Modulators of receptor for advanced glycation end products signalling in the human endometrium.

White, Amy Katherine

Modulators of Receptor for Advanced Glycation End products signalling in the Human Endometrium

By
Amy Katherine White; BSc

School of Medicine, Institute of Life Sciences
Swansea University
September 2011

A Thesis submitted to Swansea University in fulfilment of the requirements for the Degree of Doctor of Philosophy

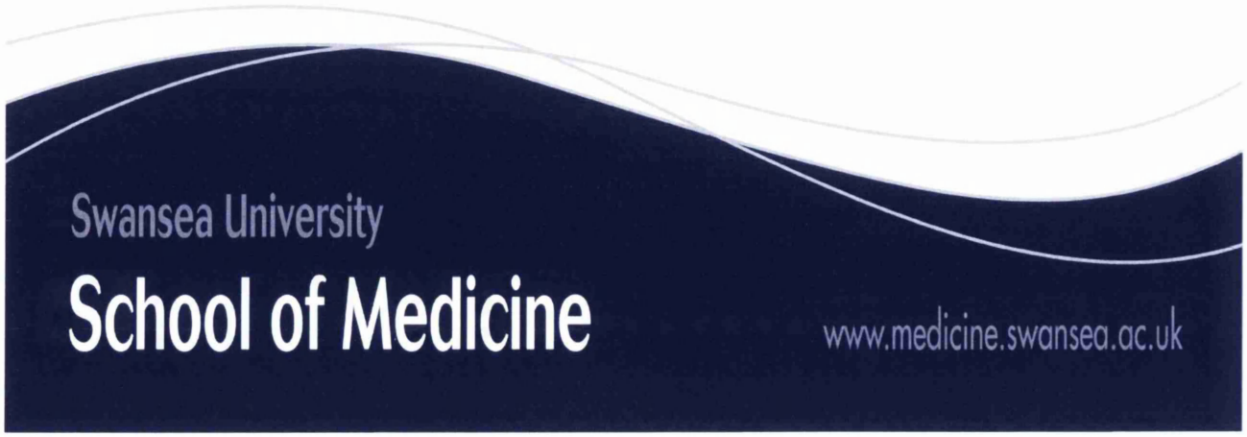

SUMMARY

The immunoglobulin-like, transmembrane Advanced Glycation End product (AGE) Receptor (RAGE) is a pattern recognition receptor implicated in the transduction of pro-inflammatory signalling and processes. Over the past decade a substantial body of evidence has accrued implicating RAGE in the pathogenesis of several chronic inflammatory and vascular diseases such as diabetes, rheumatoid arthritis, amyloidosis, atherosclerosis and renal failure. More recently RAGE has been linked to cancer progression, possibly through its role in the inflammatory process. AGE products have been shown to exert their intracellular effects through ligation of their cognate receptor RAGE and the subsequent transactivation of NFκB signalling in several cellular contexts. Polycystic Ovary Syndrome (PCOS) is a reproductive endocrine disorder characterized by hyperandrogenism, chronic anovulation and insulin resistance, thus increasing the risk of diabetes mellitus in these patients. Non-enzymatically glycated AGEs are formed at an accelerated rate and accumulate in tissues in conditions of high glucose and oxidative stress. Interestingly, young normoglycemic women with PCOS exhibit higher serum AGE levels and increased RAGE expression in poly-cystic ovaries. RAGE is also regulated through the activity of the estrogen receptor (ER). The natural cyclical expression of estrogen throughout the menstrual cycle is perturbed in endometriosis even post menopause, suggesting that RAGE could also be dysregulated. Finally PCOS has been implicated in increased risk to endometrial cancer progression as has uterine exposure to the selective estrogen receptor modulator Tamoxifen (TX) therefore it is plausible that RAGE has a function in this disease.

Objectives:

The principal aims of this thesis were to characterise RAGE expression for the first time in fertile and infertile endometriotic and PCO human endometrium, and to initiate RAGE characterisation in endometrium obtained from patients with endometrial hyperplasia and cancer. Secondly, this thesis endeavoured to elucidate the transcriptional mechanisms regulating RAGE *in vitro* in response to 17β estradiol and AGEs which are elevated in endometriosis and PCOS pathology respectively, and in endometrial cancer.

Methodology:

This project employed the use of real time Polymerase Chain Reaction (RT-PCR), Chromatin Immunoprecipitation (ChIP), Immunohistochemistry (IHC) and western blotting (WB).

Results:

Immunohistochemistry and RT-PCR data revealed that basal RAGE expression was significantly greater in PCO and endometriotic endometrium when compared to fertile controls, and significantly elevated in two cancer patients. RAGE was also characterised in endometrial cell models in which it was shown to be modulated at the mRNA and protein level by AGE-HSA, 17β estradiol (E2) and its antagonist 4-hydroxytamoxifen. Moreover, we have shown that RAGE is modulated by two distinct pathways through the estrogen receptor (ER) and NFκB. Novel ChIP results confirmed the presence of p65 and ER-alpha on the RAGE promoter at non-classical Sp1 and Ap1 sites in response to AGEs, E2 and TX.

Conclusions:

The results in this thesis may implicate endometrial RAGE expression in the infertility evident in women with PCOS and endometriosis. Furthermore, recent evidence implicates RAGE in mediating inflammation-driven tumourigenesis. Thus, over-expression of endometrial RAGE in PCOS and endometriosis, and in patients receiving tamoxifen for breast cancer treatment may predispose these women to an elevated risk of cancer.

DECLARATION

This work has not previously been accepted in substance for any degree and is not currentlv submitted in candidature for any other degree.

Signed.....(Candidate)
Date 23/3/2012

STATEMENT 1

This thesis is the result of my own investigations, except where otherwise stated.

Where corrections services have been used, the extent and nature of the corrections are clearly marked in a footnote(s). Other sources are acknowledged by footnotes giving explicit references. A bibliography is appended.

Signed..... (Candidate)
Date 23/3/2012

STATEMENT 2

I hereby give consent for my thesis, if accepted, to be available for photocopying and for inter-library loan, and for the title and summary to be made available to outside organisations.

Signed..... (Candidate)
Date 23/3/2012

CONTENTS

ACKNOWLEDGEMENTS

I owe the completion of this thesis to the expertise, guidance and support of many people. First and foremost I would like to thank Professor John White. I'd like to express my appreciation for his unfailing enthusiasm for science and my utmost thanks for his encouragement whilst guiding my research efforts. I would also like to give a literary hug and massive thanks to my supervisor Dr. Deya Gonzalez. She deserves all the praise under the sun for being generous with her time, advice, support, understanding and above all - patience. I'm so grateful for all her dedication and her confidence in my work. I would also like to thank my supervisor Dr. Steve Conlan for his management of my project, constructive criticism, guidance, coffee and the long time spent proof-reading and analysing the data. Special thanks to all my past and present colleagues in the Institute of Life Sciences at Swansea, especially to everyone in the Reproductive Biology Group: Dr. Abdulkader Azouz, Dr. Lewis Francis, Dr. Mark Roberts, Dr. Sridhar Govindarajan, Natalie DeMello, Julia Davies, Sean Griffiths, Hamidreza Saghari, Zoë Coombes, Brendan Wilson, Dr. Nurul-Huda Hamidi, Dr. Angela Richards and Dr. Kit Lucas. I'd like to mention the significant contribution of clinical samples, information and expertise that the staff in Obstetrics and Gynaecology and Pathology at Singleton Hospital have brought to my project. In particular, thanks to Dr. Lisa Joels, Dr. Lavinia Margarit and Dr. Kinza Younas. I'm especially grateful to all the women who donated clinical specimens and have given their time to this study. Special thanks go to my wonderful friends: Jim & Sara, Holly & Jack, Pete & Filly, Geoff, Dan & Amy, Matt, Dave, Mamfy, Zoulikha, Luke, Benjamin, Linda & Leigh, Bella & Dave and everyone in Christchurch, Whiteparish, DP and Indie Clique. I'd like to thank my family: Beryl & William Major, Douglas & Olive White, Dr. Martin White, Steve & Carol White, Janet & Terry Jolly, Janet & Allan Cheetham, Heather, Norman, Simon & Kim Hayter, Mark, Ruth & Roy. Last of all, I'd like to dedicate my thesis to my brilliant parents Anthony and Yvonne and my sister Lucy. Thanks for all your love, encouragement and for putting things into much needed perspective.

CONTACTS LIST

Sigma-Aldrich Company Ltd UK The Old Brickyard New Road Gillingham Dorset SP8 4XT Phone: UK 0800 717181 Fax: UK 0800 378785	**EMD Biosciences USA** 10394 Pacific Center Court San Diego, 92121, CA Phone: US 800-854-3417	**Bio-Rad Industries Ltd UK** Bio-Rad House Maxted Road Hemel Hempstead Hertfordshire, HP2 7DX Phone: UK 020 8328 2000 Fax: UK 020 8328 2550
Life Technologies Ltd UK **Gibco-Invitrogen** **Applied Biosystems** **Ambion** 3 Fountain Drive Inchinnan Business Park Paisley, PA4 9RF Phone: UK 01925 282670 Fax: UK 01925 282503	**Star Lab UK** 4 Tanners Drive Blakelands Milton Keynes Buckinghamshire MK14 5NA Phone: UK 01908 283800 Fax: UK 01908 283802	**GE Amersham Healthcare Life Sciences UK** Amersham Place Little Chalfont Buckinghamshire, HP7 9NA Phone: UK 0800 616 928 Fax: UK 01494 542018
Insight Biotechnology Ltd UK **Santa Cruz** PO BOX 520 Wembley Middlesex HA9 7YN Phone: UK 0800 073 3133 Fax: UK 0800 953 0268	**Millipore Limited UK** Suite 3 & 5 Building 6 Croxley Green Business Park Watford WD18 8YH Phone: UK 0870 900 46 45	**Active Motif Europe** 104 Avenue Franklin Roosevelt 1330 Rixensart Belgium, BE Phone: BE 26560459 Fax: BE 26530050
Thermo Fisher Scientific UK Bishop Meadow Road Loughborough LE11 5RG Phone: UK 01509 555 954	**Ventana Medical Systems Inc.** 1910 E Innovation Park Drive Tuscon Arizona 85755 Phone: US 520 887 2155 Fax: US 800 277 2155	**Mini Tab Ltd. UK** Brandon Court, Unit E1-E2 Progress Way Coventry CV3 2TE Phone: UK 0247 643 7500

FIGURES AND ILLUSTRATIONS

ABBREVIATIONS

A

ABC	Avidin-Biotin peroxidase Complex
ACTR	Activator of Transcription nuclear Receptor (see SRC-3, AIB-1)
ATCC	American Type Culture Collection
AGE(s)	Advanced Glycation End product(s)
AGE-BSA	Bovine Glycated Albumin
AKT	Serine/Threonine Protein Kinase
AGE-HbA_1C	Glycated Haemoglobin
AGE-HSA	Human Glycated Serum Albumin
AGER	Receptor for Advanced Glycation End products
AGER1	Oligosaccharyl Transferase-4 (OST-48)
AGER2	Phosphoprotein 80K-H, Protein Kinase C substrate
AGER3	Galectin-3
AIB-1	Amplified in Breast Cancer-1 (see also SRC-3, RAC-3, ACTR)
Anov	Anovulatory
ANOVA	Analysis of Variance Statistical Model
AP-1	Activator Protein-1
APS	Ammonium Persulphate
AR	Androgen Receptor
ART	Assisted Reproductive Techniques

B

BD	Band Density
BME	Basal Medium Eagle
BMI	Body Mass Index
BPTI	Bovine Pancreatic Trypsin Inhibitor
BSS	Balanced Salt Solution

C

cAMP	Cyclic Adenosine Monophosphate
CD36	Cluster of Differentiation 36
ChIP	Chromatin Immunoprecipitation
CML	N-epsilon (carboxymethyl) Lysine
CML-HSA	Human Serum Albumin N-epsilon (carboxymethyl) lysine
CREB	cAMP Response Element Binding protein (also CBP)
Ct	Cycle Threshold
CVD	Cardiovascular Disease

D

DAB	Diaminobenzidine
$\Delta\Delta$Ct	Delta Delta Threshold Cycle
DCC-FBS	Dextran-Coated Charcoal-treated Foetal Bovine Serum
DBD	DNA Binding Domain
DHT	DiHydroTestosterone
DM	Diabetes Mellitus
DMT1	Diabetes Mellitus Type I
DMT2	Diabetes Mellitus Type II
DMEM/F-12	Dulbecco's Modified Eagle Medium: Nutrient Mixture F-12
DNA	Deoxyribonucleic Acid (gDNA: genomic DNA)
DPBS	Dulbecco's Phosphate Buffered Saline
DPX	Di-n-butylPhthate

E

E	Primer PCR Efficiency
E2	17-beta Estradiol
EC	Extracellular region
ECC-1	Endometrial Carcinoma Cell line
ECCAC	European Collection of Cell Cultures
ECV304	Human Endothelial Vascular Cell Line
EDTA	Ethylenediaminetetraacetic acid
EE	17-alpha-ethinylestradiol
EGFR	Epidermal Growth Factor Receptor
EMSA	Electrophoretic Mobility (Super) Shift Assay
Endom	Endometriosis
esRAGE	Endogenous Secretory Receptor for AGE
ER	Estrogen Receptor
ERK	Extracellular Signal-Regulated Kinases
ERE	Estrogen Responsive Element
ERR	Estrogen Related Receptor
ESR1/2	Estrogen Steroid Receptor genes I and II
ETS-1	Protein C-ets-1
F	
FBS	Foetal Bovine Serum
FSH	Follicle Stimulating Hormone
FL-RAGE	Full-length Receptor for Advanced Glycation End products
FIGO	International Federation of Gynaecology and Obstetrics
G	
Gal-SRC-1	Gal-steroid receptor coactivator 1 (see also NcoA-1, SRC-1)
GAPDH	Glyceraldehyde 3-phosphate dehydrogenase (also G3PDH)
GDM	Gestational Diabetes Mellitus
GDP	Glucose Degradation Products
GIFT	Gamete Intra-Fallopian Transfer
GLUT-4	Glucose Transporter Type 4
GnRH	Gonadotropin-releasing Hormone
GRIP	Glucocorticoid Receptor Interacting Protein 1 (NcoA-2, SRC-2)
GSK-3	Glycogen Synthase Kinase 3
H	
HSA	Non-Glycated Human Serum Albumin (also abbreviated HA)
HDAs	Histone Deacetylases
HBSS	Hanks' Balanced Salt Solution
hCG	Human Chorionic Gonadotropin
HEC-1	Human Endometrial Adenocarcinoma Cells
HMGB-1	High-Mobility Group Box- protein 1
HMVEC	Human Micro Vascular Endothelial Cell
HPLC	High Performance Liquid Chromatography
HPS	Hydrogen Peroxide Solution
HRP	Horseradish Peroxide
HUVECS	Human Umbilical Vein Endothelial Cells
I	
IC	Intracellular Region
IgG	Immunoglobulin Antibody
IGFBP1	Insulin-like Growth Factor-Binding Protein 1
IHC	Immunohistochemistry
IKBα/β	Inhibitor of Kappa B alpha and beta
IKK	Inhibitor of Kappa B Kinase

IL	Interleukins (IL-1beta, IL-2, 4, 6, 8, 10 and 12)
IP	Immunoprecipitation
IR	Insulin Receptor
IRS-1	Insulin Receptor Substrate-1
IVF	*In Vitro* Fertilisation
L	
LBD	Ligand Binding Domain
LH	Luteinising Hormone
LIF	Leukaemia Inhibitory Factor
LPS	Lipopolysaccharide
M	
MAPK	Mitogen-activated Protein Kinase
MEKK	Mitogen-activated Protein Kinase Kinase Kinase
MHC	Major Histocompatability Complex
MS	Mass Spectrometry
MSR	Macrophage Scavenger Receptors
MUC1	Mucin -1 (MUC-1)
N	
NCAM-1	Neuronal Cell Adhesion Molecule
NcoA-1	Nuclear coactivator-1 (see also Gal-SRC-1, SRC-1)
NcoA-2	Nuclear coactivator-2 (see also SRC-1, GRIP, TIF-2)
NcoR1/2	Nuclear receptor corepressor 1/2 (see also SMRT for NcoR2)
NΔ-RAGE	N-terminally truncated Receptor for AGE
NEAA	Non-Essential Amino Acids
NIK	Nuclear Factor Kappa B inducing kinase (also MAP3K14)
NO	Nitric Oxide
NR	Nuclear Receptors
NFκB	Nuclear Factor Kappa B
NFκB-p65	Nuclear Factor Kappa B Protein 65 (also known as RelA)
O	
O-GalNAc	O-linked N-Acetylated Galactosamine
O-GlcNAc	O-linked N-Acetylated Glucosamine
Ov	Ovulatory
P	
PBS(X)	Phosphate Buffered Saline (with 0.5% Triton X-100)
pERK 1/2	Phosphorylated Extracellular-signal Regulated Kinases I and II
PIC	Proteinase Inhibitor Cocktail
PI-3K	Phosphatidylinositol 3-kinase
PKA/B/C	Protein Kinase A, Protein Kinase B (AKT), Protein Kinase C
PMSF	PhenylMethaneSulfonylFluoride
PCOS	Polycystic Ovary Syndrome (Stein-Leventhal syndrome)
pRas	Phosphorylated RAt Sarcoma protein
p21	Transforming protein 21 (see Ras)
PR	Progesterone Receptor
PRR	Pattern Recognition Receptor
PVDF	Polyvinylidene Fluoride (membrane)
Q	
Q-RT-PCR	Quantitative Real Time Polymerase Chain Reaction
R	
RA	Rheumatoid Arthritis
Ras	RAt Sarcoma proteins
RAC-3	Receptor Associated Coactivator-3 (see SRC-3, AIB)

RAGE	Receptor for Advanced Glycation End products
RFU	Relative Fluorescence Units
RhoA	Ras homolog gene family member A
RICD	RAGE Intracellular Domain
RIPA	Radioimmunoprecipitation Assay (Buffer)
RLT	Buffer RLT Lysis Buffer (Qiagen)
RNA	Ribonucleic Acid (mRNA; Messenger Ribonucleic Acid)
RCO	Reactive Carbonyl Compounds
ROS	Reactive Oxygen Species
RPL19	Ribosomal Protein L19
RT-PCR	Real Time Polymerase Chain Reaction
S	
SD	Standard Deviation
SDS	Sodium Dodecyl Sulphate
SDS-PAGE	Sodium Dodecyl Sulphate - Polyacrylamide Gel Electrophoresis
SERM(s)	Selective Estrogen Receptor Modulator(s)
SHBG	Sex Hormone Binding Globulin
SMRT	Silencing Mediator for Retinoid and Thyroid hormone receptor
SP	Signal Peptide
SP1	Specificity Protein
sRAGE	Soluble Receptor for Advanced Glycation End products
SRC-1	Steroid Receptor Co-activator 1 (NcoA-1, Gal-SRC-1)
SRC-2	Steroid Receptor Co-repressor 2 (NcoA-2, GRIP, TIF-2)
SRC-3	Steroid Receptor Co-activator 3 (RAC-3, AIB-1, ACTR)
STIs	Sexually Transmitted Infections
T	
TBS(X)	Tris-Buffered Saline (with 0.5% Triton X-100)
TGFα/β	Transforming Growth Factor Alpha/Beta
THP-1	Human Acute Monocytic Leukaemia Cells
TIF-2	Transcriptional Intermediary Factor-2
TNFα	Tumour Necrosis Factor Alpha
TM	Transmembrane
Tm	Melt Temperature
TLR	Toll-Like Receptors
TTBS	TBS-Tween-20 Solution
TRAF2	Tumour Necrosis Factor Receptor Associated Factor 2
TX	Tamoxifen, 4-hydroxytamoxifen
U	
UIF	Unexplained Infertility
V	
VEGF	Vascular Endothelial Growth Factor
VNTR	Variable Number Tandem Repeat
W	
WHO	World Health Organisation
X	
XBP1 enh 1	X-box binding protein -1 (enhancer region 1)

Chapter 1

Introduction

1. Introduction

1.1 Reproductive Biology

Mammalian reproductive biology is a broad field of science encompassing diverse research areas linked by a central focus on sexual reproduction. Human reproduction is reliant on the success of several complex, precisely-timed and highly-regulated biological processes namely gametogenesis, ovulation, fertilisation, implantation, gestation and parturition of live offspring. Specifically, a clinical branch of reproductive biologists has been established in Obstetrics and Gynaecology to address female-centric factors affecting the outcome of clinical pregnancy. Furthermore, collaboration between surgical clinicians, gynaecologists and molecular biologists in this field has led research on the aetiology of disease in the female reproductive tract, gestational complications, infertility, and raised awareness of contraceptives and sexually-transmitted disease. This knowledge has also aided the development of assisted reproductive techniques (ART) such as in vitro fertilisation (IVF) and gamete intra-fallopian transfer (GIFT).

1.2 Physiology of the Human Female Reproductive System

1.2.1 The Ovaries and Fallopian Tubes

Ovaries are rounded sac-like bodies which are attached to the broad ligament, one at either side of the uterus however their position may be displaced during pregnancy. Ovarian tissues comprise of vessel-rich stroma, connective fibers and granulosa beneath a layer of squamous peritoneum and a cortical layer of graafian follicles which contain the ova (eggs) and follicular fluid. When the dominant follicle matures it nears the ovarian surface and ruptures to release the ovum through the outermost layer of columnar

epithelium into the ovarian fimbria of the fallopian tube (oviduct). Passage of the ovum along the fallopian tube is facilitated by the inner mucosal layer of ciliated epithelial cells (Drake 2010).

1.2.2 The Uterine Cavity

In humans, the fully-developed uterus is a large pear-shaped organ which facilitates all stages of pregnancy from blastocyst implantation and a nine month gestational period of embryo-foetal development that ultimately ends with parturition. In the foetus, the uterus is located within the abdominal cavity and with the onset of puberty descends deeper into the pelvic region. The position of the uterus within the pelvic region is flexible due to its suspension by cardinal, uterosacral and broad ligaments. The uterine cavity comprises of thick muscular walls (*tunica muscularis*) surrounded by a layer of protective peritoneum called *tunica serosa*, a mucosal layer of ciliated and glandular epithelium (*tunica mucosa*), endometrium and myometrium. The ectocervix adjoins the cervix, the cylindrical narrowed region at the uterine base, to the vagina. Vaginal walls are comprised of outer fibrous, *muscularis* and inner protective mucosal layers which are essential to accommodate childbirth when both the cervix and vagina must dilate (Drake 2010).

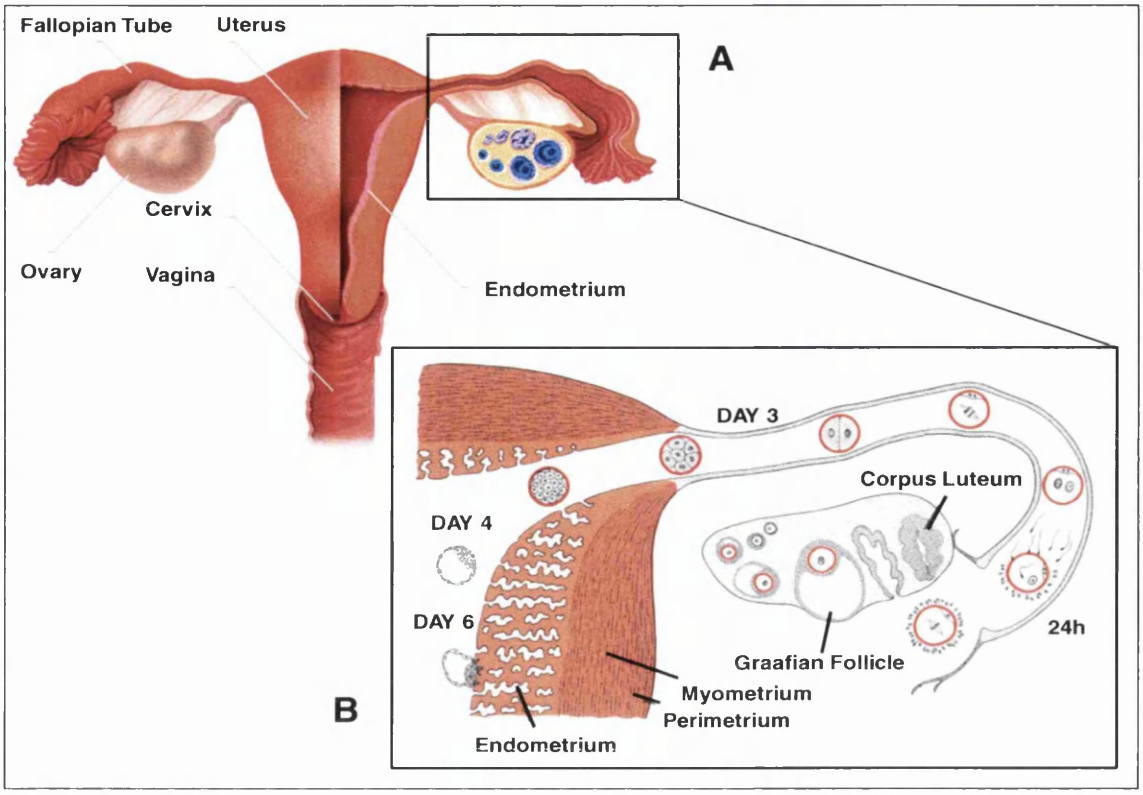

Figure 1-1 The organs of the female reproductive system *in situ*

Diagram of the organs of the female reproductive system *in situ* shows the position of the fallopian tubes, cervix, vagina, ovaries and endometrium in relation to the uterine cavity (A) http://www.artreproductivecentre.com/uterine-cervical.html. The highlighted schematic diagram (box) depicts oocyte development within the fallopian tube including the time of DNA replication at 24h post-fertilisation and blastocyst attachment into the thickened endometrial lining at day 6. Post-ovulation the ruptured follicle disintegrates to form the corpus luteum (B) http://www.victoriafertility.com/14p_in-vitro_fertilization.htm.

1.2.3 The Endometrium

The endometrium is the innermost lining of the uterus comprising largely of mesodermal-derived glandular and luminal epithelia supported by basal lamina and cell and blood vessel-rich stromal connective tissue (Arnold, Kaufman et al. 2001). The endometrial epithelium protects the opposing muscular uterine walls (myometrium) from abrasion or self-adhesion. It is

also the first point of contact for the fertilised blastocyst and provides an adhesive interface through the expression of numerous epithelial selectins and adhesion molecules (Horne, Lalani et al. 2005). The endometrium consists of two principal layers, the *stratum functionale* which is shed through menstruation and mainly comprises of columnar and glandular epithelium and the *stratum basale* from which the *stratum functionale* regenerates. It is generally accepted that during the proliferative phase, new functional epithelium emerges from the basal layer primed by increases in estrogen, vascular endothelial growth factor (VEGF) and extensive angiogenesis (Gargett and Rogers 2001). Stromal cells in the *stratum basale* may also be responsible for generating paracrine signals to promote the growth and differentiation of the overlying epithelium (Arnold, Kaufman et al. 2001). In addition, the presence of small endothelial progenitor cell populations within this *stratum basale* layer may also facilitate endometrial regeneration, vascularisation and new stroma (Gargett and Rogers 2001; Masuda, Matsuzaki et al. 2010). In the secretory phase, the endometrium undergoes progesterone-induced morphological changes characterised by decidualisation and glandular penetration of the stroma, endometrial thickening and increases in epithelial microvilli. Late secretory phase endometrium is characterised by the lack of epithelial microvilli. It is thought that the microvilli fuse in order to give rise to a membrane pinopod structure to which the blastocyst can attach and is indicative of the receptive window (Stavreus-Evers, Nikas et al. 2001). Consequently, successful implantation is dependent on adequate preparation of the endometrial epithelial interface for possible pregnancy. Central to this process is the cyclical proliferation,

shedding and re-growth of the endometrial epithelium in response to synergistic pituitary and ovarian hormonal stimulation.

1.3 Ovarian and Menstrual Cycles

The menstrual cycle describes endometrial changes regulated by the hypothalamic-pituitary axis and can be described as discrete phases. The ovaries undergo the follicular and luteal phase, whereas there are three uterine phases; proliferative, secretory and menstrual orchestrated by the timed release of specific pituitary gonadotropins and ovarian steroids: follicle stimulating hormone (FSH), luteinising hormone (LH), estrogen and progesterone. The ovarian follicular phase (days 0-14) begins on the first day of the endometrial menstrual phase (day 0-5) when the ovary is stimulated to produce ovum-bearing follicles by the release of FSH from the pituitary gland. Follicle maturation releases the sex steroid estrogen as it relocates to the ovary surface (Strowitzki, Germeyer et al. 2006). Elevated estrogen levels, particularly 17β estradiol the most abundant circulating plasma estrogen, correlate with the onset of the uterine proliferative phase (day 5-14) where it exerts an agonistic effect on ERα and ERβ signalling to induce endometrial epithelial cell proliferation (O'Brien 2006). Simultaneously, estrogen also has a pivotal physiological role in coordinating controlled proliferation of luminal epithelial cells in the breast. Specifically, cell differentiation to form terminal-end lobular milk-synthesising structures in the ducts is driven by 17β estradiol in preparation for lactation (Nilsson, Makela et al. 2001; Anderson 2002). Ovulation occurs midway through the cycle when estrogen levels peak and signal for the transient release of LH from the pituitary. This LH surge ruptures ovarian follicles to release the ovum sparking the onset of the ovarian luteal and endometrial secretory phases (day 14-28). During the

follicular phase, ovules develop in the follicles until one matures to form the primary oocyte (ovum) which is released from the corpus luteum (ovulation) along with estrogen and progesterone, the latter being in excess (Strowitzki, Germeyer et al. 2006). While sex steroids maintain the proliferation and thickening of the endometrial lining throughout the secretory phase, if fertilisation does not occur, the corpus luteum degrades and the levels of the sex steroids decrease causing shedding of the *stratum functionale*. Conversely, elevated progesterone and estrogens are disruptive of this systemic feedback loop regulating gonadal function and are exploited in the hormonal contraceptive which prevents FSH-induced follicle maturation and LH-induced ovulation through the down-regulation of gonadotropin-releasing hormone (GnR.

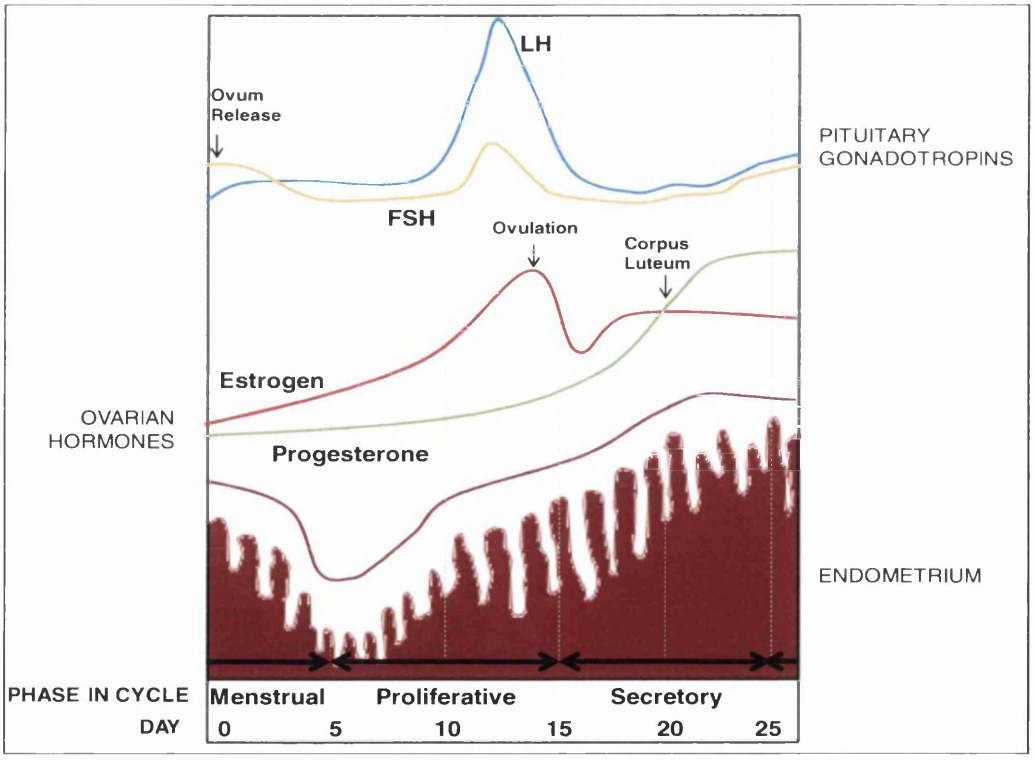

Figure 1-2 Diagram of the 28 day ovarian and menstrual cycles

Diagram shows main stages of ovulation (arrowed) coupled with the timed release of pituitary hormones; LH and FSH and ovarian steroids E2 and PR. LH surge coincides with ovulation and the onset of the secretory menstrual phase.

1.4 Female Infertility and Reproductive Disorders

Infertility is estimated to affect 1 in 6 couples in the United Kingdom (HFEA). Globally, 50-80 million are involuntarily childless equating to approximately 10% of the global reproductive population, with a further 10-25% unable to have more than one child (WHO 1992; Van den Akker 2002). Consequences of childlessness and infertility are profound having several social, economic and psychological effects on both sexes. Most couples conceive within the first year of trying to get pregnant with the chances of success almost 95% after two years (Cooke 1981). Thus, infertility is defined as the inability to conceive after two consecutive years of unprotected intercourse. Common causes of infertility are extremely varied ranging from behavioural (anxiety, anorexia), endocrine (anovulation), sexual dysfunction (immunogenic), congenital (Klinefelter disease), STIs (Chylamdia/tubal disease) and cancer (prostate/ovarian) to name but a few (Edelmann 1998; Van den Akker 2002). Obesity presents an important risk factor for reduced fecundity and infertility in both sexes. In women, obesity is particularly prevalent amongst gynaecological maladies exhibiting abnormal metabolic profiles, such as Polycystic Ovary Syndrome (PCOS) and endometriosis. Exact mechanisms behind obesity-associated infertility remain elusive however current research has implicated dislipidemia-induced dysregulation of the hypothalamic-pituitary axis. Specifically, central obesity and subcutaneous fat is linked to hyperinsulinaemia which has been shown to decrease sex-hormone binding globulin (SHBG) levels, increase hyperandrogenism and excess steroidogenesis in ovarian granulosa cells and adipose tissue (Pasquali, Gambineri et al. 2006). Furthermore, follicle exposure to inappropriate levels of gonadotropins and hyperestrogenism may accelerate ovarian cellular

differentiation and prevent follicle maturation for ovulation (Diamanti-Kandarakis and Bergiele 2001). Nevertheless, 30% of infertility cases have no identifiable cause attributable to either partner and are deemed to have 'unexplained infertility' (UIF). In most incidences, female infertility is a secondary problem associated with a diagnosable pathology some of which are investigated in this project.

1.4.1 Polycystic Ovary Syndrome (PCOS)

Polycystic Ovary Syndrome, previously known as Stein-Leventhal syndrome was first described in 1935 and diagnosed based on rudimentary observations such as hirsutism, central obesity and amenorrhea (Stein 1935). Today, PCOS is the most common female reproductive endocrinopathy affecting 5-10% of women of reproductive age (20-45yrs). PCOS can be characterised by a broad spectrum of symptoms that can vary in severity including hyperandrogenism, oligomenorrhea, hyperinsulinaemia, sleep apnea, infertility, skin problems, alopecia and premenstrual syndrome-like symptoms (Harris 2000; Futterweit 2006). In fact, PCOS symptoms such as oligomenorrhea, hyperseborrhea and acne in pre-adolescents are often mistaken for the onset of puberty (Balen 2004). Since 2003, PCOS has been diagnosed based on the Rotterdam criteria which were later revised and published in *Human Reproduction* (Criteria 2004). The consensus was that for diagnosis, two of the three following criteria must be met; biochemical and/or clinical hyperandrogenism, oligo- or anovulation and presence of multiple ovarian cysts by gynaecologic ultrasound; and exclusion of etiologies with shared symptoms such as androgen presenting tumours and Cushing's syndrome (Criteria 2004; Diamanti-Kandarakis 2006). The exact aetiology of PCOS is unknown however many studies point to underlying insulin

resistance as the root cause (Tan, Hahn et al. 2005; Fica, Albu et al. 2008). PCOS arises when the ovaries are over-sensitized by excessive luteinizing hormone (LH) or from hyperinsulinaemia where free insulin in the blood stream stimulates the ovaries to overproduce androgens. Ovaries with several small pearl-like cysts are the classical feature of PCOS. Cysts form when matured egg follicles rupture upon non-release from the ovary as a consequence of excess hormones (Homburg 2009). Insulin resistance is a prominent characteristic of PCOS, with studies finding its prevalence to be 30% and 75% in non-obese and obese cohorts respectively (Dunaif, Segal et al. 1989; Conway, Jacobs et al. 1990). Development of insulin resistance in PCOS is said to have a genetic component but is largely due to an unhealthy lifestyle (Diamanti-Kandarakis, Kandarakis et al. 2006). PCOS women are prone to hyperglycaemia and hyperinsulinaemia due to impaired glucose uptake mechanisms and reduced number of insulin receptor (IR) sites (Fornes, Ormazabal et al. 2010). Specifically, impairment or down-regulation of IRS-PI-3K-stimulated endocytic uptake of AGEs by macrophage scavenger receptor-1 (SR-A) in PCOS has been reported (Dunaif, Wu et al. 2001; Diamanti-Kandarakis, Piperi et al. 2005). Hyperandrogenism also promotes an increase in estrogens which, if sustained in excess over a long time, can cause thickening of the endometrium (hyperplasia) and increase the risk of endometrial cancer. Hyperglyceamia in PCOS causes more glucose to be converted to glycogen by the liver and is stored as fat in adipose tissues. Dislipidemia in PCOS can lead to weight gain, exacerbation of insulin resistance and allow for increased estrogen production in the fat tissues. Specifically, increased levels of 17β-hydroxysteriod dehydrogenase type 1 (17β HSD1) and sulfatase activity have been reported in PCO

endometria when compared to fertile controls. These enzymes are involved in the pathways metabolizing androgens to E2 (Leon, Bacallao et al. 2008). Excess insulin and glucose in PCOS can lead to the development of diabetes mellitus type II (DMT2). In fact, 40% of obese women with PCOS develop pre-diabetes or DMT2 by the age of 26 yrs (Talbott, Zborowski et al. 2001).

1.4.2 Endometriosis

Endometriosis is a condition of unknown aetiology where endometrial-like tissue forms outside of the uterus. It is thought an auto-immune deficiency may not protect against natural retrograde bleeding through the fallopian tubes allowing endometrial tissue in the menstrual fluid to adhere to organs outside the uterine wall. It may also result from deficiencies in the signalling or function of scavenger cells to clear retrograde endometrial cells following menstruation (Garry 2004). Endometriosis can vary in severity. It is classed in stages according to the 1985 American Fertility Society criteria points system from stage I (minimal, 1-5) to stage IV (severe, >40) (Breitkopf 1993). Endometriotic adhesions are responsive to sex-steroid stimulation during the menstrual cycle and are sometimes shed in menarche. Moreover, estrogens are overproduced in endometriosis resulting in lesion inflammation and proliferation. Like PCOS patients, women with endometriosis are often infertile or have difficulty achieving pregnancy to full-term. This may be due to numerous factors such as ectopic pregnancy and miscarriage from blastocyst implantation on endometriotic lesions or endometriotic ovaries preventing ovulation.

1.4.3 Current Infertility Therapy

There are two main 'infertility' drugs that have been used with varying degrees of success for women with PCOS and UIF; Metformin and

Clomiphene Citrate. The former was first developed to alleviate the metabolic aberrations of type II Diabetes and has been shown to ameliorate insulin resistance in PCO women (Futterweit 2006). It frequently promotes ovulation, weight loss and tissue sensitivity to insulin as well as slowing the release of glucose from glycogen stores in the liver. Specifically, Metformin is thought to suppress hepatic gluconeogenesis through the activation of adenosine monophosphate-activated protein kinase (AMPK) which inhibits production of lipogenic and gluconeogenic enzymes and stimulates glucose uptake by GLUT-4 transporters in skeletal muscle (Zhou, Myers et al. 2001; Diamanti-Kandarakis, Economou et al. 2010). Metformin is often used in conjunction with Clomiphene Citrate to aid ovulation and reduce hyperandrogenism (Futterweit 2006; Craggs-Hinton 2008). In cases of amenorrhea, progestogen is administered to induce an artificial menstrual cycle prior to Clomiphene Citrate treatment (Craggs-Hinton 2008). Clomiphene Citrate stimulates FSH gonadotropin release from the pituitary glands by sensitizing the estrogen receptor to bind circulating estrogens (Futterweit 2006). In fact, ovulation is usually restored in 80% of women administered Clomiphene Citrate and Metformin, however successful conception rates are only 40% after 6 months treatment and carry a risk of multiple pregnancies (Craggs-Hinton 2008). Treatment for endometriosis patients is further limited with only one approved drug available. Danazol is a synthetic male hormone that shrinks endometriotic lesions thus unblocking ovum and sperm passage to the uterus and improving fecundity. However over 90% of patients experience incapacitating side effects (Breitkopf 1993). Ultimately, there is a huge requirement for new infertility drugs or methods to ameliorate the reproductive and hormonal problems of PCOS and endometriosis.

1.5 Potential Factors affecting Uterine Receptivity

Coincident with steroid-regulated morphological changes, several endometrial factors influence blastocyst apposition, attachment and invasion into the receptive endometrium. The initial stages of blastocyst-endometrial recognition are said to be facilitated by pinopode protrusions formed at the apical epithelial surface in response to increased serum progesterone and decreased glandular ERα and PR-B (Stavreus-Evers, Nikas et al. 2001). In addition, a plethora of cytokines, chemokines, integrins, mucins and cadherins have been implicated in the transformation of the endometrial surface to a receptive state. Specifically, potential roles in implantation for the leukaemia inhibitory factor (LIF), interleukins (IL) 11, 6 and 1β, IGFBP-1, VEGF and transforming growth factor alpha (TGFα) and beta (TGFβ) have been elucidated (Casslen, Sandberg et al. 1998; Dimitriadis, White et al. 2005; Jones, Stoikos et al. 2006; Stoikos, Harrison et al. 2008). In particular VEGF in the *stratum functionale* and its receptors VEGFRI and II in the endothelium are markedly up-regulated during the receptive window and correlate with decidualisation and increased estrogen, vascular permeability and angiogenesis (Meduri, Bausero et al. 2000; Sugino, Kashida et al. 2002). Increased endometrial VEGF is likely due to estrogen-induced recruitment of ERα to its promoter via Sp1 interaction (Koos, Kazi et al. 2005). In addition, IL-11 is regulated by IL-1β and TGFβ and shows maximal expression in decidualised stroma. It is also secreted by the trophoblast potentially to aid placentation. Interestingly, IL-11 is abnormally expressed in endometriosis (Popovici, Kao et al. 2000; Dimitriadis, Stoikos et al. 2006). Similarly, IL-6, also regulated by IL-1β, is elevated during this putative implantation window and continues into menstruation. Like IL-11 and LIF, IL-

6 requires gp130, a signal transduction molecule to exert its effects through receptor binding. Soluble gp130, an antagonist of gp130 is decreased mid-secretory phase in women with UIF and may lead to increased IL-6, 11, LIF and TNFα signalling (Cork, Tuckerman et al. 2002; Sherwin, Smith et al. 2002). Endometrial TNFα is negatively regulated by E2 and so its elevated expression in the receptive window coincides with falling estrogen in the secretory phase. During this time, TNFα, ERα and IL-1β may accelerate synthesis of the glycoprotein Mucin-1, the dysregulation of which is linked to implantation failure (Tabibzadeh, Satyaswaroop et al. 1999; Thathiah, Brayman et al. 2004). Furthermore, MUC1 has been shown to directly bind to p53, EGFR, ERα, NFκB-p65 and β-catenin in pathways that promote cancer cell growth by inhibition of apoptosis, up-regulation of cytokines and cell-cell adhesion in several cell models (Wei, Xu et al. 2005; Wei, Xu et al. 2006; Pochampalli, Bitler et al. 2007; Ahmad, Raina et al. 2009; Bitler, Goverdhan et al. 2010). Underlying endometrial inflammation could be attributed to repeat exposure to or over-expression of these factors and may be the root cause of miscarriage and elevated risk of endometrial cancer development in infertile women.

1.5.1 Endometrial Cancer

Most women who develop endometrial cancer present with various gynaecological abnormalities prior to its detection such as uterine bleeding post menopause, infertility, PCOS and endometrial hyperplasia which is now considered a cancerous prerequisite (Dobrzycka and Terlikowski 2010). Malignant endometrial tissue assumes either an endometrioid (type I), papillary serous or clear cell (type II) carcinoma and is graded according to the 2009 International Federation of Gynaecology and Obstetrics (FIGO)

criteria (Bokhman 1983). Type I endometrioid carcinomas account for 70-80% of cases and are characterised by the estrogen-dependant solid growth of the uterine glands, β-catenin mutations and good survival prognosis (Bokhman 1983; Sherman 2000). In contrast, type II serous carcinomas are rarer, poorly differentiated, metastatic tumours presenting with micropapillae, p53 mutations and hormonal insensitivity (Bokhman 1983; Garg, Leitao et al. 2010). In order to eliminate ambiguity in classification of morphologically indistinct carcinomas having endometrioid and serous qualities, studies have suggested that p16, p53, and nuclear receptor (NR) immunohistochemistry could be used in conjunction with histology (Alkushi, Kobel et al. 2010; Dobrzycka and Terlikowski 2010; Garg, Leitao et al. 2010; Prat 2010).

1.6 Advanced Glycation End products (AGE)

1.6.1 Formation and Detection of AGEs

Advanced Glycation End products (AGEs) are a heterogeneous group of reactive cross-linking molecules formed when circulating proteins, lipids and nucleic acids undergo a series of non-enzymatic glycation events known as the Malliard reaction. The Malliard reaction is so named after the French chemist Louis-Camille Malliard who, in 1912, discovered the first interactions between the reactive carbonyl group of reducing sugars and the amino group of free amino acids or proteins (Malliard 1912). The initial stage of the Malliard reaction begins with a condensation event unifying nitrogen in the amino group to a carbon within the carbonyl group to form imines; glycated protein intermediates termed Schiff bases (Malliard 1912). Schiff bases cyclise to form N-substituted glycosylamine intermediates; aldosylamines and ketosylamines, which are formed from the reaction between amino

compounds and aldose (glucose) and ketose (fructose) sugars respectively. In the early stages of the Malliard reaction, the formation of Schiff bases is reversible in the presence of water (Isdale 1993); however, these intermediates can undergo Amadori re-arrangement or isomerisation to form more stable cross-linked structures called Amadori products (Hodge 1953; Hodge 1967; Namiki 1988). Upon further glycation and modifications such as dehydration and oxidation-reduction reactions, Amadori product intermediates become fluorescent, highly reactive and irreversibly glycated AGEs (Ledl 1999; Peppa 2003). The chemical nature of the reducing sugar and amino compound affects the rate of reaction and consequently formation of AGEs. Xylose, galactose and fructose are considered ten times more reactive than glucose, and proteins containing lysine residues, which have two amino groups are more likely to interact with reducing sugar carbonyl groups (Ashoor 1984). Many other factors affect the rate of AGE formation including the concentration of glucose, presence of glucose degradation products (GDP) and pH (Wieslander 2001). It has been suggested that acidic conditions (low pH) slow AGE formation due to the donation of positive charged protons from acids to oxygen molecules within the carbonyl group, thus making the sugar less reactive. One of the most studied AGE products N^{ε}-(carboxymethyl) lysine, or CML, has been shown to be formed at an accelerated rate in alkaline conditions from oxidative cleavage of Amadori products at the second or third carbon in the carbohydrate chain (Nagai, Ikeda et al. 1998). *In vivo*, AGEs can be loosely categorized into two types; those formed from protein or fatty acid oxidation such as CML and pentosidine, and those formed by oxidative stress precursors known as carbonyl compound (RCO) such as imidazolone and pyrraline (Miyata 1999;

Miyata 2000; Bohlender 2005). AGEs form at a slow constant rate throughout the normal aging process beginning at embryonic development and increasing in environments of high glucose concentration and oxidative stress (Peppa 2003). Nagai, et al (1998) also showed that hydrogen peroxide, a free-radical indicative of oxidative stress, and iron compounds found at high concentration in the blood plasma, could give rise to CML production from glycated human serum albumin (Kato 1981). AGEs can be detected due to their chemical fluorescence, a property which is proportional to the stage of advanced glycation and provides an index for AGE quantification. Early studies have revealed the glycating potential of reducing sugars is dependent on the relative abundance of its cyclic versus the acyclic form which participates in glycation (Krajcovicova-Kudlackova, Sebekova et al. 2002). Consistent with this premise, fructation of human serum albumin (HSA) increases AGE-HSA fluorescence to a greater extent than glycation (Jakus, Carsky et al. 1998). Study of the glycation process and AGE quantification in clinical diagnostics has been limited due to lack of efficient analytical procedures (Makita 1992; Yim 2001). However, High Performance Liquid Chromatography and Mass spectrometry have recently been employed to identify glycated peptide precursors for CML, imidazolone and pyrraline in plasma serum (Ahmad 2008). Elevated AGE has also been detected using antibodies raised against AGE-specific epitopes in aging, diabetic, renal failure and polycystic ovary tissues (Dyer 1993).

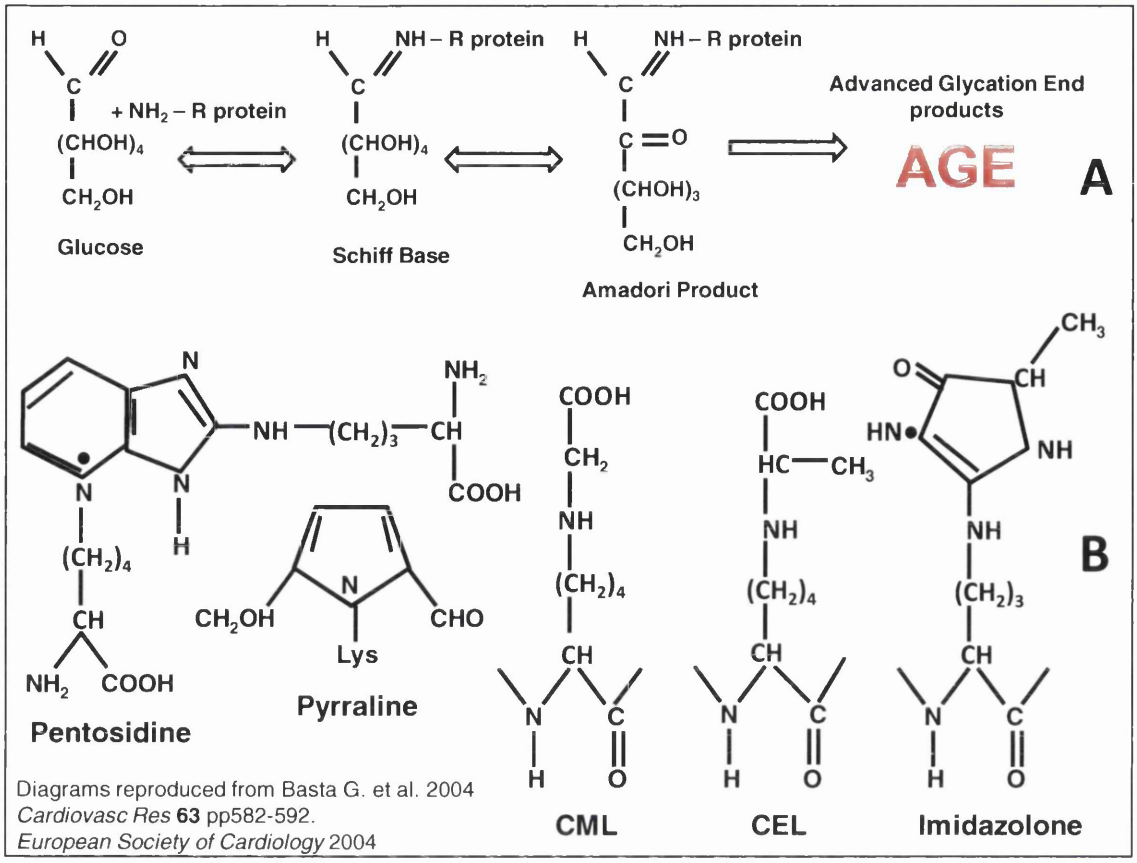

Figure 1-3 The chemical structures of some common Advanced Glycation End products.

Simplified representation of the chemical structures of two types of AGE: those made from lipid oxidation (CML and Pentosidine) and those formed from reactive carbonyl compounds (Imidazolone and Pyrraline) (B). The Malliard Reaction for the formation of AGEs is shown above (A).

1.6.2 AGEs and Nutrition

The Malliard reaction is an example of non-enzymatic glycation or browning that is accelerated when sugars are heated with lipid or proteins during typical food preparation and cooking methods (Uribarri, Woodruff et al. 2010). Studies have highlighted the contribution of highly reactive synthetic AGEs to our dietary and subsequent corporal intake of exogenously-formed AGEs to be proportional to AGE-related damage and oxidative stress (Thornalley 1990; Koschinsky, He et al. 1997; Takeuchi, Makita et al. 2000; Peppa 2003). Indeed, vegetarianism increases levels of CML, an AGE implicated in the

pathophysiology of diabetic complications and oxidative stress, due to high dietary intake of the reducing sugar fructose (Krajcovicova-Kudlackova, Sebekova et al. 2002). The level of natural AGE formation throughout the aging process (Peppa 2003) has been shown to be genetically pre-determined and to be independent of genes that influence fasting glucose levels, (Leslie 2003) thus indicating pre-disposition to development of disorders such as obesity and Diabetes Mellitus Type 2 (DMT2). However, conditions of transient high glucose accelerate AGE formation beyond the pre-determined level. This is especially significant for women with Polycystic Ovary Syndrome (PCOS) who have increased susceptibility to DMT2 as a result of increased AGE levels (El-Osta 2008).

1.6.3 Removal of AGEs: Hypothesis for the AGE Receptors

AGEs are biologically characterised by their binding to AGE-specific receptors such as the complex of OST-48 (AGE-R1), 80K-H (AGE-R2) and Galectin-3 (AGE-R3) (Pricci, Leto et al. 2000), macrophage scavenger receptors (MSRs) SR-A I and II, SR-B I and II, CD36 (Ohgami, Nagai et al. 2001; Ohgami 2002; Ilchmann, Burgdorf et al. 2010) and the Receptor for Advanced Glycation End products RAGE/AGER (Bierhaus 2005; Ramasamy, Yan et al. 2007). Despite the identification of many AGE-binding receptors, most do not partake in AGE-mediated signal transduction and exist as AGE elimination mechanisms (Thornalley 1998; Ohgami, Nagai et al. 2001; Rocken, Kientsch-Engel et al. 2003). Under normal physiological conditions, corporal AGEs are removed through kidney glomerular ultra-filtration and excreted in urea (Agalou, Ahmed et al. 2005). Circulating plasma AGEs are also locally removed by rapid cellular endocytic uptake. In animal models, MSRs are crucial to this process in hepatic Kupffer and endothelial cells,

renal epithelial tubular cells and macrophages (Smedsrod, Melkko et al. 1997; Sano 1998). Further investigation revealed that AGE endocytic uptake is not regulated by CD36 but is likely mediated by MSRs; class A SR-A II and class B SR-B I and II (Matsumoto, Sano et al. 2000; Hansen, Arteta et al. 2002; Nakajou, Horiuchi et al. 2005). Galectin-3 is unable to anchor cell membranes so it associates with OST-48 and 80K-H in an AGE-receptor complex, the function of which is attributed to Galectin-3 following its *in vivo* knock-down in mice (Vlassara, Li et al. 1995; Pugliese, Pricci et al. 2001; Iacobini, Amadio et al. 2003). Galectin-3, OST-48 and class A MSR expression inversely correlates with increased RAGE and 80K-H in diabetic complications. Furthermore, non-complexed 80K-H and RAGE receptors can mediate AGE-associated signal transduction (Pugliese, Pricci et al. 2001; Wendt 2003). In contrast, Galectin-3 and OST-48 may act as decoy receptors to confer cellular protection against the effects of AGEs (Vlassara, Li et al. 1995). Interestingly, CD36 expression is positively regulated by RAGE and may serve as an AGE-binding competitive inhibitor to impede AGE-mediated RAGE auto-regulation (Xanthis, Hatzitolios et al. 2009).

1.7 Receptor for Advanced Glycation End products (RAGE/AGER)

1.7.1 RAGE Structure and Function

Human RAGE is a 404 amino acid (aa) peptide encoded by the AGER gene located in the class III locus of the major histocompatability complex (MHC) on chromosome 6p21.3 (Sugaya, Fukagawa et al. 1994). RAGE is a member of the immunoglobulin superfamily of molecules and shares the closest homology with neuronal cell adhesion molecule (NCAM-1) an epithelial cell surface selectin receptor (Neeper, Schmidt et al. 1992). RAGE is antibody-like in structure comprising a signalling peptide (22aa), extracellular domain,

hydrophobic transmembrane region (19aa) and 41aa cytosolic tail (Raucci 2008). The extracellular (EC) region comprises of two constant 'C' and one variable 'V' immunoglobulin domains. The 'V' domain contains two N-glycosylation sites to which ligands such as AGEs bind at the N-terminus (Srikrishna 2002; Yonekura, Yamamoto et al. 2003). In fact, RAGE is often described as a pattern recognition receptor (PRR) for its ability to be liganded by a diverse group of molecules (Xie, Reverdatto et al. 2008). This 'V' domain is fundamental to RAGE PRR function as it does not distinguish between amino acid sequences but rather interacts with ligands that share homologous 3-D structures (Pullerits, Brisslert et al. 2006). The C-terminal cytosolic tail of RAGE is highly charged and is required for intracellular signalling through activation of extracellular signal-regulated kinases (ERK) (Bucciarelli 2002; Hudson, Kalea et al. 2008). RAGE is naturally expressed at low levels in several tissues but its exact innate functionality is unknown. Originally considered an essential signalling mediator in neuronal cell differentiation, increased neuronal RAGE was observed during human and rodent embryonic development (Hori, Brett et al. 1995; Wang, Li et al. 2008). Later, RAGE was discovered to be constitutively expressed in lung, specifically in pulmonary alveolar tissues; the first point of contact to airborne pathogens (Kreiger 2001). Consequently, as is the case with other PRRs, RAGE may have a role in innate immunity to recognise heterogeneous foreign bodies such as bacteria. Indeed, the observation that RAGE protein increases at sites of inflammation and oxidative stress, has lead to the notion that truncated RAGE isoforms may have been an evolutionary mechanism to combat environmental exposure to antigens (Kreiger 2001).

1.7.2 RAGE Protein Isoforms

Several carboxyl-terminal truncated forms of RAGE receptor have been identified demonstrating that RAGE undergoes alternative splicing events following transcription (Schlueter, Hauke et al. 2003; Hudson, Carter et al. 2008). Proteolytic cleavage of the full-length transcript encoded membrane-tethered form is through the action of membrane sheddases belonging to the ADAM family of metalloproteases (Raucci 2008; Zhang, Bukulin et al. 2008). Specifically, sheddase ADAM10 cleaves transmembrane RAGE to produce four stable isoforms recognised *in vivo* at the protein level: two soluble sRAGEs, N-truncated RAGE and the full-length RAGE (Yonekura, Yamamoto et al. 2003; Ding and Keller 2005; Hudson, Carter et al. 2008). A fifth isoform termed endogenous secretory esRAGE is thought to arise from alternative splicing of exon 9 (Harashima, Yamamoto et al. 2006). The esRAGE isoform comprises the signal peptide (SP) and extracellular region (EC), lacks the transmembrane (TM) and has a unique 16aa C-terminus instead of the usual 41aa intracellular region as a result of splicing at the mRNA level (IC). N-truncated RAGE is devoid of the SP and 'V' immunoglobulin domain of the EC region. It does however have the 'C' domains of the EC, TM and IC (Yonekura, Yamamoto et al. 2003; Raucci 2008). Proteolytic cleavage for esRAGE by ADAM10 leaves the IC domain intact. However, identification of free C-terminal fragment termed the RAGE intracellular domain (RICD) in the cytoplasm is thought to arise from calcium-dependent γ-secretase degradation of the IC domain (Galichet, Weibel et al. 2008). Over 20 human RAGE spliced variants have been described but do not appear to translate to protein perhaps due to a lack of sequence on exon 1 which is important for stability. Consequently, it is thought that these

transcripts might be made unstable by nonsense-mediated decay or perhaps are immediately targeted for rapid protein degradation post translation (Sparvero, Asafu-Adjei et al. 2009). Numerous studies have identified esRAGE and sRAGE soluble truncated isoforms as therapeutic targets for ameliorating diabetic complications through competitive inhibition and blockage of RAGE signalling in several tissues (Zhang, Tasaka et al. 2008). The levels of these protective soluble RAGE forms are significantly reduced in diabetics and inversely correlate with increases in circulating AGEs (Katakami 2005; Basta, Sironi et al. 2006; Grossin 2008).

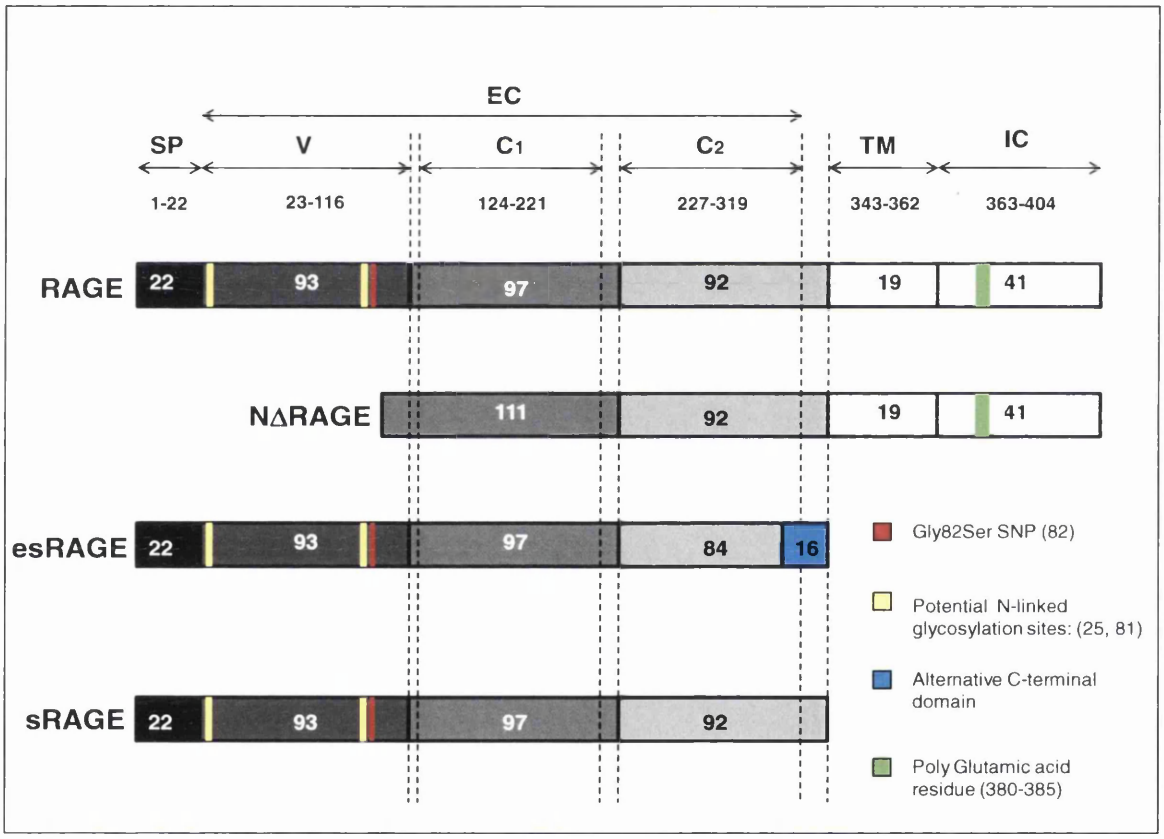

Figure 1-4 Schematic diagrams representing the structural domains of several characterised RAGE isoforms.

Indicated are the respective amino acid lengths of each protein domain, the positions of cleavage and glycosylation sites important for AGE binding. EC; extracellular domain, TM; transmembrane region, IC; intracellular domain (C-terminus), SP; signal peptide (N-terminus).

1.7.3 RAGE Ligands and Signalling

In essence, RAGE ligands are heterogeneous in structure and origin. However, these molecules can occupy the receptor owing to common binding-site homology possibly β-sheet fibrils (Yan, Chen et al. 1996; Huttunen 1999). Indeed, glycation induces restructuring of amino acids into β-sheet conformation and β-amyloid fibrils during AGE formation. These fibrils can refold to make a 'cross-beta' quarternary structure that RAGE may recognise (Bouma, Kroon-Batenburg et al. 2003). RAGE was first characterised as the receptor for AGEs in 1992 (Schmidt, Vianna et al. 1992). Identification of Amphoterin/High-Mobility Group Box-1 (HMGB-1) as a high affinity RAGE ligand lead to debate over authenticity of AGEs as the natural ligands. Initially, the consensus was AGEs displayed 'accidental occupation' of the receptor due to a high degree of binding site similarity to the HMGB-1 cytokine (Hori, Brett et al. 1995). However, RAGE was characterised as a pattern recognition receptor when it could ligate structurally diverse β-amyloid peptides, lipopolysaccharide (LPS), integrin Mac-1, and S100 calgranulins (Hori, Brett et al. 1995; Hofmann, Drury et al. 1999; Chavakis, Bierhaus et al. 2003; Figarola, Shanmugam et al. 2007). RAGE mediates, at least in part, the same signalling pathway *in vivo* as the Toll-Like Receptors (TLRs) specifically TLR2, 4 and 9 which also bind HMGB-1 and LPS (Tian, Avalos et al. 2007; Qin, Dai et al. 2009). In fact, convergence and augmentation of combined RAGE and TLR-mediated signalling is witnessed with HMGB-1 (van Beijnum, Buurman et al. 2008). In line with a possible evolutionary role for RAGE in innate immunity, RAGE has been implicated in perpetuating inflammatory cascades in response to ligation by S100b, a member of the S100 calgranulin family. Recently, hyperglycaemia-induced ROS production

has been shown to increase expression of AGEs, RAGE, HMGB-1 and S100 calgranulins S100A8 and S100A12 in human tissues (Yao and Brownlee 2010).

1.7.4 RAGE Gene and Polymorphisms

The RAGE proto-oncogene is located on chromosome 6 in the class III region of the MHC, a gene-rich region containing many overlapping genes that are susceptible to splicing and polymorphisms. In particular, the RAGE glycine 82 serine polymorphism correlates with increased sRAGE in inflammation and breast cancer (Jang, Kim et al. 2007; Tesarova, Kalousova et al. 2007). Other polymorphisms are also associated with disease progression in gastric cancer, diabetes mellitus type II, diabetic retinopathy and cardiovascular problems in rheumatoid arthritis (RA)(Carroll, Frazer et al. 2007; Gao, Xu et al. 2007; Gu, Yang et al. 2008; Zhang, Chen et al. 2009).

1.8 AGE-RAGE axis in the pathogenesis of disease

AGE-RAGE signalling is known to induce numerous biological responses implicated in the development of disease, in particular chronic inflammation and metabolic dysfunction. The ability of AGEs to modulate the expression of their cognate transmembrane receptor is well characterized in a variety of tissues, notably in skin, kidney and lung endothelium where RAGE is constitutively expressed (Bierhaus, Illmer et al. 1997; Basta, Lazzerini et al. 2002; Ramasamy, Yan et al. 2005; Sun, Liang et al. 2009). Differential expression of RAGE transcript has also been reported in fibroblast, myometrium and breast tissues to name but a few (Schlueter, Hauke et al. 2003).

1.8.1 AGE and RAGE in Neurological Disorders

In addition to AGEs, RAGE has been identified as a receptor for amyloid Aβ peptides thus evidence is accruing for a potential role for RAGE in the pathogenesis of Alzheimer's disease (AD). RAGE positively correlates with Aβ protein and AGE accumulation in cerebral blood vessels, neurons and astrocytes, and is elevated in AD hippocampus and inferior frontal cortex in comparison to normal brain (Lue, Walker et al. 2009). Specifically, it is thought to increase trafficking of Aβ across the blood-brain-barrier resulting in β-amyloid oligomerization, neuronal plaque formation, synapse dysfunction and cell death (Chen, Walker et al. 2007; Origlia, Righi et al. 2008; Takeuchi and Yamagishi 2008). Plasma AGEs CML and pentosidine show a positive association with decreased cognitive impairment and may synergistically up-regulate neuronal p38 MAPK and NFκB with Aβ proteins via RAGE-induced ERK 1/2 MAPK activation (Southern, Williams et al. 2007; Origlia, Righi et al. 2008). Moreover, antibodies against the RAGE V and C_1 domain prevent Aβ–induced toxicity and ERK activation and apoptosis respectively suggesting that RAGE isoforms may differentially contribute to AD pathology (Sturchler, Galichet et al. 2008). In fact, administration of soluble RAGE appears to have a neuroprotective role acting as a decoy receptor for AGE/Aβ-RAGE mediated β-amyloidosis and is found at reduced levels in Alzheimer's disease (Emanuele, D'Angelo et al. 2005).

1.8.2 AGE-RAGE and Cardiovascular Disease

Cardiovascular disease (CVD) accounts for 50% of chronic kidney disease mortalities, with 75% of these cases resulting from coronary artery disease (Koyama and Nishizawa 2010). In oxidative stress or sites of localized

inflammation, the AGE-RAGE axis is up-regulated and increased plasma AGEs CML and pentosidine may contribute to cardiovascular complications (Yan, Ramasamy et al. 2009). AGE accumulation in vasculature may induce arterial stiffness and expansion of the extracellular matrix by extensive cross-linking with integral collagen and elastin fibres (Koyama and Nishizawa 2010). Furthermore, arteriole wall atherosclerotic plaque formation is a prominent feature of diabetic vasculature where AGEs and β-amyloid proteins accumulate thus increasing blood pressure and risk of myocardial infarction (Kilhovd, Juutilainen et al. 2005; Peppa and Raptis 2008; Koyama and Nishizawa 2010; Nin, Jorsal et al. 2011).

1.8.3 AGE-RAGE and Diabetes Mellitus Type II

Diabetes mellitus (DM) is a chronic disease principally characterised by persistent hyperglycaemia and insulin resistance. Its incidence is fast approaching worldwide epidemic with 220 million diabetics at the time of writing, and is expected to reach over 336 million by 2030 (WHO). In the UK, the number of diabetics is 4.3% of the overall population (Diabetes UK). It is diagnosed based on specific parameters: fasting and non-fasting plasma glucose levels and glycated haemoglobin AGE-HbA_1C (WHO). Early onset DMT1 arises from insulin production deficiency in pancreatic β-cells in the islets of Langerhans or loss of β-cells by idiopathic T-cell action. Polyuria, polydipsia, polyphagia and rapid eyesight deterioration are symptomatic of diabetes. Multiple studies have reported AGE-related macular degeneration and increased vascular permeability in diabetic retinal endothelial cells (Ishibashi 1998; Barile and Schmidt 2007; Sugiyama, Okuno et al. 2007; Glenn and Stitt 2009; Sheikpranbabu, Kalishwaralal et al. 2009). Late onset

DMT2 results from reduced insulin secretion and desensitisation and impairment of the insulin receptor (IR) to mediate cellular glucose uptake. Insulin resistance has been attributed to AGEs, acromegaly and hyperandrogenism-mediated dysfunction in insulin signalling pathways. AGE-RAGE signalling has been implicated in the development of diabetic nephropathy through the promotion of p38 phosphorylation, ERK 1/2 activation and production of growth factors and cytokines TNFα, TGF1β and IL-1β in the kidney (Adhikary 2004). Cytokine accumulation in diabetic glomeruli, serum and macrophage, parenchymal, fibroblast and endothelial cells has been linked to AGE-induced activation of the MAPK pathway in a multitude of studies (Daoud 2001; Hsu 2001; Yeh 2001; Adhikary 2004). Indeed, elevated p38 expression has been observed in diabetic human and murine kidney and correlated not only with renal hypofunction and fibrosis but also levels of glycated haemoglobin HbA_1c, a common serum AGE (Ulrich 2001; Adhikary 2004). Studies in endothelial cells (HUVECs) have demonstrated AGE-human serum albumin (AGE-HSA) up-regulation of pro-inflammatory cytokines IL-6 and 8 specifically through activation of p38, ERK 1/2, c-Jun protein kinases and NFκB (Liu, Zhao et al. 2009). Inhibition showed a requirement for involvement of all these pathways to activate NFκB target genes, however marked abrogation of cytokine transcripts were seen with blockage of phosphorylated p38 and NFκB suggesting that these are key players in mediating AGE-RAGE signalling (Liu, Zhao et al. 2009).

Table 1. Levels of Advanced Glycation End-products (AGE) and their receptor RAGE in normal and PCOS women

	Control Group (N=22)	PCOS Group (N=29)	P Value (Means ± SE)
Serum AGE (U/ml)	5·11 ± 0·16	9·81 ± 0·16	< 0·0001***
RAGE Expression (% +ve)	7·97 ± 2·61	30·91 ± 10·11	< 0·02*

Table 2. Levels of Advanced Glycation End-products (AGE) and oxidation products (AOPP) in healthy (HS) and diabetes mellitus (DM) subjects

	Diabetes Mellitus Type I (N=18)	Diabetes Mellitus Type II (N=34)	Healthy Subjects (N=24)
AGEs (AU)	$3.56\pm0.74\times10^{5}$**		$3.06\pm0.56\times10^{5}$
	$3.15\pm0.68\times10^{5}$	$3.78\pm0.68\times10^{5}$***#	
AGEs (AU/g)	$4.77\pm1.12\times10^{3}$*		$4.08\pm0.71\times10^{3}$
	$4.14\pm0.86\times10^{3}$	$5.11\pm1.25\times10^{3}$***#	
AOPP (µmol/l)	136.7±69.3***		79.80±23.72
	97.5±30.9*	157.5±75.2***#	

Means ± SD *** p<0.001, ** p<0.005, * p<0.05 vs. HS. # p<0.005 vs. DM Type I

Figure 1-5 Levels of serum AGEs in PCOS women and in diabetes mellitus compared to normal healthy subjects

Table 1 Fig. 1-5 (reproduced from Diamanti-Kandarakis, E et al 2005) shows that serum AGE and monocyte RAGE expression levels in PCOS women are higher than in normal women. Table 2 Fig. 1-5 (adapted from Kalousova, M et al 2002 *Physiol. Res.* 51:597-604) shows serum AGE levels are greater in diabetes mellitus when compared to normoglycaemic subjects and are highest in type II diabetes.

1.8.4 AGE-RAGE and Diabetic Renal Dysfunction

While insulin-related dysfunction in diabetes can be monitored, it cannot be cured. Long-term complications arising from the metabolic imbalance particularly exacerbate vascular dysfunction. Removal of endogenously formed AGEs through the filtration across basement membranes of kidney glomeruli is inefficient in diabetics. In the hyperglycaemic context, kidney is a primary target tissue for AGE accumulation (Wendt 2003), the most prevalent form being N^{ε}(carboxymethyl)lysine (CML) which is found at elevated levels in human renal micro vessels, mesangial matrix and glomerular basement membranes (Horie 1997; Schleicher 1997). Studies in streptozotocin-induced diabetic murine mesangial and glomerular cells exhibited increased vascular permeability to albumin, hyperglycaemia, increased expression of vascular

endothelial growth factor (VEGF) and activation of NFκB (Kumar 2001; Sheetz 2002). RAGE is highly expressed in podocytes (glomerular epithelium) and it has been strongly suggested that the AGE-RAGE axis is responsible for albuminuria, mesangial expansion, glomerular sclerosis and renal dysfunction. Not surprisingly, diabetes is the lead cause of end-stage renal failure (Ritz 1999; Wendt 2003; Wendt 2003).

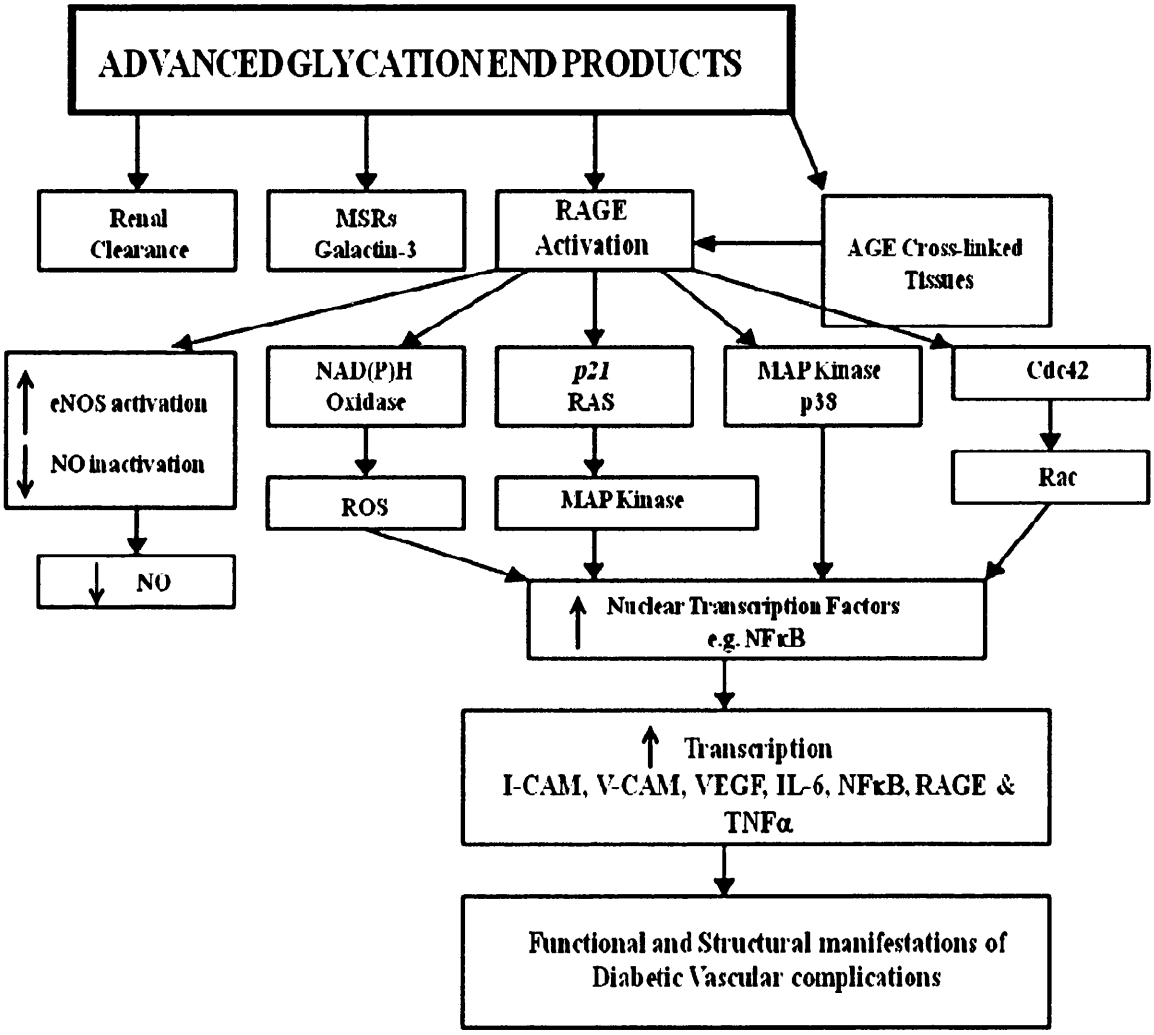

Figure 1-6 Involvement of the AGE-RAGE axis in the pathogenesis of diabetic vascular endothelial complications

Diagram adapted from Goh and Cooper (2008) *J Clin Endocrinol Metab* **93** (4): 1143-52. Flow diagram shows how AGE products are linked to the development of Diabetes and the prion diseases through the activation of ROS, MAP kinases, inflammatory cytokines and NFκB.

1.9 RAGE signalling in Inflammation and Cancer

RAGE mediates signal transduction for a broad repertoire of ligands promoting up-regulation of several pro-inflammatory cytokines, MAPKs and the oncogenic transcription factor NFκB in several cellular contexts. Evidence has accrued implicating RAGE in fuelling the initial stages of a pre-cancerous inflammatory state despite the fact that its immediate targets remain elusive (Riehl, Nemeth et al. 2009). To date, only two cytoplasmic binding partners have been shown to directly associate with the RAGE c-terminus; ERK, a member of the MAPK signalling pathway and Diaphanous-1 a RhoA effector, which stimulate release of Cdc42, Rac1, Src and TIF2 (Ishihara, Tsutsumi et al. 2003; Hudson, Kalea et al. 2008). RAGE may promote tumourigenesis through several means: 1) RAGE-mediated perpetuation of TNFα, IL-6, IL-1, TGFβ, EGF and extracellular ligand secretion, 2) RAGE-mediated up-regulation and *de novo* synthesis of NFκB-p65 and 3) recruitment of myeloid cells, leukocytes and lymphocytes to the site of inflammation (Riehl, Nemeth et al. 2009). Indeed, RAGE has been characterized in several malignancies namely breast, ovary, prostate, melanoma, lung, colon and pancreatic cancers and solid tumours over-expressing s100 calgranulins, HMGB1 and AGEs (Gebhardt, Nemeth et al. 2006; Ellerman, Brown et al. 2007; Logsdon, Fuentes et al. 2007; Abe and Yamagishi 2008). In the inflammatory milieu, RAGE competes with cell surface TLRs for mutual extracellular stimuli to synergistically regulate common MAPK signalling cascades that promote NFκB and Ap1 activation (van Beijnum, Buurman et al. 2008; Rojas, Figueroa et al. 2010) as shown in Fig. 1.9. Furthermore, the presence of NFκB-p65 sites on RAGE may facilitate a feed-forward loop whereby the expression of RAGE and NFκB target genes can be sustained (see Ch 4).

NCBI SEQUENCE for RAGE promoter: 1604 bp

```
1604  tacttacctc atacgcagct catcttaaac caatagaatc gctcggtgga cgagagtgtc
1544  tgactcagat atctacctcg gagggagttt ctgctacttt agggaattat tgactgggct
1484  ttggggttga actttttttt ttttaaagaa agaaaaagaa accctgggat ccatctgttt
1424  tttttgttgt tgttgttgtt tttgttgttg gtggtggtgg tggtggtggt ggttcttaat
1364  ttttaattta gtttggggaa gtagcttgtt tttttttta taaatatgtt gatttcttgt
1304  ctttttttt tatttcttac tttcccatat taggggtgat agccaaaggg gttctggtaa
1244  gagaaagggg gacaaacaga actggtaaag aggccccct ggctccaggc ctgtccatca
1184  ggaagtaaat tttacagggc accaagcttt gccccctaaa atcccttagg tgttctttgt
1124  tcatgcaggc aggtttctgc cgcatttgat gtggaggcag tgaagggctt gccctgctgg
1064  cctctcatcc cccttcttcc cacaaccctt gggcagggct ggactcagta attttgagga
1004  aattgaagat gccatcttcc cctgtgagtg acatgtcttt aatttttaa aaaactacta
 944  tttgaaaatt ggaggggggaa gaatgggaag ggagttattg ccaaatatgt taaatatggg
 884  ttggggtgct tgtatatgta tcttcctcaa tttccccata aatgaggtat ctttttgtca
 824  caccaaaatc aaggggtagg gagagggagg aggttgcaaa aagccagatg tgggggaaaa
 764  gtaacatcaa cactgtccca tcctcagccc tgaactagct accatctgat cccctcagac
 704  attctcagga ttttacaaga ctgtcagagt ggggaacccc tcccattaaa gatccgggca
 644  ggactgggga caggttggaa gtgtgatggg tgggggggtg ggaggcatgg gccgggggca
 584  gttctctcct cacttgtaaa cttgtgtagt ttcacagaaa aaaaacaaaa tgcagtttta
 524  aataaagaaa tttctttttt ccctgggttt agttgagaat ttttttcaaa aaacatgaga
 464  aaccccagaa aaaaaatgat tttctttcac gaagttccaa acaggtttct ctcctgttcc
 404  ccagccttgc cttcatgatg caggcccaat tgcacccttg cagacaacag tctggcctga
 344  accctattga tgcaactttg cgcaatcaag atggggctcc agtgggtcac caggcagccc
 284  tgatggactg atggaataaa taggatcggg ggctctgagg gaatgagacc ctagagggta
 224  cactccccat cccccaggga agtgactgta cccagaggct ggtagtaccc aggggtgggg
 164  tgataattat ttctctagta cctgaaggac tcttgtccca aaggcatgaa ttcctagcat
 104  tccctgtgac aagacgactg aaagatgggg gctggagaga gggtgcaggc cccacctagg
  44  gcggaggcca cagcagggag aggggcagac agagccagga ccct
```

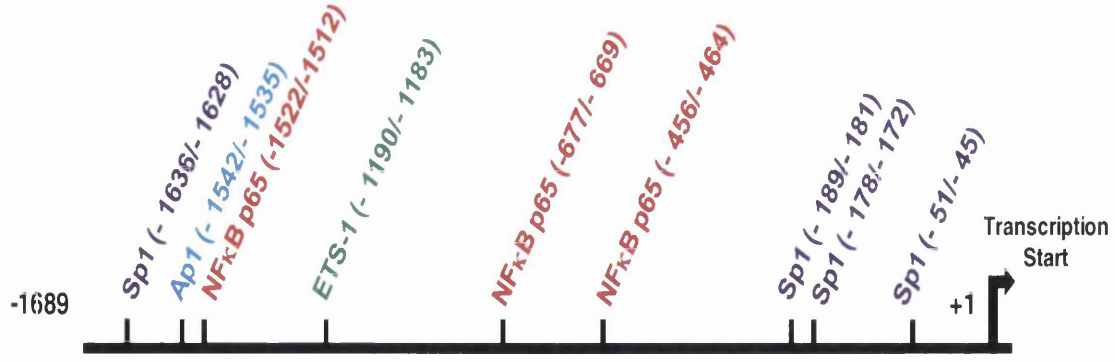

Figure 1-7 DNA sequence and schematic representation of the human RAGE promoter

Characterisation of the RAGE promoter has revealed the presence of multiple transcription factor binding sites for Nuclear Factor Kappa B (NFκB), Activated Protein-1 (Ap1), Specificity protein-1 (Sp1) and ETS-1 (Protein C-ets-1). The sites are colour-coded according to which transcriptional factor they bind. The exact positions of the sites are shown within the DNA promoter sequence to which the genomic primers were designed for qRT-PCR after ChIP. The NFκB site at - 456/ - 464 on the RAGE promoter was thought to be functionally inactive and does not bind p65 in endometrial epithelial Ishikawa or Heraklio cells.

1.10 Role of RAGE in Polycystic Ovary Syndrome

Soluble RAGE correlates with increased AGEs in the serum of PCOS women (Diamanti-Kandarakis, Piperi et al. 2005). The expression of the full-length membrane-tethered receptor has also been shown by IHC to be elevated in PCO ovarian granulosa and theca cells, and to co-localise with accumulated AGEs and NFκB (Diamanti-Kandarakis, Piperi et al. 2007). The aforementioned study showed NFκB-p65 expression was greater in PCO granulosa cells (Fig.1.8B) when compared to normal ovaries (Fig.1.8A) whereas no difference in p50 expression was observed. In poly-cystic ovaries, NFκB-p65 expression was primarily localised to the nucleus (Fig. 1.8C). It was therefore hypothesised that AGE-RAGE signalling could lead to the activation of p65 in PCO tissue and perhaps could be a mechanism involved in RAGE signalling in the endometrium (Diamanti-Kandarakis, Piperi et al. 2007).

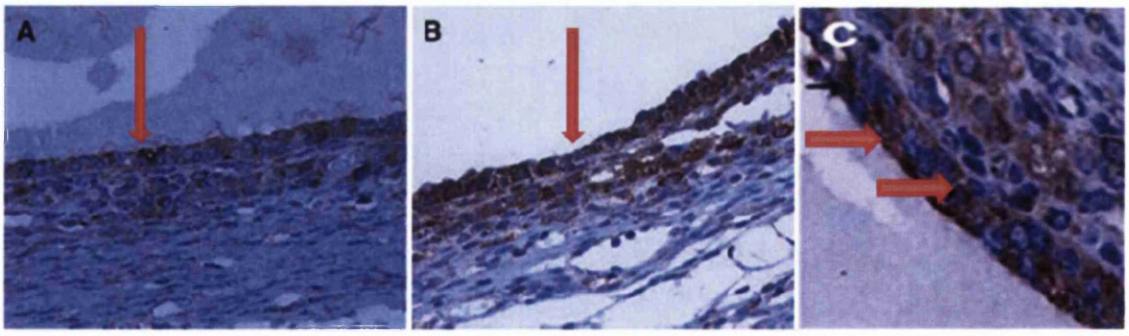

Localisation of p65 in Normal (A) and PCO (B) Ovaries. Nuclear localisation (C) Diamanti-Kandarakis E. et al 2007Histochem Cell Biol. (6):581-9

Figure 1-8 NFκB expression in polycystic (PCO) and normal ovaries

Immunohistochemistry shows that there is greater NFκB expression in the ovarian granulosa cells of PCO patients (B) than in normal ovaries (A). Strong staining for NFκB p65 was observed in the nucleus of PCO granulosa cells (arrowed, C).

1.10.1 Possible implications of the AGE-RAGE signalling pathway in the endometrium

Diabetic pregnancies are often at risk of hypertension-related complications in which the AGE-RAGE signalling axis has been implicated. Serum sRAGE levels fluctuate throughout physiological pregnancy, peaking in the second trimester in healthy women. Conversely, plasma sRAGE is significantly decreased in same stage pre-eclampsic pregnancy, women who underwent pre-term labour and in diabetics (Germanova, Koucky et al. 2009; Pertynska-Marczewska, Glowacka et al. 2009). In addition, plasma AGEs (HbA_1C), TNFα and IL-6 were elevated and sRAGE reduced during the diabetic third trimester with respect to third trimester euglycemic controls (Pertynska-Marczewska, Glowacka et al. 2009). AGEs, RAGE, ROS and NO-derivatives were also significantly elevated in full-term pre-eclampsic placenta (Chekir, Nakatsuka et al. 2006). Human trophoblasts isolated from aborted first trimester chorionic villi expressing RAGE, also exhibited increased MIP1α and MIP1β chemokine secretion, apoptosis and significantly decreased hCG production in response to AGEs (Konishi, Nakatsuka et al. 2004). Thus, AGE-RAGE signalling may inhibit trophoblastic invasion and/or placentation by altering the uterine immunological profile, increasing oxidative stress and perhaps disrupting the trophoblast hCG feedback signals for continued maintenance of the endometrium by progesterone.

1.11 Nuclear Factor Kappa B (NFκB) Pathway

NFκB is a eukaryotic transcription factor that is implicated in the pathogenesis of a multitude of diseases through the regulation of oncogene transcription. It therefore plays a prominent role in apoptotic pathways and the progression of cancer as well as the perpetuation of the inflammatory

response through activation of interleukins IL-1β, IL-2, 4, 6, 8, 10 and 12 and cytokine TNFα (Li, Schwabe et al. 2005; Tian, Nowak et al. 2005; Brasier 2006; Fitzgerald 2007; Liu, Zhao et al. 2009). Not surprisingly, NFκB signalling is vast, complex and exists in most cell types. NFκB exists in a homodimer or heterodimer of Rel/ NFκB proteins of which five have been identified; p65 (also known as Rel-A), Rel-B, p50 (also known as NFκB1), p52 and c-Rel (Nabel 1993). Interaction of NFκB with κB DNA binding motifs on target genes requires dimerization of these subunits, the combination of which may affect binding affinity with other transcription factors (Ch. 5 section 5.8). It is generally accepted that of these five proteins, only p65, Rel-B and c-Rel participate in gene transcription for they possess c-terminal transactivation domains. However, studies have also shown p50 is capable of gene activation when it is partnered with p65 as a heterodimer (Li and Verma 2002). Consequently, studies have primarily focused on the p65/p50 protein subunits that are sequestered in the cytoplasm bound to an inhibitor protein IκB which is itself a dimerized complex of subunits; IκBα and IκBβ. Under the influence of exogenous stimulants, activated MAPK proteins can phosphorylate IκB inducing a conformational change that results in the release of dimerized Rel subunits, most commonly the p65/p50 heterodimer into the cytoplasm (Tian 2003; Gilmore 2006; Perkins 2007). Subsequent nuclear translocation of NFκB to initiate target gene transcription has been demonstrated in neural and diabetic kidney endothelium, breast cancer and polycystic ovary tissue (Lindsey, Caughman et al. 2000; Diamanti-Kandarakis, Piperi et al. 2007; Panzer, Steinmetz et al. 2009; Tse, Zhu et al. 2010) where AGEs are proposed to be accountable for this NFκB activation.

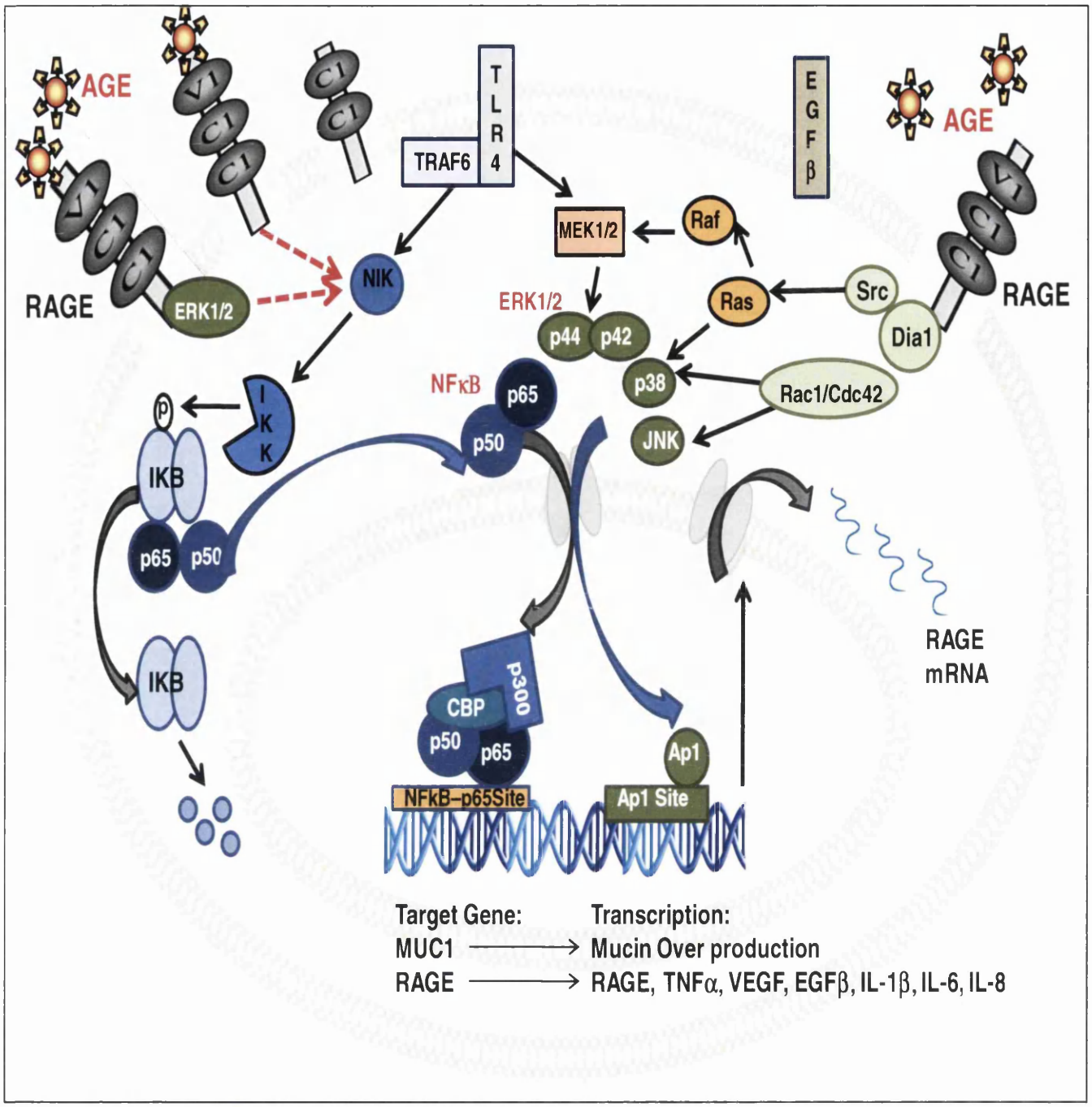

Figure 1-9 Cartoon of the potential pathways involved in AGE-RAGE-mediated NFκB transactivation.

Indicated in Fig. 1.9 are the signalling events mediated by the TLRs which are likely to show convergence with RAGE downstream signal transduction. There are two main molecules associated with the c-terminal end of RAGE; Diaphanous-1 and ERK 1/2 which can activate several members of the rac and ras proteins to phosphorylate the MAP kinases. In turn, the MAP kinases initiate NFκB dimer dissociation from the cytoplasmic inhibitor protein IκB and allow for nuclear translocation. Subsequently, transcriptional machinery such as p300, CBP and Ap1 proteins are recruited to the

promoters of NFκB target genes (Fig. 1.9). NFκB is an oncogenic transcription factor that up-regulates a plethora of inflammatory and angiogenic growth factors and cytokines (TNFα, TGFs and interleukins), some of which are cyclically elevated throughout the menstrual cycle or play a role in placental development. In disorders where RAGE is over-expressed such as PCOS and Diabetes, RAGE may also represent a molecular 'switch' for a pre-cancerous mechanism that amplifies inflammation. In fact, uterine proliferation, natural killer and leukocyte immune cell invasion and neovascularisation in the menstrual cycle proliferative phase are analogous with the initial stages of endometrial tumourigenesis.

1.12 Estrogen Receptor (ER) Pathway

1.12.1 ER Isoforms

The estrogen receptors are nuclear transcription factor receptors that mediate the intracellular steroidal activity of 17β estradiol (E2). The estrogen receptor, encoded by the ESR1 gene (6q25.1) and later known as ERα, was first sequenced in 1986 by Walter and Greene in a study investigating androgen regulated genes (Walter, Green et al. 1985; Greene, Gilna et al. 1986). However, identification of a second ER encoded by the ESR2 gene (14q23.2) a decade later, lead to the renaming of the subtypes ERα (66kDa) and ERβ (56kDa) (Kuiper, Enmark et al. 1996; Mosselman, Polman et al. 1996). Since then, spliced variants of the ER subtypes, termed estrogen related receptors (ERRs) have been discovered. Namely, two ERα isoforms of 36 and 46kDa and five ERβ variants, some of which may be biologically active when co-expressed and dimerized with the full-length receptor (Moore, McKee et al. 1998; Shi, Dong et al. 2009). Despite extensive documentation of the presence of ER splice variants in breast and endometrium, little is known about the regulatory behaviour of these truncated proteins in pathogenesis of disease (Jazaeri, Shupnik et al. 1999; Fasco, Keyomarsi et al. 2000; Herynk and Fuqua 2004; Witek, Paul-Samojedny et al. 2007).

Briefly, the ERs comprise of five functional domains for transactivation, DNA binding (DBD), anchorage, ligand binding (LBD) and agonist/antagonist recognition (Fig. 1.10). Despite a slight variation in size, 595 and 530 amino acids respectively, ERα and ERβ form homodimers (αα or ββ) or heterodimers (αβ) and equally activate gene transcription due to a high degree of sequence homology (96%) in their DBD (Hall, Couse et al. 2001; Nilsson, Makela et al. 2001; Fox 2008). However, some studies have indicated heterodimers appear to emulate ERα-ERα function and affinity for classical estrogen response elements which was greater than ERβ-ERβ (Scobie, Macpherson et al. 2002; Li, Huang et al. 2004). ERα and ERβ display distinct regulatory activity from each other in different cellular contexts. The popular consensus is that the respective affinities of ERα and ERβ for, and the bioavailability of, a select faction of co-regulatory proteins contribute to this differential response (Shang, Hu et al. 2000; Shah and Rowan 2005; Romano, Adriaens et al. 2010).

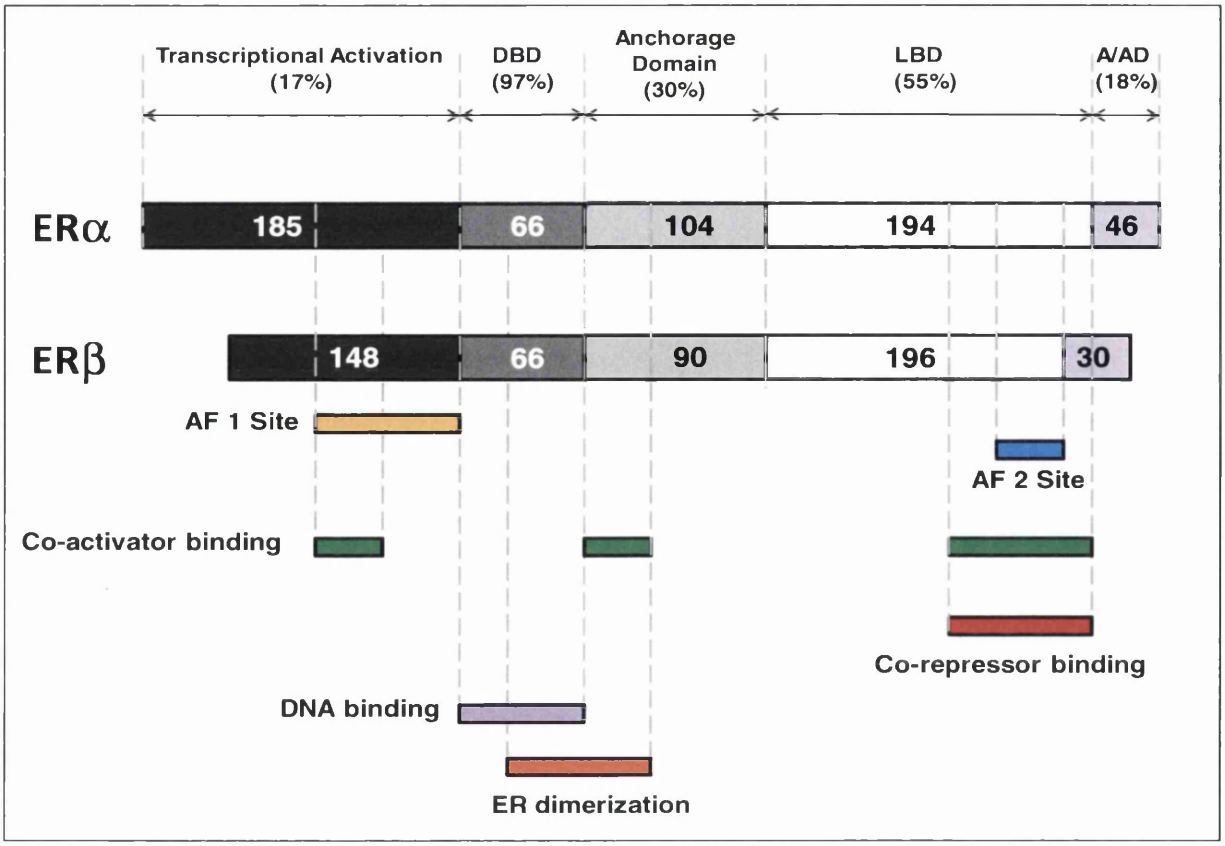

Figure 1-10 Schematic diagram comparing the protein structure of the estrogen receptor subtypes α and β

Indicated are the positions of the AF 1/2 domains, % sequence homology, amino acid length and the areas important for dimerization, DNA binding and coactivator/repressor recruitment.

1.12.2 Classical and Non-Classical ER Signalling

Classically, as with most steroid receptors upon ligation, ER is released from chaperone HSPs enabling it to dimerize for nuclear translocation and occupy promoter-specific estrogen responsive elements (EREs) of target genes (Klinge 2001). In order to evoke tissue, cell and even gene-specific transcription, ER recruits additional co-regulators, the most studied of which are the steroid receptor family of p160 coactivators. These transcription factors are documented in the literature under various acronyms as follows: SRC-1 (Nuclear coactivator-1 (NcoA-1) [Gal-steroid receptor coactivator 1], SRC-2 (Nuclear coactivator-2 (NcoA-2) [glucocorticoid receptor interacting

protein 1(GRIP)/transcriptional intermediary factor-2 (TIF-2)] and SRC-3 (activator of the thyroid and retinoic acid receptor (ACTR) [amplified in breast cancer-1(AIB1)/receptor associated coactivator-3 (RAC-3)] (Shah and Rowan 2005). These co-regulatory proteins mediate transcription by modifying chromatin structure by the recruitment of histone acetylases and deacetylases. However many genes, of which RAGE is one, display estrogen responsiveness in the absence of classical promoter estrogen responsive elements and are targeted by way of ER protein-protein interaction. Several studies have shown the involvement of the activating protein (Ap1) and specificity protein (Sp1) transcription factor complexes at alternative non-consensus sites (Paech, Webb et al. 1997; Saville, Wormke et al. 2000) . The Ap1 transcription factor unit comprises of dimerized basic leucine zipper proteins c-Fos and c-Jun that interact with DNA via base pair hydrogen bonding to its consensus sequence in the DNA major groove (Glover and Harrison 1995; Hess, Angel et al. 2004). Similarly, Sp1 also interacts with DNA in the major groove through binding its consensus sequence 5'-(G/T)GGGCGG(G/A)(G/A)(C/T)-3 which is recognised by the triple Cys_2His_2 zinc finger tandem motif in its structure (Nagaoka, Kondo et al. 2002).

1.13 Mechanisms of ER modulation in Uterus

It is widely accepted that ligand-ER binding induces conformational changes that facilitate its differential AF domain activation and subsequent regulation by co-regulatory partners. Ligand-independent and -dependent AF domains are located on ER at the opposite terminal ends yet can act both cooperatively and independently to activate gene transcription (Klinge 2001; Fox 2008). Several studies have observed that E2 constitutively activates and recruits the SRC-1 and SRC-3 coactivators to the AF-2 domain, whereas

agonist action of TX is solely thought to be facilitated by the recruitment of the shared coactivator SRC-1 to AF-1 as shown in Fig. 1.10 (Glaros, Atanaskova et al. 2006). In fact, the AF-1 domain is critical for TX agonistic potency in the endometrium (Sakamoto, Eguchi et al. 2002; Scafonas, Reszka et al. 2008). Conversely, TX acts antagonistically on ER by actively competing with E2 for the LBD and promoting NcoR and SMRT corepressor occupancy of the AF-2 domain (Tremblay, Tremblay et al. 1999; Pendaries, Darblade et al. 2002).

Several potential mechanisms have been implicated in driving ER agonism within the human endometrium. It is thought that ER activation requires phosphorylation at the N-terminal serine residues 118 and 167, as mutation of serine 118 to alanine significantly reduced ER transcriptional activity and SRC-1 association (Kato, Endoh et al. 1995; Castano, Vorojeikina et al. 1997). Indeed, rapid phosphorylation of ERα at these serine residues by c-Src kinase was shown to correlate with increased SRC-1 activity and E2-induced ERα binding to ERE-luciferase constructs in Ishikawa and HEC1A endometrial cells (Shah and Rowan 2005; Acconcia, Barnes et al. 2006). These studies also illustrated that Src kinase-activated AKT kinase was essential for stabilizing ERα-ERE interaction on endometrial gene promoters and specifically activated SRC-1 and cAMP response element binding protein (CREB) transcription and not SRC-2 or SRC-3 (Shah and Rowan 2005). E2 or TX agonist action on this c-Src complex can activate ER responsive mitotic genes, actin cytoskeleton remodelling and dissolution of cell-cell anchorage thus promoting cell motility (Acconcia, Barnes et al. 2006). Tamoxifen may evoke agonistic/antagonistic action on E2-mediated signalling in the uterus by either aiding or inhibiting ERα interaction with the SRC-1 co-activator (Shah and Rowan 2005; Daverey 2009). Interestingly, Ishikawa cells over-

express SRC-1 in comparison to MCF-7 cells, whereas the latter expresses greater NcoR, suggesting differences in TX agonistic/antagonistic potential in breast and uterus could be due to the relative availability of these co-regulatory proteins (Sakamoto, Eguchi et al. 2002).

Altered ER coactivator/corepressor expression and/or recruitment have been implicated in cancer. Comparison of normal versus malignant phenotype endometrium revealed up-regulation of several coactivator/repressor proteins; SRC1, SRC2, SRC-3, NcoR and SMRT, in particular SRC-3 was significantly elevated in atypical hyperplasia and adenocarcinoma (Kershah, Desouki et al. 2004; Shah and Rowan 2005; Balmer, Richer et al. 2006). It is thought that E2 and TX are agonists of both ER subtypes and bind to each receptor with equal affinity in non-malignant and cancerous endometrial cells (Barsalou, Gao et al. 1998; Castro-Rivera and Safe 1998; Sakamoto, Eguchi et al. 2002; Blauer, Heinonen et al. 2008; Gielen, Santegoets et al. 2008). Investigations in non-malignant pre- and postmenopausal endometrium revealed that 10nM E2 and 40nM TX both induced ERα-mediated glandular epithelial proliferation to a greater extent in postmenopausal endometrium (Punyadeera 2008). Additionally, in co-culture models of pre-menopausal endometrium mimicking *in vivo* paracrine epithelial-stromal interaction, 10nM E2 increased cell proliferation whereas TX had no proliferative effect and retained its antagonism of ER (Blauer, Heinonen et al. 2008). In endometrial HEC1A, breast MCF-7 and cervical HeLa cells varying the E2 concentration affected ER subtype activation which may contribute to cell-specific selective estrogen receptor modulator activity. In particular, both ERs were responsive to saturation with 100nM E2, however only ERα was active at the physiological sub-saturating 10nM dose (Hall 1999; Hall and Korach 2002).

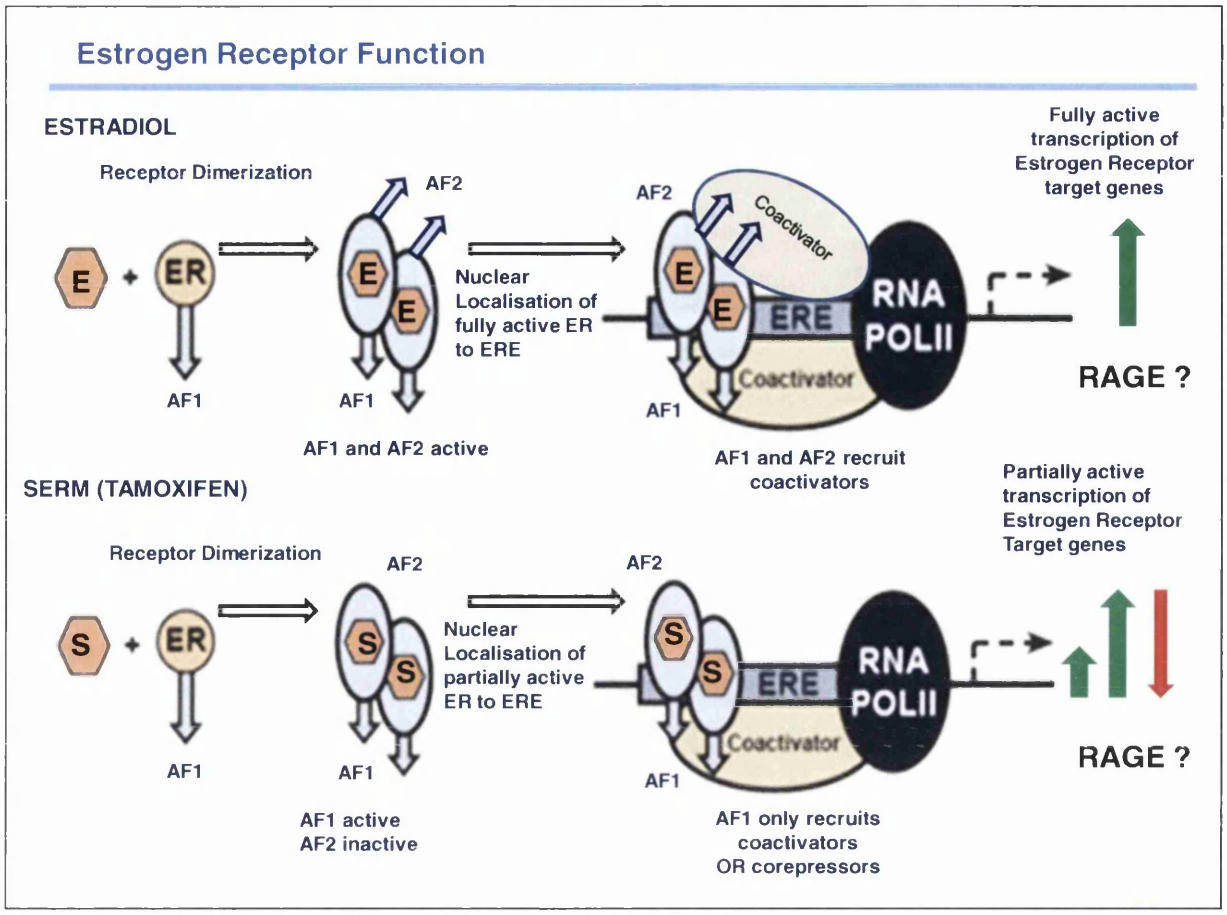

Figure 1-11 Mechanisms of E2 and Selective Estrogen Receptor Modulator action on ER signalling.

Figure 1.11 shows the known mode of action for both E2 and antagonistic SERMs on the estrogen receptor. However, the effects of the selective estrogen receptor modulator Tamoxifen on transcriptional outcome are both cell-type and gene specific. Depending on the cellular context, Tamoxifen can either act as an antagonist (repressor) of gene transcription (red arrow), a partial agonist (short green arrow) or a full agonist (activator) of gene transcription (green arrow). The uterus is an estrogen-regulated tissue and therefore it is likely that most genes will be turned on (green arrow) following E2 stimulation.

Activation of one or both AF domains and differential recruitment of transcription factors may account for the cell-specific differences in ER signalling. Studies in endothelial cells have demonstrated that non-consensus Sp1 sites on RAGE are responsive to 17α-ethinylestradiol (EE), an ERα-selective estrogen commonly found in the oral contraceptive, and E2, a natural circulating plasma estrogen, stimulation (Barkhem 1998; Tanaka,

Yonekura et al. 2000; Mukherjee, Reynolds et al. 2005). It is also likely that E2 will have an agonistic effect on RAGE in the uterus. Based on recent findings, the general consensus is that TX exhibits both antagonistic and estrogenic-like behaviour in the uterus which may be dependent on estradiol concentration.

1.13.1 Selective Estrogen Receptor Modulators (SERMs)

Selective estrogen receptor modulators or SERMs define a class of non-steroidal synthetic compounds initially designed to antagonise the cellular effects of estrogen through competitive ligation of ER. Later, it became evident that selective estrogen receptor modulators exhibit differential agonistic/antagonistic tissue-specific effects adding to the complexity of selective estrogen receptor modulator modality (Bentrem 2001). Of the clinically relevant selective estrogen receptor modulatorss, the active tamoxifen metabolite 4-hydroxytamoxifen (TX) and raloxifene (RX) are the best characterised (Dardes, Schafer et al. 2002; O'Regan, Gajdos et al. 2002; Miki, Suzuki et al. 2009). 4-hydroxytamoxifen (TX) is best known for its anti-estrogenic properties in breast tissue where it actively competes with 17β estradiol (E2) to ligand ER. Its subsequent mode of action in breast is to induce a conformational change that discriminates against E2-recruited coactivators at the AF-2 site yet promotes ER association with NcoR and SMRT corepressor proteins (Glaros, Atanaskova et al. 2006). It is for this reason that TX has long been exploited as an adjuvant therapy for ER positive breast cancers and after five consecutive years, has been shown to reduce the risk of disease return most likely through the perturbation of cancer cell growth (Gielen, Santegoets et al. 2008). Similarly, agonism of

estrogenic activity in bone makes Raloxifene (RX) beneficial for the treatment of post-menopausal osteoporosis which is characterized by reduced bone mineral density in estrogen depleted tissues (Miki, Suzuki et al. 2009). Conversely, 4-hydroxytamoxifen is an agonist in the uterus, particularly in post-menopausal endometrium (Wilder, Shajahan et al. 2004). Studies have attributed a single point mutation of the amino acid aspartate 351 on ERα to induce conformational changes that promote TX agonist action. Selective estrogen receptor modulators TX and GW5638 both possess carboxylic acid side chains but unlike GW5638, the side chains of TX may interact with this aspartate residue rather than repel it perhaps making ERα more accessible to co-activator recruitment (Dardes, O'Regan et al. 2002). Current research has thus recognised the need to develop clinically relevant selective estrogen receptor modulatorss of proven antagonist behaviour in breast that do not elicit an agonistic response in the uterus as, over time or with repeat exposure, tamoxifen therapy appears to lose its antagonistic potential (Dardes, O'Regan et al. 2002). Alternative therapies to tamoxifen with fewer agonistic effects are currently being explored for clinical use. To date, synthetic tamoxifen derivatives EM800 and GW5638, raloxifene and aromatase inhibitors have been shown to possess only anti-estrogenic properties in murine mammary gland, uterus and human Ishikawa cells (Dardes, O'Regan et al. 2002; Farnell 2003).

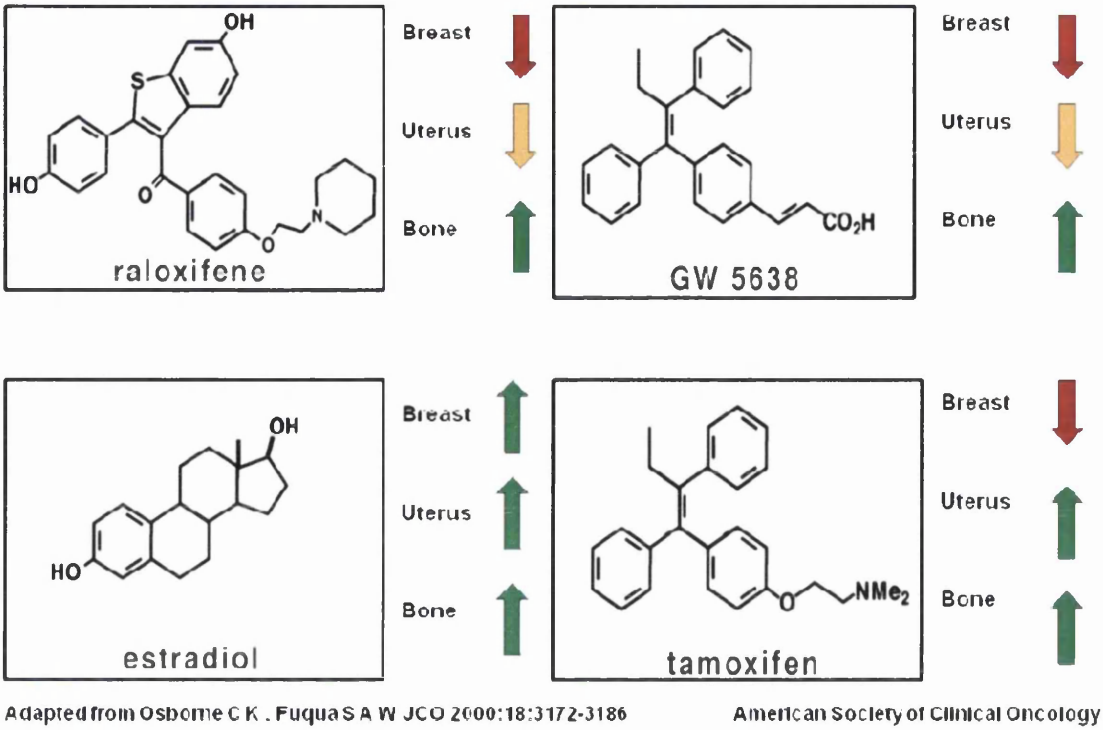

Figure 1-12 Chemical structures of 17β estradiol (E2) and selective estrogen receptor modulators (SERMs).

Figure 1.12 Chemical structures of 17β estradiol (E2), selective estrogen receptor modulators and their respective agonist (green), antagonist (red) and partial agonist/antagonist (orange) effects in breast, uterus and bone models. Tamoxifen: first generation triphenylethylene selective estrogen receptor modulator that metabolises to form 4-hydroxytamoxifen (TX) in the cell. GW5638: triphenylethylene tamoxifen derivative that metabolises to form active GW7604 in the cell and possesses a unique carboxylic acid side chain. E2: natural circulating estrogen, authentic ligand of ER. Raloxifene: second generation benzothiophene selective estrogen receptor modulator.

1.14 Tamoxifen Agonism in Uterus

Studies in Ishikawa cells have revealed that 10nM E2 and 1μM 4-hydroxytamoxifen induces ERα-mediated cell proliferation, Ap1 and ERE luciferase reporter gene activity and agonism of VEGF expression. Interestingly, TX lacked agonist potential in ERα positive ECC-1 endometrial cancer cells yet failed to down-regulate genes involved in endometrial proliferation such as EGFR which may provide a mechanism for progression towards TX resistance (Dardes, Schafer et al. 2002). Development of

endometrial polyps and hyperplasic pathology in tamoxifen-treated breast cancer patients is reported to be as high as 36% (Gielen, Santegoets et al. 2008). In fact, one study showed that TX agonism in endometrial cells was comparable to the endometrial effects of two breast cancer drugs; levormeloxifene and idoxifene, withdrawn from clinical use due to increased incidences of endometrial proliferation and polyps (Scafonas, Reszka et al. 2008). Numerous studies have reported post-menopausal endometrium to have a 2-7% elevated risk of developing endometrial cancer when compared to pre-menopausal women (Blauer, Heinonen et al. 2008). This has been evidenced by increases in cell proliferation markers such as Ki67, mitotic genes and the nuclear receptors themselves (Blauer, Heinonen et al. 2008). Interestingly, experiments in ERα knockout and ERα mutant mice showed that E2- and TX-induced hyperplasia, nuclear expansion and proliferation of endometrial lumen and glands was specifically mediated through ERα (O'Brien 2006). Uterine weight increase is thought to be mediated by ERα signalling at non classical elements on candidate proliferative genes such as Cyclin-D2 which undergoes nuclear translocation post E2 and TX challenge in endometrial luminal epithelium (O'Brien 2006). These effects appear to be both TX and ERα specific as Raloxifene (RX) has no effect on endometrial proliferation due to a greater affinity to bind to ERβ, which in the endometrium can repress ERα function by 25% (Hall 1999).

1.15 Research Aims

The principal aim of this thesis is to present novel evidence for the expression of RAGE in human fertile and infertile eutopic endometrium and to relate these observations to key features of common reproductive endocrinological maladies namely PCOS and endometriosis. Secondary to this, was to establish *in vitro* models in which to study the impact of agents clinically relevant to PCO and endometriosis pathology on the expression of endometrial RAGE. In order to explore the endometrial effects of AGEs and 17β estradiol known to modulate RAGE in other cellular contexts, a series of *in vitro* stimulation experiments for mRNA and protein analyses were conducted in the model endometrial cell lines. Finally, this thesis endeavoured to elucidate the possible mechanisms behind the regulation of endometrial RAGE by AGEs, E2 and its antagonist 4-hydroxytamoxifen. In order to achieve this, ChIP experiments were employed to identify the presence of candidate transcription factors NFκB and ER on the RAGE promoter. The work undertaken in this thesis is relevant to the aetiology of the PCOS and endometriosis infertility disorders which are characterised by elevated AGEs and estrogens respectively among other metabolic aberrations. Given the extensive body of evidence within the literature implicating RAGE in propagating chronic inflammatory signalling, this project aimed to establish a link between PCO and endometriotic pathology and a RAGE-altered uterine environment. Recent evidence has implicated RAGE in underlying inflammation preceding tumourigenesis. Consequently, RAGE may prove to be an effective therapeutic target to ameliorate the inflammatory complications in PCO and endometriosis patients and reduce the incidence of endometrial malignancy.

CHAPTER 2

Materials and Methods

2. Methods and Materials

2.1 Collection of Primary Cells

Endometrial tissue was isolated by way of endometrial biopsy taken from women admitted as outpatients to the Gynaecology Infertility and London Women's IVF clinics at Singleton Hospital, Swansea. In the majority of cases endometrial tissue was extracted using the Pipelle catheter in a standard outpatient clinic procedure. In other cases or upon patient request, endometrial samples were obtained in theatre under general anaesthetic by way of dilatation and curettage (D&C). This technique uses a metal cannula, a rod-like instrument serrated at one end, attached to a syringe. This method applies a suction force to remove a small section of the endometrium cut away by the cannula (Oehler and Rees 2003). There were a number of reasons as to why women were referred to the clinic including laparoscopy as a sterilisation procedure or for diagnostic purposes to determine endometriosis, ovarian cysts, pelvic inflammation or disease. Endometrial biopsy specimens are usually required to investigate causes contributing to menorrhagia and abnormal intermenstrual vaginal bleeding or for women who have displayed a thicker than normal endometrium (>5mm) upon routine trans-vaginal ultrasound investigations (Nutis, Garcia et al. 2008). Collection of all primary tissues was subject to ethical approval from the Abertawe Bro Morgannwg University Trust Hospital Research and Ethics committee (LREC nr. 05/WMW02/45). Patients recruited to the study were asked for their formal written consent. Biopsies were grouped into four categories according to pathology:

1. Control Group: Fertile Patients
2. Study Group: Infertile Endometriosis
3. Study Group: Infertile PCOS
4. Study Group: Unexplained Infertility

Endometrial tissues taken from patients classified as fertile were from women with proven parity and were attended theatre for sterilisation or surgery for reasons not relating to fertility. These biopsies were taken from women with a natural menstrual cycle ranging from 28-35 days. Cases of nulliparity due to a failure to conceive after two consecutive years, where male infertility and known reproductive, ovarian and tubal dysfunction were not considered causative, were classified as having 'unexplained infertility' (UIF). Endometriosis samples were taken from infertile women who continued to ovulate regularly and showed no signs of tubal dysfunction, yet presented with eutopic endometriosis of varying disease severity. PCOS endometrium was obtained from both ovulatory and anovulatory infertile women diagnosed according to the 2003 Rotterdam group criterion. Women with PCOS present with a variety of symptoms, however according to the criteria to be considered to have the syndrome, these patient would have two of the following indications: chronic anovulation/menorrhagia/oligomenorrhea, excess free androgens (FAI) and/or the presence of pearl-like ovarian cysts. Women with sexually transmitted diseases, endometrial hyperplasia, endometrial carcinoma and polyps were excluded for the RAGE IHC and RT-PCR study and those selected were matched for age and BMI.

2.1.1 Culture of Primary Cells

Biopsy material was collected in Dulbecco's Modified Eagle Medium: Nutrient Mixture F-12 (DMEM/F-12) supplemented with 10% Foetal Bovine Serum (FBS), 1% glutamine 1.5mM, sodium bicarbonate 1mM, sodium pyruvate 1mM and 1% antibiotic-antimycotic solution containing 10,000 µg penicillin, 10,000 µg streptomycin, 25 µg of amphotericin B/ml utilizing penicillin G (sodium salt), streptomycin sulfate, and amphotericin B as Fungizone® Antimycotic in 0.85% saline (Gibco-Invitrogen). DMEM/F12 media has been specifically formulated for the growth of human diploid cells and primary cultures which require lower calcium content (1.05M) to counterbalance the high calcium concentration within the FBS supplement. This protects against the toxic influx of calcium which can occur when cell membranes become damaged from oxidative and enzymatic processes during sub-culture[1]. Endometrial tissue was washed twice in calcium and magnesium free PBS (Lonza-BioWhittaker, Verviers, Belgium), sliced by scalpel (Swann-Morton Limited, Owlerton Green, Sheffield. UK) to a size of $1mm^2$ before enzymatic digestion in 10mL DMEM/F-12 cell media supplemented with 250µl collagenase type A (000.9g collagenase powder in 1mL filter sterilised PBS) and 250µl deoxyribonuclease type 1 (Sigma-Aldrich Company Ltd, Dorset, United Kingdom). Tissues were incubated for 1h at 37°C in a 5% CO_2 humidified incubator. Digested samples were centrifuged for 5 min at <1200g, resuspended in 10mL supplemented DMEM/F-12 as described above and left in culture overnight. Epithelial cells were separated from stromal and fibroblast cells through differential plating after 24h. All cell culture reagents were purchased from Gibco-Invitrogen (Invitrogen Ltd, 3 Fountain Drive, Inchinnan Business Park, Paisley, United Kingdom) unless stated otherwise.

[1] http://www.sigmaaldrich.com/life-science/cell-culture/learning-center/media-expert/calcium.html

2.2 Introduction to Endometrial Cell Lines

HEC-1 cells were originally isolated in 1968 by H. Kuramoto and colleagues from the well differentiated endometrial adenocarcinoma of a 72 year old Japanese patient. The tumour was described as a stage 1A tumour, meaning that, at the time of its removal, it had been restricted to the epithelial endometrial layer and metastases to the myometrium or cervix had not yet occurred (Kuramoto, Tamura et al. 1972). Despite originating from the same stage tumour, HEC-1A and its sub-strain HEC-1B exhibit morphological, karyotypic and functional differences. Unlike HEC-1A, HEC-1B cells display a stationary growth period whilst in culture and this causes changes to its cell morphology from a raised to a flattened shape with a distinct pavement pattern in later passages (Kuramoto 1972). HEC1A cells are diploid with a modal chromosome number of 49 whereas the HEC1B subline has a near tetraploid karyotype (Satyaswaroop, Fleming et al. 1978). The HEC-1 cells also differ in the expression of their nuclear receptors (NRs) for estrogen (ER) and progesterone (PR). HEC-1A, described as an ER positive cell line, expresses both the alpha and beta isoforms of the estrogen and progesterone receptors (Navo, Smith et al. 2008). HEC-1B is considered to be an ER negative cell line as it doesn't express the ER alpha isoform or the progesterone (PR)A receptor. It does however, express the ER beta isoform which is expressed throughout the menstrual cycle at constant levels (Guseva, Dessus-Babus et al. 2005; Bombail, MacPherson et al. 2008; Francis, Lewis et al. 2009). These cells provide us with arguable *in vitro* model systems in which to investigate sex steroid regulation in the

epithelium. Ishikawa is a well characterised epithelial cancer cell line developed from the endometrial adenocarcinoma of a 39 year old patient of Asian ethnicity (Nishida, Kasahara et al. 1985). It has been used extensively as a model for the epithelial endometrium and expresses both ER and PR. Heraklio, also an epithelial endometrial adenocarcinoma-derived cell line and sub-strain of Ishikawa, functions as an ERα and PRα negative cell line. The HEC-1 cell lines were purchased from the American Type Culture Collection (ATCC) and Ishikawa and Heraklio were purchased from the European Collection of Cell Cultures (ECCAC) for use in this study.

2.2.1 Culture of Cell Lines

Adherent Ishikawa, Heraklio and HEC-1A cells were cultured in plastic culture vessels (Falcon T25, 75, 125) in Dulbecco's Modified Eagle Medium: Nutrient Mixture F-12 (DMEM/F-12) supplemented with 10% Foetal Bovine Serum (FBS), glutamine 1.5mM, sodium bicarbonate 1mM, sodium pyruvate 1mM and 1% antibiotic-antimycotic solution at 37°C in a 5% CO_2 humidified incubator. HEC-1B cells were cultured in Basal Medium Eagle (BME) with 1.5mM glutamine and Earle's Balanced Salt Solution (BSS) adjusted to contain sodium bicarbonate 1.5mM, sodium pyruvate 1mM and 0.1mM non-essential amino acids (NEAA). The cells were sub-cultured as follows (according to guidelines given by the ATCC and ECCAC): Ishikawa was sub-cultured 1:5 (sub-confluent 70-80%), Heraklio sub-cultured 1:8 (sub-confluent 70-80%), HEC-1A sub-cultured 1:8 when confluent (90-100%) and HEC-1B sub-cultured also when confluent (90-100%) and the cell pellet split no greater than 1:6. Phosphate Buffered Saline or PBS (Lonza-BioWhittaker) free of calcium and magnesium was used to wash the cell monolayer to maintain pH, osmotic balance and to promote cell detachment. Proteins

involved in cell attachment such as integrins and cadherins require calcium and magnesium for adhesion. The wash with PBS therefore, primarily serves to remove traces of DMEM/F12 growth media containing calcium, magnesium and bovine pancreatic trypsin inhibitor (BPTI) found in FBS which can inhibit the action of trypsin (Borjigin and Nathans 1993). Cells were removed from the culture substrate by incubation <5 min at 37°C with 0.25% Trypsin 1mM EDTA (pH 8) in Hanks' Balanced Salt Solution (HBSS) containing phenol red and without $CaCl_2$, $MgCl_2$, and $MgSO_4$ (Gibco Invitrogen Cat No: 25200-056). Cell detachment was confirmed by use of inverted light microscope. Trypsin was neutralised with 10mL supplemented DMEM/F12 media. Cell culture solution was aspirated from culture vessel and transferred to sterile 15mL centrifuge tubes (Corning) for centrifugation for 5 min at 1200g. Cell pellets were resuspended in 10mL supplemented DMEM/F12 cell media and re-incubated at 37°C in a limited 5% CO_2 atmosphere. All tissue culture reagents were sourced from Gibco-Invitrogen unless stated otherwise.

2.3 Preparation of Cell Treatments

2.3.1 Advanced Glycation End Products (AGE)

Commercial bovine glycated albumin (AGE-BSA) stock at 10mg/mL was used in the generation of preliminary data (Cat: JM-2221-10 Caltag-Medsystems). Commercially available lyophilised human glycated albumin (AGE-HGA) 25mg was restored in 2.5mL of distilled water for a stock of 10mg/mL, aliquoted and stored at -20°C (Cat: A8301-25MG SIGMA). Non-glycated human serum albumin (HA) 99% essentially fatty acid free (100mg) was used as negative control after being restored in 10mLs distilled water (10mg/mL stock) and frozen at -20°C (Cat: A3782-100MG SIGMA).

2.3.2 17β Estradiol (E2) and 4-hydroxytamoxifen (TX)

Powdered17β Estradiol 0.2724g (Cat: E8875 >98% SIGMA) was added to 10mL of absolute ethanol (Fisher-Scientific) and filter-sterilised using a 0.2mm filter cap and 10mL syringe (BD Plastipak) to a concentration of 1mM, 100μL of 1mM stock was then added to 10mL ethanol to give a final stock of 1μM. Powdered 4-hydroxytamoxifen 0.3715g (Cat: T5648 >99% SIGMA) was added to 10mL absolute 100% ethanol, filter-sterilised using filter cap and syringe. 100μL of the 1mM stock was then added to 10mL of absolute ethanol to give a final stock of 1μM. All stocks were aliquoted and stored at -20°C for long-term storage in 2mL glass vials with aluminium-lined lids (SIGMA) to prevent leaching of the hormone.

2.4 Treatments of Cell Lines for RNA and Protein Analysis

Prior to being seeded, cell pellets were resuspended in 10mL culture medium. The number of cells in 1mL was counted using a glass slide haemocytometer designed so that the number of cells in one 16 corner square grid is equivalent to the number of counted cells x 10^{-4}/mL media^2. Counts were made on 4 separate grids on the haemocytometer and an average cell count calculated. The cell suspension was adjusted to a total cell number of 4-6 x 10^8 with addition of the appropriate volume of media and seeded into 6-well (vol. 9.6 cm²) plates (Greiner Bio-One Ltd, Stroudwater Business Park, UK). Ishikawa and Heraklio were seeded in 200μL aliquots containing 9.2 x 10^4 cells, allowed to adhere to plastic substrate for 3 min before 1.8mL DMEM/F-12 (10% FBS) was added. HEC-1A was seeded in 300μL aliquots containing 9.2 x 10^4 cells, allowed to attach before 1.7mL

DMEM/F-12 (10% FBS) media was added. HEC-1B was seeded in 600µL aliquots per well containing 2.7 x 10^5 cells, left to adhere for 3 min and supplemented with 1.4mL BME 10% FBS. Cells were maintained at 37°C in a humidified 5% CO_2 atmosphere. Prior to treatment and at cellular confluence, cells were serum-starved for 24h to make the cells quiescent to potential steroidal and growth factor influence. In brief, Ishikawa and Heraklio were cultured in DMEM/F-12 reduced glucose (5mM) media formulated by combining F12 nutrient mixture with DMEM without D-glucose. No further adjustment was required to the working concentration of glucose (5.5mM) in BME media for the culture of HEC1B cells. The level of 5-5.5mM glucose that these media contain equates to the level of corporal blood sugar[3], thus creating an authentic reflection of the *in vivo* state, in which preformed AGEs may exist (Tuttle, Johnson et al. 2005). HEC1A cells however became unhealthy, granulated and exhibited stunted growth rate in reduced-glucose DMEM/F12 media, only retaining structural integrity in 10mM glucose DMEM/F12. During exposure to experimental conditions FBS was substituted for 10% dextran-coated charcoal-treated foetal bovine serum (DCC-FBS, Gibco).[2]www.abcam.com/ps/pdf/protocols/haemocytometer_cell_counts.pdf

[3]http://www.sigmaaldrich.com/life-science/cell-culture/learning-center/media-expert/glucose.html.

Human glycated albumin (AGE-HSA) and human albumin (HSA) were added to cells maintained in 6 well culture plates for 4 or 24h at the following concentrations:

Treatment	[Stock]	Dilution	[Final] in 2mL Media
AGE-HSA	10mg/mL	1:100	100µg/mL
		1:200	50µg/mL
		1:400	25µg/mL
		1:1000	10µg/mL
		1:2000	5µg/mL
HSA	10mg/mL	1:200	50µg/mL
		1:1000	10µg/mL

Estradiol (E2) and Tamoxifen (TX) were added to cells maintained in 6 well culture plates for 4h at the following concentrations:

Treatment	[Stock]	Dilution	Final Concentration	Treatment (µL in 2mL Media)
E2	1µM	1:100	10nM (10^{-8} M)	20
TX	1µM	1:100	10nM (10^{-8} M)	20

Media from control cultures were aspirated and replaced with 2mL fresh culture media supplemented with 10% dextran-coated charcoal-treated foetal bovine serum (DCC-FBS) and left untreated without vehicle. After incubation time, each cell medium was aspirated and monolayer washed twice with 10mL Dulbecco's Phosphate-Buffered Saline (Lonza BioWhittaker) without calcium and magnesium for all adherent cell types. For RNA analysis, cells were collected in appropriate volumes of buffer RLT (Qiagen) for direct cell lysis of cells grown in a monolayer according to the culture dish diameter: 300µl for a plate or well with a diameter less than 6cm or 600µl for a dish or well with a diameter between 6-10cm. Cell lysates were collected with rubber policeman scrappers (Greiner) and stored at -20°C. For protein analysis: cells were collected in appropriate volumes of RIPA buffer (SIGMA) according to culture dish size: 200µl per well (6 well plate) or 1mL per 1-5 x 10^7 cells. Cells

were incubated in RIPA buffer on ice or at 4°C for 5 min prior to collection with rubber policeman then stored at -20°C. For immediate use, lysates were centrifuged 8,000g (12,000 rpm) at 4°C for 10 min and protein aggregates removed from the supernatant. If the samples were to be used for immunoblotting of a phosphorylated protein, RIPA buffer was substituted for phosphosafe buffer (EMD Biosciences, San Diego, CA, USA) which contains four phosphatase inhibitors; sodium fluoride, sodium vanadate, β glycerophosphate and sodium pyrophosphate to help preserve the integrity of the protein.

2.4.1 Treatments of Cell Lines for Chromatin Immunoprecipitation

Cell lines were adjusted to a total cell number of 4-6 x 10^8 and seeded (approximately 1.5 x 10^7 cells when 80-90% confluent) in 14cm diameter sterile cell culture dishes with lid and vent (Cat: 157150 NUNC). Prior to treatment, cells were serum-starved for 24h as previously described, in media substituted with 10% dextran-coated charcoal-treated foetal bovine serum (DCC-FBS, Gibco-Invitrogen). Cells were maintained at 37°C in a humidified 5% CO_2 atmosphere. Treatments Estradiol (E2), Tamoxifen (TX), Human Glycated Albumin (HGA) and Human Albumin (HA) were added to the cells for 4h at the following concentrations:

Treatment	[Stock]	Dilution	Final Concentration	Treatment (μL in 25mL Media)
E2	1μM	1:100	10nM (10^{-8} M)	250
TX	1μM	1:100	10nM (10^{-8} M)	250
HGA	10mg/mL	1:1000	10μg/mL	25
HA	10mg/mL	1:1000	10μg/mL	25

Cell media was aspirated after the 4h incubation time and the monolayer washed with 10mL DPBS without calcium and magnesium (Lonza

BioWhittaker). Cells grown in confluent monolayer in 14cm culture dishes were fixed with 20mL serum free culture media supplemented with 0.54mL 37% formaldehyde to give a final concentration of 2.5M (Cat No. F8775, SIGMA), and placed on a rotary agitator at room temperature for 10 min. Fixative was aspirated and cells neutralised for 5 min in 5mL Glycine Stop-Fix Solution: 4mL 1.25M (10X) Glycine (Active Motif Europe), 36mL distilled MilliQ water (Millipore). The cell monolayer was washed with ice-cold 1X PBS (Lonza BioWhittaker) between incubation steps to prevent carry-over of fixative/buffer. Cells were scraped with rubber policemen in 5mL ice-cold 1X PBS supplemented with 5µL phenylmethanesulfonylfluoride (serine protein inhibitor PMSF, 100mM), centrifuged 10 min at 5,000g at 4°C and supernatant discarded. The cell pellet was either used immediately for ChIP or frozen at -80°C with 5µL PMSF and 5µL Proteinase Inhibitor Cocktail (PIC, supplied in ChIP-IT Express kit, Active Motif, Europe) to prevent degradation and crystallisation of cells on freezing.

2.5 Isolation and Quantification of RNA

Total RNA was isolated from confluent monolayers scrapped in RLT buffer according to the manufacturer's protocol for Total RNA Isolation from Animal Tissues (see Appendix A). In brief, cell lysates were homogenised in Qiashredder spin columns, RNA isolated and purified on-column using an RNeasy-Plus Mini Kit including gDNA Eliminator spin columns for the removal of genomic DNA. The membrane in the RNeasy spin column binds RNAs longer than 200 nucleotides in order to isolate mRNA. In cases of high cell yield (>1 x 10^7 cells), RNeasy Mini Kit with integrated on-column DNase 1 digestion step was used instead to prevent overloading of gDNA Eliminator spin columns and co-purification of DNA/RNA. RNA was eluted in 30µL of

RNase-free water into 1.5mL collection tubes (supplied in kit) and quantified by spectrophotometer (Nanodrop ND-1000 - Nucleic Acid program v3 1.2).

2.6 Isolation and Quantification of Protein

Protein was quantified using the Bradford assay. In brief, 1mL ready to use Bradford reagent (Cat No: B6916, SIGMA) was added to 100µL sample diluted 1:100 in 0.15M sodium chloride (0.438g NaCl to 50ml of ddH_2O) in a 1mL cuvette (Fisher Scientific), inverted to mix and incubated for 5 min at room temperature. The Brilliant Blue G dye in the Bradford Reagent works by forming complexes with the proteins present and changing the optical density, determined using a Beckman DU 650 spectrophotometer, from λ 465nm to λ 595nm to be proportional to the amount of protein. The absorbance was quantified against the optical densities of a BSA (0.5mg/mL) standard curve of known concentrations ranging from 0-20mg/mL (see table).

Standard	BSA (µL)	NaCl 0.15M (µL)	[Final] mg/mL
A	0	100	0.0
B	5	95	0.025
C	10	90	0.05
D	15	85	0.075
E	20	80	0.1

2.7 Reverse Transcription (RT) Synthesis of RNA to cDNA

RNA (12µL total volume) was adjusted to a concentration of 100µg/mL in RNase-free water (Qiagen) and 2µL reserved for PCR negative control (un-transcribed template). Next, 2µL random decamers at 50µM (RETROscript, Ambion, UK) were added to the remaining 10 µL RNA in thin-walled 0.2mL PCR tubes (Corning). The samples were briefly spun and heated for 3 min at 85°C in a thermo cycler (i-cycler Bio-Rad) to allow for heat denaturation of the RNA. The remaining components (RETROscript, Ambion, UK) were added per sample: 2µL 10X RT buffer (500 mM Tris-HCl, pH 8.3, 750mM KCl, 30

mM $MgCl^2$, 50mM DTT), 4µL dNTP Mix containing 2.5mM of each dNTP, 1µL RNase Inhibitor (10 units/µL) and 1µL Reverse Transcriptase MMLV enzyme (100 units/µL) to a final volume of 20µL. Samples were heated for 1h at 44°C to allow for cDNA synthesis, followed by 10min at 92°C then held at 4°C until removed from the machine. cDNA was stored at -20°C or for long-term storage -80°C. Serial dilutions were made from cDNA stock in distilled MilliQ water (Millipore) at 1:5, 1:10, 1:100 and 1:1000 to be used for standard curve calibration plots. cDNA 1:10 was used as the working template for analysing target gene expression.

2.8 Quantitative Real Time Polymerase Chain Reaction (Q-RT-PCR)

RT-PCR was used to amplify cDNA using gene specific primers (Beacon Design 2.0, Premier Biosoft, USA; Primer Express v3.0 Applied Biosystems, USA) to a PCR product of approximately 75-150bp. Ribosomal Protein 60S L19 (RPL-19) was used as an internal reference (amplicon 144bp), and genomic DNA, RNase-free water (Qiagen) and RNA 1:10 template were used as positive and negative controls respectively. PCR reactions were made to a total volume of 20µL with 10µL of Power Sybr Green Master Mix containing iTaq polymerase (Applied Biosystems), 5µL of primer mix containing 2.5µL sense primer and 2.5µL anti-sense primer at 4µM, and 5µL of sample 1:10 cDNA. RT-PCR reactions were performed in triplicate per sample in clear 96 well optical reaction plates (Sartedf Aktelangesellachaft & Co.) sealed in optical tape (Bio-Rad) and run in the MyIQ5 i-cycler (Bio-Rad). Plates were heated for 95°C for 15 minutes to initiate the iTaq DNA polymerase enzyme that requires a hot start and Real Time (RT) data collected during 50 cycles comprising of 94°C for 15 sec, 30 sec at optimum annealing temperature for

specific primer sets and 72°C for 30 sec to allow for primer extension. Next, 1 cycle annealing step for 30 sec at 55°C and 1 cycle denaturation step for 30 sec at 95°C. Melt curve data was collected after 43 cycles of 15 sec at 53°C, increasing the set point in 1°C increments to an end-point temperature of 95°C. No products were amplified when using negative control RNA or distilled water directly in the PCR reactions.

2.8.1 Detection of PCR products using Real-Time

Quantitative Real-Time PCR allows for quantification of a specific starting amount of complementary DNA. Following binding to double stranded DNA, Sybr Green I dye produces a fluorescent emission at λ521nm. The intensity of the signal is measured per cycle and increases with the extension of the PCR product by gene specific primers. The amplification of the PCR product is displayed as a sigmoidal amplification curve when fluorescence, measured in relative fluorescence units (RFU), is plotted against the number of cycles. The threshold cycle represents the number of PCR cycles the exponential doubling of the DNA template has reached to be detected. Threshold cycle values (Ct) for each sample were generated from the amplification curve in the analysis software where the amplification is proportional to the fluorescent signal. The Ct value is the cycle at which the amplification curve intercepts the baseline threshold and is used to calculate the starting amount of DNA in the PCR reaction. The baseline threshold is automatically set by the software at the level of the earliest detectable signal where there is no product amplification, usually a few cycles before the earliest signal crosses the threshold. Fluorescence detected beneath the baseline threshold represents noise e.g. non-specific signal from inefficient binding of Sybr Green, contamination or primer-dimer artefacts. It can also be manually set at

the up-turn of the curve at the beginning of the log-linear phase of amplification (Qiagen 2010).

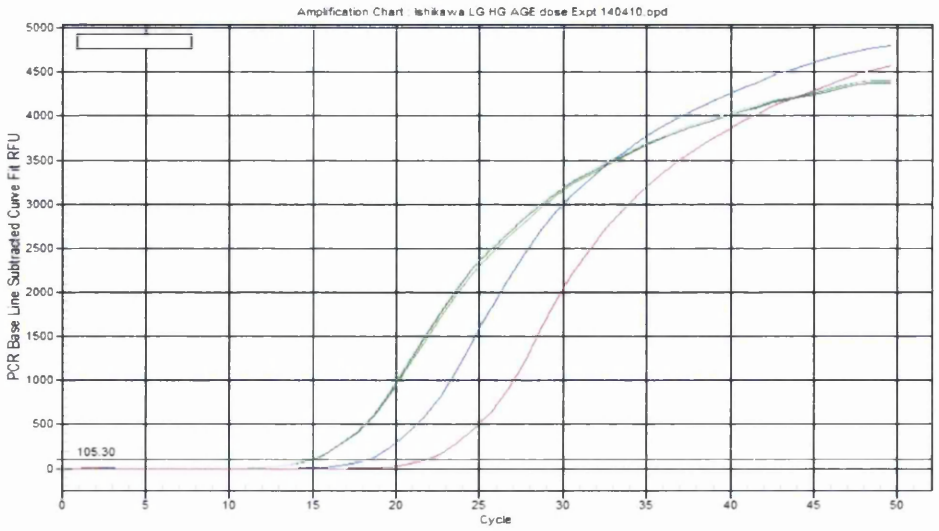

Figure 2-1 Amplification plot of an Ishikawa cDNA standard curve

Figure 2.1 shows amplification plot of an Ishikawa cDNA standard curve crossing the baseline and demonstrating the threshold cycle (Ct) for each dilution.

Melt curves for each primer pair were checked for a single peak at the correct inflection for the specific amplicon that would indicate the absence of contamination, primer dimers or the product resulting from an incorrectly annealed primer.

2.8.2 Generation of a Standard Curve

Serial dilutions from $2x10^{-1}$ to $1x10^{-3}$ of 5µL reference cDNA were performed in triplicate on the 96 well plates starting at the highest concentration in the first row to the lowest concentration in the fourth row. Next, 15µL of Master Mix containing 10µL Power Sybr Green with iTaq polymerase and 5µL specific primer at 4µM were added to each well for a total sample volume of 20µL. Serial dilutions were made for every gene evaluated in the experiment to generate a calibration curve against which Ct values for that gene could be plotted to quantify expression. Standard curves were generated by plotting a

graph of the Log Starting Quantity (StQ) of each standard against its Ct value. The trend line function, equation for the gradient and Y-axis intercept were applied to the graph. The R^2 efficiency of the calibration curve was checked for a strong correlation (between 0.95 and 1.00) and alignment of dilution standards with the gradient of the graph between -3.3 and -3.8. If the PCR is 100% efficient (R^2 =1.00) then the slope of the standard curve -3.322 which shows the PCR product is doubled with each cycle (Qiagen 2010).

Well	Fluor	Type	Replicate #	Threshold Cycle (Ct)	Ct Mean	Ct Std. Dev	Starting Quantity (SQ)	Log Starting Quantity
B02	SYBR1	Std	2	12.99	12.98	0.039	1.000E-01	-1.000
B03	SYBR1	Std	2	13.01	12.98	0.039	1.000E-01	-1.000
B04	SYBR1	Std	2	12.93	12.98	0.039	1.000E-01	-1.000
B05	SYBR1	Std	3	16.34	16.34	N/A	1.000E-02	-2.000
B06	SYBR1	Std	4	19.81	19.81	N/A	1.000E-03	-3.000

Figure 2-2 Threshold cycle (Ct) and Log StQ values of Ishikawa samples

Figure 2.2 shows the threshold cycle (Ct) values and Log StQ values of the above Ishikawa samples used to make a standard curve for RPL19.

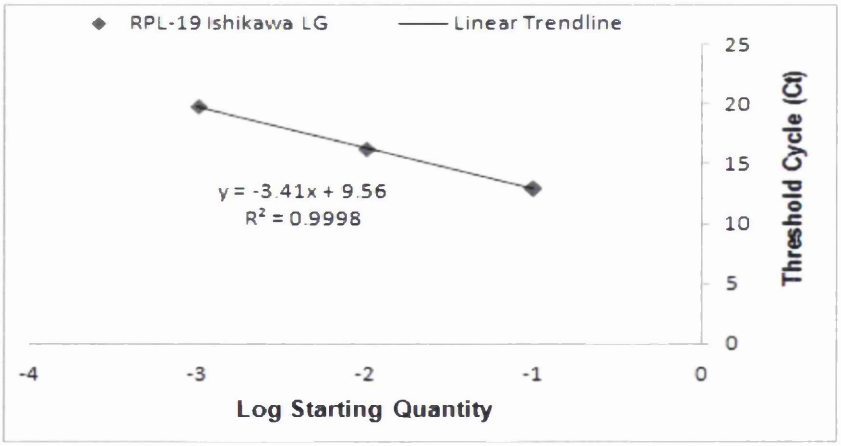

Figure 2-3 Standard curve of the above Ishikawa samples for RPL-19

Figure 2.3 shows the standard curve of the above Ishikawa samples for the RPL-19 gene (Fig. 2.2). The equation can be used to quantify the starting amount of RPL19 in each sample.

2.8.3 Analysis of Quantitative Real-Time PCR Results

Relative quantification of gene expression data was determined from triplicate Ct values for each sample. Triplicate Ct values were copy-pasted into Excel worksheets as raw data. If necessary, one outlying Ct value per sample in triplicate was excluded from the analysis and the average Ct value calculated. Samples were quantified from the average Ct value and the known concentrations of the dilution series. The Log Starting Quantity for each sample was calculated using the equation of the curve:

$$Y = (X - Z)/- M$$

Where Y = Log Starting Quantity
X = Average Ct value
M = Slope of the Standard curve
Z = Curve Intercept on Y axis

The starting quantity for each sample is calculated by using the Power (10, Y) function in Excel, where Y is the Log Starting Quantity. The average starting quantity of the target gene was normalized against the average starting quantity value obtained for the endogenous reference gene RPL-19. Gene expression was calculated as a ratio of transcript levels between untreated (control) and treated samples (fold expression). Standard deviation, to show the statistical significance of the results, was calculated from the starting quantities of the individual Ct values.

Primers for RT-PCR were designed using the Beacon Designer software v2.0 from NCBI gene sequences and were purchased from Sigma-Aldrich as custom made oligos. Upon arrival, the appropriate volume of RNase/DNase-free water was added to reconstitute the lyophilised primer to a starting stock concentration of 100μM. RT-PCR primers were stored at -20°C until use.

2.8.4 Primers used for Real-Time PCR

Name	Primer	Primer Sequence	Tm	Position in Seq.	Amplicon
GAPDH	sense	GTCCACTGGCGTCTTCAC	54.5	291	Tm = 90.5 Ta = 54.7 145bp
	antisense	CTTGAGGCTGTTGTCATACTTC	54.6	435	
RPL-19	sense	CCTGTGACGGTCCATTC	50.5	160	Tm = 91 Ta = 54.3 144bp
	antisense	AATCCTCATTCTCCTCATCC	50.8	303	
RAGE	sense	CAGTGTGGCTCGTGTCCTTC	58	219	Tm =89.2 Ta = 54.8 108bp
	antisense	GTCTCCTTTCCATTCCTGTTCATTG	58.2	326	
Mucin-1	sense	TGGTGCTGGTCTGTGTTCTG	57.1	545	Tm = 89.8 Ta = 55 134bp
	antisense	CTCGCTCATAGGATGGTAGGT	57.5	678	
ER alpha	sense	CCTCATCCTCTCCCACATCAG	56.5	1524	Tm = 88 Ta = 53.5 115bp
	antisense	GGCGTCCAGCATCTCCAG	56.6	1638	
ER beta	sense	TGCTGAACGCCGTGACCGATG	63.1	1286	Tm = 86.4 Ta = 54.2 73bp
	antisense	ATGGATTGCTGCTGGGAGGAGA	62.5	1358	
p65	sense	TCAAGATCAATGGCTACAC	49.0	182	Tm = 93.5 Ta= 55.1 235bp
	antisense	TTGTTGTTGGTCTGGATG	48.7	416	

Figure 2-4 Table of primers used for real time PCR

2.8.5 Statistical Analysis of Real Time PCR

Triplicate normalised starting quantity (StQ) values per sample were analysed using a two-tailed students T-Test. Treated samples were compared against the untreated controls where P value <0.05 was considered statistically significant. Real time data for endometrial biopsies: Mean normalised StQ values per sample were grouped according to pathology. For each pathology data set the Anderson-Darling normality test was performed. Non-parametric Kruskall-Wallace and Mann-Whitney tests for

categorical data were performed using the MiniTab software to compare inter-individual variability within, and inter-pathology variability between groups. P value <0.05 for the Mann-Whitney test was considered statistically significant.

2.9 Western Blotting

2.9.1 SDS-PAGE

Polyacrylamide gels (10%) were prepared for SDS-PAGE as described below, adding polymerizing catalyst 10% ammonium persulphate (APS) last to polymerise the gel matrix in a reaction with TEMED. Gels were set between 1.5mm separated glass plates (Bio-Rad). 2mL 70% water-saturated butanol (Fisher Scientific) was used to create a flat interface between resolving and stacking gels and to prevent dehydration of the resolving gel whilst setting. Butanol was removed with distilled MilliQ water (Millipore) and filter paper (Whattman).

Gel Reagent	Resolving Gel (10%)	Stacking Gel (4%)
MilliQ Distilled Water (Millipore)	6mL	3mL
30% Acrylamide/Bis Solution 37.5:1 (Bio-Rad)	5mL	650µL
1.5M Tris, pH 8.8	3.75mL	-
1.0M Tris, pH 6.8	-	1.25mL
10% SDS (Fisher Scientific)	150µL	50µL
10% APS (SIGMA)	75µL	25µL
TEMED (GIBCO)	15µL	5µL

Protein samples (30µg) were quantified as previously described (section 2.6) and diluted 1:2 in 2x concentrated Lamelli buffer in preparation for SDS-PAGE. Samples were incubated for 5 min at 95°C in a heat block to solubilise, denature and apply a negative charge to the protein structure. Equal amounts of protein (30µg) were loaded per well plus 9µL of Dual Colour Protein Standards (Bio-Rad) and run on a 10% SDS-polyacrylamide gel in ice-cold 1% SDS electrophoresis buffer for 1.5 h at 120 V or until dye-

front reached base of gel. To make 1 litre 5% electrophoresis buffer pH 8.3 - Tris Base 15.1g, Glycine 72.g, Sodium Dodecyl Sulphate (SDS) 5.0g in 1000mL distilled water. Buffers were tested for correct pH before use.

Blotting Reagent	1X Transfer Buffer (1.5L)	5X Tris-Buffered Saline TBS (1L)
Sodium Chloride (SIGMA)	-	40g
Distilled Water	1200mL	1000mL
Tris Base (SIGMA)	3.63g	12.1g
Glycine (Fisher Scientific)	16.8g	-
Ethanol (Fisher Scientific)	300mL	-

PVDF membrane with 0.2μM pore size and protein binding capacity of 150-160 $\mu g/cm^2$ (Bio-Rad) was cut to size and activated at room temperature in the following a) Absolute methanol (Fisher Scientific) 15 sec b) distilled MilliQ water (Millipore) 5 min and allowed to equilibrate in c) Transfer buffer 10 min. Separated proteins were transferred by electrophoresis onto activated PVDF membrane in ice-cold transfer buffer for 70 min at 100 V. Membranes were blocked overnight at 4°C in 10mL 10% milk in 1X TBS-Tween-20 solution (TTBS, 200mL 5X TBS, 800mL MilliQ distilled water, 10mL Bio-Rad 10% Tween-20) or for antibodies not compatible with milk protein, 10% BSA in 1X TTBS. Membranes were placed at room temperature on a rotary agitator and washed five times for 5 min in 1X TTBS. Membranes were cut according to molecular weight of protein of interest (RAGE 46KDa, ERα 66KDa, and ERβ 56KDa) and to allow incubation of membrane in a control antibody for normalisation (GAPDH 37KDa). Membranes were incubated at 4°C for 2h with rabbit anti-RAGE polyclonal antibody (H300 sc: 5563) diluted 1:500 in 0.5% milk-TTBS or rabbit anti-GAPDH polyclonal antibody (FL-335 sc: 25778) diluted 1:1000 in 0.5% milk-TTBS (Santa Cruz). Immunoblots for ERα were incubated at 4°C for 1h with rabbit anti-ERα polyclonal antibody (HC-20

sc: 543) diluted 1:1000 in 0.5% milk-TTBS. Immunoblots for ERβ were incubated overnight at 4°C with goat anti-ERβ diluted 1:500 (L20 sc: 6822). Phospho-NFκB-p65 (ser276) antibody (Cell Signalling #3037) was incubated in 0.5% BSA-TTBS (Sigma) as a substitute for milk that contains natural phosphotases. Membranes were then washed several times with 1X TTBS. The blots were incubated at room temperature on a rotary agitator for 1h with either goat anti-rabbit or donkey anti-goat horseradish peroxide (HRP) linked secondary antibodies (Amersham GE Healthcare) diluted 1:1000 in 0.5% milk-TTBS. Membranes were washed five times for 5 min in 1X TTBS to reduce non-specific binding. All antibodies were sourced from Santa Cruz biotechnology unless stated otherwise. Protein was visualized after 2-3 min incubation at room temperature in enhanced chemiluminescence solution (Western C, Bio-Rad) and detected on the ChemiDoc System Bio-Rad Imager (Bio-Rad). Protein band intensity was quantified using the volume rectangle tool function on the Quantity One® imaging software (Bio-Rad). This allowed the signal of each band to be contained within equal defined boundaries and be adjusted against the background level of non-specific binding. The signal for the protein of interest per sample, expressed as a function of volume data (intensity/mm^2) was then normalised to the signal of the house-keeping protein.

2.10 Chromatin Immunoprecipitation (ChIP)

Cells were collected as previously described (section 2.4.1) and ChIP performed using ChIP-IT Express kits (Active Motif, Europe). Cell pellets were thawed (if necessary), resuspended in 1mL ice-cold Lysis Buffer supplemented with 5μL Proteinase Inhibitor Cocktail (PIC) and 5μL serine

protein inhibitor PMSF (100mM) and incubated on ice 30 min. Cells were transferred to a 1.7mL tube and centrifuged at 10,000g for 10 min at 4°C to pellet nuclei. The supernatant was discarded and pellet was resuspended in 350µL of Shearing Buffer and placed on ice. DNA was sheared to 200-350bp under previously optimised conditions (see Appendix B1) using a hand-held probe sonicator (Vibracell VC 130, Sonics) or water tank sonicator (Bioruptor, Diagenode). The sonicated chromatin was centrifuged at 4°C at 18,000g for 10 min and the supernatant containing sheared DNA was transferred to a 1.7mL Eppendorf tube, stored at -80°C for long term storage or used immediately for ChIP. Before freezing, 50µL sheared chromatin was removed for a DNA clean-up step to assess DNA concentration and chromatin shearing efficiency prior to gel analysis (see Appendix B2). Following DNA clean-up, 16µL sheared chromatin (7-25µg) was added to 4µL 6X loading dye (Bio-Rad) and loaded in two different volumes (5µL and 10µL) to a 1% TAE agarose (SIGMA) gel to prevent over- or under-loading. Gels were run at 100 V for 1 h until loading dye reached ¾ of the gel length. Optimal shearing should result in a smear at 200-1000bp on the gel. Efficiency of DNA shearing was visualised on the gel using the Chemidoc (Bio-Rad) imager.

For immunoprecipitation (IP), ChIP reactions were set up in 8-well 0.2mL PCR strips (SIGMA) as follows, adding the ChIP-validated antibody last: 25µL Protein G Magnetic Beads, 10µL ChIP Buffer 1, 1µL PIC, Sheared Chromatin approx. 7µg (20-60µL), 10µL of 0.2µg/mL specific antibody and MilliQ distilled water (Millipore) to total volume of 100µL. The volume of chromatin per reaction was dependant on DNA quantification (see Appendix B2), and standardised between samples to contain 5µg.

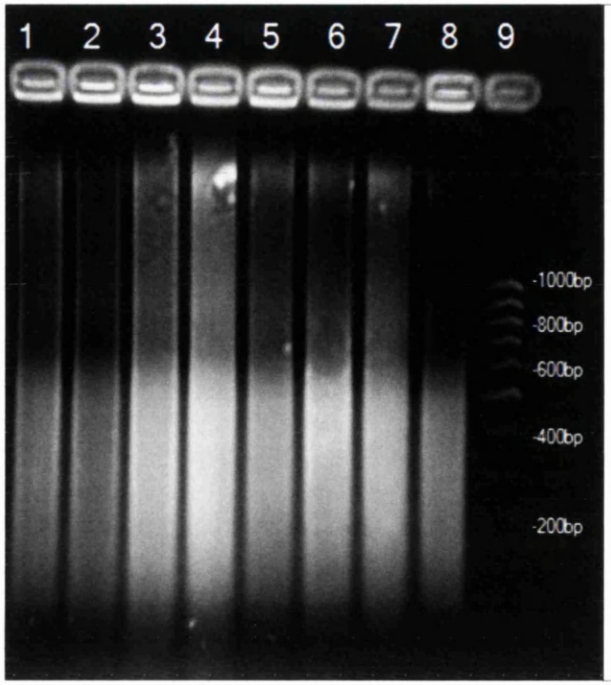

Figure 2.5 Gel analysis of optimal shearing by sonication using the ChIP-IT Express Kit (Active Motif, Europe).

Epithelial endometrial HEC-1A (Lanes 1-4) and HEC-1B cells (Lanes 5-8) were fixed 10 min with 37% formaldehyde in BME serum free media. Chromatin was sheared with 5 pulses of 1min 40sec each at 40% power using a Vibracell VC 130 sonicator (Sonics) in 300mL Shearing Buffer on ice.

Chromatin was subject to cross link reversal, RNase A and Proteinase K treatment and purified according to the manufacturers' instructions. Optimally sheared samples produce a smear between 250-1500bp. Lane 9 contains a 100bp - 1000bp ladder (Bio-Rad)

Figure 2-5 Gel analysis of optimal shearing by sonication using the ChIP-IT Express Kit

Next, 5µg chromatin per sample (equal to the volume in the IP reaction) was also reserved in 0.2mL tubes to be the 'input' controls in PCR analysis. Input samples were stored at 4°C for use within 6 h or -20°C within 24 h. Tubes were briefly vortexed and placed on an end-to-end rotator for 4h at 4°C. Following a brief spin, beads were pelleted on a magnetic stand and supernatant discarded. Beads were washed four times with 200µL ChIP Buffer 1, three times with 200µL ChIP Buffer 2 and resuspended in 50µL Elution Buffer AM2 using a 200µL 8 channel pipette (StarLab). Beads were incubated for 15 min on an end-to-end rotator at room temperature to elute chromatin. 50µL Reverse-Cross-linking Buffer was added and tubes immediately placed on magnetic stand. The supernatant containing the chromatin was transferred to new 8-well PCR strip tubes on ice. Reserved 'input' samples were added to 2µL 5M NaCl (SIGMA) and ChIP Buffer 2 to a total volume of 100µL and heated for 15 min in a thermocycler at 95°C along

with the ChIP samples. Samples were briefly centrifuged and incubated at 37°C 1h with 2µL Proteinase K (0.5µg/µL). The action of Proteinase K was stopped with 2µL Proteinase Stop Solution (100mM PMSF diluted 1:20 in distilled water) and samples were either stored at -20°C or purified using the QIAQuick PCR Purification Kit (Cat No. 28104 Qiagen) to give a final volume of 100µL purified DNA for use in qPCR after ChIP. All reagents were supplied in the ChIP-IT Express kit (Active Motif, EU) unless stated otherwise.

2.10.1 ChIP-validated Antibodies

Antibody	Type	Source	Product Code	Specificity & Target	References
Anti-ER alpha	Rabbit Polyclonal	Santa Cruz Ltd	HC-20 sc:543	(h)ER-alpha C terminus	Evans, R.M. 1998
Anti-ER beta	Rabbit Monoclonal	Millipore Ltd	04-824 (68-4)	Full length ER-beta (h, r, m)	Zhu, Y., et al. 2002
Anti-ER beta	Rabbit Polyclonal	Pierce Ltd	PA1-311	55KDa ER-beta (h, m)	*Biol.Reprod.*, **60**:691-697, 1999
Anti-ER beta	Mouse Monoclonal	Calbiochem	GR40	53KDa ER-beta (h)	Shughrue, P.J. et al. 1998
Anti-ER beta	Mouse Polyclonal	Gene Tex Inc.	GTX70182 (7B10.7)	ER-beta (h)	Nicole. R. Bianco., et al. 2003
(NFκB) Anti-p65	Rabbit Polyclonal	Santa Cruz Ltd	C-20 Sc: 372	NFκB p65 C-terminus (h)	Meyer, R., et al 1991
Secondary Rabbit IgG	Whole Molecule IgG	Rockland Ltd	011-0102	Precipitated against Anti-Rabbit Serum and IgG	Active Motif Europe
Secondary Mouse IgG	Whole Molecule IgG	Rockland Ltd	010-0102	Precipitated against Anti-Mouse Serum and IgG	Active Motif Europe

Figure 2-6 Table of Antibodies used for Chromatin Immunoprecipitation and references

2.10.2 Q-RT-PCR post ChIP

Q-RT-PCR reactions were set up as follows: 12.5µL Power Sybr Green Master Mix containing iTaq polymerase (Applied Biosystems), 3.5µL distilled MilliQ water (Millipore), 2µL sense and 2µL antisense primer at 5µM (SIGMA) per sample. Q-RT-PCR reactions were performed in triplicate in translucent MicroAmp Fast Optical 96-well reaction plates and run on the StepOnePlus Real-Time PCR Thermal Cycling Block (Applied Biosystems). Plates were heated for 95°C for 10 minutes to initiate the DNA polymerase enzyme that requires a hot start and Real Time (RT) data collected during 39 cycles comprising of 95°C for 15 sec and 1h at optimum annealing temperature for specific primer sets. Melt curve data was collected during 1 cycle of 15 sec at 95°C, 1h at 60°C followed by a set point increase in 0.3°C increments to an end-point temperature of 95°C. Q-RT-PCR data was analysed on the StepOnePlus v2.1 Software (Applied Biosystems) and the CFX Manager v1.6 Software (Bio-Rad).

2.10.3 Genomic Primers for Q-RT-PCR post ChIP

Specific genomic primers for NFκB (p65), Sp1 and Ap1 (ER) sites were designed by inputting the NCBI promoter sequence for RAGE and MUC1 into the Primer Express v3.0 software (Applied Biosystems, USA) and verified using the Beacon Design 2.0 program (Premier Biosoft, USA). Primer Express software design parameters were left unchanged if suitable primers of an amplicon length between 50-150bp could be generated with annealing temperature (Ta) of 60°C. If necessary, the following parameters were amended to avoid the formation of secondary structures and dimers: amplicon length, % of C&G base content (40-70%) and number of C&G

bases at the 3' end. It was recommended by the manufacturers of the ChIP-IT Express Kit, Active Motif, that the difference between the melt temperature (Tm) of sense and anti-sense should not exceed 3°C. Prior to use in Q-RT-PCR, primers were optimised for concentration against serial dilutions of HeLa (0.45ng/mL, Invitrogen) genomic DNA template. The standard curves were checked for an R^2 efficiency of between 0.90 (95%) and 1.10 (110%). Melt curves were also checked for the absence of primer dimers at low DNA template concentrations and one single inflection, indicating the amplification of a single product (see Appendix B3).

Promoter Site	Primer	Primer Sequence 5'-3'	Amplicon
NFκB p65 Site 1 (-1518/-1510bp) **Ap1 Site** (-1542bp)	For	ATAGAATCGCTCGGTGGACG	Tm = 77.98 Ta = 60 101bp
	Rev	GTTCAACCCCAAAGCCCAGT	
NFκB p65 Site 2 (-671/-673bp)	For	AGTAACATCAACACTGTCCCATCCT	Tm = 77.9 Ta = 60 99bp
	Rev	GGTTCCCCACTCTGACAGTCTT	
NFκB p65 Site 3 (-467/-458bp)	For	AAAAAACATGAGAAACCCCAGAAA	Tm = 76.96 Ta = 60 104bp
	Rev	AATTGGGCCTGCATCATGA	
ER Sp1 Site 1 (-189/-181bp)	For	CCCCCAGGGAAGTGACTGTA	Tm = 77.3 Ta = 60 88bp
ER Sp1 Site 2 (-172/-166bp)	Rev	GGACAAGAGTCCTTCAGGTACTAGA GA	
ER Sp1 Site 3 (-45/-39bp)	For	AATTCCTAGCATTCCCTGTGACA	Tm = 84.72 Ta = 60 158bp
	Rev	GCCATCCTGCTTCCTTCCA	

Figure 2-7 Table: Genomic primer sequences for the p65, Sp1 and Ap1 sites on the RAGE promoter

Promoter Site	Primer	Primer Sequence 5'-3'	Position	Amplicon
NFκB Site 1 (-584bp)	For	GGGACAGGGAGCGGTTAG	464	93bp Tm=80.4 Ta=53.4
	Rev	GGCTGGATAATGAGTGGAC TAG	556	
NFκB p65 Site 2 (-444bp) ER site 1 (-452bp) ER Site 2 (-432bp) ER Site 3 (-417bp) ER Site 4 (-411bp)	For	CCGCTCTGCTTCAGTGGAC	573	101bp Tm=83.1 Ta=56.7
	Rev	AGCCAGCTAGGTCGAGGTC	673	

Figure 2-8 Table: Genomic primer sequences for the p65 and ER sites on the MUC1 promoter

2.11 Analysis of Quantitative Real Time PCR for ChIP

The 'pull down' of an antibody is defined as the amount of DNA to which the protein of interest has bound for a particular site, region or length of DNA (specified by the genomic primer). The Input sample is the same chromatin used in the experiment (standardized across biological samples), but does not undergo immunoprecipitation (IP) with the antibody. In these experiments, it represents the total amount of DNA at the site or defined region in 20μg of sheared chromatin starting material.

2.11.1 ER-alpha ChIP

Real Time Quantitative PCR Data for ER-alpha ChIP on the RAGE promoter was analysed on the Step One Plus Version 2.1 Software program (Applied Biosystems) using the analysis method provided by researchers at epigenetics company Active Motif Europe (Rixensart, Belgium) who manufacture the ChIP-IT Express kit utilised in this project. Q-RT-PCR for ChIP was performed in triplicate per sample as described (section 2.10.2). On the Step One Plus software, the threshold cycle (Ct) value for an

individual sample on the PCR plate is calculated against an individual baseline threshold automatically set by the program. In order to compare the Ct values of the Input, Antibody and IgG samples relative to each other, the baseline threshold of these samples must be set the same. Therefore, the individual baseline threshold values of the selected Input, Antibody and IgG data were exported into an Excel spreadsheet to calculate the average baseline threshold. In the analysis, the Input, Antibody and IgG data for each target were highlighted and the average baseline threshold value manually set against the samples by deselecting the automatic default settings and pasting in the new baseline threshold. Once the analysis settings were applied, the Ct values in the well table were re-analysed automatically. The re-analysed Ct values are now calculated from where the amplification signal (measured in RFU) from the Input, Antibody and IgG sample crosses the average baseline threshold. The PCR Ct values were then exported into Excel worksheets as raw threshold cycle data for further analysis.

2.11.2 NFκB p65 ChIP

Real Time Quantitative PCR Data for NFκB-p65 on the RAGE and MUC1 promoters was analysed on the CFX Manager Version 1.6 Software program (Bio-Rad) using the same analysis method as on the Step One Plus Software (Applied Biosystems). In the CFX analysis program, Input, Antibody and IgG samples were highlighted and grouped per target and an auto-calculated baseline threshold was assigned to the data. The auto-calculated baseline in the CFX software is already the average baseline threshold of all the samples within the group. For this reason it is not necessary to export individual thresholds into Excel to calculate it. In order to compare the threshold cycle (Ct) values of Input, Antibody and IgG samples relative to each other, the

same auto-calculated baseline threshold was applied across all biological samples within an experiment. In this way, Input, Antibody and IgG pull-down for a specific target in the untreated ChIP sample will be relative to the Input, Antibody and IgG pull-down for the same target in the treated ChIP sample. The PCR Ct values were then exported into Excel worksheets as raw threshold cycle data for further analysis.

2.11.3 Analysis of ChIP Data using the ΔΔCt Method

This method of analysis of Q-RT-PCR is known as the ΔΔCt method (Livak and Schmittgen 2001). Application of the ΔΔCt method relies on the primer efficiency for the Input, ChIP antibody and negative IgG samples being equal. To achieve this, genomic Q-RT-PCR primers were optimised for concentration against genomic HeLa DNA standard curves of various template dilutions prior to ChIP experiments (section 2.10.3). Furthermore, Input, Antibody and IgG samples were run under the same conditions on the same 96 well plate. Primers were designed to have amplicons less than 150bp and all had an R^2 efficiency value between 0.9-1.0. In this study, chromatin was used un-diluted in the ChIP reactions therefore the dilution factor is 1. The amount of target DNA (bound by protein of interest at a specific site) is simply subtracted from, and is relative to, the reference Input sample (total DNA). The formula for calculating the binding of the antibody and negative IgG using the ΔΔCt method, where the dilution factor is one and primer efficiency (E) is 100%, is as follows:

ChIP Antibody Pull Down (%)

= (2^(Input Ct - ChIP Antibody Ct))*Dilution Factor*E

Negative Control IgG Antibody Pull Down (%)

=(2^(Input Ct - IgG Antibody Ct))*Dilution Factor*E

Threshold (Ct) values for the Input, Antibody and negative control antibody (IgG) for each biological sample were exported into a Microsoft Excel spreadsheet. If necessary, one outlying Ct value per sample in triplicate was excluded from the analysis. The 'pull-down' of the antibody was calculated as a percentage of the DNA in the Input sample (% Input DNA) for each Ct value using the above formula. The average 'pull-down' value was calculated for the ChIP Antibody and IgG antibody from the individual pull down values generated from the individual Ct values. Average pull-down values were plotted on an Excel graph as a % of the Input DNA. Error bars were generated from the standard deviation (SD) of the individual pull-down values.

G4 =(2^(C4-D4))*F4*100

	A	B	C	D	E	F	G	H	I	J	K	L
2		Sample	Input (Ct)	AB (Ct)	IgG (Ct)	DF	AB (%)	IgG (%)	Mean AB	Mean IgG	SD AB	SD IgG
3		A	22.325224	34.01531	38.9826	1	0.030265	0.000967	0.016104	0.001395	0.002884	0.000605
4			22.325657	34.75391	38.06927	1	0.018144	0.001823				
5			22.28038	35.07597	38.43841	1	0.014065	0.001368				
6		B	22.555117	33.62119	34.2614	1	0.046642	0.029927	0.044603	0.0273829	0.002884	0.003597
7			22.453661	33.65173	34.42875	1	0.042564	0.024839				
8		C	23.717905	32.70681	35.10784	1	0.196821	0.037264	0.214629	0.0292178	0.028048	0.011379
9			23.710665	32.67568	35.91623	1	0.200107	0.021172				
10			23.867149	32.52865	35.44514	1	0.246961	0.03271				

Figure 2-9 Example of Q-RT-PCR ChIP data analysis in Excel spreadsheet

Figure 2.9 shows an example of the analysis for Q-RT-PCR ChIP data. The equation in the formula bar shows the equation for the antibody pull-down calculation of the highlighted cell.

2.12 Immunohistochemistry (IHC) for ERα and ERβ in HEC-1 cells

Preparation of IHC slides for cultured cells was as follows: Cells were washed twice in 10mL DPBS in culture vessel and removed from the culture substrate by incubation <5 min at 37°C with 1mL 0.25% Trypsin 1mM EDTA (pH 8) in Hanks' Balanced Salt Solution (HBSS) containing phenol red (without $CaCl_2$ and $MgCl_{2)}$. Cells were checked for detachment using an inverted light microscope and the trypsin neutralised with the addition of 10mL media. Cells were centrifuged at 12,000g for 5 min at room temperature and 2mL basic culture medium (DMEM/F12 for HEC-1A, Ishikawa and Heraklio and BME for HEC-1B) supplemented with 10% DCC-FBS was used to resuspend the cell pellet. 100µL of cell suspension (1×10^5 approx.) were fixed to glass slides with 5 min cytopspin centrifugation. Slides were air dried and fixed 10min at -4°C in absolute (100%) methanol. Slides were briefly air-dried to evaporate the methanol, placed in a metal slide rack inside a pressure cooker to boil for 3 min in Antigen Retrieval Buffer (10mL/L Citrate Buffer pH 6.0 Cat. No: H3300). Slides were cooled under running water to room temperature and washed twice for 5 min in 1X Tris-Buffered Saline (TBS): 8g Sodium Chloride (SIGMA), 2.42g Tris Base (SIGMA) in 1L distilled MilliQ water (Millipore) supplemented with 0.5% Triton X-100 (SIGMA). Slides were blocked for 1h at room temperature in 1X TBS (990µL) with 10% (10µL) Goat serum and 1% BSA (10mg) filter-sterilised using 0.2mm cap and 10mL syringe (BD Plastipak). IHC for ER-beta expression used a primary antibody raised in goat so the serum in the blocking solution was substituted with 10% (10µL) donkey serum. Slides were gently washed twice with 1X TBS with 0.5% Triton X-100 (TBSX) to remove blocking solution. Slides were incubated at 4°C overnight on a rotary agitator in either

100µL rabbit anti-ERα antibody (HC-20 sc: 573, Santa Cruz) diluted 1:100 in 1% BSA-TBS or goat anti-ERβ antibody (L-20 sc: 6822, Santa Cruz) diluted 1:50 in 1% BSA-TBS. The following day, excess primary antibody was removed by gentle washes with TBSX. Slides were incubated at room temperature for 30 min in secondary antibody (2.5µL) diluted (1:400) in 970µL Phosphate Buffered Saline with 0.5% Triton X-100 (PBSX) and goat/donkey serum (30µL). Avidin-Biotin peroxidase Complex (ABC, Vector Laboratories Ltd, UK) was immediately prepared (reagent A 9µL, reagent B 9µL 1:1 in 500µL TBSX) in a dark room. Slides were washed briefly in TBSX to remove excess secondary antibody. 100µL vector ABC stain was administered to each slide and left to incubate for a further 30 min in the dark room. Slides were washed twice in TBSX for 5 min. Whilst in the last wash, the DAB stain solution was prepared in a fume hood: 1 drop Buffer pH 7.5 (BSS), 2 drops diaminobenzidine (DAB) and 1 drop hydrogen peroxide solution (HPS) in 2.5mL distilled MilliQ water (Millipore). Slides were left in the dark room for 5-25 min to stain for the secondary antibody in 100µL of DAB stain solution. After this time, the DAB solution was removed and transferred into a sealed container and disposed as biohazard clinical waste (appropriate for carcinogenic substances). Slides were washed briefly in distilled water (Millipore) and stained for 1min in Haematoxylin (nuclear stain) followed by another brief wash in MilliQ water. Slides were washed 3 min in weak alkaline Scott's tap water which acts upon the Haematoxylin stain and deepens it's colour from red to reddish-brown thus aiding microscopy. To stain for cell cytoplasm, slides were incubated 1 min in Eosin stain, followed by incubation 3 min in a dilution series of 50%, 70%, 90% ethanol. Slides were left for 5 min in 100% xylene before being air-dried and mounted with

cover slips in a fume hood using xylene with di-n-butylphthate (DPX). Slides were left 2h or overnight in a fume hood before inspection under microscope.

2.12.1 Immunohistochemistry (IHC) for paraffin-embedded samples

Immunohistochemistry on archived paraffin-embedded samples was undertaken at Singleton Hospital, Swansea. Samples were previously fixed in 10% formaldehyde for 24h at the time of endometrial biopsy, paraffin embedded and sectioned to 4μm. Sections were removed of paraffin (de-waxed) with xylene, incubated through a series of methanol grades and fixed onto slides for staining with haematoxylin and eosin for the nuclear and cytoplasmic compartments respectively. The Ventana machine (Ventana Biotek Solutions, Tucson, AZ, USA) at Singleton Hospital uses a barcode system to recognise each slide. Slides were heated in citrate buffer CC1 (Ventana) on a benchmark XT processor to 100°C for 1h for antigen retrieval. 100μL of primary antibody was added per slide and incubated at a specific temperature and length of time according to the antibody requirements. The Ventana machine uses a multiple biotinated secondary antibody detection kit which is compatible with all primary antibodies except those raised in goat. Staining was visualised using the Ventana I View DAB solution that is sensitive to the interaction between Avidin-Biotin peroxidase Complex (ABC) solution and the secondary biotinated antibody. Slides were counter-stained 1 min with 100μL Haematoxylin stain at room temperature, incubated in xylene 5 min, left to air-dry and mounted in DPX.

2.12.2 Scoring and Statistical Analyses

Immunohistochemical data was generated using a scoring system where slides are scored simultaneously by three independent observers on a multi-headed microscope (Lai, Shih Ie et al. 2005). Slides for established cell lines were produced in triplicate per sample and a representative area of 20 cells chosen per slide. Positive red-brown stain was scored for intensity where 0 is absent and 4 is very strong. Slides were also scored for stain distribution throughout the tissue section as follows: 0 - absent, 1 - less than 30%, 2 - 30-60%, 3 - more than 60% and 4 - 100%. Positive (human lung tissue) and negative (endometrial tissue lacking antibody) control sections were used for reference. Primary tissues exhibit non-uniform cellular staining therefore the tissues were scored independently for the epithelium, stroma and glandular lumen compartments. The sections were first scored according to the % distribution of positive staining across the tissue and scored again for stain intensity. Data was subject to the Kolmogrovov-Smirov normality test to find whether the stain was normally distributed ($p = >0.150$) or not normally distributed ($p = <0.150$). Normally distributed data was analysed using the ANOVA (SPSS) test for parametric data. If the data was not normally distributed, the scoring results for the combined data of all the samples was analysed using the Kruskall Wallace test followed by the Mann Whitney test (Margarit, Gonzalez et al. 2009). These tests will show the significance of differences within the whole combined data set and the significance of the differences between the grouped pathologies respectively.

CHAPTER 3

Expression of Receptor for Advanced Glycation End products (RAGE) in fertile and infertile human endometrium

3. Expression of Receptor for Advanced Glycation End products in fertile and infertile human endometrium

3.1 Introduction

The endometrium is a complex tissue comprising of mesenchymal-derived stroma, glandular and luminal epithelia, vascular smooth muscle and leukocytes. Its unique cyclical disintegration and regeneration is closely regulated by pituitary-released gonadotropins and ovarian sex steroid hormones (Chan 2004). Consequently, the natural state of the endometrium is governed by factors impacting on ovarian function and may be reflected in the expression of RAGE. During the late proliferative and secretory phase of the menstrual cycle, the endometrium responds to estrogens released during ovum maturation prior to ovulation. Endometriosis is a disorder of the endometrium which can largely be attributed to abnormal or excessive estrogen levels causing proliferation of endometrial-like cells outside the uterine cavity (Garry 2004). Endometriotic and PCO endometrial cells show significantly greater expression of ERα than fertile controls suggesting that pathology-associated excess estrogen could increase transcriptional activity of ERα target genes (Lessey, Palomino et al. 2006; Margarit, Taylor et al. 2010). Promoter studies of RAGE in human and bovine aortic, and human skin endothelial cells have identified it as an ER target gene directly regulated by ERα recruited by the Sp1 transcription factor (Li 1998; Tanaka, Yonekura et al. 2000). Studies have shown that the membrane-tethered receptor RAGE and its soluble form sRAGE are elevated in the ovaries and serum of women with PCOS (Diamanti-Kandarakis, Piperi et al. 2007; Diamanti-Kandarakis, Katsikis et al. 2008). In the same way endometriotic lesions respond to

elevated levels of estrogen, PCO endometrium responds to excess androgens and AGEs.

Upon RAGE ligation AGEs have been shown to activate dissociation of β-catenin from its anchorage to E-cadherin on the cell membrane in bovine and human vascular endothelium (Otero 2001). Liganded androgen receptor (AR) has been shown to form a transcriptional complex itself with free β-catenin upon its release (Yang, Li et al. 2002). AGE-RAGE interaction indirectly stimulates ERK 1/2 MAP kinases bound to the RAGE cytoplasmic c-terminal domain (Ishihara, Tsutsumi et al. 2003). ERK 1/2 phosphorylates the steroid receptor TIF2 which post translocation assembles with the androgen/AR/β-catenin complex in the nucleus (Song, Herrell et al. 2003). Here, this complex induces chromatin remodelling, polymerase and p300 recruitment and initiates transcription of AR target genes including MUC1. In this way RAGE could potentially increase AR and NFκB transcriptional activity through the up-regulation of β-catenin and the MAPK pathways. Basal levels of cellular RAGE are influenced by levels of AGE, free androgens and expression of AR. Thus, it can be hypothesised that hyperandrogenism, specifically free testosterone, excess estrogen and elevated AGEs in infertile disorders lead to over-expression of RAGE and possibly MUC1, the latter perhaps being RAGE dependent (see Ch.4). Moreover, it could also be argued that RAGE displays cyclical basal expression and may reflect the estrogenic cellular environment during the secretory phase due to maintenance of estrogen levels in endometriosis (Lessey 2002). The work in this chapter aims to characterise basal RAGE transcript expression in endometrial epithelial cell lines and primary endometrial tissue and epithelial cells. Endometrial biopsy specimens were grouped according to menstrual cycle phase to ascertain

whether RAGE expression is influenced by the stage of endometrial development. RAGE expression was also investigated at the protein level in glandular and luminal endometrial epithelium and endometrial stroma from infertile PCO and endometriotic pathology compared to fertile controls.

3.2 Clinical Data and Patient Demographics for RAGE IHC

Patient data was analysed using the statistical Anderson-Darling and two-tailed student T-tests (Fig. 3.1). Patients with a BMI over 40 and/or over 45 years of age were excluded from the study. In total eighty seven (87) patients were enrolled into this study. 32 endometrial samples were obtained from patients in the proliferative phase, 41 samples were obtained during the secretory phase of the cycle at LH+6 and 14 samples were from patients with anovulatory PCOS. These samples were classified into 4 groups: fertile (n=21), endometriosis (n=29), ovulatory PCOS (n=23) and anovulatory PCOS (n=14). There were no statistically significant differences in the mean age and BMI between the fertile and infertile patient cohorts (Fig. 3.1).

	Fertile	Endometriosis	Ovulatory PCOS	Anovulatory PCOS
AGE	29.58 ± 4.12	28.63 ± 4.55 P=0.727	28.72 ± 5.06 P=0.777	25.1 ± 4.4 P=0.267
BMI (Kg/m^2)	26.70 ± 4.82	27.54 ± 3.08 P=0.753	26.65 ± 3.34 P=0.985	28.15 ± 2.3 P=0.591

Figure 3-1 Patient demographics for human endometrial biopsy specimens

Table shows mean age and body mass index (BMI) ± SD of patients recruited to the study assessing RAGE expression in endometrial pathologies by IHC.

3.3 RAGE is expressed in fertile and infertile proliferative phase endometrium

RAGE protein expression has previously been characterised in ovarian tissues from PCOS patients (Diamanti-Kandarakis, Piperi et al. 2007) and in ectopic endometriotic stromal cells (Sharma, Dhawan et al. 2010). However, at the time of writing, expression of RAGE in human eutopic endometrium was yet to be determined. In the following study, RAGE expression was investigated in 32 endometrial samples in the proliferative phase of the cycle and 14 anovulatory PCOS patients. Localisation of RAGE to the glandular and luminal epithelium and stroma of proliferative endometrium was confirmed using a RAGE-specific antibody. Immunohistochemistry from fertile, endometriosis, ovulatory PCOS and anovulatory PCOS patients were scored for intensity and distribution of RAGE positive red-brown stain (H-score) and analysed using the Mann-Whitney statistical test for non-parametric data. Data was determined to be non-parametric by the Anderson-Darling and Kruskall-Wallace normality and distribution statistical tests.

A

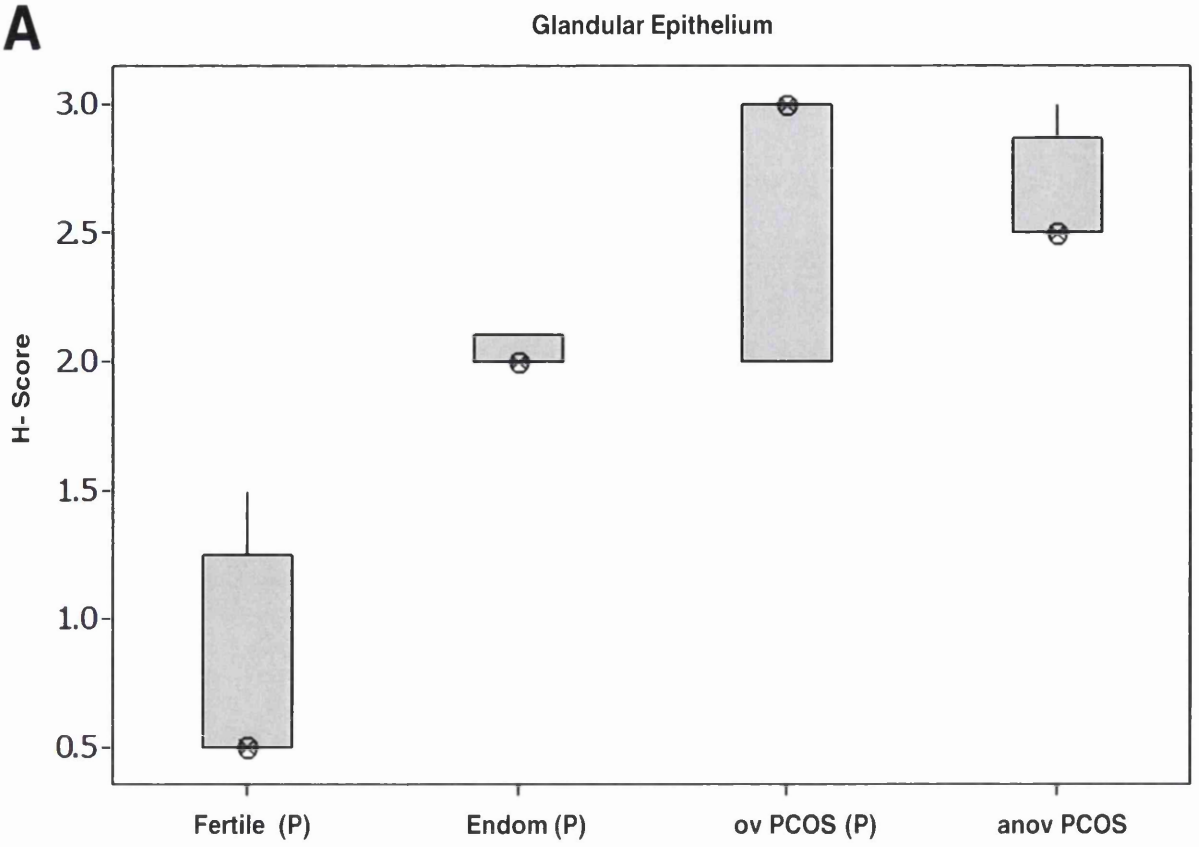

B

Glands	Endom (P)	ovPCOS (P)	anov PCOS
P values. Fertile (P) vs	0.041	0.041	0.040
Fold Change	4.0	6.0	5.0

Figure 3-2 RAGE is expressed in proliferative phase fertile and infertile endometrial glandular epithelium.

Box plot shows RAGE protein levels in endometrial biopsy specimens in the proliferative (P) phase of the menstrual cycle by IHC (A). 46 patients were grouped by pathology as follows: Fertile (n=9), Endometriosis (n=11), ovulatory (ov) PCO (n=12) and anovulatory (anov) PCOS (n=14). IHC samples were scored blind in triplicate by three independent observers. Values given are mean H-score. Data was analysed using the statistical Mann-Whitney test. Data shown is group P value vs. Fertile (P) group where P<0.05 is significant (B).

Figure 3.2A shows statistically significant elevated RAGE protein expression in the glandular epithelium of infertile pathologies versus fertile controls. The median H-score for RAGE protein expression in endometriotic glands was 4 fold greater than levels in fertile proliferative phase glandular epithelium (Fig. 3.2B, p=0.041). Individuals in the proliferative ovulatory PCO group showed more variation in glandular RAGE expression than the anovulatory PCOS

women. However, the median H-score of both PCO groups was 6 and 5 fold greater than in proliferative phase fertile glands (Fig. 3.2B, p=0.041, p=0.040). Stronger staining for RAGE protein in the proliferative phase glands can be seen in Fig. 3.6 in infertile endometrium and was particularly elevated in glandular epithelium of ovulatory PCO pathology.

A

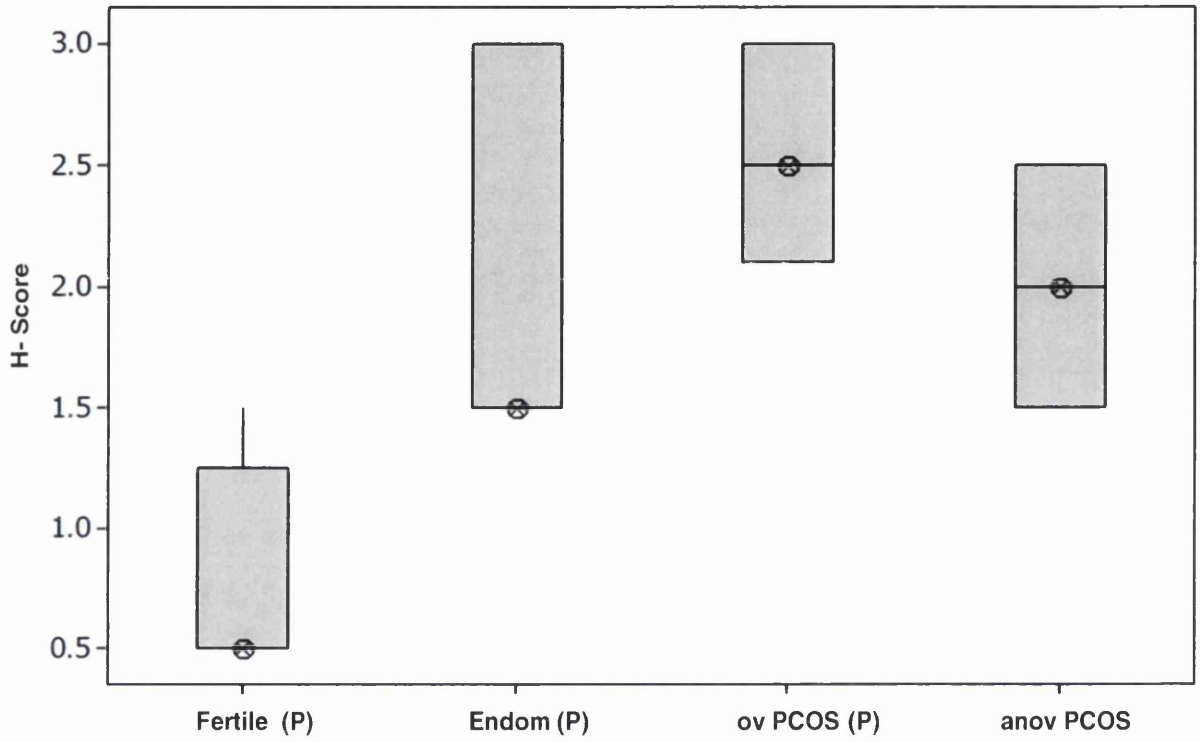

B

Lumen	Endom (P)	ovPCOS (P)	anov PCOS
P values. Fertile (P) vs	0.157	0.044	0.042
Fold Change	3.0	5.0	4.0

Figure 3-3 RAGE is expressed in proliferative phase fertile and infertile endometrial luminal epithelium.

Box plot shows RAGE protein levels in endometrial epithelial lumen in the proliferative (P) phase of the menstrual cycle by IHC (A). 46 patients were grouped by pathology as follows: Fertile (n=9), Endometriosis (n=11), ovulatory (ov) PCO (n=12) and anovulatory (anov) PCOS (n=14). IHC samples were scored blind in triplicate by three independent observers. Values given are mean H-score. Data was analysed using the statistical Mann-Whitney test. Data shown is group P value vs. Fertile (P) group where P<0.05 is significant (B).

Figure 3.3A shows a distinct 3 fold increase in the median H-score for luminal epithelial RAGE expression in proliferative phase endometriosis compared to fertile controls. However, there was no statistical difference between the two groups (Fig. 3.3B, p=0.157) which may be due to greater variation between individuals in the endometriosis group. Basal RAGE expression was significantly greater in the endometrial luminal epithelium of women with proliferative phase ovulatory and anovulatory PCOS than in fertile controls (Fig. 3.3B, p=0.044, p=0.042). Compared to proliferative phase fertile endometrium, the median H-score for RAGE protein was 5 fold higher in the ovulatory, and 4 fold higher in anovulatory PCO epithelial lumen (H=2.5 and 2.0 vs. 0.5). Some individuals within the proliferative phase ovulatory PCOS group displayed greater RAGE expression in the luminal epithelium than those who did not ovulate. With regard to the median H score across all infertile endometrial pathologies, the expression of glandular RAGE (Fig 3.2A) appeared to be greater than in the lumen (Fig. 3.3A) however this has not been statistically proven. The results in Fig. 3.2A and Fig. 3.3A did demonstrate however, that the receptor was differentially expressed in fertile and infertile endometrial epithelium.

A

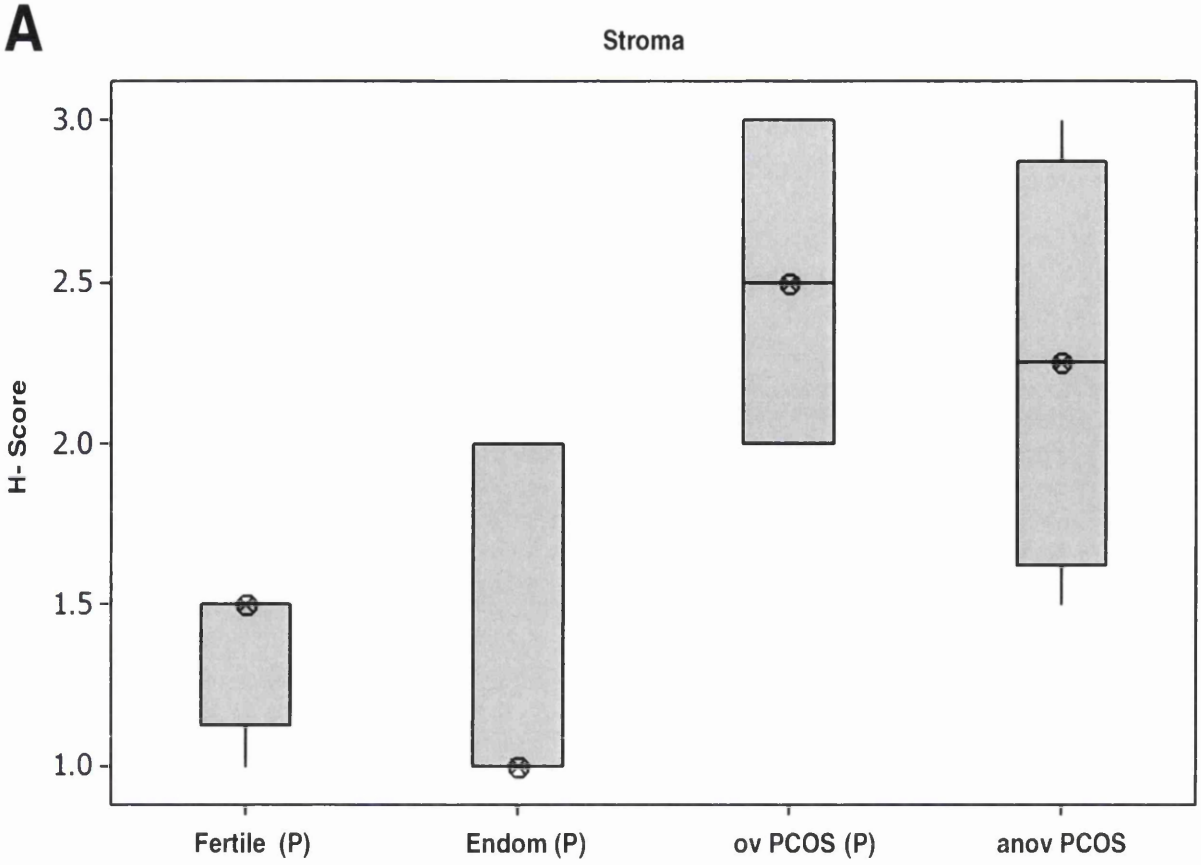

B

Stroma	Endom (P)	ovPCOS (P)	anov PCOS
P values. Fertile (P) vs	0.643	0.048	0.044
Fold Change	0.7	1.7	1.5

Figure 3-4 RAGE is expressed in proliferative phase fertile and infertile endometrial stroma.

Box plot shows RAGE protein levels in endometrial stromal cells in the proliferative (P) phase of the menstrual cycle by IHC (A). 46 patients were grouped by pathology as follows: Fertile (n=9), Endometriosis (n=11), ovulatory (ov) PCO (n=12) and anovulatory (anov) PCOS (n=14). IHC samples were scored blind in triplicate by three independent observers. Values given are mean H-score. Data was analysed using the statistical Mann-Whitney test. Data shown is group P value vs. Fertile (P) group where P<0.05 is significant (B).

Figure 3.4A shows RAGE protein expression in proliferative phase endometrial stroma of women with endometriosis was reduced 0.7 fold than in fertile controls. However, this reduction in endometriotic stromal RAGE was not statistically significant from the fertile group (Fig. 3.4B, p=0.643). When compared to fertile epithelium, increased stromal RAGE was only

observed in the PCO pathologies (Fig. 3.4A). The anovulatory PCOS women had a higher median H-score for stromal RAGE than the fertile women (1.5 fold) however, the greatest RAGE expression was observed in proliferative phase ovulatory PCO stromal cells (1.7 fold vs. fertile group). Similarly, when compared to fertile women, RAGE also showed greater expression in PCO glands (Fig. 3.2A) and lumen (Fig. 3.3A). Immunohistochemical images demonstrated how RAGE staining was strongest in the proliferative phase stroma of PCO pathology, whereas proliferative phase fertile and endometriotic stromal cells presented weaker positive staining for RAGE (Fig. 3.6).

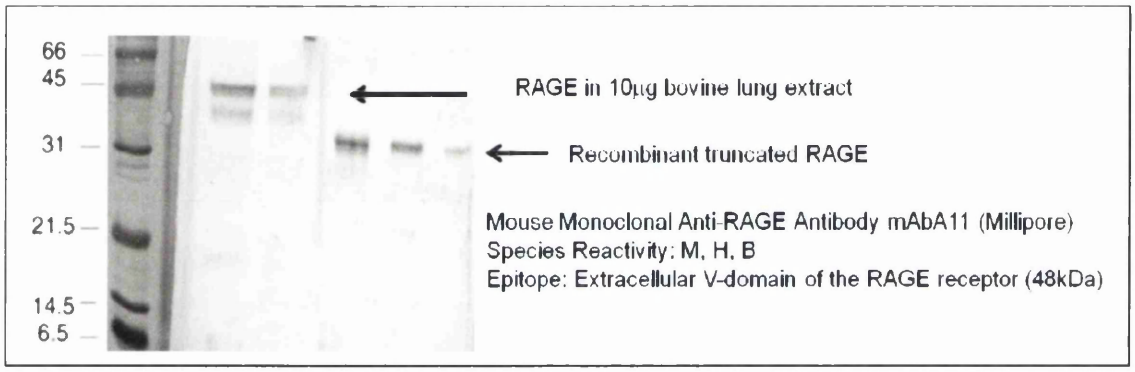

Figure 3-5 Anti-RAGE antibody used in the RAGE IHC study on human fertile and infertile endometrial specimens

The mouse monoclonal Anti-RAGE antibody was specific to the extracellular domain of RAGE and recognises both natural and recombinant protein. This antibody therefore would identify the full-length membrane tethered protein as well as various forms of soluble and secreted RAGE that possess the protein N-terminal variable (V) domain.

Representative IHC images taken of fertile and infertile endometriotic and PCO human endometrium in Fig. 3.6 and Fig. 3.10 showed a lack of membrane staining for RAGE. Therefore it is likely that the mAbA11 antibody used in this study preferentially binds to other RAGE isoforms possessing the extracellular region.

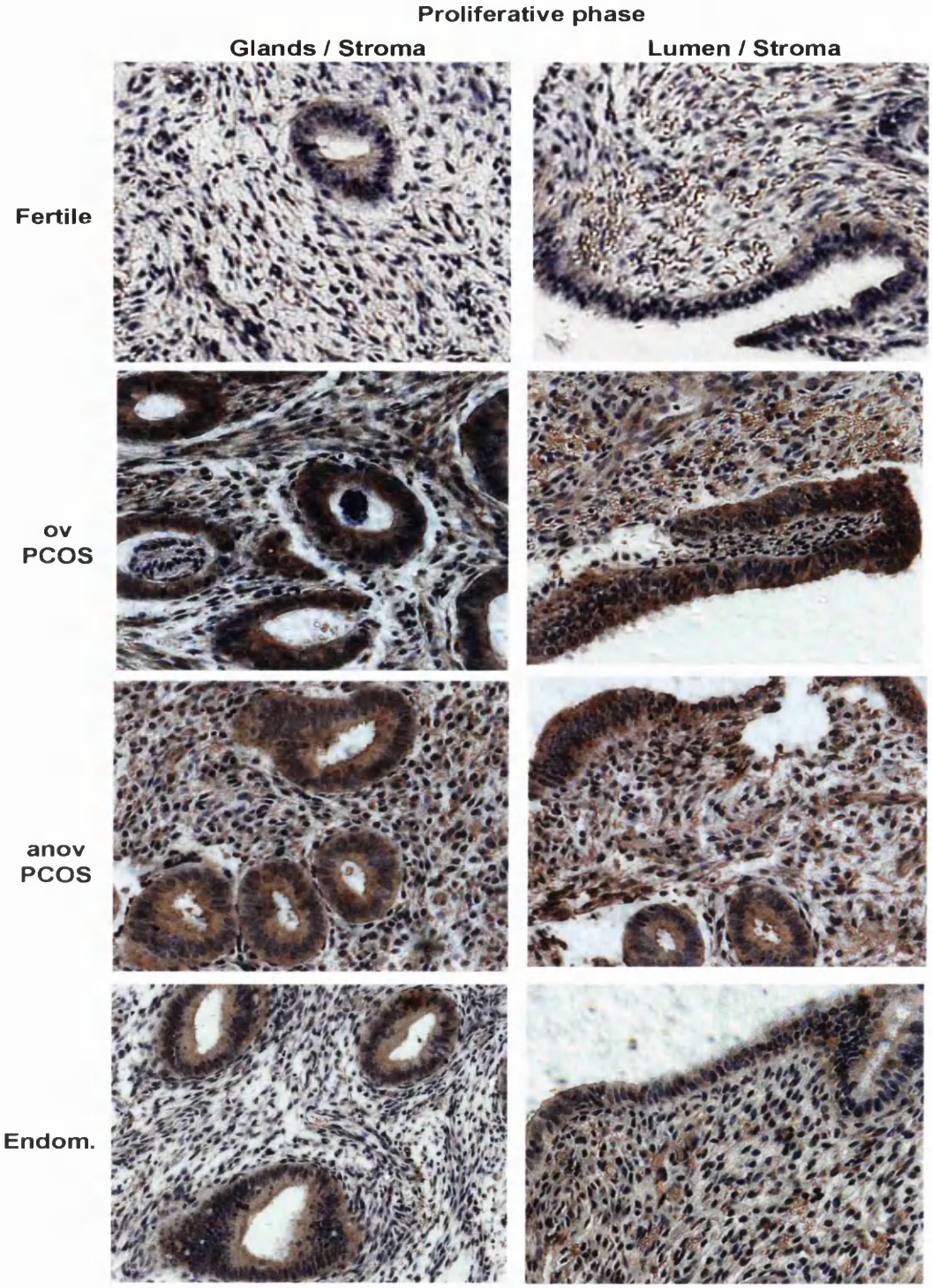

Figure 3-6 Immunohistochemical localisation of RAGE in the proliferative phase endometrium of fertile and infertile patients.

RAGE expression in proliferative phase endometrial glands, lumen and stroma of fertile women, and infertile women with endometriosis, ovulatory PCOS and anovulatory PCOS (as indicated). Slides were stained with negative purple H&E stain for the nuclear and cytoplasmic cell compartments. RAGE protein is indicated by positive red-brown staining. Representative IHC images were taken using the Axio CamHRc colour camera (Zeiss) at x20 magnification.

Figure 3.6 shows visualisation of RAGE protein in the proliferative endometrium. Epithelial RAGE staining in proliferative phase endometrium was stronger in infertile ovulatory PCOS, anovulatory PCOS and endometriosis than in fertile epithelium (Fig. 3.2A, Fig. 3.3A and Fig. 3.6). RAGE staining was predominantly strongest in the glands of infertile endometriotic, ovulatory PCO and anovulatory PCO endometrium when compared to luminal epithelial RAGE. In contrast, there was no difference between the intensity of staining for glandular and luminal RAGE in fertile endometrium (Fig 3.6). Increased stromal RAGE staining was evident in infertile PCO versus endometriotic and fertile endometrium. In addition, endometriotic stroma displayed weaker staining for RAGE than in fertile stroma (Fig. 3.4A and Fig. 3.6). Taken together, these novel results demonstrate that proliferative phase fertile and infertile endometrial cells express RAGE. RAGE was particularly elevated in ovulatory and anovulatory PCO endometrium across all cell subtypes in comparison to fertile controls, whereas endometriotic cells displayed greater epithelial RAGE and comparable stromal RAGE levels to fertile endometrium (Fig. 3.6).

3.4 RAGE is expressed in fertile and infertile secretory phase endometrium

In the following study, RAGE expression was investigated in 41 endometrial samples in the secretory phase of the cycle and 14 anovulatory PCOS patients. Localisation of RAGE to the glandular and luminal epithelium and stroma of secretory endometrium was confirmed using a RAGE-specific antibody. Immunohistochemistry from fertile, endometriosis, ovulatory PCOS and anovulatory PCOS patients were scored blind by three independant

observers for the intensity and distribution of RAGE positive red-brown stain (H-score) and analysed using the Mann-Whitney statistical test for non-parametric data. Data was determined to be non-parametric by the Anderson-Darling and Kruskall-Wallace statistical normality and distribution tests.

A

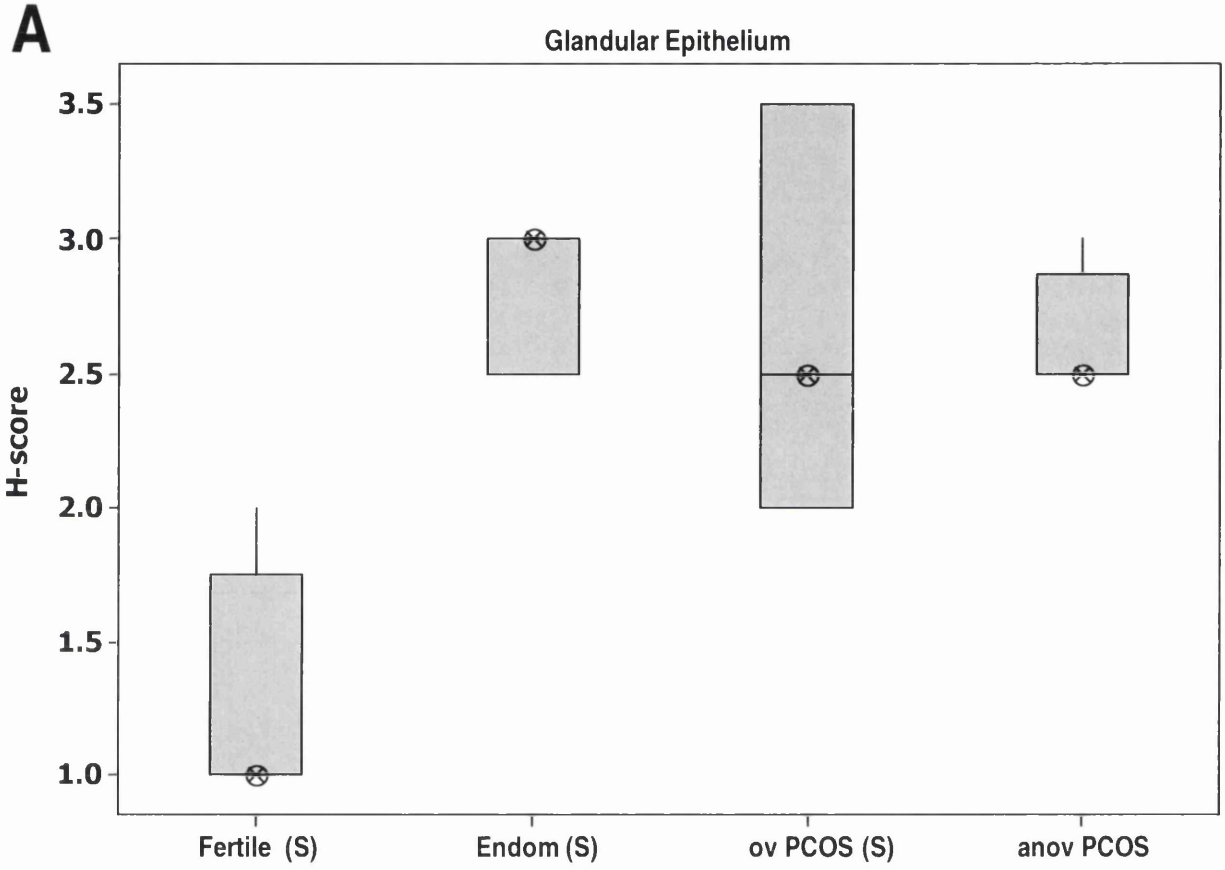

B

Glands	Endom (S)	ovPCOS (S)	anov PCOS
P values. Fertile (S) vs.	0.031	0.046	0.016
Fold Change	3.0	2.5	2.5

Figure 3-7 RAGE is expressed in secretory phase fertile and infertile endometrial glandular epithelium.

Box plot shows RAGE protein levels in endometrial biopsy specimens in the secretory (S) phase of the menstrual cycle by IHC (A). 55 patients were grouped by pathology as follows: Fertile (n=12), Endometriosis (n=18), ovulatory (ov) PCO (n=11) and anovulatory (anov) PCOS (n=14). IHC samples were scored blind in triplicate by three independent observers. Values given are mean H-score. Data was analysed using the statistical Mann-Whitney test. Data shown is group P value vs. Fertile (S) group where P<0.05 is significant (B).

Figure 3.7A shows significantly elevated RAGE expression in secretory phase glandular epithelium of the infertile pathologies versus fertile controls. The median H-score for RAGE protein expression in secretory phase endometriotic glands was 3 fold greater than in fertile glands (p=0.031). In endometriosis, epithelial RAGE was only significantly elevated in secretory phase glands when compared to fertile controls (Fig. 3.7A). These results suggest that the elevated RAGE mRNA in secretory phase endometriotic epithelium (Fig. 3.14A) may only translate to an increase in glandular RAGE protein. In secretory phase endometriotic endometrium, glandular RAGE appeared to be higher than in proliferative phase endometriotic endometrium (H=3.0 Fig. 3.2A vs. H=2.0 Fig. 3.7A), despite a smaller fold difference (3 fold vs. 4 fold) when compared to fertile glands. This is likely due to elevated RAGE in the fertile glands during the secretory phase, however cross comparisons between tissue subtype and menstrual cycle stage have not been statistically proven. In fact, anovulatory PCOS patients were evaluated independently of menstrual cycle phase due to characteristic anovulation and amenorrhea. Glandular epithelial RAGE in the secretory phase was more varied amongst individuals in the ovulatory PCOS group than the anovulatory PCO women, with some individuals scoring highly for RAGE (H=3.5). However, the median H-score for both PCO groups was 2.5 fold greater than in secretory phase fertile glands (Fig. 3.7B, p=0.046, p=0.016). These findings indicate similar levels of glandular RAGE in secretory phase ovulatory PCO and anovulatory PCO endometrium (Fig. 3.7A, H=2.5).

A

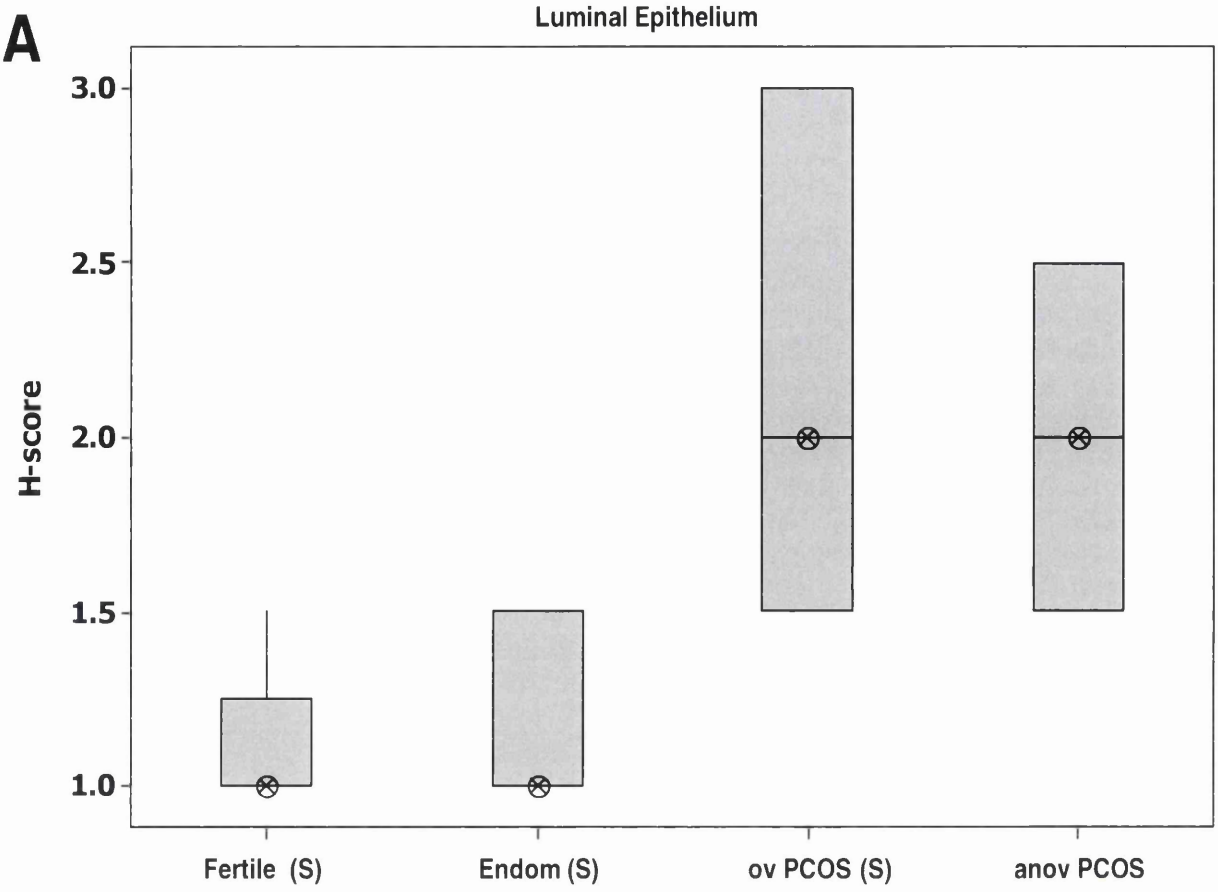

B

Lumen	Endom (S)	ovPCOS (S)	anov PCOS
P values. Fertile (S) vs.	0.863	0.038	0.026
Fold Change	0.0	2.0	2.0

Figure 3-8 RAGE is expressed in secretory phase fertile and infertile endometrial luminal epithelium.

Box plot shows RAGE protein levels in endometrial epithelial lumen in the secretory (S) phase of the menstrual cycle by IHC (A). 55 patients were grouped by pathology as follows: Fertile (n=12), Endometriosis (n=18), ovulatory (ov) PCO (n=11) and anovulatory (anov) PCOS (n=14). IHC samples were scored blind in triplicate by three independent observers. Values given are mean H-score. Data was analysed using the statistical Mann-Whitney test. Data shown is group P value vs. Fertile (S) group where $P<0.05$ is significant (B).

Figure 3.8A demonstrated that the basal level of RAGE in the secretory phase epithelial lumen of ovulatory and anovulatory PCOS women was 2 fold greater than in secretory phase fertile endometrium (Fig. 3.8B, p=0.038, p=0.026). Overall, the median H-score for luminal RAGE expression was the

same for secretory phase ovulatory PCOS and anovulatory PCOS (H=2.0), however some individuals within the ovulatory PCOS group expressed RAGE highly (H=3.0). There was no statistical difference between luminal epithelial RAGE expression in the secretory phase endometrium of fertile and infertile endometriosis pathology (Fig. 3.8B, p=0.86).

A

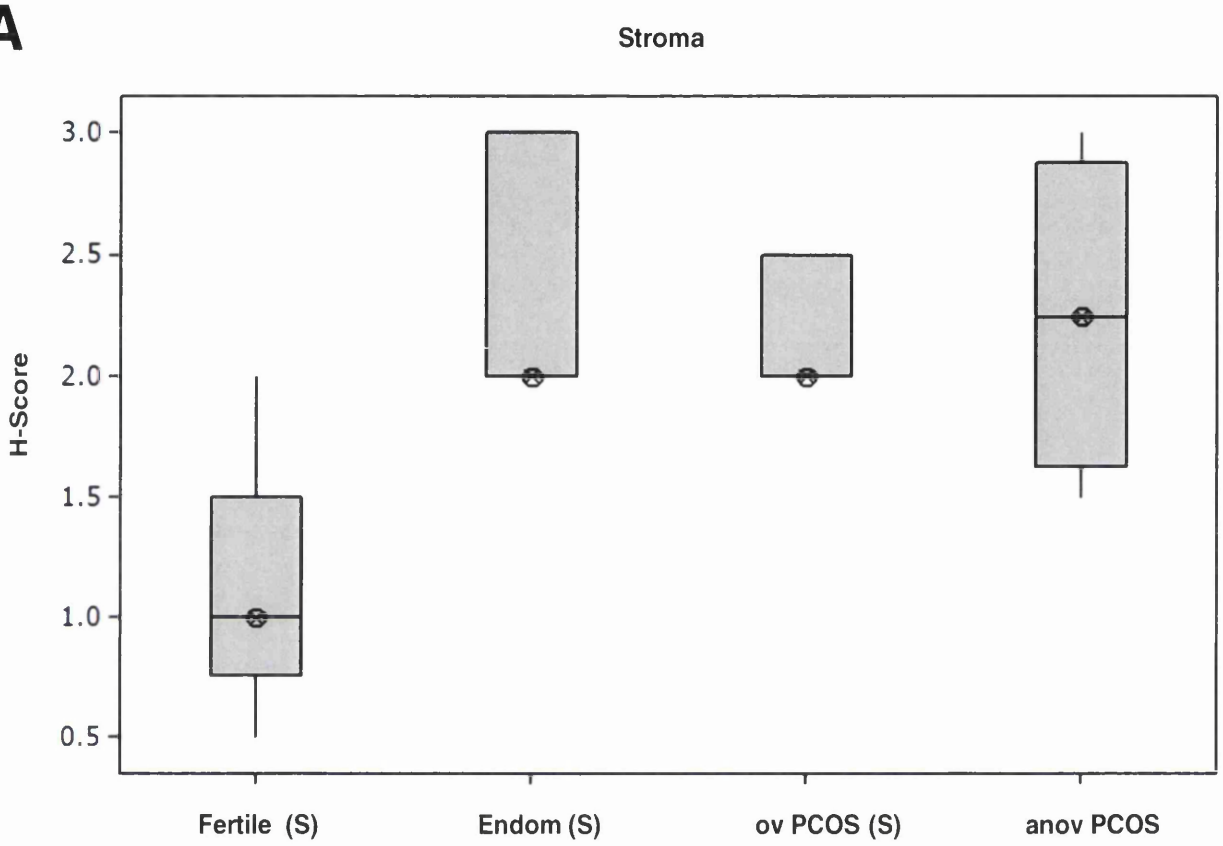

B

Stroma	Endom (S)	ovPCOS (S)	anov PCOS
P values. Fertile (S) vs.	0.037	0.037	0.045
Fold Change	2.0	2.0	2.3

Figure 3-9 RAGE is expressed in secretory phase fertile and infertile endometrial stroma

Box plot shows RAGE protein levels in endometrial epithelial stroma in the secretory (S) phase of the menstrual cycle by IHC (A). 55 patients were grouped by pathology as follows: Fertile (n=12), Endometriosis (n=18), ovulatory (ov) PCO (n=11) and anovulatory (anov) PCOS (n=14). IHC samples were scored blind in triplicate by three independent observers. Values given are mean H-score. Data was analysed using the statistical Mann-Whitney test. Data shown is group P value vs. Fertile (S) group where P<0.05 is significant (B).

Figure 3.9A shows the median H-score for RAGE protein expression in the endometrial stroma of secretory phase endometriosis and ovulatory PCOS was twice (H=2, p=0.037) that observed in the fertile group (H=1). Furthermore, anovulatory PCO stroma also showed slightly greater (2.3 fold) basal RAGE protein expression (H=2.25, p=0.045) in comparison to secretory phase fertile stroma (Fig. 3.9B). These results indicate that stromal RAGE is elevated in the secretory phase endometrium of infertile endometriosis and PCOS patients with respect to fertile controls. However, unlike PCO stroma, endometriotic stroma only expressed significantly elevated RAGE during the secretory phase (Fig. 3.4A and Fig. 3.9A, B).

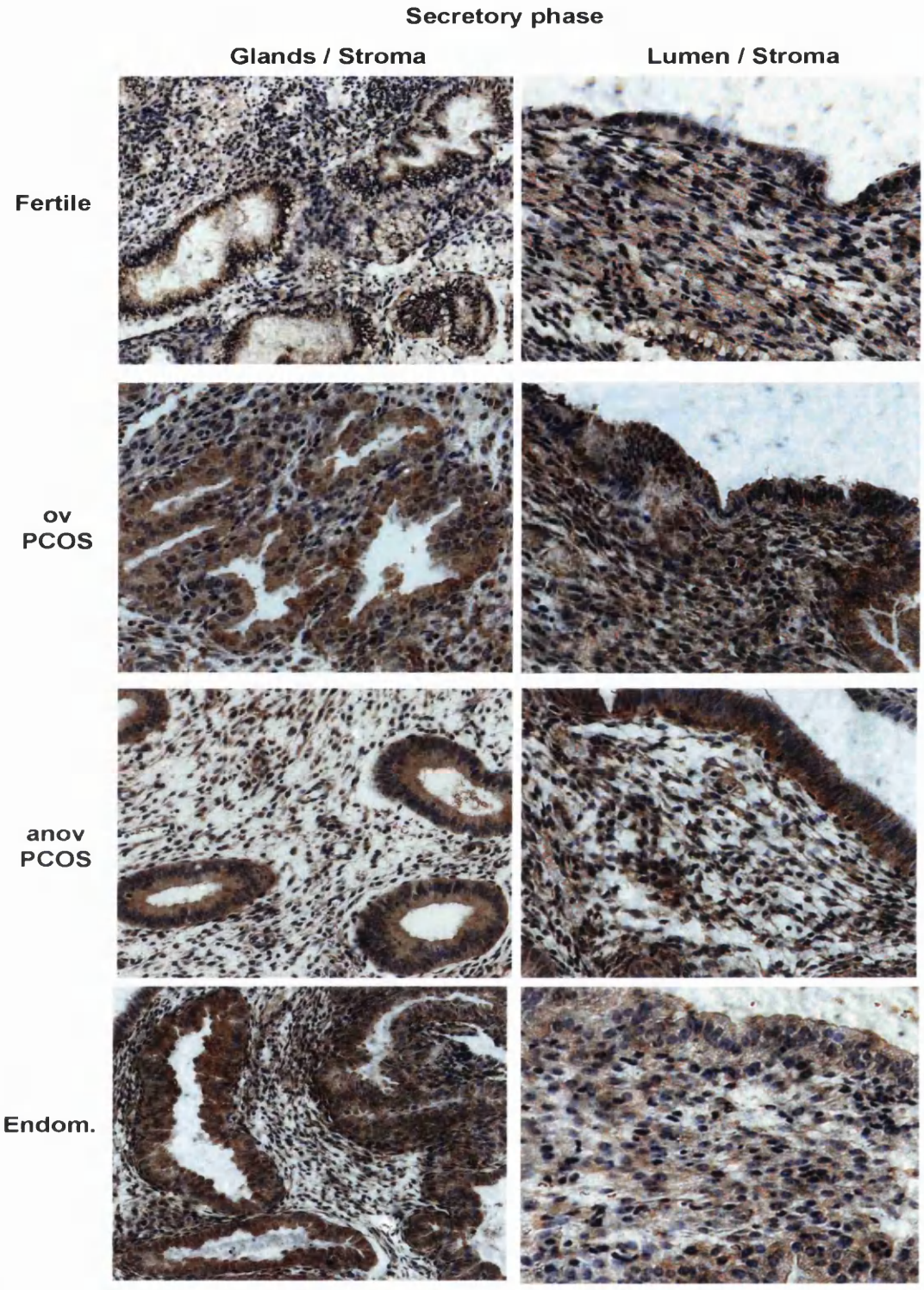

Figure 3-10 Immunohistochemical localisation of RAGE in the secretory phase endometrium of fertile and infertile patients.

RAGE expression in secretory phase endometrial glands, lumen and stroma of fertile women, and infertile women with endometriosis, ovulatory PCOS and anovulatory PCOS (as indicated). Slides were stained with negative purple H&E stain for the nuclear and cytoplasmic cell compartments. RAGE protein is indicated by positive red-brown staining. Representative IHC images were taken using the Axio CamHRc colour camera (Zeiss) at x20 magnification.

3.5 Clinical Data and Patient Demographics for RT-PCR

In total forty eight (48) patients were enrolled into this study. Whole endometrial tissue (epithelia and stroma) and epithelial endometrial cells were obtained from 16 patients in the proliferative phase. 22 samples were obtained during the secretory phase of the cycle at LH+6 and 10 samples were from patients with anovulatory PCOS. These samples were classified into 3 groups: fertile (n=18), endometriosis (n=20) and anovulatory PCOS (n=10). No PCOS patients were shown to be ovulatory and so this particular faction of PCOS women could not be assessed for RAGE transcript in this study.

	Fertile	Endometriosis	Anovulatory PCOS
AGE (Years)	33.27 ± 4.73	31.85 ± 5.57 P=0.510	29.13 ± 6.71 P=0.131
BMI (Kg/m^2)	25.13 ± 3.44	25.69 ± 4.13 P=0.678	24.14 ± 3.18 P=0.527

Figure 3-11 Patient demographics for human endometrial biopsy specimens. Table shows mean age and body mass index (BMI) ± SD of patients recruited to the study used to assess RAGE mRNA in endometrial pathologies by real time PCR.

Patient data in Figure 3.11 was analysed using the statistical Anderson-Darling normality test and two-tailed student T-test. Patients with a BMI over 40 and/or over 45 years of age were excluded due to evidence that levels of corporal endogenous AGEs naturally increase with time and are elevated in obese individuals. There were no statistically significant differences between the mean age and BMI of the fertile and infertile patient cohorts recruited to the RT-PCR study (Fig. 3.11).

3.6 RAGE transcript is expressed in whole tissue and epithelial cells isolated from fertile and infertile proliferative phase endometrium

RAGE expression has been demonstrated in endometrial epithelium and stroma of fertile women and infertile women with endometriosis and PCOS (Fig. 3.6 and Fig. 3.10). RAGE mRNA expression was therefore investigated in whole endometrial tissue and epithelial cells isolated from fertile, endometriotic and PCO endometrium to determine whether RAGE transcript varies with menstrual cycle phase or between fertilities. Upon investigation all endometrial PCOS samples were found to be anovulatory. In total, 16 whole and 10 epithelial samples in proliferative phase, and 20 whole and 11 epithelial samples in secretory phase were collected from patients recruited to this study and were analysed by real time PCR (see Fig. 3.11).

A

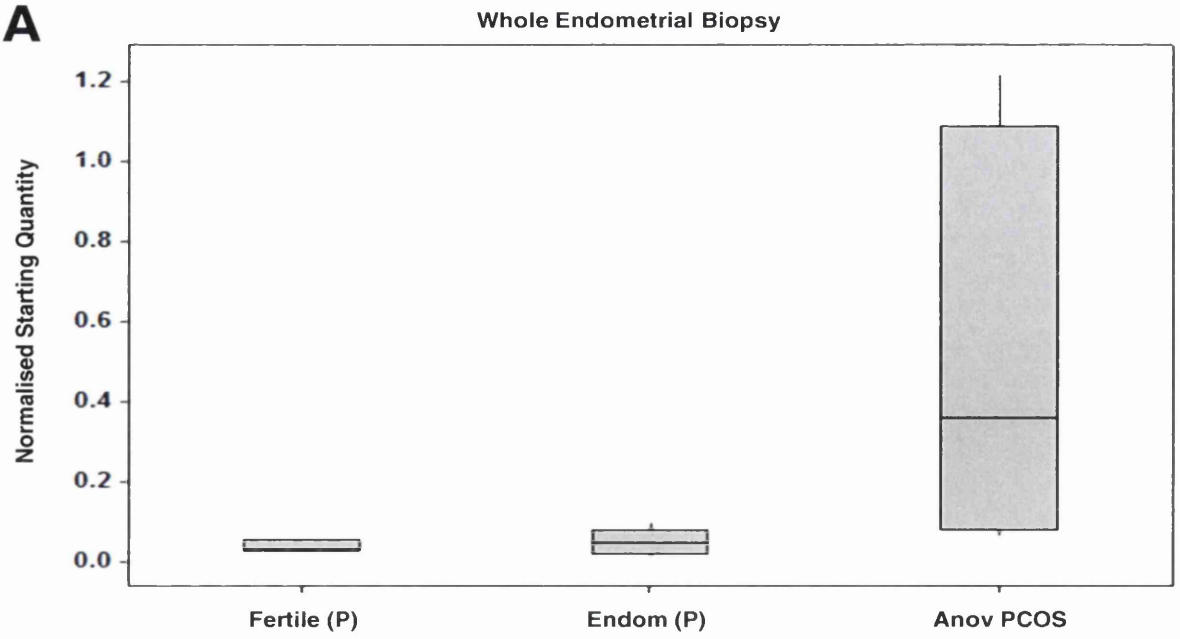

B

Total Biopsy	Endom (P)	anov PCOS
P values. Fertile (P) vs	0.897	0.023
Fold Change	1.5	11.2

Figure 3-12 RAGE transcript is expressed in proliferative phase fertile and infertile human endometrium.

Box plot shows RAGE mRNA levels in whole tissue biopsy specimens in the proliferative (P) phase of the menstrual cycle by real time PCR (A). Values given are mean starting quantity (StQ) from PCR triplicates per sample normalised to RPL19. 16 patients were grouped by pathology as follows: Fertile P (n=3), Endometriosis P (n=6) and anovulatory (anov) PCOS (n=7). Data was analysed using the statistical Mann-Whitney test. Data shown is group P value vs. Fertile (P) group where P<0.05 is significant (B).

Fig. 3.12A demonstrates that RAGE transcript levels in the endometrium of infertile anovulatory PCO pathology were significantly greater than in fertile endometrium. This was reflected in a statistically significant (Fig. 3.12B, p=0.023) 11.2 fold increase in the median normalised StQ for RAGE transcript compared to the fertile group. The slight 1.5 fold increase in the median normalised StQ for RAGE expression, proliferative phase endometriotic endometrium was not statistically different from the fertile controls (Fig. 3.12B, p=0.897). These results indicated that RAGE mRNA

was elevated in proliferative phase whole endometrial tissue of anovulatory PCOS women but not in proliferative phase endometriosis when compared to fertile individuals (Fig. 3.12A). The levels of RAGE transcript were consistent with the significantly elevated RAGE protein expression in PCO endometrium and were also consistent with less prominent increases in protein in endometriotic tissue (Fig 3.2A, Fig. 3.3A and Fig. 3.4A). In order to assess the relative contribution of RAGE mRNA specifically within the epithelium, epithelial cells were isolated from proliferative phase endometrial tissue and the above experiments repeated.

A

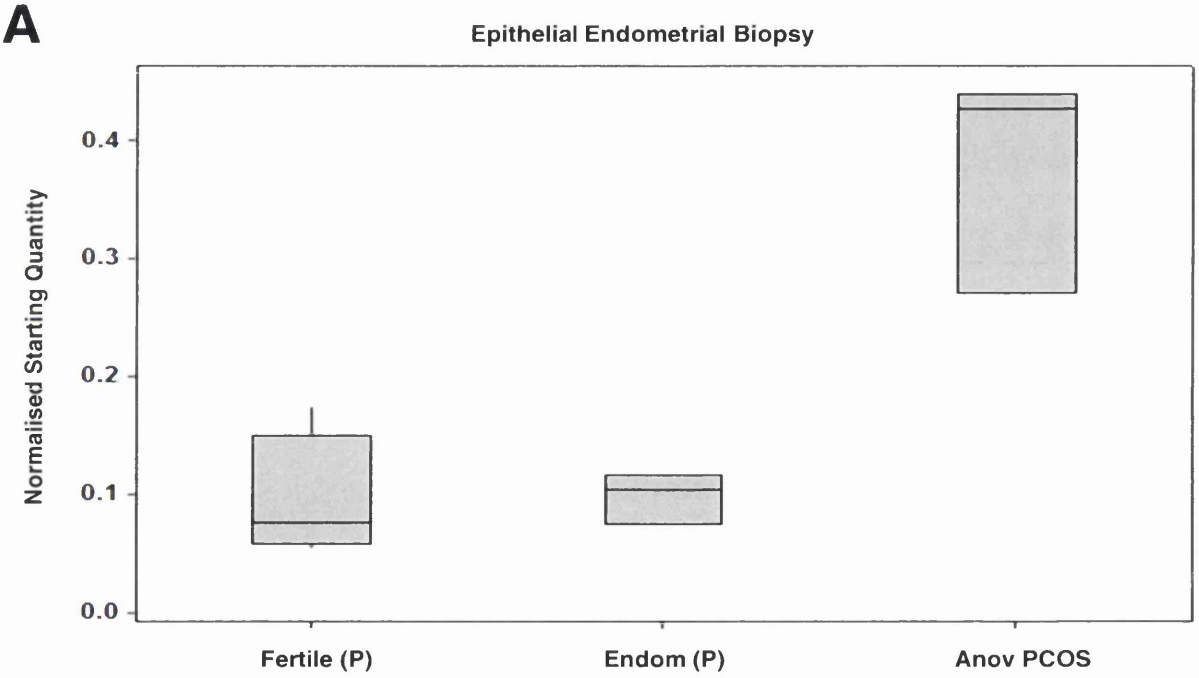

B

Epithelial Biopsy	Endom (P)	anov PCOS
P values. Fertile (P) vs	0.859	0.052
Fold Change	1.4	5.6

Figure 3-13 RAGE transcript is expressed in proliferative phase fertile and infertile human endometrial epithelium.

Box plot shows RAGE mRNA levels in epithelial endometrial biopsies in the proliferative (P) phase of the menstrual cycle by real time PCR (A). Values given are mean starting quantity from PCR triplicates normalised to RPL19. 10 patients were grouped by pathology as follows: Fertile P (n=4), Endometriosis P (n=3) and anovulatory (anov) PCOS (n=3). Data was analysed using the

statistical Mann-Whitney test. Data shown is group P value vs. Fertile (P) group where P<0.05 is significant (B).

The results in Figure 3.13A demonstrate epithelial RAGE mRNA was 5.6 fold greater in proliferative phase endometrium of infertile anovulatory PCOS women than in fertile controls (p=0.052). In contrast, RAGE mRNA was only elevated 1.4 fold in proliferative phase endometriotic epithelium which was not statistically significant when compared to fertile controls (Fig. 3.13B, p=0.859). These data indicate that RAGE transcript was increased in proliferative phase anovulatory PCO endometrial epithelium but not in endometriotic epithelium. These results also correlate with the protein levels observed for RAGE in proliferative phase ovulatory and anovulatory PCO epithelial glands and lumen in the IHC experiments (Fig. 3.6).

3.7 RAGE transcript is expressed in whole tissue and epithelial cells isolated from fertile and infertile secretory phase endometrium

Secretory phase PCO and endometriotic endometrium expressed more RAGE in the epithelial glands (Fig. 3.7A) and stroma (Fig. 3.9A) than in fertile endometrium. In addition, secretory phase ov and anovulatory PCO endometrium also expressed greater luminal RAGE (Fig. 3.8A) than fertile women. It was therefore of interest to investigate the level of RAGE mRNA in secretory phase whole endometrial tissue and epithelial cells isolated from fertile and infertile women.

A

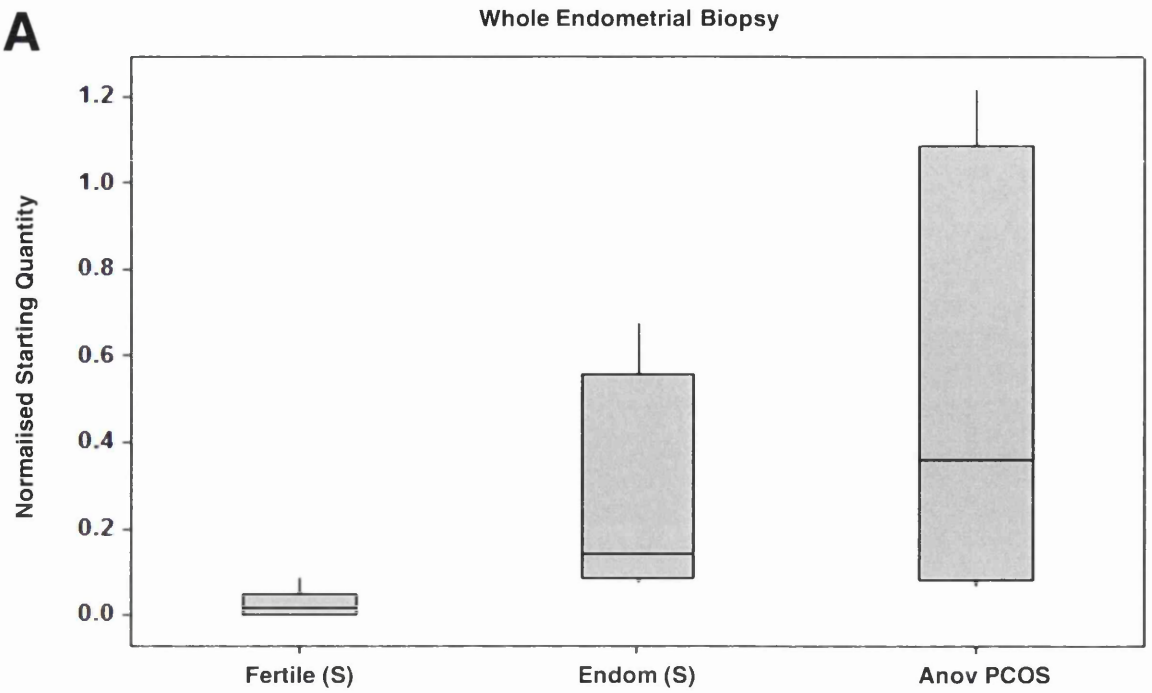

B

Total Biopsy	Endom (S)	anov PCOS
P values. Fertile (S) vs	0.008	0.008
Fold Change	9.3	23.6

Figure 3-14 RAGE transcript is expressed in secretory phase fertile and infertile human endometrium.

Box plot shows RAGE mRNA levels in whole tissue biopsy specimens in the secretory (S) phase of the menstrual cycle by real time PCR (A). Values given are mean starting quantity (StQ) from PCR triplicates per sample normalised to RPL19. 20 patients were grouped by pathology as follows: Fertile S (n=6), Endometriosis S (n=7) and anovulatory (anov) PCOS (n=7). Data was analysed using the statistical Mann-Whitney test. Data shown is group P value vs. Fertile (S) group where P<0.05 is significant (B).

Results in Figure 3.14A showed RAGE transcript levels in the endometrium of infertile endometrial pathology were significantly greater than in fertile endometrium. This was reflected in a statistically significant (Fig. 3.14B, p=0.008) 9.3 fold increase in the mean normalised StQ for RAGE mRNA in secretory phase endometriosis with respect to fertile tissue. Furthermore, the mean normalised StQ for RAGE mRNA was distinctly elevated 23.6 fold in secretory phase anovulatory PCO tissue when compared to fertile

endometrium (Fig. 3.14B, p=0.008). These findings suggest that RAGE mRNA expression in endometriosis may be influenced by the menstrual phase as significantly elevated RAGE mRNA was only observed in secretory endometriotic endometrium (Fig. 3.14A).

A

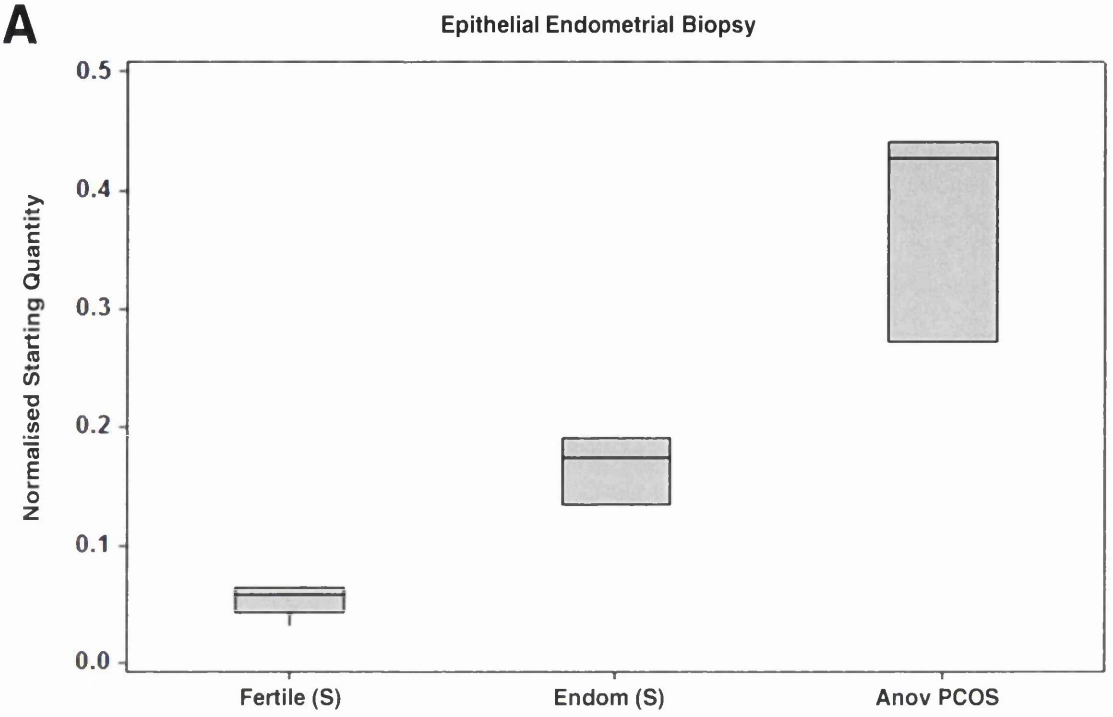

B

Epithelial Biopsy	Endom (S)	anov PCOS
P values. Fertile (S) vs	0.036	0.036
Fold Change	2.9	7.4

Figure 3-15 RAGE transcript is expressed in secretory phase fertile and infertile human endometrial epithelium.

Box plot shows RAGE mRNA levels in epithelial endometrial biopsies in the secretory (S) phase of the menstrual cycle by real time PCR (A). Values given are mean starting quantity from PCR triplicates normalised to RPL19. 11 patients were grouped by pathology as follows: Fertile S (n=5), Endometriosis S (n=3) and anovulatory (anov) PCOS (n=3). Data was analysed using the statistical Mann-Whitney test. Data shown is group P value vs. Fertile (S) group where P<0.05 is significant (B).

Finally, the expression of RAGE transcript in secretory phase endometrial epithelium was assessed. The results in Figure 3.15A demonstrated RAGE mRNA was greater in secretory phase endometrial epithelium of infertile

pathology than in fertile controls. RAGE mRNA was significantly increased 2.9 fold in secretory phase endometriotic and 7.4 fold in anovulatory PCO endometrial epithelium (Fig. 3.15B, p=0.036) when compared to fertile controls. As observed in whole endometrial tissue, endometriotic epithelial cells showed elevated RAGE mRNA in secretory but not proliferative phase epithelium (Fig. 3.13A and Fig. 3.15A). Despite limited epithelial sample numbers, an increase in RAGE transcript was evident across all secretory phase infertile endometrial pathologies (Fig. 3.15A).

3.8 RAGE transcript is expressed in human endometrial epithelial cell lines

This work has characterized RAGE expression for the first time in eutopic human endometrium at different stages of endometrial development *in vivo*. In other studies, RAGE expression has recently been demonstrated in ectopic ovarian endometriotic stroma (Sharma, Dhawan et al. 2010). It was not feasible to obtain sufficient primary endometrial samples to investigate the mechanisms behind RAGE regulation in *in vivo* experiments. Thus, RAGE mRNA expression was determined in four epithelial cell lines derived from endometrial adenocarcinoma to provide *in vitro* experimental models in which to continue further studies.

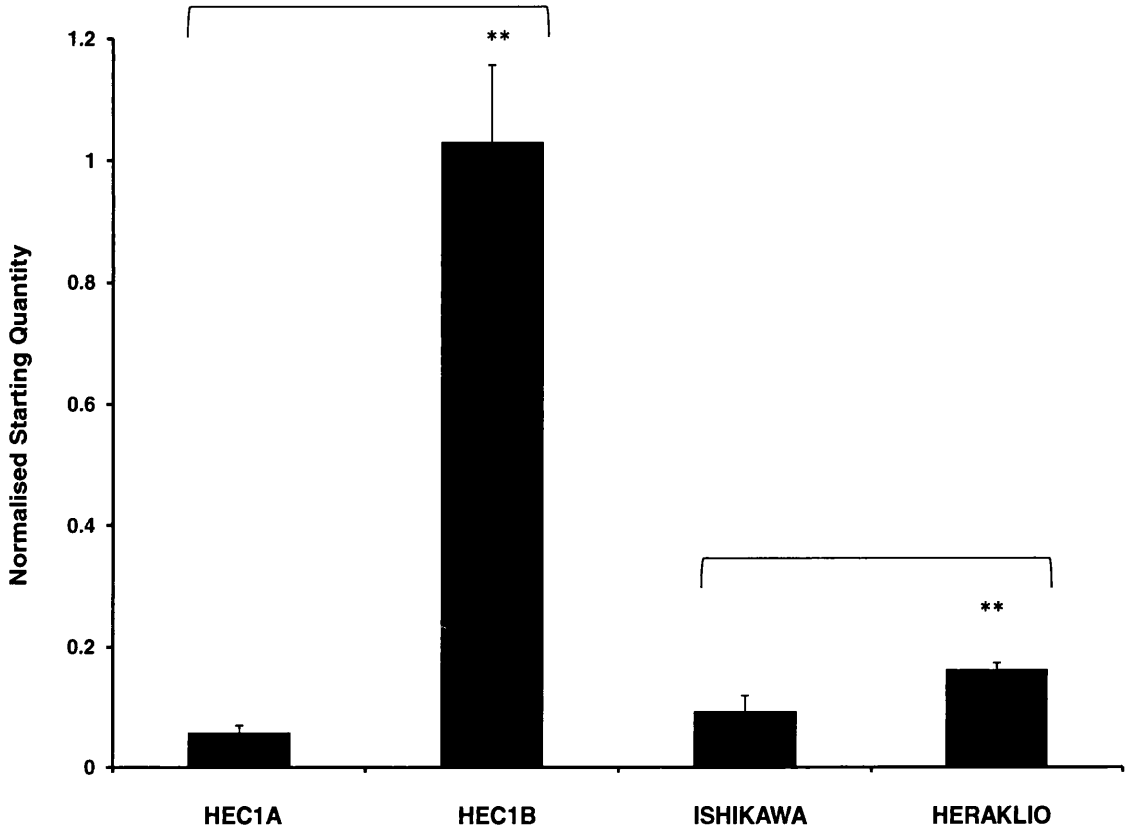

Figure 3-16 RAGE is expressed in endometrial epithelial adenocarcinoma cell lines.

Bar graph shows RAGE transcript levels in four endometrial epithelial cell lines derived from two well-differentiated stage 1 adenocarcinomas; HEC1 (HEC1A, HEC1B) and Ishikawa (Ishikawa, Heraklio) by real time PCR. Untreated cells were grown to confluent monolayers in 6 well culture plates. RNA was collected using the RNeasy Mini Kit (Qiagen) according to manufacturer's instructions. RNA was reverse transcribed and analysed by real time PCR as described in materials and methods (Ch2 section 2.7). Values given are the mean starting quantity (StQ) normalised to RPL19 ± STDEV from triplicate values. Data was analysed using a two-tailed students T-test ** P< 0.01 vs. HEC1A cells.

Real time PCR revealed that RAGE transcript was expressed in the selected cell line models (Fig. 3.16). Ishikawa (ERα positive) and Heraklio (ERα negative) cells displayed 1.6 and 2.8 fold greater basal RAGE mRNA

compared to HEC1A cells, which expressed the lowest level of RAGE transcript in the four cell lines tested. Basal RAGE mRNA was significantly greater in HEC1B than all other cell lines, and had 18 fold higher RAGE transcript than HEC1A from which it was derived. Interestingly, basal RAGE transcript was greater in both HEC1B and Heraklio which did not express ERα in comparison to their counterpart ERα positive parent strains HEC1A and Ishikawa. The possibility of endometrial RAGE modulation by the ER receptors α and β was further explored in HEC1A and HEC1B cell lines in Chapter 5.

3.9 Discussion

Prior to this work, RAGE expression in eutopic endometrium had only been demonstrated at the mRNA level in a small cohort of fertile women (n=4) (Fujii, Nakayama et al. 2008). RAGE expression in fertile and infertile eutopic endometrium and its tissue subtype localisation was still undetermined when this work was undertaken. RAGE expression in anovulatory PCO endometrium could not be assigned to a specific stage in the menstrual cycle due to the chronic anovulation and irregular menses of the patients. Nevertheless, immunohistochemistry revealed that irrespective of tissue subtype localisation or menstrual cycle phase, RAGE protein expression was consistently elevated 1.7 fold or more in ovulatory and anovulatory infertile PCO endometrium when compared to fertile controls. However, differential RAGE expression in the endometrium of fertile and infertile PCOS women was most apparent in proliferative phase glands (Fig. 3.2A, >5 fold vs. fertile). In addition, RAGE mRNA was significantly elevated in whole tissue (11.2 and 23.6 fold) and epithelial cells (5.6 fold and 7.4 fold) isolated from infertile anovulatory PCO endometrium when compared to fertile controls, particularly

in secretory phase (Fig. 3.12-15). In contrast to PCOS where RAGE was overexpressed in all endometrial tissue compartments, significantly elevated RAGE expression was confined only to proliferative phase epithelium (>3 fold) and secretory phase glands (3 fold) and stroma (2 fold) in endometriosis patients when compared to fertile women. Luminal RAGE expression in endometriotic endometrium was not significantly different from fertile controls. However, infertile endometriotic endometrium had greater RAGE transcript levels than fertile controls irrespective of menstrual cycle phase (Fig. 3.12-3.15. These novel results indicated that endometrial RAGE may be over-expressed in endometriosis and PCOS throughout the menstrual cycle, with particularly high levels of RAGE in infertile endometrium of ovulatory PCO pathology. Furthermore, these results suggest that RAGE expression at the protein level may be influenced by or fluctuate with the menstrual cycle in endometriotic tissue.

Finally, RAGE transcript was differentially yet notably expressed in four cell models of the endometrial epithelium, with distinctly high basal expression observed in HEC1B cells, thus indicating that these cells models were suitable for the study of RAGE. It can be hypothesised that pathology-specific endocrine factors mediating RAGE expression may lead to an altered uterine environment. Central to this hypothesis is the observation that RAGE is elevated in endometriotic and PCO endometrium in comparison with fertile controls, both at the transcriptional (Fig. 3.12-3.15) and protein level (Fig. 3.2-3.4 and Fig. 3.7-3.9). It is my hypothesis that RAGE is over-expressed in the endometrium of infertile anovulatory and ovulatory PCOS and endometriosis patients potentially as a result of altered hormonal profiles, elevated AGE and possible NFκB activation, which is further explored in Chapters 4 and 5.

3.10.1 RAGE expression is elevated in eutopic endometrium of infertile ovulatory and anovulatory PCOS women

Elevated RAGE positively correlates with the level of AGEs in the serum and ovarian tissues of infertile PCO women in comparison to fertile controls (Diamanti-Kandarakis, Piperi et al. 2007). AGE-RAGE interaction positively regulates RAGE expression in an auto-regulatory feedback loop likely mediated by NFκB activation (Tanaka, Yonekura et al. 2000). Importantly, increased NFκB-p65 occupation of RAGE positively correlated with AGE treatment in endometrial epithelial cells (Ch. 4, Fig. 4.8). While these findings did not provide direct evidence, NFκB was potentially implicated as being upstream of RAGE. In fertile endometrial glands, phosphorylated (ser276) NFκB-p65 expression was significantly increased, and cytoplasmic restriction of RAGE activator TNFα lifted during the secretory phase suggesting nuclear translocation (Saegusa, Hashimura et al. 2007). Notably, TNFα is also elevated in PCO serum and monocytes (Sayin, Gucer et al. 2003; Gonzalez, Rote et al. 2006). Therefore, one possibility for the significantly elevated endometrial RAGE in PCOS could potentially be due to activated NFκB signalling. Studies have also shown ERα is elevated in PCO endometrium with respect to fertile women (Villavicencio, Bacallao et al. 2006; MacLaughlan, Palomino et al. 2007; Margarit, Taylor et al. 2010). This may provide an explanation for higher RAGE protein levels in proliferative phase ovulatory PCOS with respect to anovulatory PCO and fertile controls, correlating with the rise in E2 (Fig. 3.2-4). Elevated endometrial RAGE in anovulatory PCOS may be principally regulated by AGEs, as is the case in the ovary (Diamanti-Kandarakis, Piperi et al. 2007) or perhaps by increased estrogens synthesised from excess androgens in PCO adipose tissue (Wang,

Lu et al. 1998; Kaaks, Lukanova et al. 2002). Hyperinsulinaemia stimulates ovarian and adrenal hyperandrogenism and exacerbates hyperglycaemia-induced AGE formation in PCOS which may up-regulate RAGE *in vivo* (Zhang and Liao 2010). It can therefore be speculated that excess androgens and estrogens could elevate RAGE expression in PCOS.

3.10.2 RAGE is elevated in endometriotic eutopic endometrium of infertile women

Nuclear ERα expression and 17β estradiol are significantly elevated in eutopic endometriotic endometrium (Lessey, Palomino et al. 2006; Margarit, Taylor et al. 2010). Notably, RAGE was transcriptionally regulated by 17β estradiol in HEC-1 endometrial epithelial cells expressing both ERα and ERβ receptors (Ch.5 Fig. 5.3). However, only ERα appeared to actively regulate RAGE at the protein level, as concluded in other studies (Tanaka, Yonekura et al. 2000, Ch.5 Fig. 5.4). Furthermore, increased ERα occupation of Sp1 and Ap1 sites on RAGE was observed in response to E2 treatment in ERα positive HEC1A endometrial cells (Ch.5 section 5.5). Uterine ERα and ERβ expression is elevated during the proliferative phase mimicking the pre-ovulation increases in estrogen (King, Critchley et al. 2001). This may correlate with the greatest RAGE expression being observed in proliferative phase endometriosis (Fig. 3.2A, 3.3A). In the mid-luteal phase however, ERα levels decline due to its down-regulation by elevated progesterone and potentially, according to several reports, reciprocal down-regulation of ERα by ERβ (Weihua, Saji et al. 2000; King, Critchley et al. 2001; Weyant, Carothers et al. 2001; Trukhacheva, Lin et al. 2009). Immunohistochemistry revealed that RAGE expression remains elevated in secretory phase

endometriotic epithelial glands (Fig. 3.7A) and stroma (Fig. 3.9A) with respect to same phase fertile controls. Similarly, with respect to fertile controls, markedly elevated RAGE mRNA in endometriotic whole tissue and epithelial cells was observed in the secretory phase (Fig. 3.14-15). Coincidently, it has been reported that ERα is dysregulated in endometriotic endometrium remaining elevated during the secretory phase (Lessey, Palomino et al. 2006). Sustained elevated RAGE in endometriotic endometrium could perhaps be attributed to dysregulation of several secretory phase-specific factors; ERα signalling, NFκB and a plethora of decidua-secreted agents. In particular, abnormal dysregulation of TGFβ1, IL-6, and IL-1β and constitutive NFκB signalling which are implicated in RAGE signalling in several cellular contexts, have been reported in eutopic and ectopic endometriosis (Bergqvist, Bruse et al. 2001; Boulanger, Grossin et al. 2007; Dimitriadis, Stoikos et al. 2006; Sato, Wu et al. 2009; van Zoelen, Yang et al. 2009; Rasheed, Akhtar et al. 2011). In addition, RAGE, sRAGE and VEGF, which have been shown to be up-regulated by E2 in the endometrium, were reportedly elevated in the tissue and follicular fluid of women with ectopic ovarian endometriosis and adenomyosis (Mueller, Vigne et al. 2000; Tanaka, Yonekura et al. 2000; Fujii and Nakayama 2010; Sharma, Dhawan et al. 2010). Thus, elevated endometrial RAGE could perhaps be attributed to the highly estrogenic milieu of endometriosis and potentially contributes to the pathological process through perpetuating underlying hormone-dependent inflammation.

Chapter 4

AGEs regulate RAGE expression in human endometrial epithelial cells through the NFκB pathway

4. AGEs regulate RAGE expression in human endometrial epithelial cells through the NFκB pathway

4.1 Introduction

It is widely accepted that following engagement of RAGE by AGEs, a signalling cascade is activated that positively regulates not only its expression but also that of other NFκB target genes through the activation of p65 and the NFκB pathway (Kislinger, Fu et al. 1999; Singh 2001). The popular hypothesis of this positive feed-forward loop that sustains the expression of RAGE and NFκB has been linked to the perpetuation of inflammatory responses particularly in diabetic vasculature where AGEs accumulate (Schmidt, Yan et al. 1999; Evans, Goldfine et al. 2002; Gao, Zhang et al. 2008). Female infertility disorders have also been characterised by impaired insulin tolerance and hyperglycaemia, in particular Polycystic Ovary Syndrome (PCOS) and endometriosis (Dickerson, Cho et al.; Toprak, Yonem et al. 2001; Garry 2004; Fica, Albu et al. 2008; Caglar, Oztas et al. 2011) making these women especially susceptible to endothelial dysfunction, CVD and the onset of diabetes (Zargar, Gupta et al. 2005; Kelestimur, Unluhizarci et al. 2006; Beckman, Goldfine et al. 2007; Amini, Horri et al. 2008; Jayaraman, Subrahmanya et al. 2009; Soares, Vieira et al. 2009). Elevated AGEs have been shown to co-localise with RAGE in polycystic ovaries and have also been shown to correlate with elevated levels of RAGE in circulating monocytes of PCO women (Diamanti-Kandarakis, Piperi et al. 2005). Recently, insulin resistance and hyperinsulinaemia have been linked to increased expression of phosphorylated ERK 1/2 MAPK kinase in PCO endometrium compared to normal endometrium. Furthermore, PCOS women with endometrial hyperplasia or carcinoma irrespective of fertility status had

significantly greater activated ERK 1/2 protein levels than normal endometrium (Song, Zhang et al. 2010). Hyperinsulinemic PCO endometrium, in comparison to normoinsulinemic PCO and control endometrium without this metabolic defect, exhibits lower epithelial insulin receptor substrate (IRS-1) and diminished GLUT-4 protein expression despite having comparable levels of Insulin Receptor (IR) at the cell surface (Fornes, Ormazabal et al. 2010). This suggests that while epithelial endometrial cells possess the machinery to maintain glucose homeostasis, deficiency in glucose transportation could increase the availability of free glucose, AGE formation and occupation of RAGE in PCO endometrium (Rosenbaum, Haber et al. 1993; Fornes, Ormazabal et al. 2010; Johansson, Feng et al. 2010). Diminished GLUT-4 and IRS-1 expression in glandular epithelial endometrium has also been reported following testosterone stimulation mimicking the androgenic milieu of PCOS. This effect however was partially reversed using AGE-inhibitor Metformin (Zhang and Liao 2010). Furthermore, metabolic aberrations arising from transient high glucose, impaired IR signalling and elevated AGEs have more recently been implicated in complications associated with infertility and pregnancy such as preeclampsia, foetal-maternal inflammation and preterm birth particularly in diabetic and PCO women where the affects of AGEs are prevalent (Amini, Horri et al. 2008; Hajek, Germanova et al. 2008; Harsem, Braekke et al. 2008; Germanova, Koucky et al. 2009; Noguchi, Sado et al. 2010).Taken together, the aforementioned studies highlight the importance of elucidating the possible effects of an endometrial AGE-RAGE axis on NFκB activation, expression of RAGE and its potential downstream target MUC1 that may perhaps impact on fertility and progression towards endometrial cancer in

female infertility disorders. The effect of AGEs on the transcriptional regulation of endometrial RAGE is, at the time of writing, still yet to be determined. With this in mind, the work in this chapter investigates the effects of glycated human serum albumin (AGE-HSA) treatment on the expression of RAGE in epithelial endometrial cell lines both at the transcriptional and protein level. The effect of AGE-HSA on the levels of phosphorylated p65, a transcriptional factor involved in the modulation of RAGE in other cell systems, was also explored in Ishikawa and Heraklio endometrial cells. Chromatin immunoprecipitation was employed to determine p65 binding to the RAGE promoter and the promoter of MUC1 in order to give evidence for the involvement of the NFκB pathway in the regulation of RAGE by AGE-HSA.

4.2 Effect of AGE on RAGE transcript expression in human endometrial epithelial cells

The RAGE receptor was originally thought to exist to mediate signalling that aided neuronal cell differentiation however it is found naturally in a variety of tissues expressed at low basal levels. RAGE expression can be influenced by numerous factors including increased androgens, free β-catenin, ROS and cytokines; all characteristic of diabetic and endocrine metabolic aberrations, the most documented of which are the AGEs (Otero 2001; Csiszar and Ungvari 2008; Pertynska-Marczewska, Glowacka et al. 2009; Diamanti-Kandarakis, Lambrinoudaki et al. 2010). Cellular exposure to AGEs is hypothesised to activate the proto-oncogenic MAPK kinase pathway which orchestrates the nuclear translocation of phosphorylated NFκB subunits and subsequent activation of genes involved in chronic inflammation and disease (Csiszar and Ungvari 2008; Liu, Zhao et al. 2009; Liu, Liang et al. 2010). It is

the popular hypothesis that engagement of the RAGE receptor by AGEs is required for these signalling events to occur, however this association remains unverified in human endometrium. For this study, human epithelial endometrial adenocarcinoma cells were used to assess the effect of AGE-HSA on RAGE transcript levels in the uterus. HEC1 cells have been shown to be model cell lines for the epithelial endometrium and have previously been used to further explore mitogenic activity of growth factors and their outcome on endometrial cell proliferation and apoptosis (Bergman, Talavera et al. 1997; Connor, Talavera et al. 1997; Kurarmoto, Hamano et al. 2002; Cong, Gasser et al. 2007). Furthermore, Ishikawa and Heraklio (ERα negative Ishikawa) cells have been extensively exploited to investigate the effect of sex steroid and protein kinase signalling on uterine dysfunction, proliferation and blastocyst implantation failure (Hata and Kuramoto 1992; Nishida 2002; Guo, Wei et al. 2004; Guo, Wei et al. 2006; Lessey, Palomino et al. 2006; Schaefer, Fischer et al. 2010). These cell lines therefore provide appropriate models for investigating an AGE-RAGE signalling cascade that may affect uterine receptivity.

HSA is the most abundant protein in human serum. Its structure is a protein chain of 585 amino acids coupled by 17 disulphide bonds (Peters 1996) and has been studied alongside haemoglobin - another commonly glycated serum protein in diabetic conditions (Thornalley 2000; Ulrich 2001; Ahmed 2005). In *in vitro* experiments mass spectrometry has been used to investigate the specific glycation of the commercially available glycated HSA used in this study (~95% protein and 99% pure HSA glycated *in vitro,* giving 8.0 mol modified sites per mol protein, Sigma Aldrich, St. Louis, M.O) (Wa 2007). This *in vitro* glycation models the formation of AGEs from HSA in

plasma and serum *in vivo* (Gugliucci 1996; Lapolla 2005). Lysine residues 159, 212, 286,413 and 432 and arginine residues 81, 114 and 218 were shown to be the primary sites targeted for glycation. Glycation at these specific sites gives rise to different forms of glycated HSA (Wa 2007; Barnaby, Wa et al. 2010). For example, glycation at lysine residues 159 and 286 gave rise to the AGEs pyrraline and CML-HSA respectively (Wa 2007). Therefore, the effect on RAGE transcript seen in this study occurs through exposure to multiple HSA-derived AGE isoforms. The physiological impact of AGE-HSA on RAGE transcript levels in other cell models has previously been characterised (Fujita; Cortizo 2003; Yamagishi, Matsui et al. 2008; Sourris and Forbes 2009; Tanikawa 2009; Koyama and Nishizawa 2010). Studies leading up to this project using AGE-BSA showed that AGE could induce RAGE transcript in two endometrial epithelial cell lines HEC1A and HEC1B (Fig. 4.1). Briefly, AGE-BSA was generated by incubating 2g BSA with 10mL 1.5M D-glucose in 50mL 0.1M PBS pH 7.4. The BSA solution was filter sterilized and incubated at 37°C for 9 weeks in a CO_2 monitored incubator before use to allow for the glycation process as described in Tanaka et al 2000.

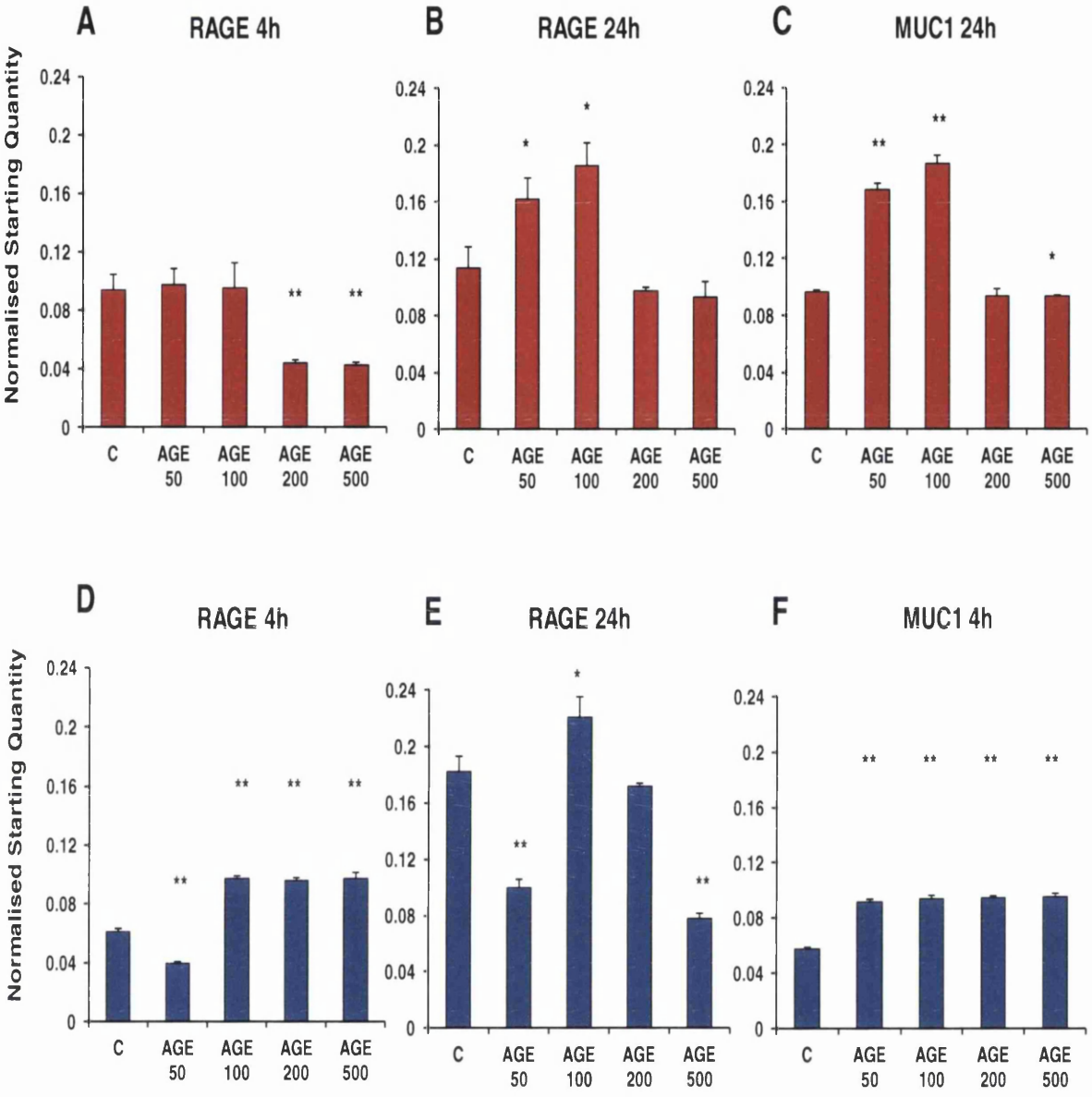

Figure 4-1 AGE-BSA induces RAGE and MUC1 expression in HEC-1 endometrial epithelial cells.

Bar graphs show the effect of varying AGE-BSA concentrations on RAGE and MUC1 transcript levels in HEC1A (A, B, C) and HEC1B (D, E, F) by real time PCR. HEC-1 cells were treated with 50, 100, 200 and 500μg/mL AGE-BSA for 4 and 24h. Data shown is from singular experiments. Values given are mean starting quantity (StQ) normalised to GAPDH ± STDEV from StQ triplicates. Data was analysed using a two-tailed students T-test *p=<0.05, **p=<0.01 vs. Control (C).

RAGE transcript was not induced by AGE-BSA in HEC1A cells at 4h. In fact, AGE-BSA at concentrations exceeding 100μg/mL significantly reduced

RAGE expression at 4h (Fig. 4.1A). In contrast 100μg/mL AGE-BSA induced RAGE transcript by 1.6 fold after 24h in HEC1A (Fig. 4.1B). MUC1 transcript levels were induced 1.9 fold 24h post challenge with AGE-BSA in HEC1A (Fig. 4.1C). AGE-BSA at 100μg/mL induced RAGE transcript 1.6 fold in HEC1B and transcript levels remained elevated at 200μg/mL (1.57 fold) and 200μg/mL (1.59 fold) after 4h (Fig. 4.1D). RAGE induction with 100μg/mL AGE in HEC1B was reduced (1.2 fold) after 24h. Concentrations in excess of 100μg/mL appeared to repress the system at 24h (Fig. 4.1E). MUC1 transcript levels were also induced 1.6 fold 4h post AGE-BSA challenge in HEC-1B (Fig. 4.1F). These rapid responses to AGE-BSA have been demonstrated in skin and umbilical cord HMVECs with RAGE transcript increasing after just 2h and reaching a peak around 8h (Tanaka, Yonekura et al. 2000). In line with this observation most research investigating RAGE and potential RAGE-dependent NFκB target gene transcription has been undertaken within the window of 2 to 24h following RAGE-specific ligand stimulation (Tanaka, Yonekura et al. 2000; Ge, Jia et al. 2005; Cai, He et al. 2008; Zhang, Tasaka et al. 2008). The following *in vitro* studies investigate the effect of 10μg/ml commercially sourced AGE-HSA (Sigma-Aldrich) treatment on the expression of RAGE in human epithelial endometrial cell lines after 4 and 24h. Real time PCR was utilised to detect the expression of full length RAGE transcript of the membrane-bound isoform which recognises AGEs at the cell surface.

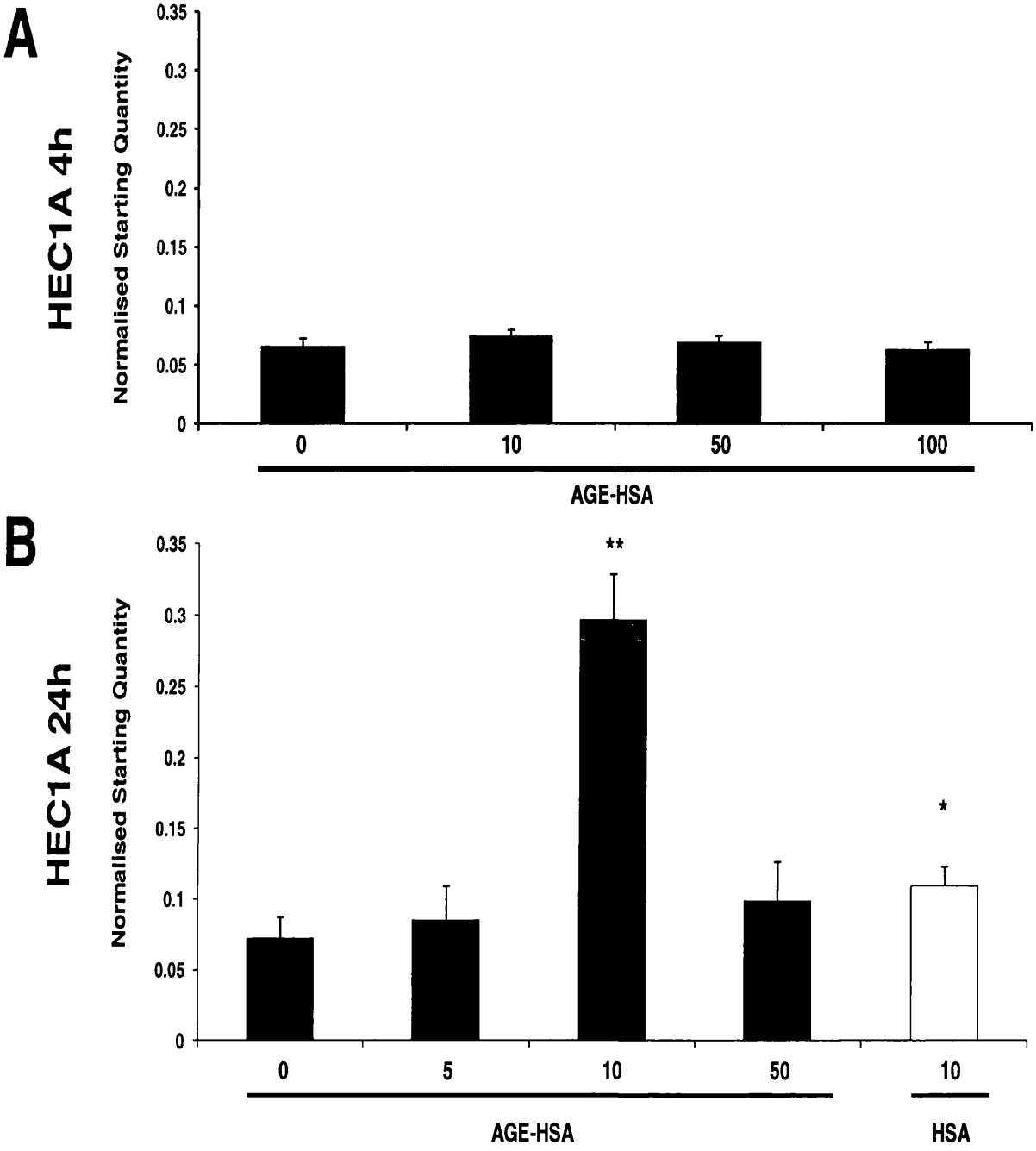

Figure 4-2 Effect of AGE-HSA on RAGE transcript levels in HEC1A endometrial epithelial adenocarcinoma cells.

Bar graphs show the effect of varying AGE-HSA concentrations on RAGE transcript levels after 4h (A) and 24h (B) by real time PCR. HEC1A cells were grown to confluent monolayer in 6 well culture plates and were either left untreated or treated with 5, 10, 50 and 100μg/mL AGE-HSA. Unmodified HSA (10μg/mL) was used as a biological negative control. Experiments were done in triplicate and typical results are shown. Values given are mean starting quantity (StQ) normalised to RPL-19 ± STDEV from StQ triplicates. Data was analysed using a two-tailed students T-Test *P<0.05, **P<0.01 vs. untreated control.

Preliminary studies in Figure 4.2A revealed that treatment with AGE-HSA for 4h had no significant effect on the level of RAGE transcript in HEC1A cells. RAGE mRNA expression remained unchanged despite stimulation with higher concentrations (100μg/mL) of AGE-HSA (Fig. 4.2A). However modulation of RAGE transcript by AGE-HSA was observed after 24h, with a statistically significant upregulation of RAGE expression (4 fold vs. control) occurring at the 10μg/mL dose (Fig. 4.2B). Whilst the effect of HSA was also statistically significant, the fold increase in RAGE expression was only 1.5 fold (Fig. 4.2B). High concentrations of AGE-HSA 50μg/mL and 100μg/mL (data not shown) however did not induce RAGE mRNA after 24h. From this, it could be suggested that RAGE modulation by AGE at the transcriptional level could be concentration dependant or perhaps involves AGE clearance mechanisms that protect the cell against AGE-induced oxidative stress or cytotoxicity. Overall, the levels of induced RAGE are higher in HEC1A cells (Fig. 4.2B) in comparison to HEC1B cells (Fig. 4.3A). The induction of RAGE transcript occurred later in HEC1A at 24h compared to the response to AGE-HSA seen at 4h in HEC1B and is likely to be a cell line specific observation (Fig. 4.1 B, D, 4.2B, 4.3A).

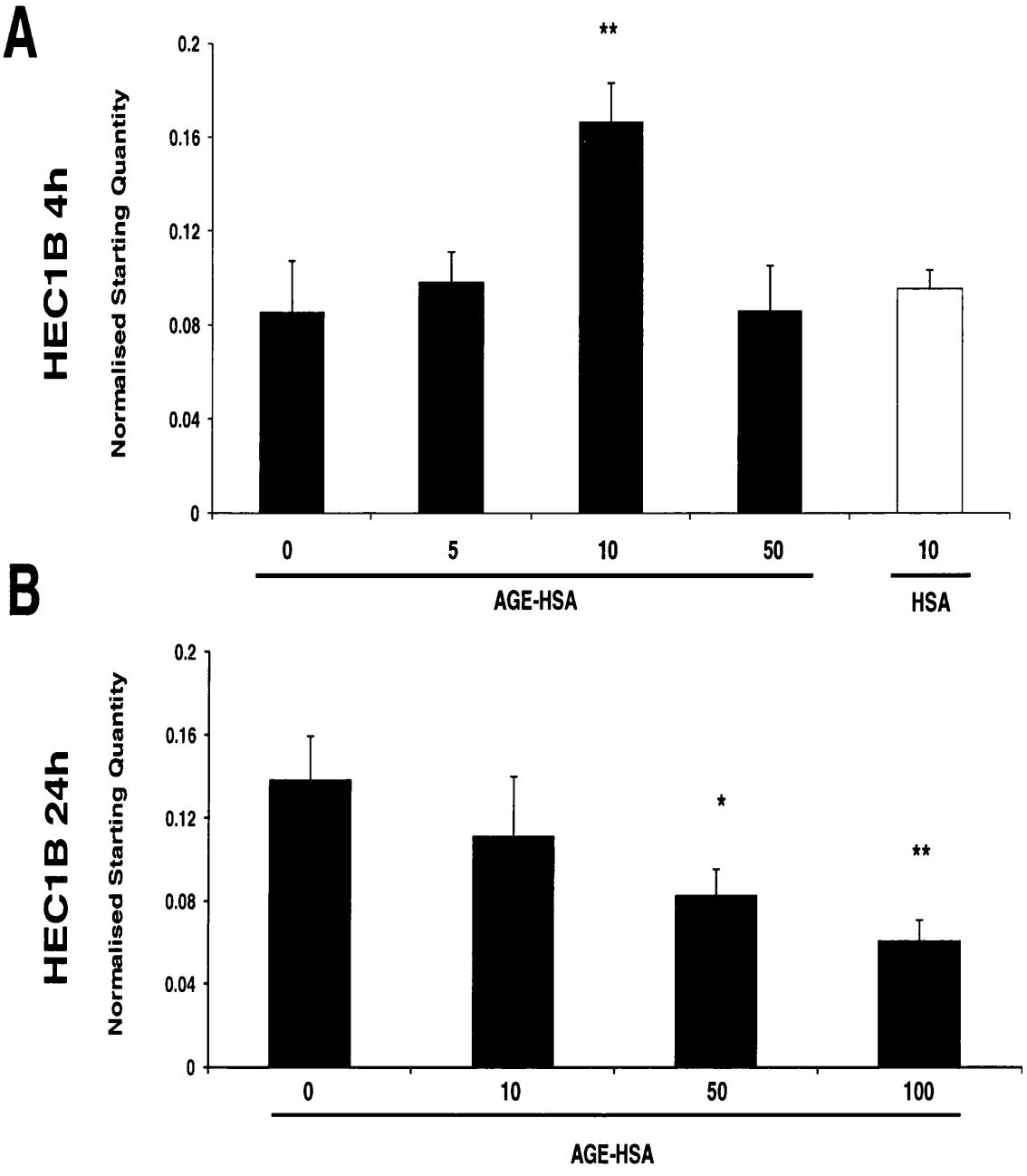

Figure 4-3 Effect of AGE-HSA on RAGE transcript levels in HEC1B endometrial epithelial adenocarcinoma cells.

Bar graphs show the effect of varying AGE-HSA concentrations on RAGE transcript levels after 4h (A) and 24h (B) by real time PCR. HEC1B cells were grown to confluent monolayer in 6 well culture plates and were either left untreated or treated with 5, 10, 50 and 100μg/mL AGE-HSA. Unmodified HSA (10μg/mL) was used as a biological negative control. Experiments were done in triplicate and typical results are shown. Values given are mean starting quantity (StQ) normalised to RPL-19 ± STDEV from StQ triplicates. Data was analysed using a two-tailed students T-Test *P<0.05, **P<0.01 vs. untreated control.

In contrast to its parent cell line HEC1A (Fig. 4.2A), incubation of HEC1B cells with AGE-HSA for 4h resulted in the modulation of RAGE transcript with a statistically significant up-regulation of RAGE mRNA (2 fold vs. control) occurring at the 10μg/mL dose (Fig. 4.3A). HSA showed no effect on RAGE transcript levels after 4h in these cells (Fig. 4.3A). However, following 24h AGE-HSA treatment, RAGE transcript levels were comparable with the untreated HEC1B cells at the inducing-concentration of 10μg/ml (Fig. 4.3B). AGE-HSA treatment for 24h at higher concentrations; 50μg/ml and 100μg/ml significantly reduced RAGE transcript levels 0.6 fold and 0.4 fold respectively when compared to the untreated control (Fig. 4.3B). In both HEC-1 cell lines, it appears that there may be a threshold dose that must be exceeded for induction to occur, and that excess AGE-HSA may repress the system. While previous studies in different cell models have noted similar effects, it cannot be ruled out that RAGE repression at high concentrations of AGE could be attributed to AGE-induced cytotoxicity (Tanaka, Yonekura et al. 2000; Cassese, Esposito et al. 2008). Basal levels of endometrial RAGE transcript were 18 fold greater in HEC1B than in HEC1A cells as described (Ch. 3, Fig. 3.16). For this reason, there is a possibility that the already high basal levels RAGE mRNA in HEC1B cells may mask AGE-HSA-mediated induction causing the AGE response to be more rapid (4h) yet less pronounced in this cell line than HEC1A in which induction occurs after 24h (Fig. 4.2B). In contrast, RAGE transcript is expressed at a low basal level in HEC1A cells (Fig. 3.16). The experimental data in Fig. 4.2B and Fig. 4.3A show for the first time that AGE products derived from HSA, a major protein component of serum (Peters 1996; Frolov and Hoffmann 2010) can induce the levels of RAGE mRNA in two *in vitro* models of the human epithelial endometrium.

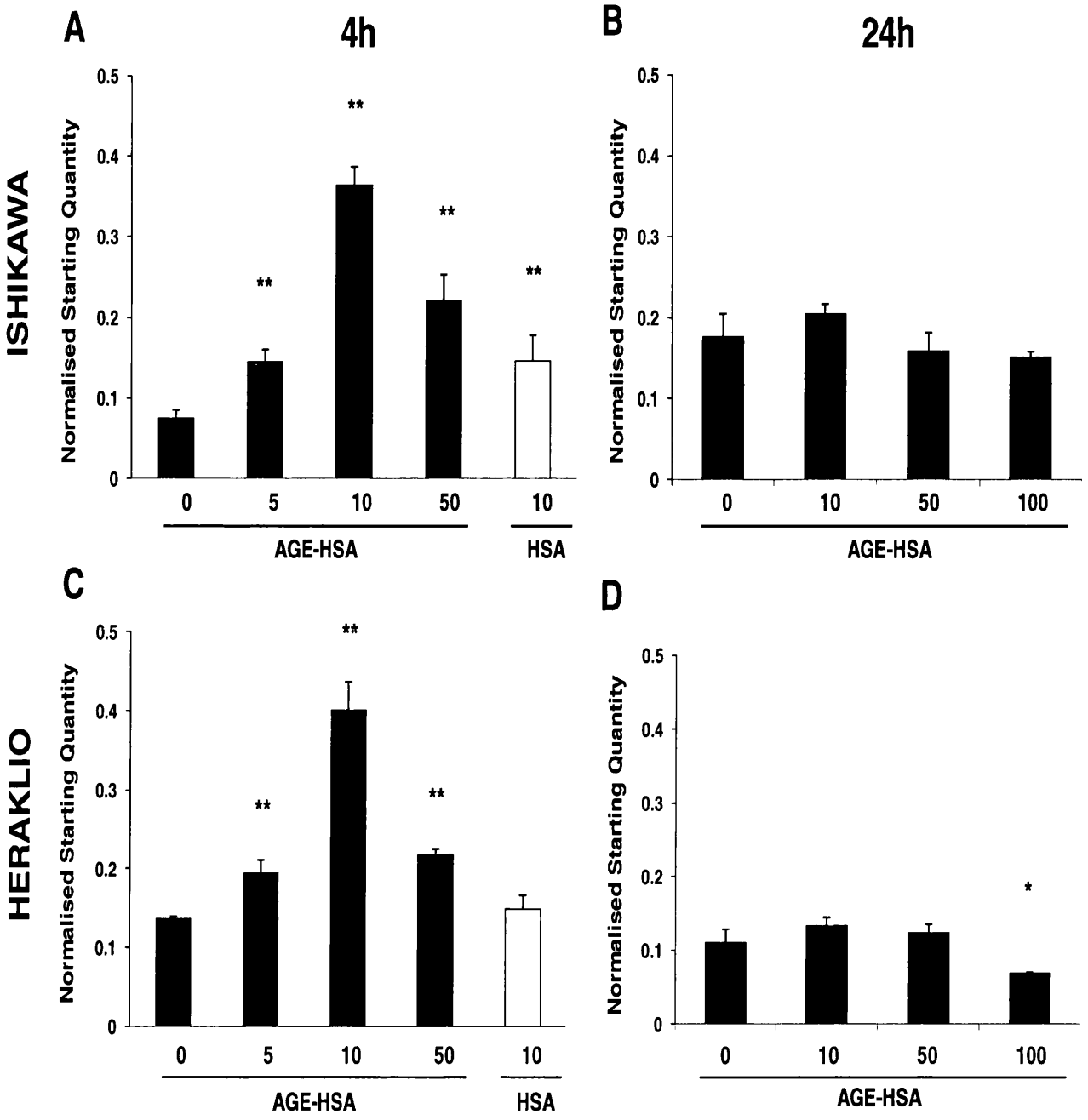

Figure 4-4 AGE-HSA up-regulates RAGE transcript levels in epithelial endometrial adenocarcinoma cells.

Bar graphs show the effect of varying concentrations of AGE-HSA on RAGE transcript levels in Ishikawa at 4h (A) and 24h (B) and Heraklio at 4h (C) and 24h (D) by real time PCR. Ishikawa and Heraklio cells were grown to confluent monolayers in 6 well culture plates and treated with 5, 10 and 50 μg/mL AGE-HSA and 100μg/mL in 24h samples (B, D). Unmodified HSA (10μg/mL) was used as a biological negative control. Experiments were done in triplicate and typical results are shown. Values given are mean starting quantity (StQ) normalised to RPL-19 ± STDEV from triplicates. Data was analysed using a two-tailed students T-Test *P<0.05, **P<0.01 vs. untreated control.

Results in Fig. 4.4 demonstrated that 4h AGE-HSA treatment could modulate RAGE transcript levels in Ishikawa (A) and Heraklio (C) cells with the greatest statistically significant induction occurring at the 10μg/mL dose in both cell lines. 10μg/mL AGE induced RAGE transcript in Ishikawa (4.8 fold vs. control) and Heraklio (3 fold vs. control) to similar levels suggesting that these cell lines respond to AGEs to the same degree (Fig. 4.4A, C). In comparison, 4h treatment with unmodified HSA did not induce RAGE in Ishikawa cells to the extent of the glycated form (1.9 fold). In Heraklio, HSA showed no effect on RAGE transcript levels. In both cell lines, AGE-HSA treatment had no real effect on RAGE mRNA expression after 24h. Transcript levels were not significantly altered from the levels observed in untreated cells (Fig. 4.4 B, D) which may indicate that AGE-induction of RAGE is a transient event, and the effect on its transcription is attenuated after 24h (Tanaka, Yonekura et al. 2000). Furthermore, the inducibility of RAGE appeared to be reduced at 4h and abolished after 24h at high AGE concentrations i.e 100μg/mL. This suggested either a dose-dependant response where high AGE saturated or repressed the system, or was due to a cell response to stress/toxicity (Fig. 4.4). These observations reveal for the first time that AGE-HSA can induce RAGE transcript levels *in vitro* in a second set of epithelial endometrial cells. Ishikawa and Heraklio cells displayed similar rapid responses to AGE-HSA treatment at 4h and were able to be cultured in media with lower glucose content thus limiting the level of exogenously formed AGEs in the environment. Utilisation of these cells was therefore favoured to the HEC-1 cells to further explore AGE-RAGE signalling in the endometrium.

4.3 Effect of AGE on RAGE protein expression in human endometrial epithelial cells

Levels of AGEs and full-length RAGE are elevated in diabetes and PCOS. These are disorders characterised by hyperinsulinaemia, insulin resistance and in the latter case, excess androgens which can augment AGE-RAGE-mediated activation of MAPK and regulation of androgen receptor (AR) and NFκB target genes (Csiszar and Ungvari 2008) including RAGE itself. Increased RAGE could possibly impact on fertilised blastocyst adhesion at the endometrial epithelial cell surface (Carson, Julian et al. 2006) through up-regulation of inflammatory cytokines and MUC1. Having determined that AGE-HSA up-regulates RAGE transcript levels at a concentration of 10μg/mL in endometrial cells it was important to determine whether this AGE-HSA concentration translates to an increase in RAGE protein.

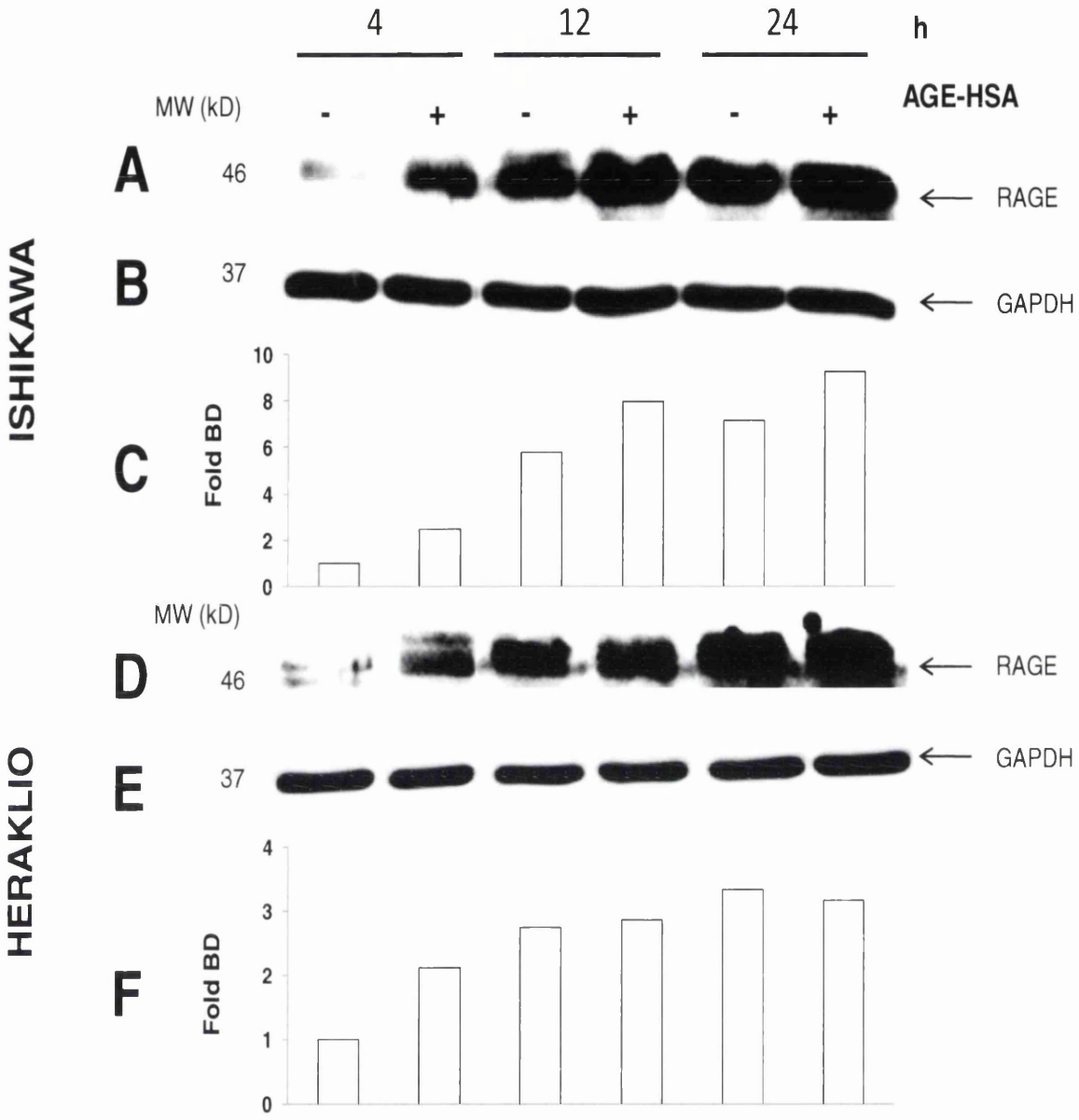

Figure 4-5 AGE-HSA up-regulates RAGE protein expression in endometrial epithelial cells.

Immunoblots show the effect of AGE-HSA treatment on RAGE protein in relation to untreated controls at 4, 12 and 24h in Ishikawa (panels A-C) and Heraklio (panels D-F). Confluent cells were incubated for 4, 12 and 24h with 10μg/ml AGE-HSA and harvested in RIPA protein buffer (SIGMA). Immunocomplexes were separated by SDS-PAGE followed by immunoblotting with RAGE specific (H300: sc-5563) and GAPDH specific (FL-335: sc-25778) rabbit polyclonal antibodies (Santa Cruz) as described in methods (Ch 2 section 2.9). Bands corresponding to the un-truncated RAGE membrane-tethered protein were detected at 46kDa.

Band Density (BD) was determined using the Quantity One software (Bio-Rad) using the volume rectangle tool for signal intensity/area mm^2. BD is displayed as the fold expression relative to 4h untreated control (Panels C and F) normalised to respective GAPDH samples (Panels B and E). Experiments were done in triplicate and typical results are shown.

Protein blot analysis revealed that treatment with 10µg/ml AGE-HSA resulted in an increase in membrane-bound RAGE protein in both endometrial cell lines examined. Following AGE-HSA treatment in Ishikawa, RAGE protein levels were 2.5 fold that observed in the respective untreated control at 4h (Fig. 4.5 panels A, C). RAGE protein is initially induced 2 fold after 4h in Heraklio cells also pinpointing a rapid response to cellular AGE exposure and is comparable with the effect seen in Ishikawa at 4h (Fig. 4.5 panels D, F). Protein levels further increased under *in vitro* conditions at 12 and 24h post AGE challenge. However, this later increase in RAGE is likely to be mediated by factors independent of AGE as RAGE inducibility is also observed in cells untreated with AGE. This is consistent with the observation that high levels of AGE may function to repress RAGE (Fig. 4.4 D). It is likely that further increases in RAGE protein past 4h are due to cellular factors not cleared from the cells in the closed nature of the experimental set-up or perhaps is a response to cellular stress. This notion is reinforced by the observation that untreated cells express RAGE at lower levels than cells treated with exogenous AGE at 4h after transfer to new media. Thus, the 4h time point is optimal for investigating the AGE regulation of RAGE within this system.

4.4 AGE products increase levels of phosphorylated NFκB-p65 in human endometrial epithelial cells

Several studies have highlighted the phosphorylation and probable involvement of p38 and ERK 1/2 Mitogen-Activated Protein Kinase (MAPK) in the up-regulation of RAGE and subsequent increased NFκB activity following AGE treatment (Yeh 2001; Li 2004; Yoon, Kang et al. 2008). This was proposed due to the attenuation of AGE-induced NFκB activity (measured by EMSA) with the use of p38 and ERK MAPK inhibitors in human THP-1 monocytes (Yeh 2001) and endothelial progenitor cells (Sun, Liang et al. 2009). Consistent with this premise, activation of AGE-induced pERK 1/2 is also repressed with the use of truncated sRAGE, neutralizing anti-RAGE antibody and ERK 1/2 MAP kinase inhibitors in epithelial kidney cells (Li 2004). In other cell systems, following the initiation of the NFκB signalling cascade, p65 is phosphorylated at numerous sites, some of which have been shown to be targeted independently of IκB, as is the case at serine residue 536 (Sasaki, Barberi et al. 2005). However, p65 phosphorylated at serine 276 is a site targeted almost immediately by protein kinase A (PKA) following p50/p65 dissociation from inhibitor complex IκB and is dependent on ERK 1/2 activation which can potentially be initiated by AGE-RAGE association (Zhong, Voll et al. 1998; Larsen, Storling et al. 2005). Phosphorylation of p65 specifically at serine 276 has also been shown to be essential for NFκB-p65 mediated cellular signalling by LPS, a ligand of RAGE and Toll-Like receptors (TLRs) shown to synergistically activate NFκB with AGE products (Okazaki, Sakon et al. 2003; Wijayanti, Naidu et al. 2008; Furusawa, Funakoshi-Tago et al. 2009; Liu, Zhao et al. 2009). In vascular endothelial cells, glycated bovine serum albumin (AGE-BSA) has been shown to induce RAGE

expression to activate pro-inflammatory mediators such as interleukin1β and tumour necrosis factor alpha TNFα (Tanaka, Yonekura et al. 2000; Gao, Belmadani et al. 2007; Gao, Zhang et al. 2008). TNFα is positively regulated by NFκB activation and contains active binding sites for the transcription factor p65 on its promoter (Goldin, Beckman et al. 2006). Studies leading up to this project also revealed TNFα can modulate RAGE transcript in endometrial Ishikawa cells. Induced RAGE transcript levels were further augmented when TNFα treatment was administered in conjunction with AGE-BSA (data not shown). This novel observation gives some evidence for NFκB involvement. AGE-activated cellular stress signalling through the MAPK, RhoA, p21*ras* or c-Jun pathways ultimately lead to downstream NFκB activation and RAGE regulation in other tissues, most notably ovarian tissue from PCO patients (Diamanti-Kandarakis, Piperi et al. 2007). Therefore, the possibility of AGE activating this pathway in endometrial cells was investigated. Previous studies have shown κB signalling is rapid and increases in cellular phosphorylated ERK 1/2 and p65 are apparent within 10 to 30 minutes (Bierhaus, Illmer et al. 1997; Lander 1997; Yeh 2001; Chan and Murphy 2003). Based on these previous observations, Ishikawa and Heraklio cells were treated with 10μg/ml AGE-HSA for a period of 30 minutes and levels of p65 protein phosphorylated at serine 276 subsequently analysed at 5 min intervals.

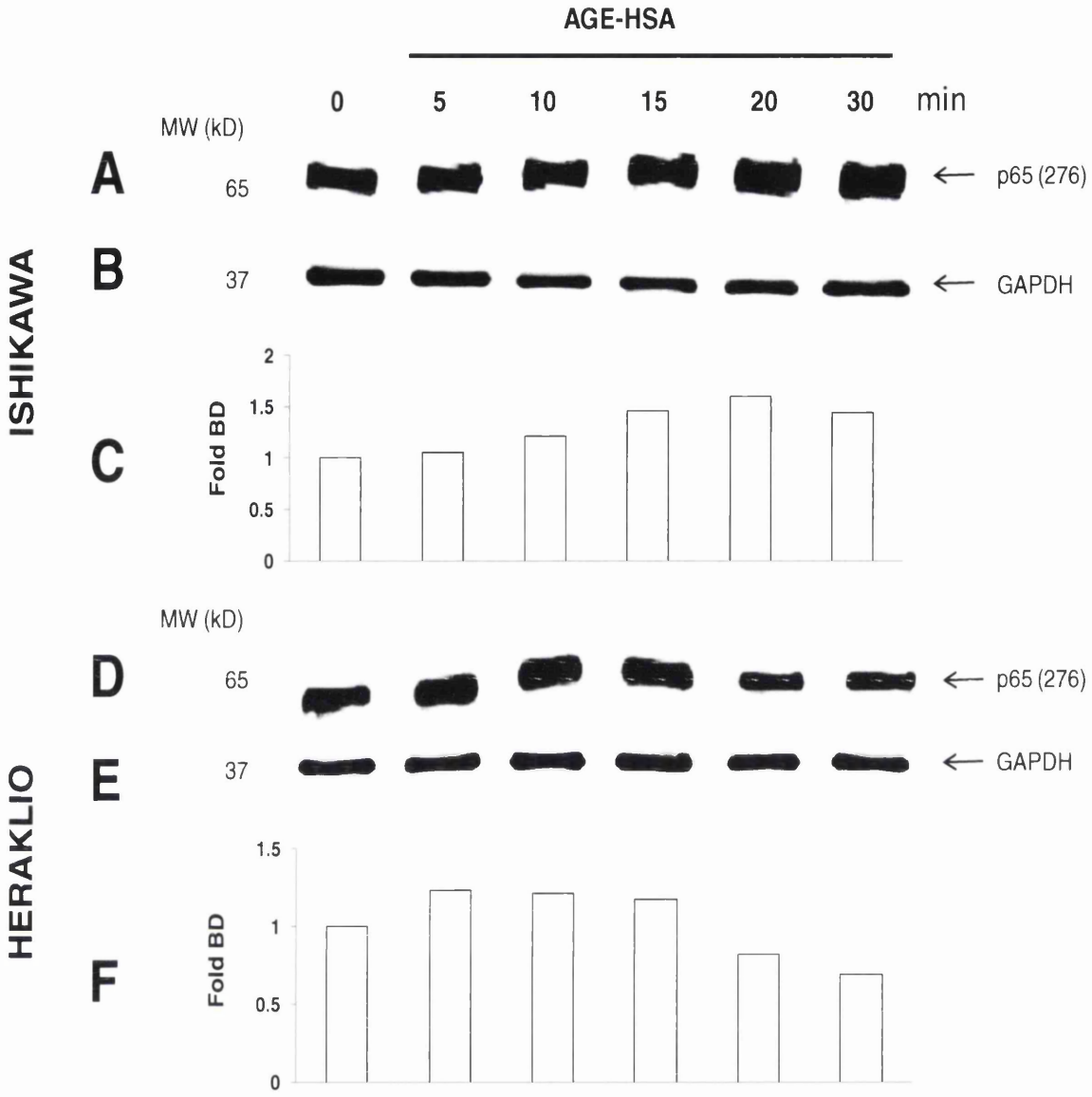

Figure 4-6 AGE-HSA increases phosphorylated p65 protein levels in epithelial endometrial adenocarcinoma cells.

Immunoblots show the effect of AGE-HSA treatment on phosphorylated p65 (serine 276) protein relative to untreated control over a 30 min period in Ishikawa (panels A-C) and Heraklio (panels D-F).

Confluent cells were incubated for 5, 10, 15, 20 and 30 min with 10μg/ml AGE-HSA and harvested in Phosphosafe buffer (EMD). Immunocomplexes were analysed by SDS-PAGE followed by immunoblotting with phospho-NFκB-p65 serine 276 specific (Cell Signalling, #3037) and G3PDH specific (Santa Cruz, FL-335: sc-25778) rabbit polyclonal antibodies as described in methods (Ch. 2 section 2.9). Bands corresponding to the p65 protein phosphorylated at the 276 serine residue were detected at 65kDa. Band Density (BD) is displayed as fold expression relative to untreated control (Panel C and F). Experiments were done in triplicate and typical results are shown normalised to G3PDH (Panel B and D).

AGE-HSA treatment increased phosphorylated/activated p65 protein levels in a time dependent manner in Ishikawa with a small 1.5 fold increase in protein levels detected after 20 min (Fig. 4.6A). In Heraklio cells, AGE-HSA treatment had an effect on activated p65 protein levels after 5 min (Fig. 4.6D), however only a small 1.25 fold increase in protein levels was observed (Fig. 4.6F). The levels of GAPDH protein remained unchanged in response to 10μg/mL AGE-HSA and provided an internal reference (Fig. 4.6B, E). These results are suggestive of AGE-activated NFκB activity in human epithelial endometrium. In control cells at time 0 phospho-p65 was detected in both cell lines indicating that despite serum starvation for 26h, NFκB-p65 is constitutively activated in these cells. This is consistent with a previous suggestion that the endometrium essentially undergoes an inflammation cycle (Clancy 2009; Sharma, Dhawan et al. 2010). Nevertheless, positive increases in p65 protein phosphorylated at serine 276 in response to AGE were observed in both cell lines.

4.5 Modulation of endometrial RAGE by AGE is NFκB dependent

Despite extensive studies of the downstream effects of the ERK 1/2 and p38-activated MAPK pathway on dominant effector NFκB subsequent to AGE-RAGE association, this signalling cascade has not yet been investigated in the human endometrium. Bierhaus and associates have described acute activation of ERK1/2 MAPK to stimulate IκB degradation and NFκB p65 nuclear translocation where degradation initiates *de novo* synthesis of IκB to act as an auto-regulatory feedback mechanism (Bierhaus 2001). However, in the hyperglycaemic state, possible sustained activation of the MAPK pathway due to excessive or prolonged AGE-RAGE interaction may lead to IκB

independent transcription of p65 and p65-DNA binding (Bierhaus 2001; Cortizo 2003). In order to further understand the mechanisms involved in the regulation of RAGE, previous research has employed the use of HMGB1 and lipopolysaccharide (LPS), alternative ligands of RAGE and TLR2 and 4 (van Beijnum, Buurman et al. 2008; Liu, Zhao et al. 2009; Qin, Dai et al. 2009; van Zoelen, Yang et al. 2009). In particular, LPS has been used to perform RAGE-luciferase reporter gene assays in bovine endothelial and rattus vascular smooth muscle cells (Li 1997). Transfection of 5' chimeric deletion constructs identified the region spanning -1543/-587 of the RAGE promoter containing three candidate NFκB–like consensus sequences (GDRRADYCCC) at -1519/-1510, -671/-663 and -467/-458 to be important in the regulation of RAGE. Upon DNase 1 footprinting and EMSA assays however, it was revealed that only the sites starting at -1519 and -671 were functionally active in response to LPS stimulation (Li 1997) . Site directed mutation of the NFκB site at -671 on the RAGE promoter was shown to abolish inducibility of both AGE-BSA and TNFα- mediated NFκB and RAGE luciferase reporter gene activity in human micro vascular endothelial (HMVEC) from skin, and the umbilical vein cell line ECV304 (Tanaka, Yonekura et al. 2000). Nuclear extracts from HMVEC and ECV304 cells exposed to AGE-BSA or TNFα for 4h showed that the DNA binding complex on the -671 site comprised of p50 and p65 NFκB proteins (Tanaka, Yonekura et al. 2000). In addition, murine sRAGE itself can stimulate rapid NFκB p65/p50 nuclear translocation after just 2h (Pullerits, Brisslert et al. 2006). Studies in renal endothelial cells also reported biphasic NFκB activation following RAGE ligand stimulation peaking early on at 3h to 6h and again after 48h (Panzer, Steinmetz et al. 2009). Supershift analysis revealed

the activated NFκB at 3-6h was comprised of p65/p50 heterodimers whereas after 48h, NFκB largely consisted of p50 homodimer, thus highlighting the involvement of p65 in transient NFκB signalling (Panzer, Steinmetz et al. 2009). Consistent with these findings, Chen-Hsiung Yeh and associates showed a RAGE-dependent 1.7 fold increase in p65 transcriptional activity after 4h treatment with AGE N^{ε}-(carboxymethyl)lysine-HSA (CML-HSA) in human monocytes (Yeh 2001). It has also been confirmed by EMSA and western blotting that synthetic anti-sense RAGE oligonucleotides can abolish AGE-HSA-induced NFκB binding activity in endothelial cells due to suppressed translocation of NFκB proteins to the nucleus (Bierhaus, Illmer et al. 1997). Given these previous observations that NFκB is regulated by the action of AGE, and that p65 is further activated in endometrial cells following AGE treatment, the direct regulation of NFκB was investigated. Chromatin immunoprecipitation (ChIP) was used to determine site specific p65 occupancy of the RAGE promoter following 10μg/mL AGE-HSA treatment in Ishikawa and Heraklio cells at the 4h time point identified in Figure 4.4 A, C.

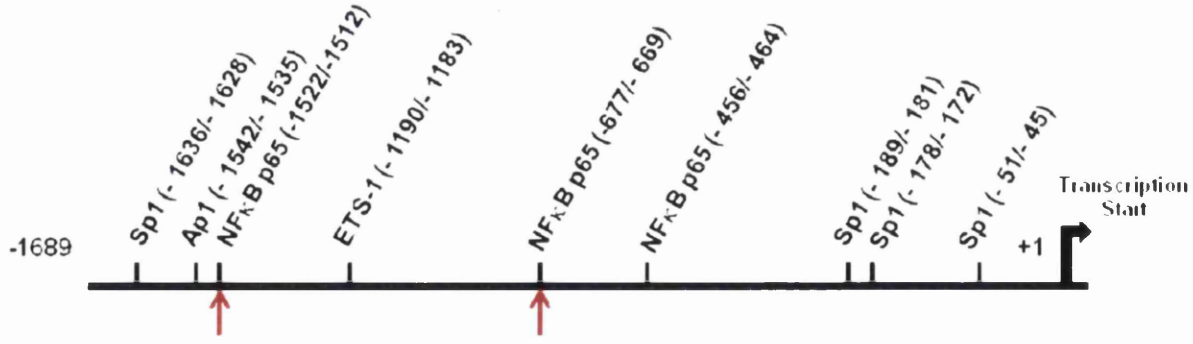

Figure 4-7 Schematic diagram of the RAGE promoter showing the position of the NFκB-p65 sites investigated using ChIP

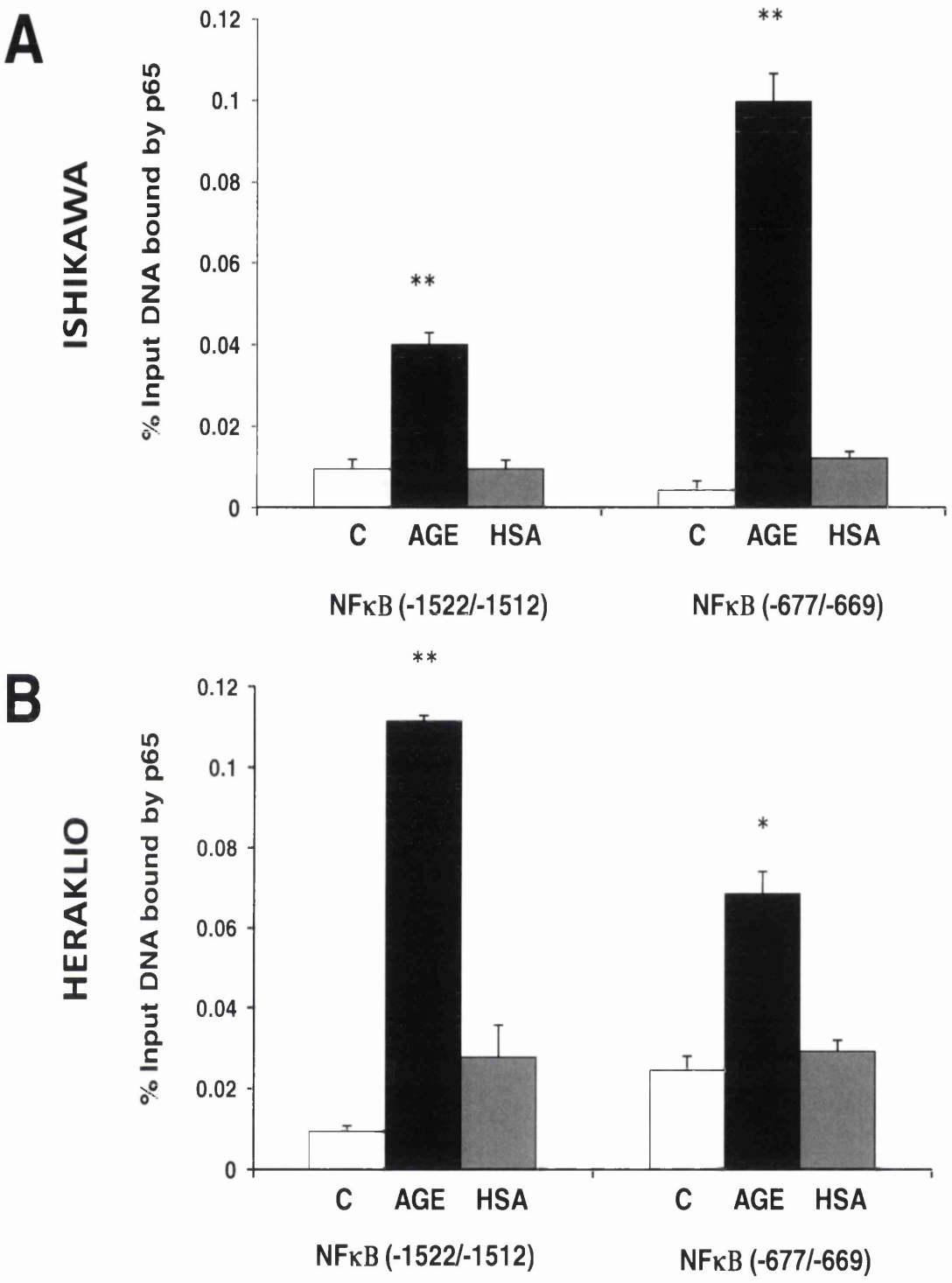

Figure 4-8 AGE-HSA increased total p65 binding at two NFκB sites on the RAGE promoter.

ChIP shows total p65 binding at two NFκB sites -1522/ -1512 and -677/ -669 respectively on the RAGE promoter after 4h in A) Ishikawa and B) Heraklio epithelial endometrial adenocarcinoma cells.

Bar graphs illustrate recruitment of p65 to NFκB sites on RAGE following 4h treatment with 10μg/ml AGE-HSA or 10μg/ml unmodified HSA as a negative control. ChIP experiments were performed in triplicate and representative results are shown. Experiments for a negative control mouse IgG detecting non-specific signal at each site were run in parallel per sample. Data presented is the mean background subtracted binding level of p65 ± STDEV of triplicates and is shown as a % of Input DNA at the site bound by p65 antibody following immunoprecipitation. Data was analysed using a two-tailed students T-Test *P<0.05, **P<0.01 vs. untreated control.

Treatment with 10μg/ml AGE-HSA for 4h resulted in a significant increase in p65 recruitment to the RAGE promoter at NFκB sites in human epithelial endometrial cells *in vitro*. This effect was likely to be AGE specific as treatment with unglycated HSA had no statistically significant effect on NFκB-DNA binding from that exhibited in untreated endometrial cells (C, control) as observed in other cell models (Yeh 2001). In Ishikawa cells (Fig. 4.8A), enrichment of p65 at NFκB site 2 (-677/-669) was more than twice that observed at NFκB site 1 (-1522/-1512) following AGE-HSA treatment. Conversely, in Heraklio cells (Fig. 4.8B) p65 occupancy was greater at NFκB site 1 than at the second site which has been shown to be responsive to AGE-BSA treatment in skin endothelial cells (Tanaka, Yonekura et al. 2000). Under unstimulated conditions, p65 is present at NFκB sites in both Ishikawa and Heraklio cells, suggesting that NFκB may regulate basal RAGE expression in the endometrium. DNA fragmentation by sonication leads to the generation of fragments in the size range 500-1000bp. ChIP analyses the native state of transcription factor binding, therefore occupancy of adjacent binding sites or indeed dynamic chromatin structure will influence the observed NFκB occupancy within different cellular contexts. Hence, in these experiments, NFκB binding may be influenced by the binding of other transcription factors and vice versa. Heraklio and Ishikawa cells differ in ERα

expression status. One possible explanation for the preferential binding of p65 to the RAGE promoter at NFκB site 2 in Ishikawa could be due to an ERα-recruited Activated Protein 1 (Ap1) transcriptional complex occupying the Ap1 site (-1542/-1535) that is in close proximity to the NFκB site 1(-1522/-1512) (arrowed, Fig. 4.7). Indeed ERα recruitment to the Ap1 site on the RAGE promoter has been demonstrated in epithelial endometrial HEC1A cells (Ch.5 Fig. 5.7). ERα expression in Ishikawa could therefore be limiting yet not abrogating p65 binding at NFκB site 1 through steric hindrance. Direct ERα and p65 interaction has been shown in the nuclei of human osteoblastic cells (Quaedackers 2007). Thus one could speculate that ERα actively competes with NFκB sites to bind phosphorylated p65 and perhaps, having greater affinity to complex Ap1, recruits p65 to Ap1 sites to aid ER signalling (Hodgkinson, Laxton et al. 2008; Chiu, Chen et al. 2010; Lin, Chang et al. 2010). This would have the added effect of decreasing the localised availability of p65. No occupancy of p65 was observed at a third NFκB site (located at -464/-456, Fig. 4.7) in either untreated or 10μg/ml AGE-HSA treated Ishikawa and Heraklio cells (data not shown). This site was also unbound by p65 in endothelial cells prior to and post challenge with LPS thus may be functionally inactive (Li 1997).

4.6 Modulation of endometrial MUC1 by AGE is NFκB dependent

MUC1 glycoproteins can confer either adhesive or anti-adhesive properties to the endometrial apical surface. Thus, MUC1 deficiency or dysregulation may lead to altered endometrial receptivity and potentially blastocyst implantation failure. Previous research has demonstrated that MUC1 expression can be regulated by sex steriods, anti-estrogenic compounds, TNFα and p65

through the action of the ERs and NFκB signalling in normal and cancerous breast, lung epithelia and uterine tissues (Hanson, Browell et al. 2001; Koga, Kuwahara et al. 2007; Lagow 2002; Croce, Isla-Larrain et al. 2003; Paszkiewicz-Gadek, Porowska et al. 2005; Brayman, Julian et al. 2006; Zaretsky, Barnea et al. 2006). Lung tissue not only constitutively expresses RAGE but is rich in endothelial cells where AGE-RAGE association may activate NFκB-DNA binding activity (Sternberg, Gowda et al. 2008; Zhang, Tasaka et al. 2008). The importance of the MUC1 promoter region spanning -598/-485 in activating expression had previously been investigated in breast cancer MCF-7 cells (Abe and Kufe 1993; Kovarik, Peat et al. 1993). Deletion mutants of the 5' flanking gene sequence cloned into vectors and further site directed mutagenesis identified a putative NFκB site located at -589/-580. EMSA of T47D nuclear extracts revealed p65 bound to this NFκB site and its involvement in mediating TNFα and IFN-γ-activated MUC1 transcription in breast cancer (Lagow 2002). MUC1 has previously been characterised in human epithelial endometrium and may potentially be a downstream target of NFκB signalling (Hey, Meseguer et al. 2003). Experiments were therefore conducted to investigate the possibility of any direct NFκB-p65 occupancy of the MUC1 promoter in endometrial cells following AGE-HSA treatment.

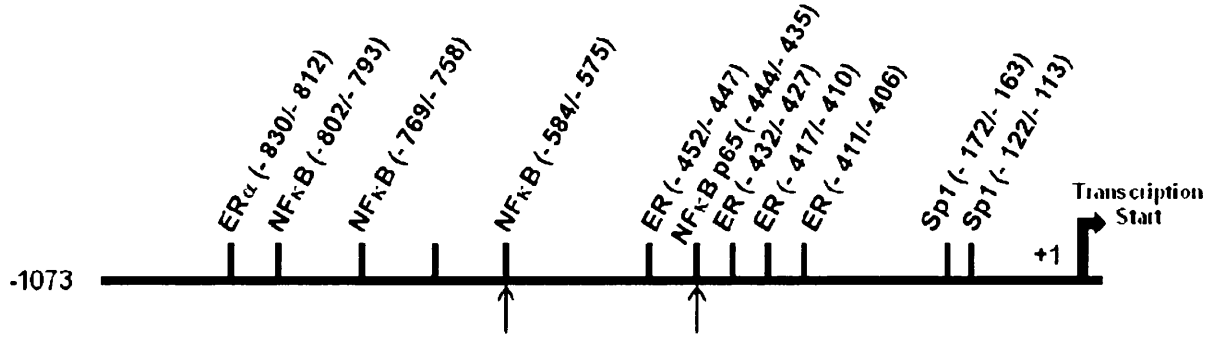

Figure 4-9 Schematic diagram of the MUC1 promoter showing the position of the NFκB sites investigated in ChIP

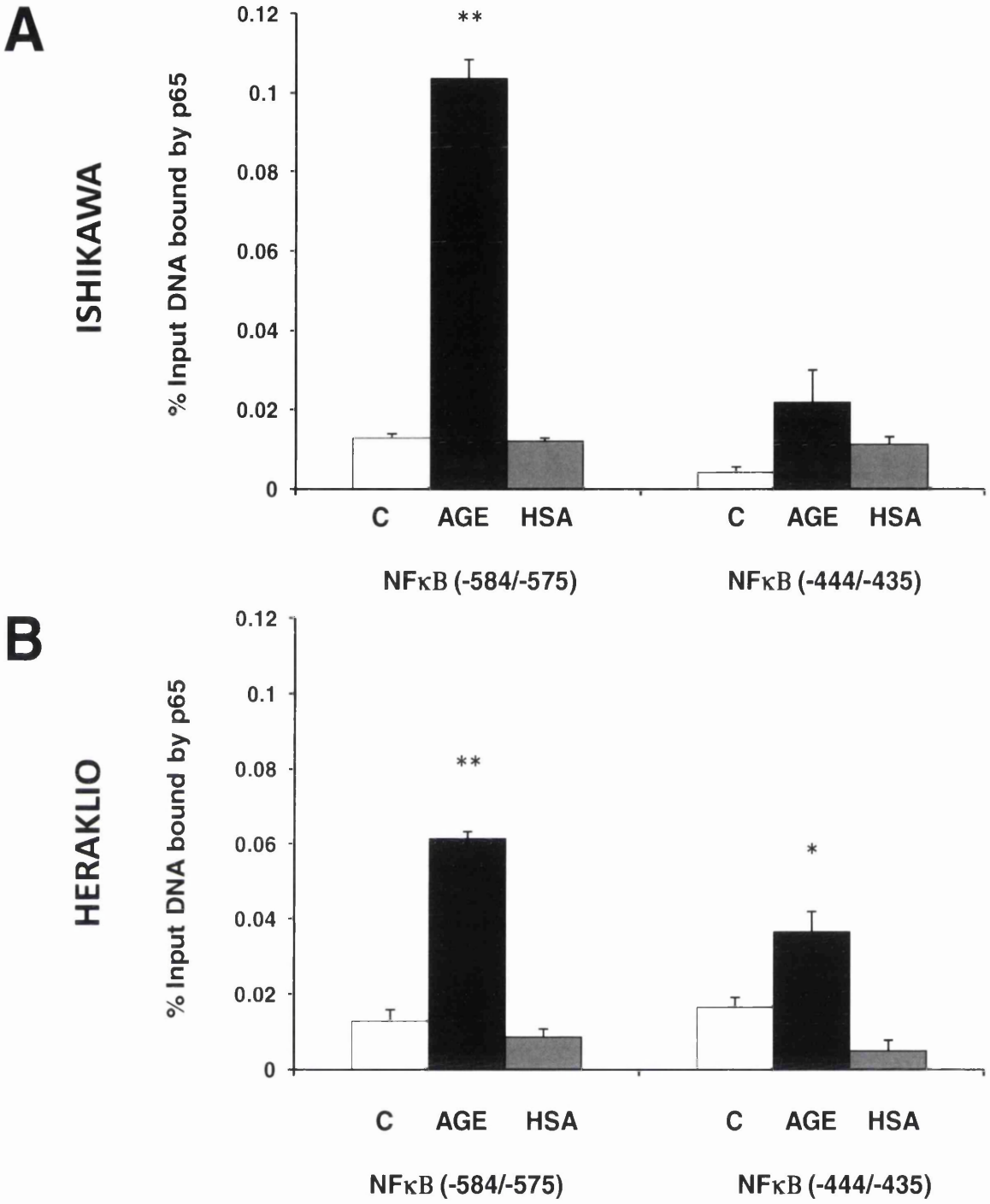

Figure 4-10 AGE-HSA increases total p65 binding to two NFκB sites on the MUC1 promoter.

ChIP shows total p65 binding to two NFκB sites at -584/-575 and -444/-435 respectively on the MUC1 promoter after 4h in A) Ishikawa and B) Heraklio endometrial epithelial adenocarcinoma cells.

Bar graphs illustrate recruitment of p65 to NFκB sites on MUC1 following 4h treatment with 10μg/ml AGE-HSA or 10μg/ml unmodified HSA as a negative control. ChIP experiments were performed in triplicate and representative results are shown. Experiments for a negative control mouse IgG detecting non-specific signal at each site were run in parallel per sample. Data

presented is the mean background subtracted binding level of p65 ± STDEV of triplicates and is shown as a % of Input DNA at the site bound by p65 antibody following immunoprecipitation. Data was analysed using a two-tailed students T-Test *P<0.05, **P<0.01 vs. untreated control.

Following 4h exposure to 10μg/ml AGE-HSA, recruitment of p65 to the MUC1 promoter in human endometrial cells was increased. AGE-HSA-induced p65 binding was observed in both Ishikawa (Fig. 4.10A) and Heraklio (Fig. 4.10B) and could perhaps indicate a role for possible AGE-stimulated NFκB-p65 in the regulation of endometrial MUC1. In Ishikawa cells, only binding of p65 to NFκB site 1 (-584/-575) was observed. No significant increase in p65 binding following AGE-HSA treatment at NFκB site 2 (-444/-435) was observed (A). In contrast, AGE-induced p65 recruitment in Heraklio occurred at both NFκB sites 1 and 2 (B). In both cell lines, unglycated HSA had no effect on the levels of p65 binding at either site (Fig. 4.10 A, B). ERα may also affect localised binding of p65 to the MUC1 promoter in the same way it may affect its binding to RAGE (Fig. 4.8 A, B). Steric hindrance by ERα binding in close proximity to NFκB site 2 at -444 is supported by the identification of a cluster of four ERE sites spanning the region -452/-411 on the MUC1 promoter (arrowed, Fig. 4.9).

4.7 Discussion

The work presented in this chapter has taken a step towards elucidating an AGE-RAGE signalling pathway in the human epithelial endometrium. This research brings to light the possible involvement of this pathway as a factor in the infertile aetiology of PCOS and endometriosis. It also provides initial evidence for the proposed role of AGE in inflammation and potentially in the progression to endometrial cancer through the possible activation of RAGE

by NFκB as described in Chapter 3 (section 3.10). The principal discovery in this chapter was that 10μg/mL AGE-HSA could transiently up-regulate RAGE in the endometrium despite relatively low basal expression in this tissue (Ch. 3 Fig. 3.16). Significant increases in RAGE transcript were observed at 4h falling to basal levels after 24h. However, inducibility was significantly reduced and even repressed at high AGE concentrations, suggesting dose-dependent saturation or more likely as a result of oxidative stress and cytotoxicity, increased AGE clearance. RAGE protein however remained highly expressed at 24h perhaps increasing independently of AGE in the experimental model. This is particularly significant, as the endometrium is targeted in women with PCOS and endometriosis by excess ROS, AGEs, androgens; estrogens (Ch.5 Fig 5.4-5) and inflammatory cyto/chemokines which in turn potentially enhance RAGE expression (Tanaka, Yonekura et al. 2000; Csiszar and Ungvari 2008; Xanthis, Hatzitolios et al. 2009; Zhang, Park et al. 2009). Indeed, basal RAGE transcript and protein levels are higher in infertile PCO and endometriotic endometrium in comparison to fertile controls (Ch. 3 Fig. 3.6, 3.10, 3.12-15) as is the expression of MUC1 transcript (data not shown). Additionally, increased ovarian follicular and plasma RAGE has been reported to correlate with CML-AGE and VEGF in patients with endometriosis (Fujii, Nakayama et al. 2008). Infertility disorders are also characterised by metabolic dysfunction in the insulin receptor pathway thus promoting accelerated generation of AGEs that can perpetuate RAGE-mediated chronic inflammation and progression towards the diabetic state (Fica, Albu et al. 2008; Fornes, Ormazabal et al. 2010). Circulating AGEs have been implicated in female fecundability odds, and links between the deleterious effects of persistent hyperglycaemia and complications in diabetic

pregnancy are well documented (Hjollund, Jensen et al. 1999; Harsem, Braekke et al. 2008; Bals-Pratsch, Grosser et al. 2011). Moreover, recent studies have shown diabetic PCOS women have a significantly greater risk of (sub) infertility, preeclampsia and miscarriage (Boomsma, Fauser et al. 2008; Hart 2008). AGEs accumulate in human chorionic villi from women who miscarried in their first trimester (6-10 weeks) correlating with increases in RAGE, chemokine secretion and apoptosis of placental trophoblasts. Increased AGEs may also alter the foetal-maternal interface by inhibiting human chorionic gonadotropin (hCG) secretion which is thought to prime placentation (Konishi, Nakatsuka et al. 2004). Studies in women with pre-eclampsia have shown elevated placental RAGE and nitric oxide-derived (ROS) AGEs in serum. RAGE-mediated cytotoxicity induced by AGE could be suppressed with NFκB inhibitors. AGEs may fuel a state of oxidative stress in pre-eclampsia leading to uteroplacental dysfunction - a leading cause of perinatal mortality (Chekir, Nakatsuka et al. 2006). Insulin sensitising AGE inhibitors such as metformin and clomiphene citrate have already been proven to ameliorate diabetic complications such as insulin resistance, levels of plasma IL-6, AGEs and endothelial RAGE expression (Ouslimani, Mahrouf et al. 2007; Diamanti-Kandarakis, Economou et al. 2009; Luque-Ramirez and Escobar-Morreale 2010). Furthermore, metformin reduces the prevalence of gestational diabetes, oligomenorrhea and anovulatory infertility arising from characteristic excess androgens and AGEs in PCO women, thus highlighting the potential for RAGE as a therapeutic target (Glueck, Wang et al. 2001; Glueck, Goldenberg et al. 2008; Begum, Khanam et al. 2009; Palomba, Pasquali et al. 2009). Metformin has recently been linked to improvements in ovulation and clinical pregnancy rates in

PCOS, however this has not been shown to correlate with successful birth rate indicating that an endometrial defect may be accountable for PCOS infertility (Tang, Lord et al. 2010). Substantial evidence from a variety of tissues has shown us the importance of numerous protein kinases, in particular key-players of the MAPK pathway p38 and ERK 1/2, in the activation of NFκB (Yoon, Kang et al. 2008; Sun, Liang et al. 2009; Liu, Liang et al. 2010).This research concentrates on the possible effects of AGE products on RAGE and on the downstream effector of the aforementioned pathway, NFκB. Here; AGE-HSA has been shown to increase, albeit modestly, the levels of activated p65 phosphorylated at serine 276 in the human epithelial endometrium (Fig. 4.6 A, D). This is further supported by ChIP experiments that demonstrate the presence of NFκB-p65 at two NFκB sites on endometrial RAGE (Fig. 4.8 A, B) and two NFκB sites on endometrial MUC1 promoters (Fig. 4.10 A, B) from which we hypothesise that RAGE and MUC1 are probably modulated in part through the NFκB pathway. Following treatment with 10μg/mL AGE-HSA, the level of p65 recruitment to these sites increased whereas no binding increase was seen with HSA treatment alone. This indicates that NFκB-p65 is likely to be activated by AGEs and that endometrial MUC1 transactivation could possibly be RAGE dependant. Taken with recent findings that ERK 1/2 MAPK protein is increased in endometriotic, hyperinsulinemic PCO and hyperplasic endometrium we suggest that putative NFκB activation is likely to be mediated by the MAPK pathway in this tissue (Song, Zhang et al. 2010). Recent studies have highlighted the elevation of RAGE in endometriotic stroma and its contribution to underlying inflammation in the pathophysiology of the disorder (Pertynska-Marczewska, Glowacka et al. 2009; Sharma, Dhawan et al.

2010). While RAGE has a role in the perpetuation of the inflammatory response, MUC1 has a role in blastocyst attachment into the endometrial epithelium and its expression can influence the receptivity of this tissue (Carson, Julian et al. 2006). It could therefore be speculated that over-expression of MUC1 from sustained AGE-RAGE-mediated NFκB transactivation is a potential causative factor of implantation failure and high miscarriage frequency evident in women with PCOS who have no known endometrial defect. These women also have a known risk of developing an endometrial cancer which perhaps could be attributed to enhanced RAGE signalling impacting on the expression of oncogenes, cytokines, and apoptotic pathways (Lim, Park et al. 2008; Kang, Tang et al. 2009; Chen, Song et al. 2010; Rasheed, Akhtar et al. 2011). Consistent with this premise, AGE products are also known to correlate with the release of β-catenin and loss of E-cadherin which is indicative of the metastatic environment (Ebert, Yu et al. 2003; Juhasz, Ebert et al. 2003; Rojas, Figueroa et al. 2010). Interestingly, loss of E-cadherin and β-catenin also allows a transcriptional complex comprising of ERK 1/2 MAPK-activated TIF2, β-catenin and androgens to target downstream AR regulated genes, one of which is MUC1 (Otero 2001). To conclude, increases in endometrial epithelial RAGE and MUC1 during the window of blastocyst implantation could be modulated through the AGE-RAGE axis, perhaps in combination with androgens found in excess in infertile disorders.

CHAPTER 5

17β Estradiol and 4-Hydroxytamoxifen modulate RAGE expression through the ER pathway in human endometrial epithelial cells

5. 17β Estradiol and 4-Hydroxytamoxifen modulate RAGE expression through the ER pathway in human endometrial epithelial cells

5.1 Introduction

The discovery that AGEs, elevated in PCO and endometriosis pathology, exhibited RAGE agonistic potency in human endometrium prompted the investigation of other RAGE modulators. Endometrial receptivity to estrogenic action is fundamental in preserving its functionality. Specifically, the cyclical sloughing and proliferative regeneration of the endometrium requires the precisely-timed regulation of a specific subset of estrogen-controlled genes in a manner likened to an inflammatory response.17β estradiol (E2) is the most abundant natural estrogen found in the circulation of premenopausal women (Barkhem 1998). E2 has previously been shown to induce RAGE expression in human micro vascular endothelial cells (HMVECs) (Tanaka, Yonekura et al. 2000; Mukherjee, Reynolds et al. 2005) however, at the time of writing, E2 modulation of endometrial RAGE was yet to be determined. The effects of E2 and selective estrogen receptor modulators (SERMs) such as 4-hydroxytamoxifen (TX) in the endometrium are thought to be both gene and cell-specific (Farnell 2003). Agonistic action of TX on ERα has been reported in non-malignant uterus and endometrial cell lines Ishikawa and HEC1A, yet in contrast, TX had no effect on cell proliferation or ERE-luciferase reporter gene activity in ERα positive ECC-1 cells (Dardes, Schafer et al. 2002; Shah and Rowan 2005). Contrasting evidence for selective estrogen receptor modulator action may be due to gene-and promoter-specific differential transcription factor recruitment by the ER α/β subtypes, both of which are expressed throughout the menstrual cycle (Critchley and Saunders 2009; King, Collins et al. 2010). Estrogen receptor (ER) signalling has been

extensively studied in a multitude of tissues, most notably in breast where E2 agonism of ER has been linked to an accelerated disease state (Anderson 2002). Several studies in T47D and MCF-7 cells have highlighted that ERα is the dominantly expressed ER subtype in breast cancer however normal breast tissue expresses very little (Herynk and Fuqua 2004). Similarly, greater expression of ERα has also been observed in myometrium and endometrial glands, lumen and stromal cells relative to ERβ (Punyadeera 2008). In non-malignant endometrium, E2 down regulates ERβ which is readily targeted for degradation and leads to stabilisation and reciprocal over-expression of the ERα isoform (Johnson, Maleki-Dizaji et al. 2007). However, in ectopic endometriotic stromal cells, E2-induced ERβ can bind to the ERα promoter via non-classical Ap1 (-237/-19) and Sp1 (+298/+591) and a classical ERE (-839/-709). This has lead to the hypothesis that ERβ represses ERα in endometriosis leading to the subsequent down-regulation of its target PR, increasing the risk of progesterone resistance and cell proliferation (Trukhacheva, Lin et al. 2009). ERβ however may have a physiological role in mediating the biological actions of estrogen in cells negative for ERα expression such as HEC1B (Hall 1999). In cell lines where both isoforms are co-expressed, ERβ signalling may be achieved through directly targeting genes or indirect regulation through the modulation of ERα action (Villablanca 2009). Unlike many other estrogen responsive genes, no classical estrogen response elements sites have been identified in the RAGE promoter (Tanaka, Yonekura et al. 2000). However, a study in endometrial Ishikawa and HEC1A cells found that pS2 and c-myc could be up-regulated by E2 and TX via a non-consensus ERE believed to be an Ap1 site (Shah

and Rowan 2005). It was therefore hypothesised that RAGE modulation involved ER occupation of non-classical sites where recruitment was dependent on Ap1 or Sp1 proteins, much like Cyclin-D1(Castro-Rivera, Samudio et al. 2001). In this chapter, endometrial adenocarcinoma HEC1A and HEC1B cells were characterised for ER expression at the mRNA and protein level. The modulation of endometrial RAGE by 17β estradiol and 4-hydroxytamoxifen was investigated at the level of mRNA and protein after 4h to explore the possibility that RAGE is an early estrogen response gene. In order to gain evidence for the involvement of the ER pathway in this regulation of endometrial RAGE, ChIP assays were performed to demonstrate direct interaction of E2 and/or TX-liganded ERα on the RAGE promoter. In endometriotic and PCO endometrium *in vivo*, RAGE expression would be influenced simultaneously by hormonal action and elevated AGEs which have also been shown to positively regulate RAGE probably through the NFκB pathway (Ch.4 Fig. 4.5, 4.6 and 4.8). From this, one may infer that cross-talk may exist between the ER and NFκB pathways with the potential to alter cellular levels of RAGE. This possibility of potential ER-NFκB interference on the level of ERα recruitment to the RAGE promoter was also investigated following co-treatment of E2 or TX with AGE-HSA in ERα positive HEC1A and Ishikawa cells.

5.2 Estrogen Receptor expression in human endometrial epithelial HEC-1 cells at the mRNA and protein level

Pivotal to the cyclical disintegration, regeneration and function of the endometrial epithelium is the modulation of a diverse subset of endometrial expressed genes in response to an estrogenic stimulus. It is widely accepted that ERα is the dominantly expressed ER subtype in human endometrial and myometrial tissue however it appears that the ERα/ERβ expression ratio may fluctuate between cellular compartments (Punyadeera 2008). In order to assess the likely hormonal regulation of endometrial epithelial RAGE expression, two cell lines, HEC1A and HEC1B, were chosen for their contrasting ERα expression status (Fig. 5.1). HEC1A has been previously characterised as an ER positive cell line expressing both receptor subtypes; ERα in excess of ERβ. HEC1B has been described as not expressing the dominant subtype ERα, however due to positive ERβ expression it provides us with model in which to investigate the ERβ-selective effects on RAGE. One report noted the presence of ERα only in the cytoplasm of HEC1B cells deemed it to therefore be transcriptionally inactive (Punyadeera 2008). It was therefore necessary to confirm the relative expression of the ER isoforms both at the mRNA and protein level in these experimental models.

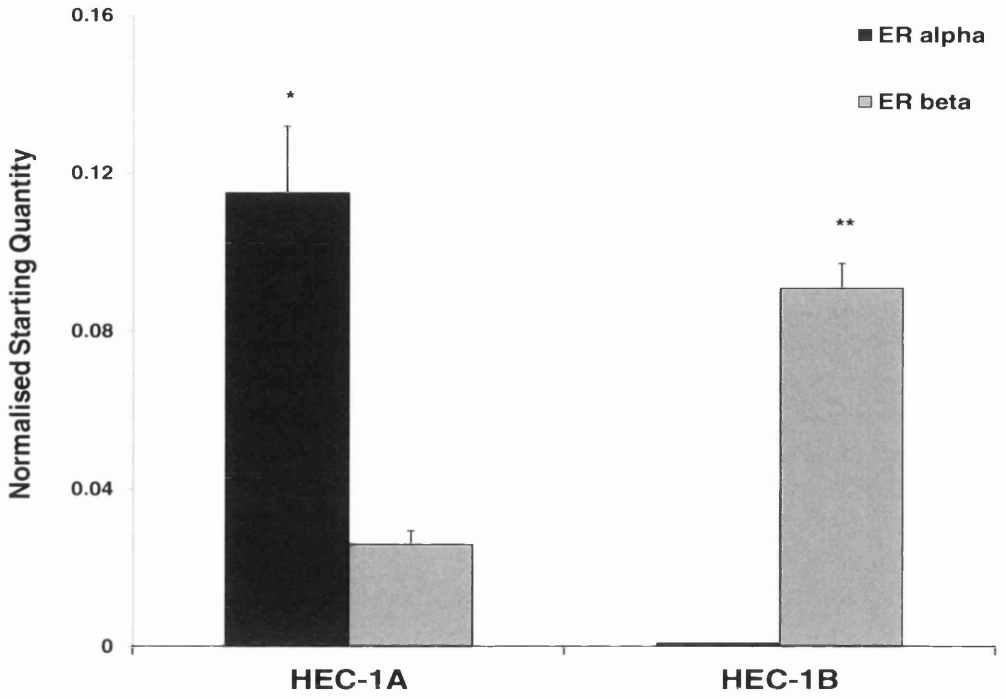

Figure 5-1 Estrogen receptors ERα and ERβ are differentially expressed in HEC1 epithelial adenocarcinoma cell lines.

Bar graphs show ER isoform transcript levels in HEC-1A and HEC-1B cells determined by real time PCR analysis.

HEC-1 cells were grown in confluent monolayers in 6 well plates and left untreated to assess basal ER transcript levels. Values given are mean starting quantity (StQ) normalised to GAPDH ± STDEV from StQ triplicates. Data was analysed using a two-tailed students T-test *p=<0.05, **p=<0.01 ERα vs. ERβ.

Figure 5.1 shows the relative expression of the two ER isoforms in HEC1A and HEC1B endometrial cells. HEC1A cells expressed both receptor subtypes however the expression of ERα was 4.4 fold greater than ERβ. HEC1B cells showed essentially no expression of ERα (ERβ 120 fold vs. ERα) and expressed 3.5 fold greater ERβ transcript than HEC1A. HEC1A cells are therefore an appropriate model in which to investigate the impact of ER signalling on RAGE, as the expression ratio of ERα to ERβ transcript is comparable with endometrial epithelium *in vivo* .

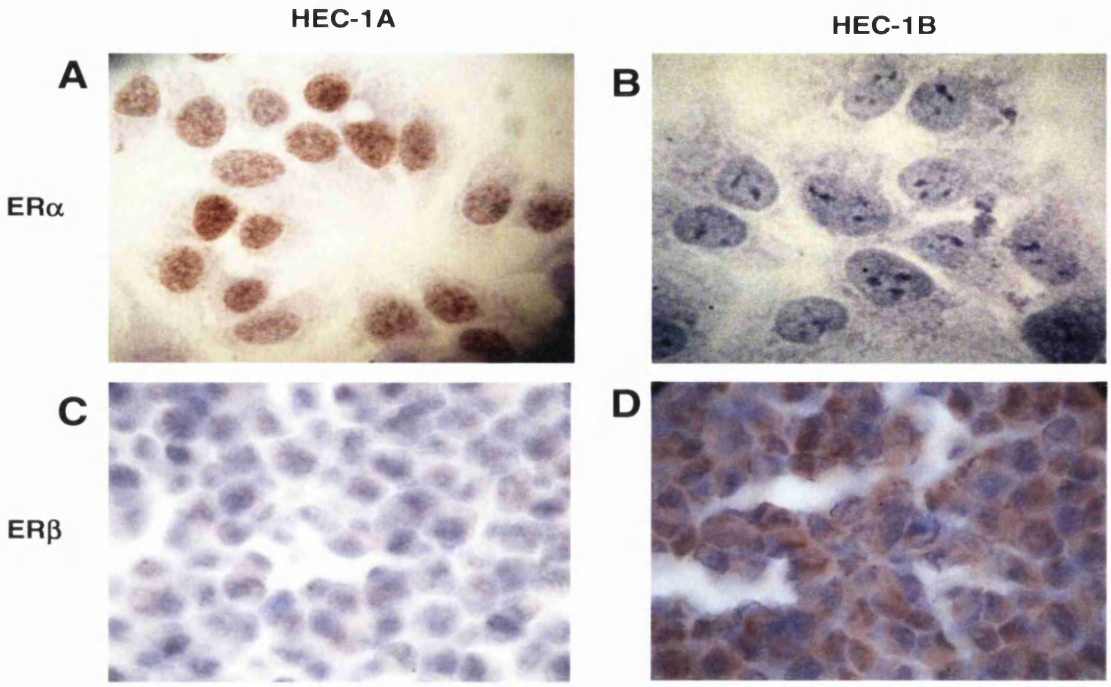

Figure 5-2 Expression of ERα and ERβ proteins in HEC-1 human endometrial epithelial cells

Images show basal ERα (A, B) and ERβ (C, D) protein expression in untreated HEC1A and HEC1B cells by immunohistochemistry. Images were taken using the AxioCam HRc camera (Zeiss) fitted to a light microscope at x100 magnification. Slides were stained with haematoxylin and eosin (H&E) for the nuclear and cytoplasmic compartments.

Figure 5.2 shows strong positive staining for ERα protein expression (A) in comparison to weak positive staining for ERβ (C) and reflects the greater relative expression of ERα mRNA in HEC1A cells (see Fig. 5.1). ERα protein expression appeared to be both nuclear and cytoplasmic in positively staining HEC1A cells (Fig. 5.2A). In contrast, HEC1B cells did not stain for cytoplasmic or nuclear ERα protein (Fig. 5.2B) whereas strong positive staining for ERβ (Fig. 5.2D) again correlated with transcript levels (Fig. 5.1). However due to dense cell seeding and low magnification it was not possible to determine the distribution of ERβ protein in either cell line (Fig. 5.2C, D). HEC1 cells incubated with secondary antibody only as a negative control showed no non-specific staining for either ER (data not shown).

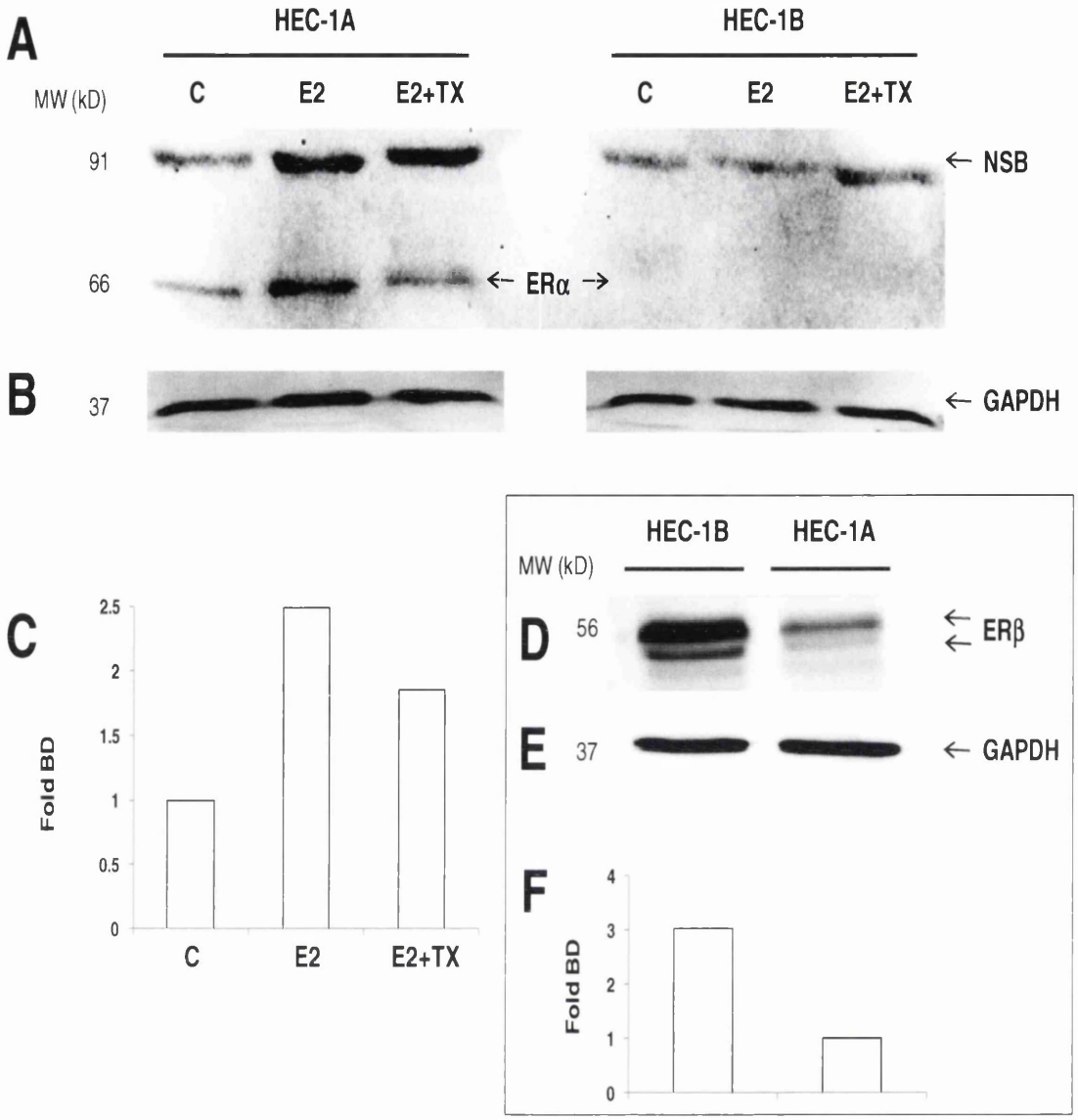

Figure 5-3 Expression of ERα and ERβ protein in HEC-1 human endometrial epithelial cell lines

Immunoblot data shows ERα protein (A) and ERβ protein (D) expression after 4h in HEC1A and HEC1B cells.

Confluent cells were either left untreated (control, C), or treated with 10nM 17β estradiol (E2) or both 10nM 17β estradiol and 10nM 4-Hydroxytamoxifen (E2+TX) for 4h (A). Proteins were separated by SDS-PAGE followed by immunoblotting with ER (ERα HC-20: sc-543, ERβ L-20: sc-6822) and GAPDH specific (FL-335: sc-25778) polyclonal antibodies (Santa Cruz). Bands corresponding to ERα 66kDa and ERβ 56kDa were detected. Non specific binding (NSB) was also detected at 91kDa as indicated by ERα antibody data sheet. Band Density (BD) was determined using Quantity One software (Bio-Rad) using the volume rectangle tool for signal intensity/area mm^2. BD is displayed as the fold expression relative to either control (C) or HEC1A (F) normalised to respective GAPDH samples (shown B, E).

Fig 5.3A shows that ERα protein expression was up-regulated 2.5 fold with 17β estradiol (E2) treatment in HEC1A after 4h. This increase in ERα was reduced to 1.7 fold increase combined with 10nM 4-hydroxytamoxifen (A). No ERα was expressed in HEC1B cells even after E2 treatment, however ERβ protein expression was 3 fold greater in HEC1B than in untreated HEC1A cells (Fig. 5.3 D, F).

5.3 17β Estradiol and 4-Hydroxytamoxifen modulate RAGE transcript in human endometrial epithelial cells

RAGE is elevated in the endometrial tissues of women with endometriosis and PCOS and therefore may play a role in the pathogenesis of these infertility related disorders. RAGE expression was significantly elevated in proliferative phase PCO endometrium coinciding with pre-ovulatory increases in estrogen levels (Ch. 3 Fig. 3.2-3.4). Previous studies have shown that 17β estradiol can transcriptionally regulate RAGE expression in skin endothelial cells (Tanaka, Yonekura et al. 2000; Mukherjee, Reynolds et al. 2005). Numerous studies have demonstrated that TX orchestrates agonistic effects on specific subsets of genes independently of E2 action in the epithelial endometrium (Blauer, Heinonen et al. 2008; Gielen, Santegoets et al. 2008). In fact, analysis of endometrium from TX users vs. matched controls revealed that several genes were specifically and differentially regulated in the endometrium via TX including NFκB, EGFR, MUC1, TP53 and β-catenin (Gielen, Kuhne et al. 2005). These genes are collectively involved in mediating apoptotic and cell-cell adhesion signalling through pathways common to RAGE, suggesting that RAGE may also be implicated in endometrial proliferation (Ch.4 Fig. 4.6 and 4.8). Furthermore, TX agonism of ERα mediated signalling on cell proliferation has been observed in murine

uterus (Stygar, Muravitskaya et al. 2003). In Ishikawa, TX was also shown to up-regulate the expression of c-myc, a gene which has been associated with endometrial cell proliferation and malignancy, through recruitment of the ERα coactivator SRC-1 between 2-4h (Shang and Brown 2002). Cell line models HEC1A and HEC1B positive and negative for ERα expression respectively were used to assess the impact of physiological (10nM) and saturating (100nM) concentrations of 17β estradiol with and without 10nM TX on endometrial RAGE transcript. In addition, RAGE expression was assessed in these cells post-challenge with 10nM TX to ascertain whether TX could assume an agonistic role independent of estrogen in the uterus. The following experiments demonstrate not only differential modulation of RAGE by the ER isoforms but also suggest that the ability of 4-hydroxytamoxifen to antagonise E2-mediated responses is influenced by E2 bioavailability and ERα status in these experimental models.

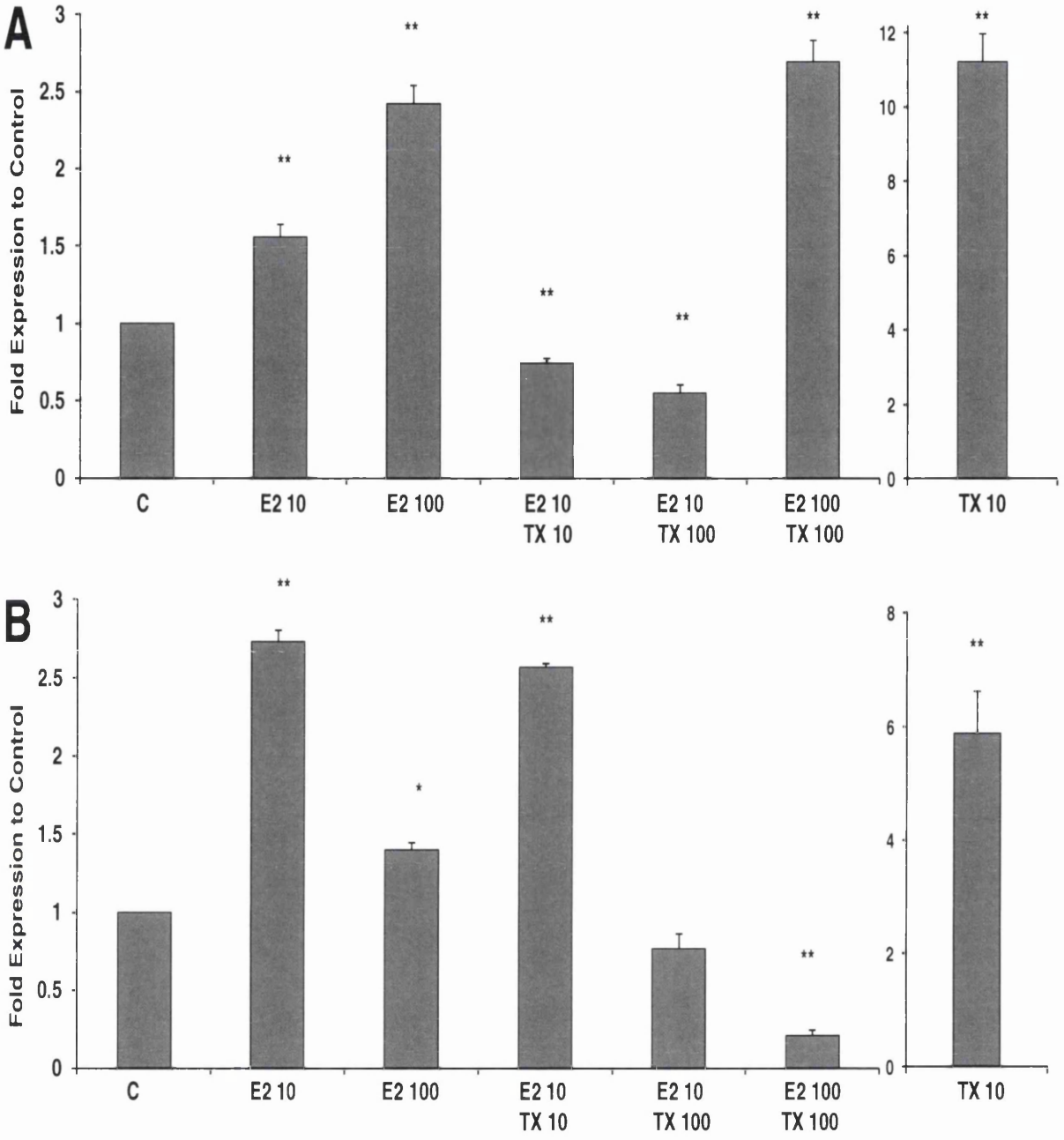

Figure 5-4 17β estradiol and 4-hydroxytamoxifen modulate RAGE transcript levels in HEC-1 endometrial epithelial cells

Bar graphs show the effects of physiological and high dose 17β estradiol and 4-hydroxytamoxifen on RAGE mRNA after 4h in HEC1A (A) and HEC1B cells (B) by real time PCR.

HEC1A and HEC1B cells were grown to confluent monolayers in 6 well culture plates and treated with 10 or 100nM 17β estradiol (E2) with or without 4-hydroxytamoxifen (TX) and with 10nM TX alone (no estrogen priming) for 4h. Cells were left untreated in cell culture medium for the negative control. Experiments were done in triplicate and typical results are shown. Values given are mean starting quantity (StQ) normalised to RPL-19 ± STDEV from StQ triplicates. Data was analysed using a two-tailed students T-Test *P<0.05, **P<0.01 vs. untreated control.

Figure 5.4 demonstrates the differential effects of 10nM E2 and TX treatment on the expression of RAGE transcript between the two HEC1 cell lines (A, B). In HEC1A, RAGE transcript was induced 1.5 fold with 10nM E2 and 2.5 fold with 100nM E2 treatment after 4h when compared to untreated control. RAGE mRNA was down-regulated when HEC1A cells were treated with E2 and TX combined treatment at 10nM and was further attenuated at higher (100nM) TX concentrations. This demonstrates that TX can act as an antagonist against E2-induced RAGE in this experimental model. However at high, non-physiological concentrations of E2 (100nM), TX was not able to antagonise E2 action in HEC1A cells (Fig. 5.4A). Fig 5.4B showed that 10nM E2 treatment up-regulated RAGE mRNA to a greater level (2.8 fold) in HEC1B than in HEC1A cells (1.5 fold) when compared to their respective controls. This suggests that in HEC1B, E2 was more effective at mediating signalling through ERβ in the absence of ERα. However, unlike HEC1A, higher concentrations of E2 (100nM) had a less marked effect than 10nM E2 on RAGE mRNA (1.4 fold vs. control) in HEC1B. Furthermore, RAGE mRNA remained up-regulated (2.5 fold) when HEC1B cells were challenged with 10nM E2 and TX in combination. This suggests that at a physiological concentration of E2, TX does not inhibit E2-induced RAGE expression in HEC1B cells and therefore potentially exerts an agonistic effect on ERβ. Conversely, TX regains its antagonistic potential at high concentrations (100nM) and can completely abolish the E2-mediated induction in HEC1B, evidenced by lower transcript levels (0.25 fold) than in untreated cells (Fig. 5.4B). Interestingly, in the absence of E2, TX displays significant agonistic potency in endometrial cells and possesses affinity for binding both ERs (Fig. 5.4). RAGE transcript was significantly up-regulated (11.2 fold) in HEC1A and

5.9 fold in HEC1B cells when challenged with 10nM TX alone for 4h. These results suggest that TX is a potent inducer of endometrial RAGE and may also have an adverse effect on the endometrium in a low or non-estrogenic setting which could be likened to post-menopausal tissue. Taken together, these results indicate that 17β estradiol induces RAGE transcript via either ERα or ERβ receptors and that 4-hydroxytamoxifen differentially modulates this response in two endometrial cell lines. If ERα is assumed to be the predominant factor in HEC1A, this study also begins to uncover the differential roles of the two ER isoforms in RAGE regulation in the endometrium.

5.4 17β Estradiol and 4-Hydroxytamoxifen can modulate RAGE protein in human endometrial epithelial cells

It was important to see if the dual antagonistic/agonistic effects of tamoxifen at the mRNA level translated to altered RAGE protein levels in the endometrium. *In vivo*, endometrial glands, lumen and stroma show significantly greater ERα expression relative to ERβ thus it is likely that most genes, RAGE included, are predominantly regulated via ERα in this tissue (Punyadeera 2008). Previous immunoblot and EMSA analyses in skin endothelial cells revealed 10nM E2-induced RAGE was mediated solely through ERα whereas ERβ had no effect on RAGE protein expression after 4-6h, indicating that RAGE rapidly responds to hormonal simulation via the ER pathway (Tanaka, Yonekura et al. 2000; Mukherjee, Reynolds et al. 2005). RAGE protein expression was therefore investigated in the HEC-1 cells stimulated for 4h with either 10nM E2 or 10nM TX and compared to untreated counterparts.

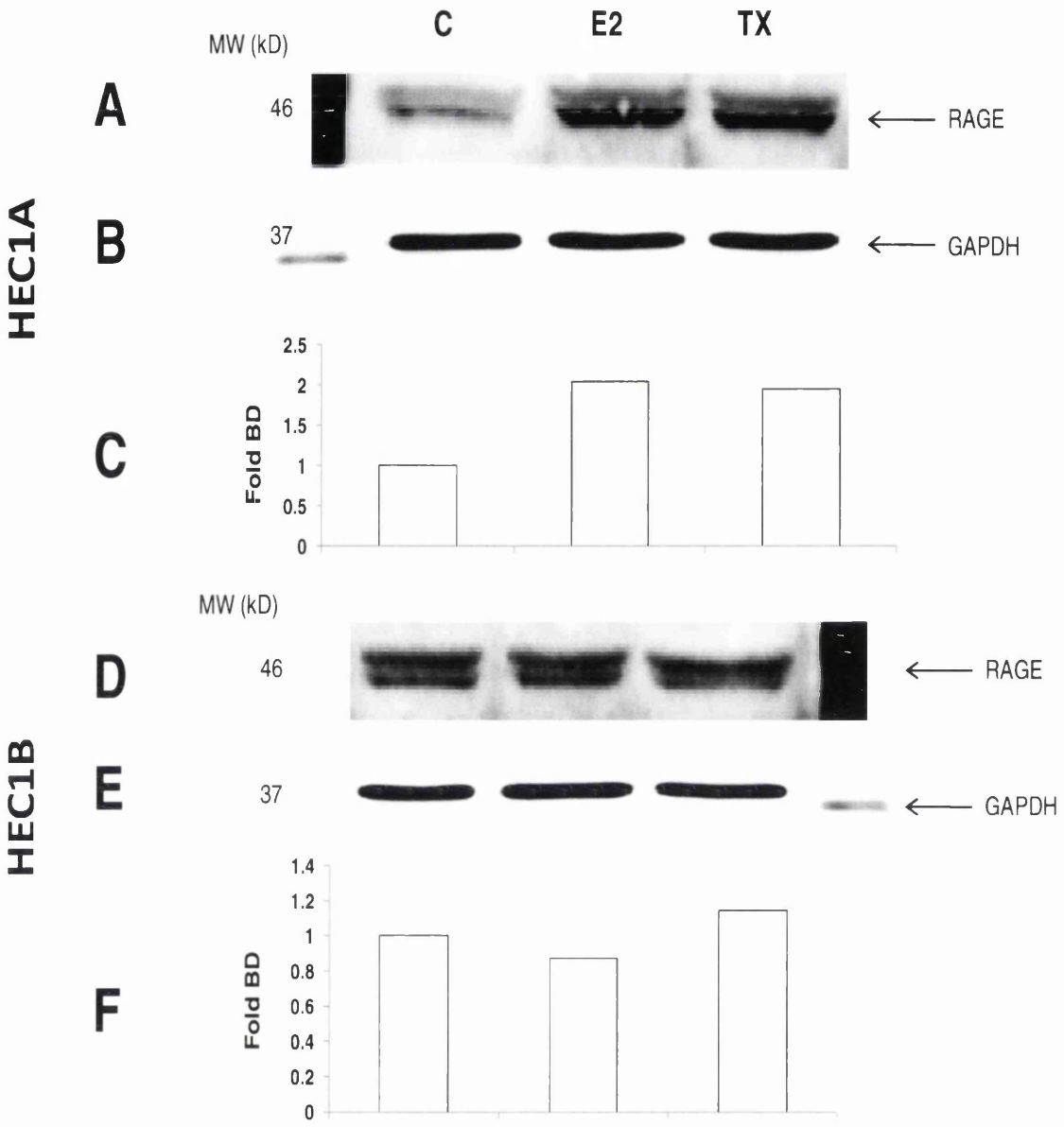

Figure 5-5 17β estradiol and 4-hydroxytamoxifen regulate RAGE protein expression in HEC-1 human endometrial epithelial cells.

Immunoblots show the effect of 10nM 17β estradiol (E2) or 10nM 4-hydroxytamoxifen (TX) treatment on RAGE protein levels after 4h in HEC1A (A) and HEC1B (D).

Confluent cells were harvested in RIPA protein buffer (SIGMA). Immunocomplexes were separated by SDS-PAGE followed by immunoblotting with RAGE (H300: sc-5563) and GAPDH specific (FL-335: sc-25778) rabbit polyclonal antibodies (Santa Cruz). Protein bands corresponding to the un-truncated RAGE membrane-tethered protein were detected at 46kDa. Band Density (BD) was determined using the Quantity One software (Bio-Rad) using the volume rectangle tool for signal intensity/area mm^2. BD is displayed as the fold expression relative to 4h untreated control (Panel C and F) normalised to respective GAPDH samples (Panel B and E).

Figure 5.5 shows that basal RAGE protein was expressed at relatively low levels in both endometrial cell lines (Fig. 5.5 A, D). Basal RAGE expression was higher in HEC1B than in HEC1A which reflects the relative mRNA levels in these cells (Ch. 3 Fig. 3.17). The doublets seen in the immunoblots reveal the presence of a truncated RAGE isoform as well as the full-length receptor in both HEC-1 cell lines. However, expression of the truncated isoform appears to be greater than the full-length RAGE protein in HEC1A (A) whereas in HEC1B cells the expression of both RAGE isoforms appear comparable (D). In HEC1A, RAGE protein is induced 2 fold in cells treated for 4h with 10nM E2 (Fig. 5.5 A, C). The same concentration of TX also increased RAGE protein levels 1.85 fold after 4h in these cells. In contrast, HEC1B cells showed no increase in RAGE protein expression after 4h with either 10nM E2 (0.9 fold) or TX treatment (1.1 fold) (Fig. 5.5 D, F). Potentially, this could be due to differences in the regulation of RAGE by ERα and ERβ. It may also be possible that the effects of these treatments at the protein level are seen at a later time however this is still to be investigated.

5.5 17β Estradiol increases ERα recruitment to the RAGE promoter via Sp1 and Ap1 sites

RAGE is an estrogen responsive gene the expression of which can be modulated transcriptionally through both ERα and ERβ in endometrial cells. However, up-regulation of RAGE at the protein level after 4h is only observed in ERα positive HEC1A cells, suggesting that RAGE is regulated via ERα at this time (Fig. 5.5A, D). Previous characterisation of the RAGE promoter revealed the presence of several non-classical estrogen response elements. In particular, Sp1 sites located in the region spanning -189 to -45 on the

RAGE promoter were shown to be responsive to E2 treatment after 4h in skin-derived HMVECs. Two Sp1 sites at -189/-181 and -178/-172 were both shown to be involved in the transcriptional regulation of RAGE following systematic deletion of the promoter in RAGE-luciferase reporter constructs (Tanaka, Yonekura et al. 2000). Furthermore, in HMVECs only ERα was recruited to Sp1 sites at -189 and -172 on the RAGE promoter after 4h (Mukherjee, Reynolds et al. 2005). In addition, the selective synthetic ERα agonist 17-α-ethinylestradiol (EE) increased ERα occupancy at the Sp1 sites 5 fold more than 17-epiestriol, an estrogen metabolite with selective ERβ agonistic potency (Mukherjee, Reynolds et al. 2005). ERα recruitment to the RAGE promoter specifically at these Sp1 sites is yet to be determined in endometrial cells. In the following ChIP experiments, ER occupation of the two Sp1 sites and a novel singular Ap1 site on the RAGE promoter was assessed prior to and 4h post challenge with 10nM E2 in HEC1A.

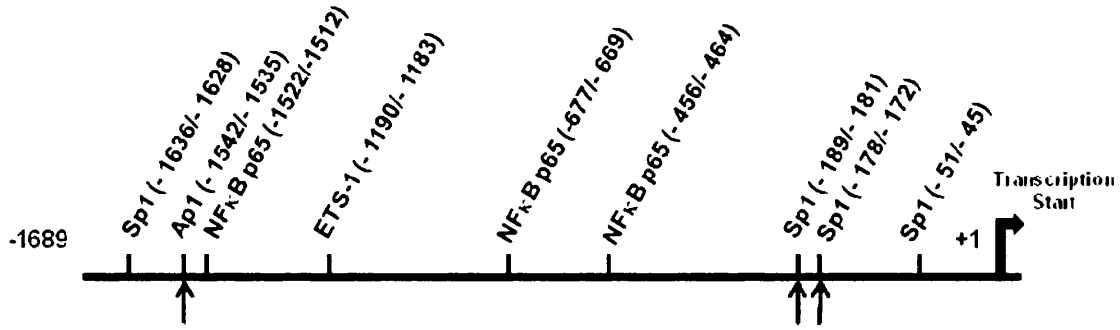

Figure 5-6 Schematic diagram of the RAGE promoter showing the position of the two Sp1 and Ap1 sites investigated

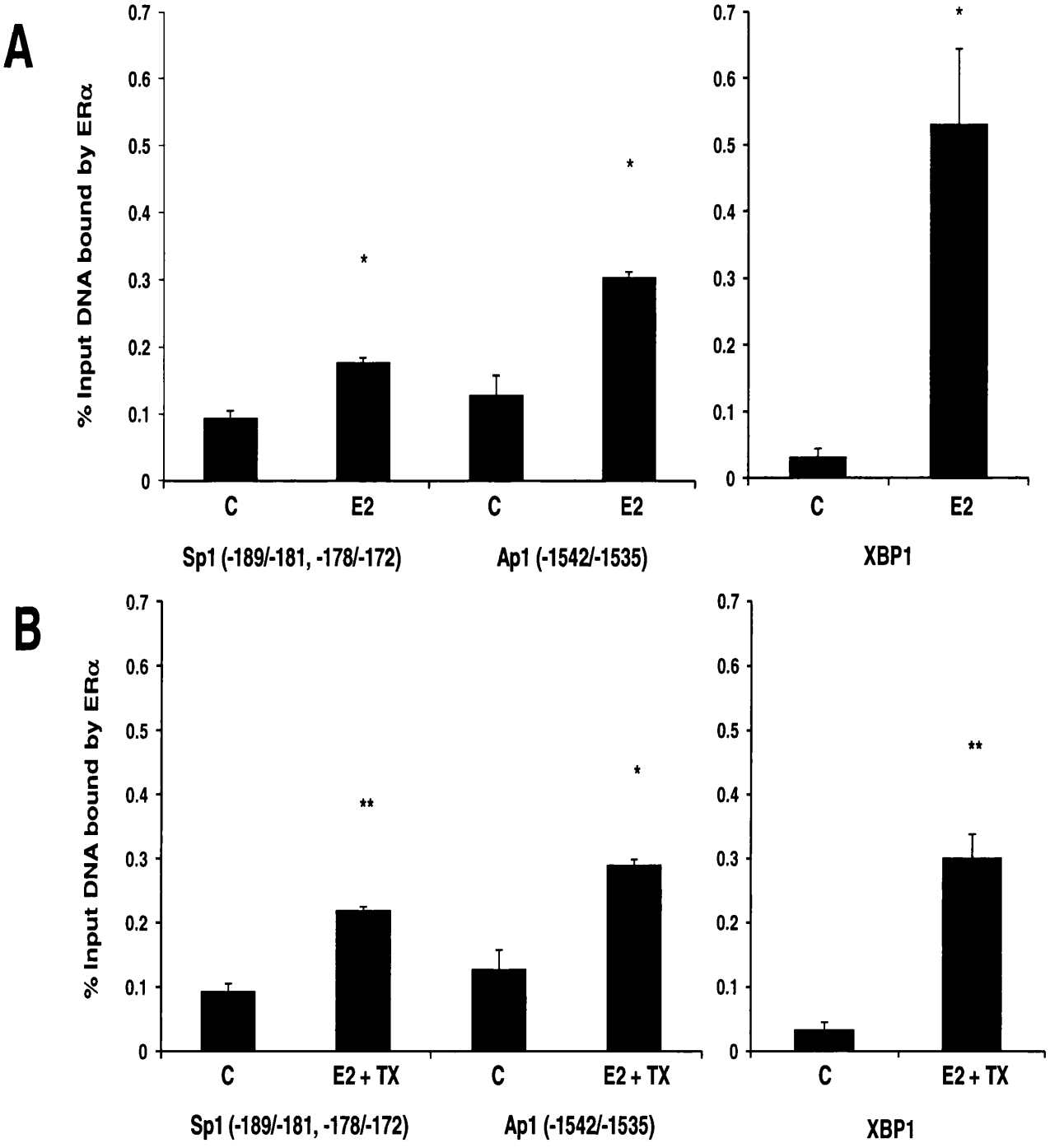

Figure 5-7 Effect of 17β estradiol with or without 4-hydroxytamoxifen on ERα binding at Sp1 and Ap1 sites on the RAGE promoter.

The data presented shows ERα binding to Sp1 and Ap1 sites at -189/ -172 and -1542/ -1535 on the RAGE promoter in HEC1A epithelial endometrial adenocarcinoma cells. Bar graphs illustrate the recruitment level of ERα to the RAGE promoter following 4h treatment with A; 10nM 17β estradiol (E2) alone or B; combined treatment of 10nM 17β estradiol (E2) and 10nM 4-hydroxytamoxifen (TX). ChIP experiments were performed in triplicate and representative results are shown.

Binding to an ERE located at -13351/-13217 on the XBP1 promoter was assessed as a positive control using the same experimental samples. ChIP reactions for a negative control mouse IgG detecting non-specific background signal at each site were run in parallel per sample. Data presented is the mean background subtracted binding level of ERα ± STDEV of triplicates and is shown as a % of Input DNA at the site bound by antibody following immunoprecipitation. Data was analysed using a two-tailed students T-Test *P<0.05, **P<0.01 vs. untreated control.

Figure 5.7 shows that 4h treatment with 10nM E2 resulted in increased recruitment of ERα protein to the RAGE promoter in HEC1A cells. ERα recruitment to a region on the RAGE promoter containing two Sp1 transcription factor sites starting at -181 and -172. In HEC1A cells following E2 treatment, the level of ERα binding to the two Sp1 sites increased by 1.9 fold (p=0.01) and by 2.4 fold (p=0.02) at a single Ap1 site located further upstream at -1542/- 1535 on the RAGE promoter (Fig. 5.7). In control experiments ERα binding increased 16 fold (p=0.02) to the classical ERE on the XBP1 promoter (-13351/-13217). It appears that ERα is recruited to both Sp1 and Ap1 sites in endometrial HEC1A cells however the exact composition of the ERα recruitment factors remains to be determined. The Ap1 transcriptional complex recruited by ERα can exist as a hetero- or homodimer of Fos and Jun proteins, of which there are several identified combinations. However, ERα is more likely to recruit a complex containing both c-Fos and c-Jun proteins to the Ap1 site on RAGE due to preferential heterodimerization of Fos proteins (Ryseck 1991; Chinenov 2001; Matthews 2006). Figure 5.8 demonstrates that ERα recruitment to the RAGE promoter following E2 (10nM) and TX (10nM) treatment at two Sp1 sites (-189/-172) was similar to the recruitment observed with 10nM E2 treatment alone in HEC1A cells (Fig. 5.8). In comparison with untreated HEC1A, 10nM E2 and TX increased ERα recruitment to Sp1 and Ap1 sites by 2.3 fold (p=0.01) and

2.2 fold (p=0.02) respectively after 4h (Fig. 5.8). These results indicate that binding of ERα to RAGE is not antagonised by TX but may be sustained; however this does not result in a repression of RAGE transcript levels in HEC1A (Fig. 5.4A). Thus, TX-complexed ERα may recruit co-repressors to the RAGE promoter. In contrast, ERα binding to the XBP1 enhancer 1 ERE (-13351/-13217) was decreased by almost 50% (0.56 fold) compared to 10nM E2 stimulation alone (16.7 fold vs. control). These findings suggest that TX antagonises E2-mediated ERα recruitment to the XBP1 consensus ERE but not to the Ap1 or Sp1 sites on RAGE suggesting the presence of promoter-specific recruitment mechanisms of transcriptional machinery(Shang, Hu et al. 2000). In addition, these data indicate the possibility of a differential response between classical ERE and non-classical estrogen regulated sites. The observations in HEC1A cells are in accordance with other studies which have shown that TX, when administered in conjunction with E2, can inhibit the agonistic effects mediated by E2 in endometrial models. In addition, genes that displayed an early response to E2 stimulation were principally regulated at non-consensus ER sites whereas after 48h, the majority of E2 responsive genes were regulated via classical estrogen response elements (Johnson, Maleki-Dizaji et al. 2007). E2 exerts a biphasic effect in uterus with a specific early response window observed between 1-4h and later after 24h (O'Brien 2006). Therefore, RAGE can be identified as an early E2 responsive gene regulated by ERα in the endometrium.

5.6 4-Hydroxytamoxifen increases ERα recruitment to the RAGE promoter via Sp1 and Ap1 sites

In earlier experiments, TX was shown to be a potent inducer of RAGE at the mRNA level in both HEC1A and HEC1B (Fig. 5.4 A, B). Additionally, in ERα positive HEC1A cells, 10nM TX induced a 1.9 fold increase in RAGE protein after 4h which was comparable to the effect of 10nM E2. Interestingly, no increase in RAGE protein was observed in HEC1B cells when challenged with 10nM TX (Fig. 5.5A, D). From these findings it was inferred that ERα was likely to be the predominant factor mediating RAGE expression in HEC1A. However, a study investigating gene regulation in breast cancer revealed that ERβ can interfere with the transcriptional activity of ERα. Incorporation of an ERβ expression plasmid into T47D cells reduced the recruitment of Ap1 transcription factor components c-Jun and c-Fos to estrogen responsive promoters as well as reducing E2-induced ERα protein expression by 50% (Matthews 2006). Consequently, it should not be ruled out that ERβ could indirectly affect the outcome of the subsequent results. Nevertheless, it was of interest to establish whether TX at a concentration of 10nM could mimic the E2-induced recruitment of ERα to the Sp1 and Ap1 sites on the RAGE promoter after 4h (Fig. 5.7 A, B).

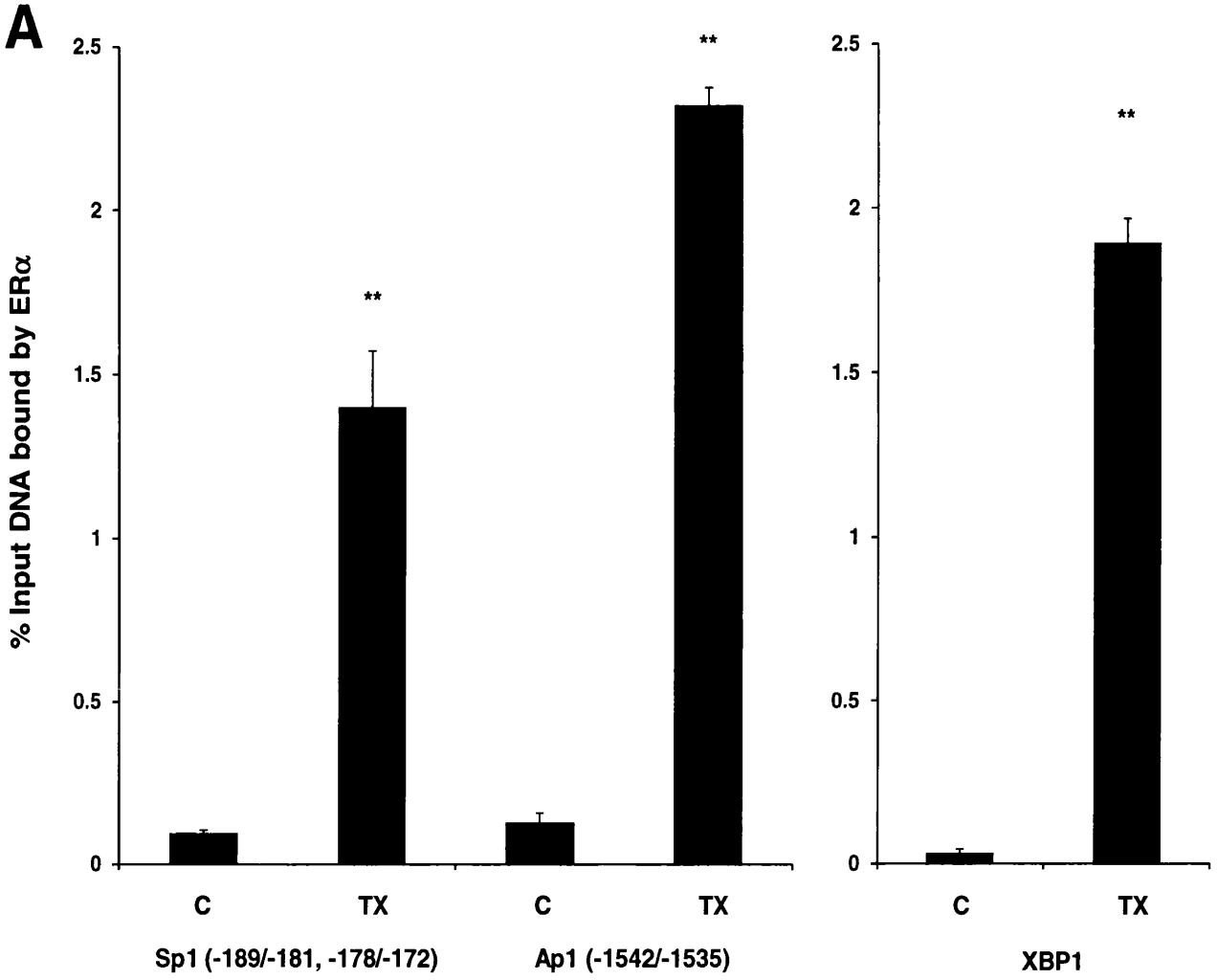

Figure 5-8 Effect of 4-Hydroxytamoxifen on the recruitment of ERα to Sp1 and Ap1 sites on the RAGE promoter

Bar graphs illustrate the level of ERα recruitment to Sp1 and Ap1 sites at -189/ -172 and -1542/ -1535 respectively on the RAGE promoter in HEC1A epithelial endometrial adenocarcinoma cells.

The data presented is the level of ERα binding to the RAGE promoter before (C) and after 4h treatment with 10nM 4-hydroxytamoxifen (TX). ChIP experiments were performed in triplicate and representative results are shown. Binding to an ERE located at -13351/-13217 on the XBP1 promoter was assessed as a positive control. ChIP reactions for a negative control mouse IgG detecting non-specific background signal at each site were run in parallel per sample. Data presented is the mean background subtracted binding level of ERα ± STDEV of triplicates and is shown as a % of Input DNA at the site bound by antibody following immunoprecipitation. Data was analysed using a two-tailed students T-Test *P<0.05, **P<0.01 vs. untreated control.

Figure 5.8 shows treatment of HEC1A cells with 10nM TX alone increased the level of ERα recruitment to the RAGE and XBP1 promoters after 4h. The level of ERα binding at the Sp1 sites (-189/-172) following 10nM TX treatment was 15 fold (p=0.01) greater than in untreated HEC1A, and 7.9 fold greater than with E2 alone (Fig. 5.7). There appears to be preferential binding of ERα to the Ap1 site (-1542/-1535) on RAGE following both E2 (Fig. 5.7) and TX stimulation. TX at a concentration of 10nM increased promoter Ap1 occupation by 18 fold vs. untreated HEC1A (p=0.0004) and 1.7 fold in comparison to Sp1. This may reflect greater affinity for TX/E2-bound ERα to form complex with Ap1 rather than Sp1 proteins in this cell model. The fact that TX induced 7.6 fold greater ERα binding at the Sp1 sites and 7.9 fold at the Ap1 site in comparison to E2 suggests that TX is a more potent ligand of ERα binding activity in HEC1A endometrial cells. Similarly, TX mediated ERα recruitment to the classical ERE on the XBP1 was increased by 59 fold with respect to untreated controls (p=0.0008).

5.7 A Clinical Case Study of RAGE expression in hyperplasic and tamoxifen treated endometrium

Hyperplasia is a risk factor for the development of endometrial adenocarcinoma with over 1 in 5 cases advancing towards malignancy and is particularly prevalent amongst PCO women (Kurman, Kaminski et al. 1985; Balen 2001; Pillay, Te Fong et al. 2006; Villavicencio, Bacallao et al. 2006). PCO women express significantly greater levels of endometrial epithelial and stromal RAGE in comparison to fertile women (Ch.3 Fig. 3.2-3.9). A substantial body of evidence has implicated RAGE and RAGE ligands in the underlying inflammatory micro-environment that precedes tumourigenesis in

several cellular contexts including endometrium (Dougan and Dranoff 2008; Sparvero, Asafu-Adjei et al. 2009; Rojas, Figueroa et al. 2010). Furthermore, endometrial RAGE can be up-regulated potentially via increased ERα-DNA binding in response to E2 and/or TX treatment (Fig. 5.4-5.8) and possibly through AGE-induced NFκB-p65 (Ch.4 Fig. 4.5-4.8). In addition to excess androgens and AGE, estrogens and ER have been shown to be elevated in PCO pathology and may promote proliferation of the endometrium (Leon, Bacallao et al. 2008; Diamanti-Kandarakis, Piouka et al. 2009; Homburg 2009; Margarit, Taylor et al. 2010). Thus, it was of interest to investigate RAGE expression from a clinical perspective.

A preliminary IHC study of two isolated cases of endometrial hyperplasia was undertaken. Biopsy specimens were taken from two patients; the first, a 35 yr old otherwise fertile woman (parity=2) having spontaneously developed endometrial hyperplasia which progressed to cancer (Fig. 5.9A), and a second patient receiving on-going tamoxifen treatment for breast cancer. The latter presented with abnormal bleeding at the time of the first biopsy which was later found to be early stage hyperplasia (ESH, Fig. 5.9B). Three months later after continued bleeding, a second biopsy confirmed atypical hyperplasia (LSH, Fig. 5.9C). IHC images of fertile endometrium (controls) are presented for comparative purposes and were discussed previously in chapter 3 (Fig 3.10). Slides in Fig. 5.9 were stained using standard Haematoxylin and Eosin (H&E) staining for the nuclear and cytoplasmic compartments respectively. Red-brown stain indicated RAGE expression as targeted by Anti-RAGE mouse monoclonal antibody (mAbA11, Millipore).

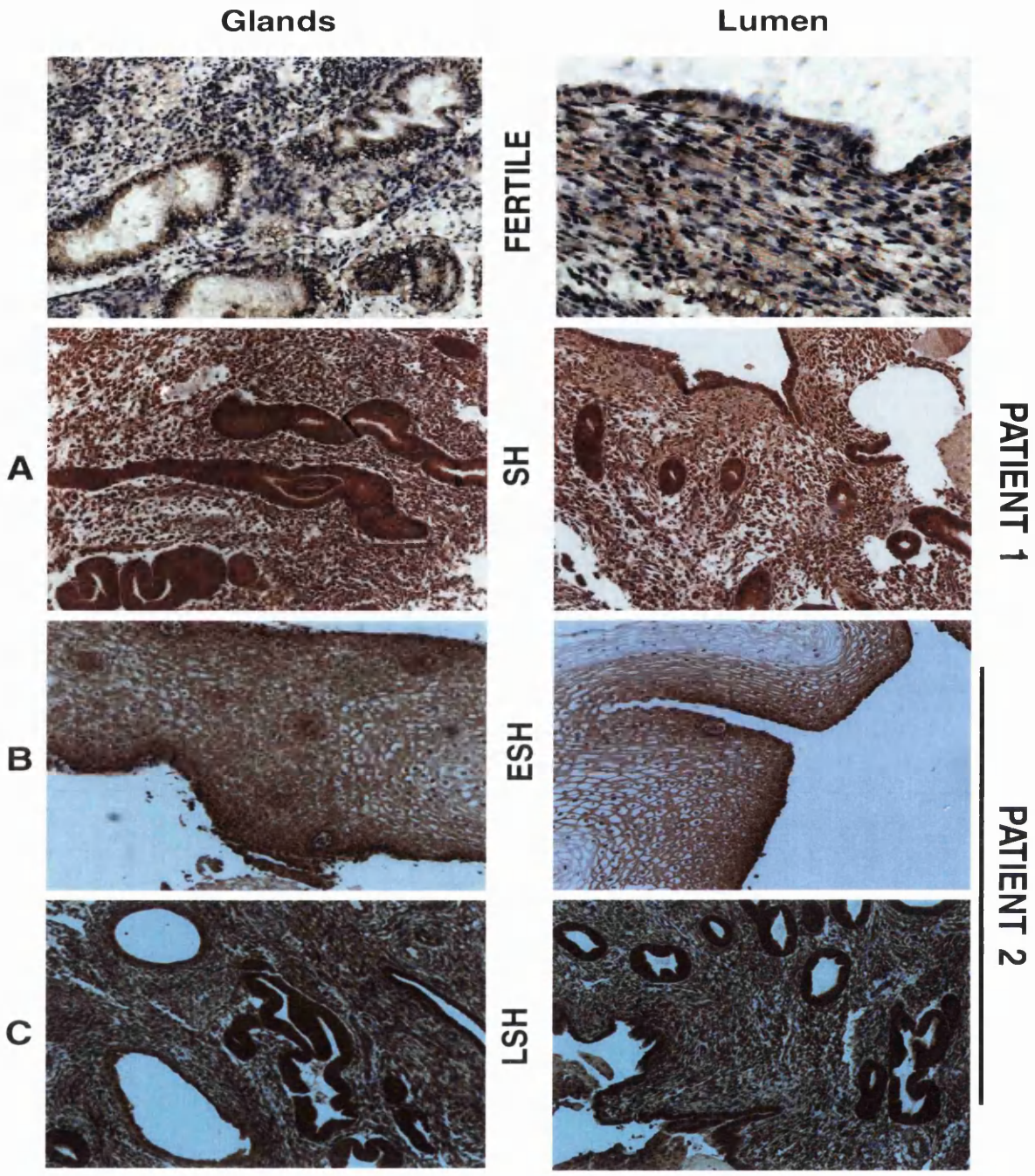

Figure 5-9 Glandular and luminal RAGE expression in hyperplasic endometrium

Panel A: Endometrium from a patient not receiving hormonal therapy who developed spontaneous hyperplasia (SH). Panel B: Initial endometrial biopsy taken from a patient receiving tamoxifen treatment for breast cancer (ESH). Panel C: Biopsy taken 3 months later from the same breast cancer patient in panel B showing confirmed hyperplasia (LSH). Slides were stained with purple (negative) H&E stain for the nuclear and cytoplasmic cell compartments. RAGE protein was identified using the Anti-RAGE monoclonal antibody mAbA11 (Millipore) and is indicated by positive red-brown stain. IHC images were taken using the AxioCam HRc camera (Zeiss) at x20 magnification.

Figure 5.9A demonstrates distinct over-expression of RAGE protein in hyperplasic endometrial epithelium and stromal cells. In particular, the epithelial glands showed intense staining for RAGE and irregular morphology characteristic to hyperplasia (Kurman, Kaminski et al. 1985). Luminal RAGE expression was also distinctly elevated and almost all stroma cells stained positively for RAGE. In the tamoxifen-treated breast cancer patient, an initial biopsy diagnosed as 'normal proliferative' endometrium showed increased epithelial RAGE expression with more intense staining in the lumen than at the glandular surface (Fig. 5.9B). Despite no signs of glandular transformation as seen in 5.9A, the stroma not only stained for elevated RAGE but appeared to show nuclear expansion which may be indicative of early stage hyperplasia (ESH). In later stage hyperplasia (LSH) from the same patient, endometrial RAGE was distinctly over-expressed in the glands and lumen when compared to ESH (Fig. 5.9C). Furthermore, the endometrial stroma had proliferated and the glands appeared to exhibit irregular morphology comparable to the hyperplasic endometrium which progressed to cancer in Fig. 5.9A. These preliminary findings suggest that RAGE may be elevated in hyperplasia and correlate with disease severity. Moreover, it may implicate tamoxifen in the development of hyperplasia due to its known agonistic effect on ER signalling which drives uterine proliferation and up-regulates endometrial RAGE.

5.8 Cross talk between the ER and NFκB pathways may alter RAGE expression in ERα positive human endometrial epithelial cells

Experiments in this chapter have demonstrated that E2 and TX are potent inducers of endometrial RAGE expression. These results, taken together with the finding that AGE-HSA up-regulates endometrial RAGE suggest receptor modulation through two distinct putative signalling pathways namely ERα and

NFκB. Several studies have investigated cross-talk between the ER and NFκB pathway on gene expression in various cell systems. Inhibitory reciprocal ER-NFκB interference has been demonstrated in human liver HepG2 cells co-transfected with ERα expression vector and ERE-luciferase constructs. Introduction of cytokine NFκB-agonists and p65 itself attenuated ERα occupation of the ERE mediated by E2 (Evans, Eckert et al. 2001). Direct ER-NFκB association in osteoblastic U2OS cells was shown to be specific to ERα and p65 either as a homo- (p65/p65) or heterodimer (p65/p50) in co-immunoprecipitation and luciferase reporter deletion assays, whereas no interaction was observed between ERβ or p50/p50 (Quaedackers 2007). Furthermore, studies investigating ER-NFκB cross-talk in human aortic smooth muscle and liver cells have evidenced reciprocal repression may involve competition for p300 or co-recruitment of CBP leading to formation of inactive or unstable complexes (Harnish, Scicchitano et al. 2000; Speir, Yu et al. 2000). More recently, the impact of functional interference between ER and NFκB has been assessed in endometrial tissue. Interestingly, both synergistic and inhibitory cross-talk between ERα-agonist E2 and NFκB-agonist IL-1β was observed between immortalised endometrial and Ishikawa cells. In normal epithelial endometrium, co-treatment had an additive effect on ER-ERE occupation, c-myc and prostaglandin gene expression, whereas in Ishikawa cells, no synergistic effect was observed after 24h (King, Collins et al. 2010). However, other endometrial studies have reported that NFκB activation significantly repressed E2 action on several genes (Feldman, Feldman et al. 2007; Guzeloglu-Kayisli, Halis et al. 2008) In contrast, simultaneous binding of

ERα and p65 to an ERE was required to synergistically up-regulate prostaglandin-E expression in breast cancer cells (Frasor, Weaver et al. 2008). These observations lead to the supposition that ER-NFκB cross-talk is both cell- and gene-specific (King, Collins et al. 2010). The subsequent experiments assess ERα RAGE occupation after 4h 10nM E2 or TX and 10μg/mL AGE treatment in ERα positive HEC1A and Ishikawa cells in order to give some possible preliminary evidence for cross-talk that could influence RAGE regulation in the endometrium.

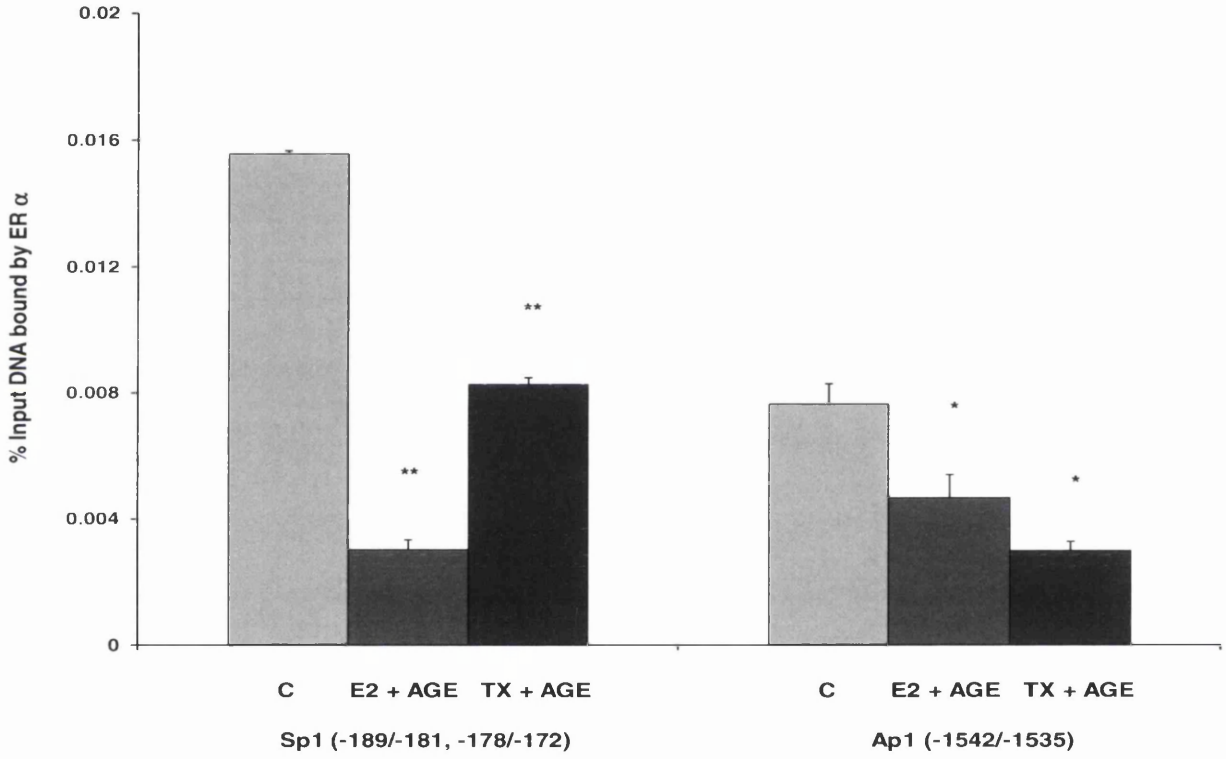

Figure 5-10 AGE-HSA inhibits 17β estradiol and 4-Hydroxytamoxifen-recruited ERα binding to Sp1 and Ap1 sites

Bar graph illustrates ERα recruitment to the RAGE promoter following 4h treatment with either 10nM E2 or TX in combination with 10μg/mL AGE-HSA in HEC1A cells. ChIP experiments were performed in triplicate and representative results are shown. ChIP reactions for a negative control mouse IgG detecting non-specific background signal at each site were run in parallel per sample. Data presented is the mean background subtracted binding level of ERα ± STDEV of triplicates and is shown as a % of Input DNA at the site bound by antibody following immunoprecipitation. Data was analysed using a two-tailed students T-Test *P<0.05, **P<0.01 vs. untreated control.

Figure 5.10 reveals the E2-induced ERα occupation of Sp1 site(s) at -189/-181 and -178/-172 on the RAGE promoter was significantly inhibited when compared to basal levels after 4h AGE treatment (reduced 0.2 fold vs. control, p=0.0003). Similarly, ERα occupation of the Ap1 site at -1542/-1535 was significantly reduced in comparison to control levels following E2 and AGE-HSA treatment (0.6 fold vs. control, p=0.0002). Furthermore 10μg/mL AGE-HSA significantly reduced TX-induced ERα occupation with respect to untreated controls at both Sp1 site(s) (0.5 fold vs. control, p=0.05) and the Ap1 site (0.4 fold vs. control, p=0.01). These results suggest that possible NFκB-ER cross talk alters ERα-RAGE interaction at the promoter, and perhaps also influences RAGE regulation at the transcription level (Fig. 5.11).

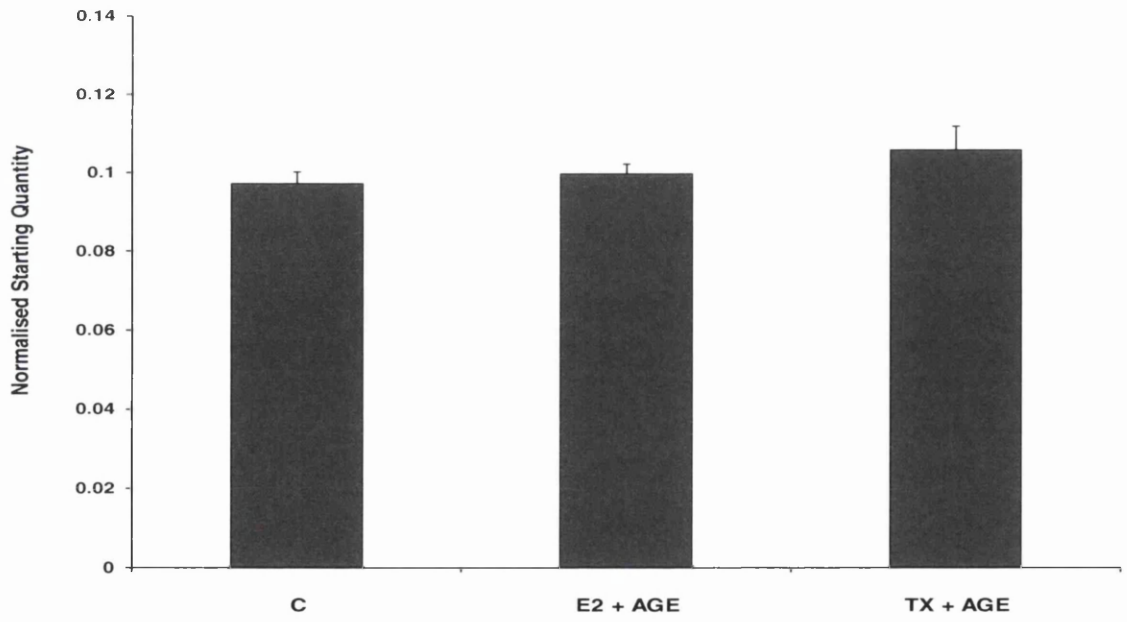

Figure 5-11 AGE-HSA inhibits the induction of RAGE transcript by 17β estradiol and 4-hydroxytamoxifen

Bar graph shows the effect of 17β estradiol (E2) and 4-hydrotamoxifen (TX) in combination with AGE-HSA on RAGE expression in HEC1A cells by real time PCR. HEC1A cells were treated with either 10nM E2 or 10nM TX with 10μg/mL AGE-HSA for 4h. Values given are mean starting quantity (StQ) normalised to RPL19 ± STDEV from StQ triplicates. Data was analysed using a two-tailed students T-test.

Figure 5.11 simply demonstrates no significant difference between RAGE mRNA expression in HEC1A cells challenged for 4h with either E2 or TX (10nM) and 10μg/mL AGE-HSA and untreated cells. These results suggest AGE-HSA may abrogate E2 and TX-induced RAGE transcript, and potentially indicate that these agents modulate RAGE through opposing regulatory pathways.

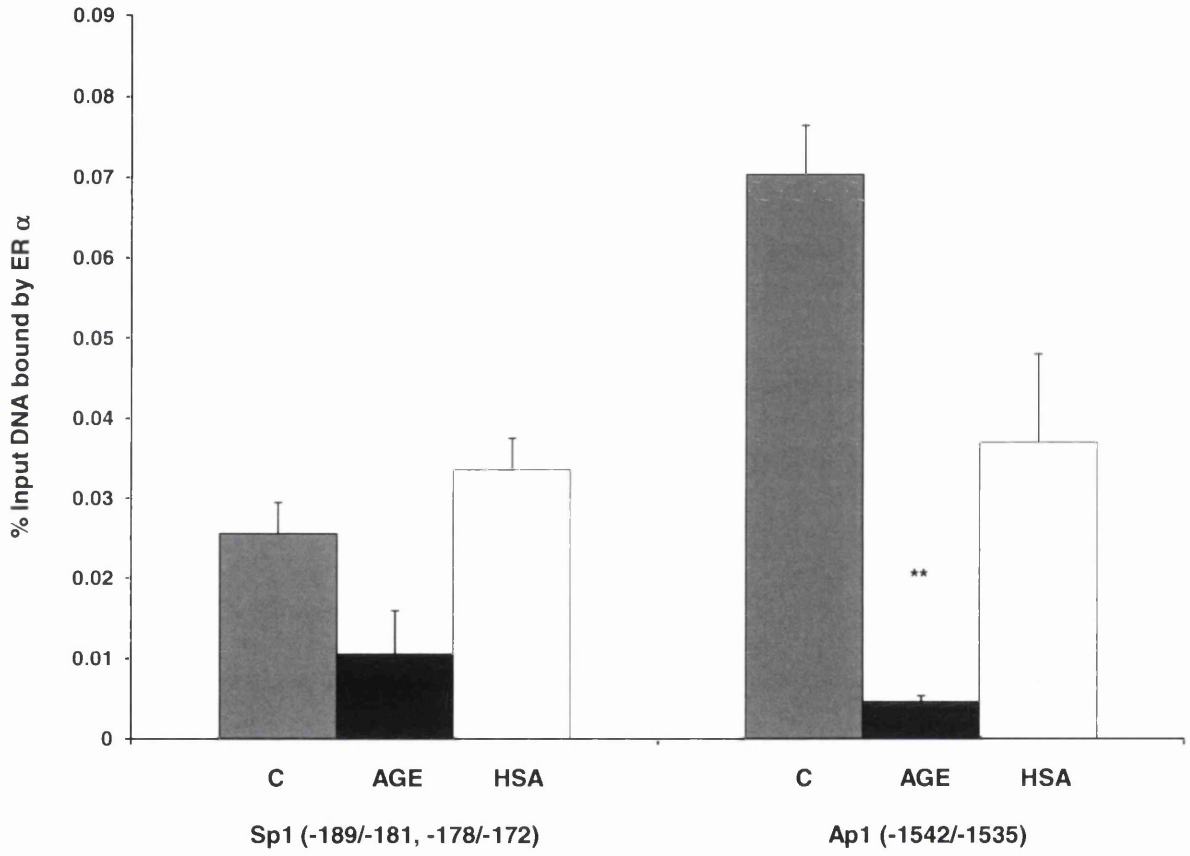

Figure 5-12 AGE-HSA inhibits ERα binding to two Sp1 sites and one Ap1 site

Bar graph illustrates recruitment of ERα to the RAGE promoter following 4h treatment with 10μg/mL AGE-HSA in Ishikawa endometrial epithelial cells. Unmodified HSA (10μg/mL) was used as a biological negative control. ChIP experiments were performed in triplicate and representative results are shown. ChIP reactions for a negative control mouse IgG detecting non-specific background signal at each site were run in parallel per sample. Data presented is the mean background subtracted binding level of ERα ± STDEV of triplicates and is shown as a % of Input DNA at the site bound by antibody following immunoprecipitation. Data was analysed using a two-tailed students T-Test *P<0.05, **P<0.01 vs. untreated control, C.

Figure 5.12 shows the effect of 10μg/mL AGE-HSA treatment on ERα recruitment to the RAGE promoter in a second endometrial cell line, Ishikawa. In comparison to untreated Ishikawa cells, 10μg/mL AGE-HSA reduced ERα recruitment to the region on the RAGE containing two Sp1 sites however this decrease in binding was not significant (0.4 fold vs. control, p=0.08). Thus, AGE-HSA does not affect occupation of Sp1 sites by ligand activated ER when the cells are treated with 10μg/mL AGE-HSA alone. Furthermore, ERα recruitment to the Sp1 sites following 10μg/mL unmodified HSA treatment remained altered from ERα occupation observed in control samples (p=0.18). In untreated Ishikawa, more ERα is bound to the Ap1 site after 4h than at the two Sp1 sites combined, suggesting that ER may have a greater affinity for Ap1 proteins or the site itself. ERα recruitment is significantly inhibited after 10μg/mL AGE-HSA treatment (0.1 fold vs. control, C) at the Ap1 site. The same concentration of unmodified HSA also reduced ERα occupation by 0.53 fold at this site however it was not found to be significantly different from the control sample (p=0.06). These results indicate that in two ERα positive cell line models of endometrial epithelium, the ambient concentration of AGEs or the possible activation of the NFκB pathway may affect the regulation of RAGE by the ER pathway.

5.7 Discussion

This chapter has endeavoured to elucidate the mechanisms behind the modulation of RAGE by 17β estradiol and 4-hydroxytamoxifen, and provides the first evidence of ERα and ERβ in mediating E2 and TX agonist action on endometrial RAGE expression. Importantly, these results demonstrate that

endometrial RAGE is induced by E2 at physiological and high concentrations at the mRNA (Fig. 5.4 A, B) and protein level (Fig. 5.5 A, C), and that administration of 10nM TX differentially modulated the E2-induced response in HEC-1 cells. For the most part, TX exhibited an antagonistic effect on E2-induced RAGE transcript in estrogen stimulated cells (Fig. 5.4). However, when cells were treated solely with 10nM TX in the absence of estrogen or low estrogenic milieu, RAGE mRNA was distinctly up-regulated in both HEC1A (11.2 fold) and HEC1B cells (5.9 fold) indicating that TX conferred ER dependent agonistic potency in the endometrium (Fig. 5.4). ChIP experiments revealed that 10nM E2 increased ERα occupation on the RAGE promoter at Sp1 and Ap1 sites in ERα positive HEC1A cells (Fig. 5.7A) but not in HEC1B (data not shown). Similarly, 10nM TX treatment increased ERα recruitment to the RAGE promoter and the level of ERα enrichment at both Sp1 and Ap1 sites was significantly greater than in E2-treated cells (Fig. 5.7, 5.8). TX partially antagonised E2-induced ERα recruitment, slightly reducing the level of binding in comparison to E2 treated cells, however more ERα was bound to the Sp1 and Ap1 sites than in untreated controls (Fig. 5.7B). Furthermore, preferential binding of E2 and TX-liganded ERα to the Ap1 site on the RAGE promoter is a novel observation (Fig. 5.7, 5.8). Based on previous observations (discussed in Fig. 5.13) differential availability and/or recruitment of ER coactivators/repressors may mediate the dynamic effects of TX in the uterus. The principal findings in this chapter have perhaps highlighted that the low estrogenic milieu post menopause may render the endometrium susceptible to potent ER agonist action in women taking tamoxifen treatment for ERα positive breast cancers. Consequently, we may have exposed this specific cohort of women receiving tamoxifen treatment to

a secondary risk of endometrial cancer due to its agonism of RAGE signalling. RAGE has been implicated in the perpetuation of pro-inflammatory responses allied to tumourigenesis in several cell systems most notably in lung and pancreatic cancer, and hypothetically could also mediate pre-cancerous mechanisms that advance endometrial malignancy (Hiwatashi, Ueno et al. 2008; Kang, Tang et al. 2009; Sparvero, Asafu-Adjei et al. 2009; Rojas, Figueroa et al. 2010). Moreover, this suggestion was reinforced with the discovery that endometrial hyperplasia that materialized both spontaneously and under tamoxifen stimulus, stained extensively for RAGE (Fig. 5.9). However, larger cohorts of patients with endometrial hyperplasia and tamoxifen-treated breast cancer would need to be recruited to this study in order to further implicate RAGE in endometrial cancer development. Finally, several studies have reported reciprocal inhibitory cross-talk between ERα, NFκB and their respective pathways in a variety of cellular contexts (Harnish, Scicchitano et al. 2000; Evans, Eckert et al. 2001; Chadwick, Chippari et al. 2005; Kalaitzidis and Gilmore 2005; Guzeloglu-Kayisli, Halis et al. 2008). These preliminary results imply that endometrial RAGE expression may be influenced by the interplay of NFκB-and ER-mediated stimuli, which perhaps could provide a means of exploiting RAGE as a therapeutic target and may be of particular importance for women with PCOS, endometriosis and tamoxifen-treated breast cancer.

Figure 5.13 depicts E2 as an agonist in the uterus recruiting specific subsets of p160 co-activators to E2 responsive genes: SRC-1, SRC-2, SRC-3, [CBP and HDAs] in MCF-7 breast and [endometrial ECC-1 and Ishikawa cells] (Fig. 5.13A) (Shang, Hu et al. 2000; Shang and Brown 2002).

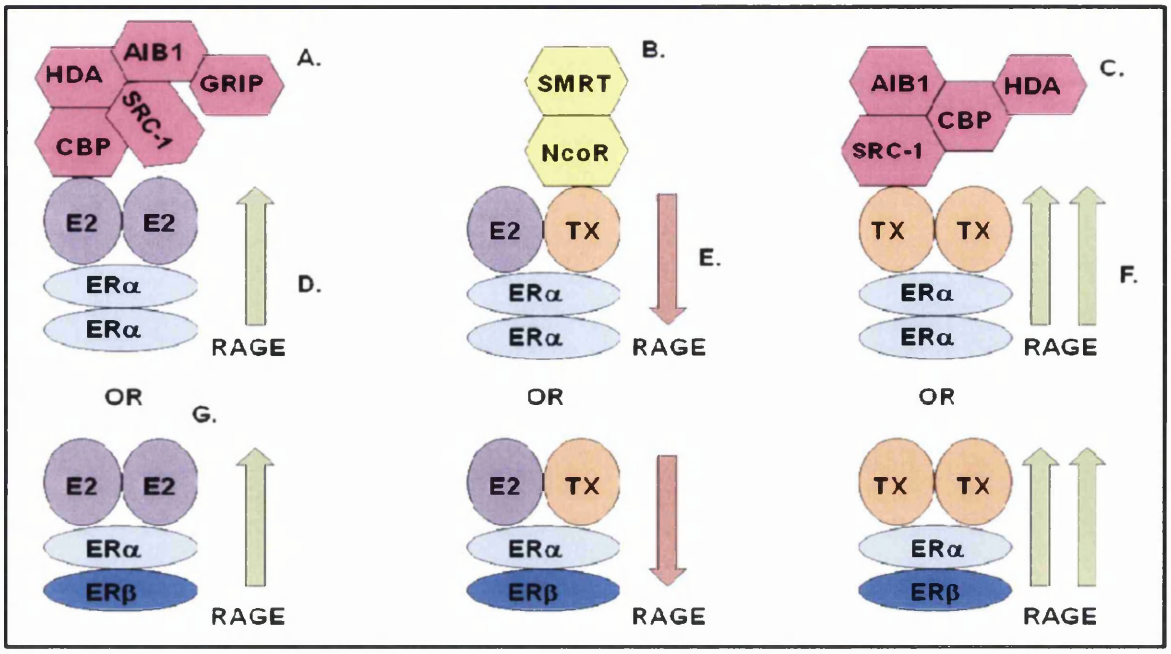

Figure 5-13 Diagram to illustrate the possible mechanisms behind the ER modulation of RAGE in the endometrium

In contrast, TX is a known ER antagonist in breast where it recruits co-repressors NcoR and SMRT to ERα (Fig. 5.13B) (Shang, Hu et al. 2000). However in uterus, TX is an agonist or antagonist depending on the gene in question. For example, TX is an ER agonist recruiting SRC-1, SRC-3 and CREB to the c-myc promoter yet behaves as an antagonist recruiting NcoR and SMRT to the cathepsin D promoter in Ishikawa (Fig. 5.13B, C) (Shang and Brown 2002). In the HEC1A models, TX acted antagonistically on ER(α) when in conjunction with E2, yet when the cells were treated with TX alone, it acted agonistically on ER(α) to induce RAGE (Fig. 5.4, 5.7, 5.8) (Scafonas, Reszka et al. 2008). It could therefore be hypothesised that E2 and TX may utilise mechanisms similar to those depicted in Fig. 5.13E and F to induce RAGE in the endometrium. Further adding to the complexity of ER signalling, ERα enrichment at Sp1 and Ap1 sites on RAGE is likely to be representative of both ERα/ERβ and ERα/ERα dimers (Fig. 5.7, 5.8 and 5.13G) which may dictate coactivator/repressor recruitment (Li, Huang et al. 2004).

CHAPTER 6

Summary
&
General Conclusions

6. Thesis Summary and General Conclusions

6.1 Thesis Summary

The novel results described in this thesis have served to characterise the expression of the AGE receptor in human eutopic endometrium. RAGE was shown to be significantly elevated in PCOS, endometriosis, hyperplasia and cancer. In addition, this project served to provide evidence for the transcriptional mechanisms involved in RAGE modulation using endometrial cell line models. Specifically, this project addresses the role of AGEs, 17β estradiol and the anti-estrogen 4-hydroxytamoxifen on the transcriptional activity of RAGE. The following discussion begins with a brief synopsis of the work accomplished in this project in order to give an overall representation of the AGE-RAGE axis in the endometrium. Thereafter, potential roles for the AGE-RAGE axis in female infertility and gynaecological malignancies are discussed.

Immunohistochemistry results in chapter 3 demonstrated for the first time that RAGE is expressed in both fertile and infertile human endometrium. However, RAGE exhibited differential expression in the glandular, luminal and stromal endometrial compartments between the fertile and the infertile PCOS and endometriosis women. RAGE was found to be significantly elevated in both ovulatory and anovulatory PCO endometrial glands, lumen and stroma with respect to fertile endometrium. Greatest RAGE expression was observed in the proliferative phase ovulatory PCOS patients across all endometrial cell subtypes, whereas secretory phase ovulatory PCO endometrium had comparable levels of RAGE to anovulatory patients. In addition, infertile endometriotic endometrium showed significantly greater RAGE protein localized solely to the glandular epithelium, and secretory

phase stroma when compared to fertile controls. In contrast, no difference in luminal RAGE expression was observed between endometriotic and fertile endometria irrespective of menstrual cycle phase. The level of RAGE transcript was assessed in whole tissue and epithelial cells isolated from endometrial biopsy. Real time PCR results revealed that

RAGE mRNA levels were significantly higher in anovulatory PCO whole endometrial tissue and cultured epithelial cells when compared to fertile controls. Increases in RAGE transcript in proliferative phase endometriosis did not reach significance over proliferative phase fertile controls either in whole endometrial tissue or the isolated epithelial cells. In contrast, RAGE mRNA was significantly greater in whole tissue and epithelial cells of secretory phase endometriotic endometrium. Finally, RAGE transcript was evaluated in endometrial epithelial adenocarcinoma cell lines; Ishikawa, Heraklio, HEC1A and HEC1B, the latter having the greatest expression. This allowed for the work in the subsequent chapters to be undertaken in these cell lines as appropriate *in vitro* models of the endometrial epithelium. Using these *in vitro* models, endometrial RAGE expression was investigated at the mRNA and protein level following stimulation with its ligand AGE.

Chapter 4 endeavoured to investigate whether endometrial RAGE could be manipulated in the *in vitro* models with the introduction of ligand. RT-PCR results conducted in the four cell lines revealed that RAGE transcript could be significantly up-regulated by AGE-HSA in a time- and dose-dependent manner. AGE-HSA at a concentration of 10μg/mL had the greatest effect on RAGE mRNA levels whereas the same concentration of HSA negative control did not. Using 10mg/mL AGE-HSA, RAGE protein levels were also up-regulated in Ishikawa and Heraklio cells after 4h however, at later times

increases in RAGE were observed that were likely due to factors acting independently of the exogenous AGE input. AGE-HSA treatment at 10μg/mL slightly elevated phosphorylated NFκB-p65 levels in Ishikawa and Heraklio after 15 min. However, within the confines of the experimental set up, phosphorylated p65 appeared to be constitutively active. Importantly, ChIP data in chapter 4 demonstrated the involvement of NFκB in the transcriptional regulation of RAGE. ChIP results revealed that post 4h challenge with AGE-HSA, occupation of NFκB-p65 at NFκB sites on the RAGE promoter was significantly increased in Ishikawa and Heraklio cells. Furthermore, AGE-induced NFκB-p65 recruitment was also observed at NFκB sites on the MUC1 promoter, a known NFκB target gene in the endometrium and breast (Lagow and Carson 2002; Thathiah, Brayman et al. 2004). It was thus demonstrated for the first time the existence of an AGE-RAGE axis in the endometrium involving the transactivation of NFκB-p65 signalling (Ch.4). NFκB pathway aside, very little was known about additional pathways involved in the modulation of RAGE. Given that endometrial tissue function is largely dependent on its responsiveness to sex steroids, experiments in the subsequent chapter attempted to elucidate a role for 17β estradiol.

The data presented in chapter 5 indicated that RAGE could be targeted through the ER pathway in the epithelial endometrium. RT-PCR, western Blot and IHC confirmed the expression of the ERα and ERβ receptors in the cell line models; HEC1A as ERα positive and HEC1B as ERα negative. Significantly, RAGE transcript was revealed to be induced by 10nM E2 in both cell lines after 4h. Conversely, RAGE appeared to be differently regulated at higher E2 concentrations. The effects of E2 and TX treatment in

these two cell lines also indicated differential agonism/antagonism of E2-induced RAGE expression specific to the two ER subtypes, thus TX differentially modulated RAGE mRNA in a cell line ER subtype- and E2 concentration-specific manner. Moreover, these results also indicated that in addition to E2, TX was also a potent inducer of RAGE expression in the endometrium. Despite greater basal RAGE expression at the protein level in HEC1B, consistent with greater mRNA levels in this cell line, no induction of RAGE was observed post challenge with E2 or TX. In contrast, RAGE protein was up-regulated by E2 and TX in HEC1A cells under the same conditions. From this, it was inferred that ERα was the predominant factor facilitating RAGE regulation in the endometrium, or that any ERβ driven RAGE protein accumulation may occur at a later time. Finally, ChIP experiments using an ERα-specific antibody revealed that ERα recruitment to the RAGE promoter was by way of protein-protein interaction with Ap1 and Sp1 transcription factors. ERα recruitment to Sp1 and Ap1 sites on the RAGE promoter was increased with 10nM E2 and furthermore increased with 10nM TX treatment when compared to untreated controls.

6.2 Significance of elevated RAGE in endometriosis and PCOS

The work in this thesis has demonstrated that endometrial RAGE is regulated at the mRNA and protein level by AGEs and E2 which are elevated in PCOS and endometriosis pathology respectively. Hyperandrogenism, particularly excess dihydrotestosterone (DHT), in combination with elevated AGEs, increase formation and activity of the β-catenin/pTIF2/AR transcription complex in HMVECs (Otero 2001). The activity of this AR complex is increased in the presence of estrogen, and AR itself can even be liganded and activated by estrogens in Ishikawa endometrial cells (Lovely, Appa Rao

et al. 2000; Truica 2003). Interestingly, endometrial epithelial β-catenin displays transient nuclear localisation during the estrogenic secretory phase (Saegusa, Hashimura et al. 2007). This AR/β-catenin complex targets and initiates transcription of AR genes one of which is MUC1 (see Figure 6.1). In addition, liganded-RAGE activates ERK1/2 MAPKs and NFκB which in turn directly up-regulate both RAGE (and MUC1) via p65-DNA binding (Yeh 2001; Li 2004; Thathiah, Brayman et al. 2004; Ahmad, Raina et al. 2009; Liu, Liang et al. 2010). One possibility is that RAGE could potentially act as an upstream effector of MUC1 which is up-regulated during a period of maximal receptivity termed the 'window of implantation'(Hey, Graham et al. 1994). MUC1 is thought to prime endometrial epithelium for blastocyst apposition. Specifically, the large MUC1 ectodomain acts as a scaffold in glandular epithelia for the recruitment of adhesive carbohydrates that ligand L-selectin expressed on the blastocyst apical surface (DeLoia, Krasnow et al. 1998; Carson, Julian et al. 2006; Margarit, Gonzalez et al. 2009). Inefficient clearance or altered MUC1 expression be it up or down regulation has been implicated in implantation failure and infertility (Hey, Graham et al. 1994; Horne, Lalani et al. 2005; Margarit, Taylor et al. 2010). Immunohistochemical appear to reflect over expression of RAGE and MUC1 in secretory endometriotic and proliferative anovulatory PCO endometrium, however the data sets are limited and more patient samples would be needed to provide more conclusive results.

6.3 Elevated RAGE expression presents a risk of endometrial cancer for women with PCOS, endometriosis and patients receiving tamoxifen for breast cancer

RAGE has been implicated in the development of several cancers particularly lung, colorectal, gastric and cervical metastasis (Tsuji 2008; Srikrishna and

Freeze 2009). Tamoxifen, has proven to be a very effective antagonist in breast and has been used for the treatment of breast cancer for years. However, tamoxifen has been phased out in favour of aromatase inhibitors and is no longer administered to post-menopausal breast cancer patients due to concern that it possesses estrogenic properties in the uterus that induce proliferation. Nevertheless, RAGE is distinctly up-regulated by TX and its expression in hyperplasic endometrium appears to correlate with progression towards endometrial cancer. Therefore, it could be speculated that enhanced RAGE expression could promote an altered endometrial pro-inflammatory cytokine profile which fuel tumourigenesis. RAGE, elevated by hyperestrogenism in endometriosis or by hyperandrogenism and AGE in PCOS, can potentiate pERK, NFκB and pro-inflammatory cytokines (Roberts, Luo et al. 2005; Honda, Barrueto et al. 2008; Sharma, Dhawan et al. 2010; Song, Zhang et al. 2010). Chronic anovulation and hyperestrogenism increase the risk of endometrial hyperplasia or carcinoma development in these patients due to prolonged action of 'unopposed' estrogens (Acconcia, Barnes et al. 2006; Giudice 2006; Zhu and Pollard 2007). Estrogen (17β-estradiol) has also been shown to up-regulate IL-6 and IL-8 promoting epithelial ovarian cancer through the MAPK/NFκB and ERα (Yang, Wang et al. 2009). AGE-RAGE can also up-regulate β-catenin which is implicated in promoting endometriotic cell survival and the *trans*-differentiation of endometrial cells to a cancerous state (Otero 2001; Saegusa, Hashimura et al. 2007; Banu, Lee et al. 2009).

6.4 The AGE-RAGE axis: Potential altered uterine environment through the transactivation of MUC1

Figure 6.1 shows a potential positive feedback loop mechanism whereby RAGE could indirectly up-regulate several uterine genes that are downstream targets of NFκB. This pro-inflammatory signalling pathway may act as a pre-cancerous mechanism that, if over-stimulated, may not only increase the risk of developing cancer but also lead to an altered uterine environment which could impact on blastocyst implantation. The menstrual cycle involves the cyclical coordinated proliferation driven by various growth factors and cytokines. It is my hypothesis that in PCO and endometriotic endometrium, this signalling pathway is constitutively enhanced due to pathology-specific excessive RAGE stimuli (i.e. AGEs, E2 and TNFα). Inflammatory cells, such as macrophages at the site of localised inflammation produce several RAGE ligands (S100, HMGB1, AGEs) which activate intracellular NFκB signalling (6.1.B) via RAGE binding (6.1.A). NFκB signalling involves the MAPK ERKs that phosphorylate IκBα to release p65/p65, p65/p50 to bind to RAGE and other target genes such as MUC1 (6.1.C) which invariably results in increased RAGE and MUC1 expression at the uterine surface. What's more, activation of NFκB leads to generation of several oxidative stress compounds (ROS) which can lead to accelerated AGEs formation to create a systemic inflammatory cycle through perpetuation of RAGE activation (6.1.D,E,F). Secondly, as previously stated, AGEs have been shown to induce E-cadherin dissociation and increased formation of the AR/β-catenin complex which can transactivate MUC1 which has not only been implicated in infertility but also acts as an oncogene in breast, colon and prostate cancers (6.1.H, I, J, K, L). There is a possibility that this signalling is promoted in PCOS and

endometriosis, characterized by excess AGEs and hyperandrogenism and excess estrogens respectively, (6.1.M) and could perhaps explain the observed over-expression of RAGE in the PCO, endometriotic, hyperplasic and cancerous endometrial specimens in this project.

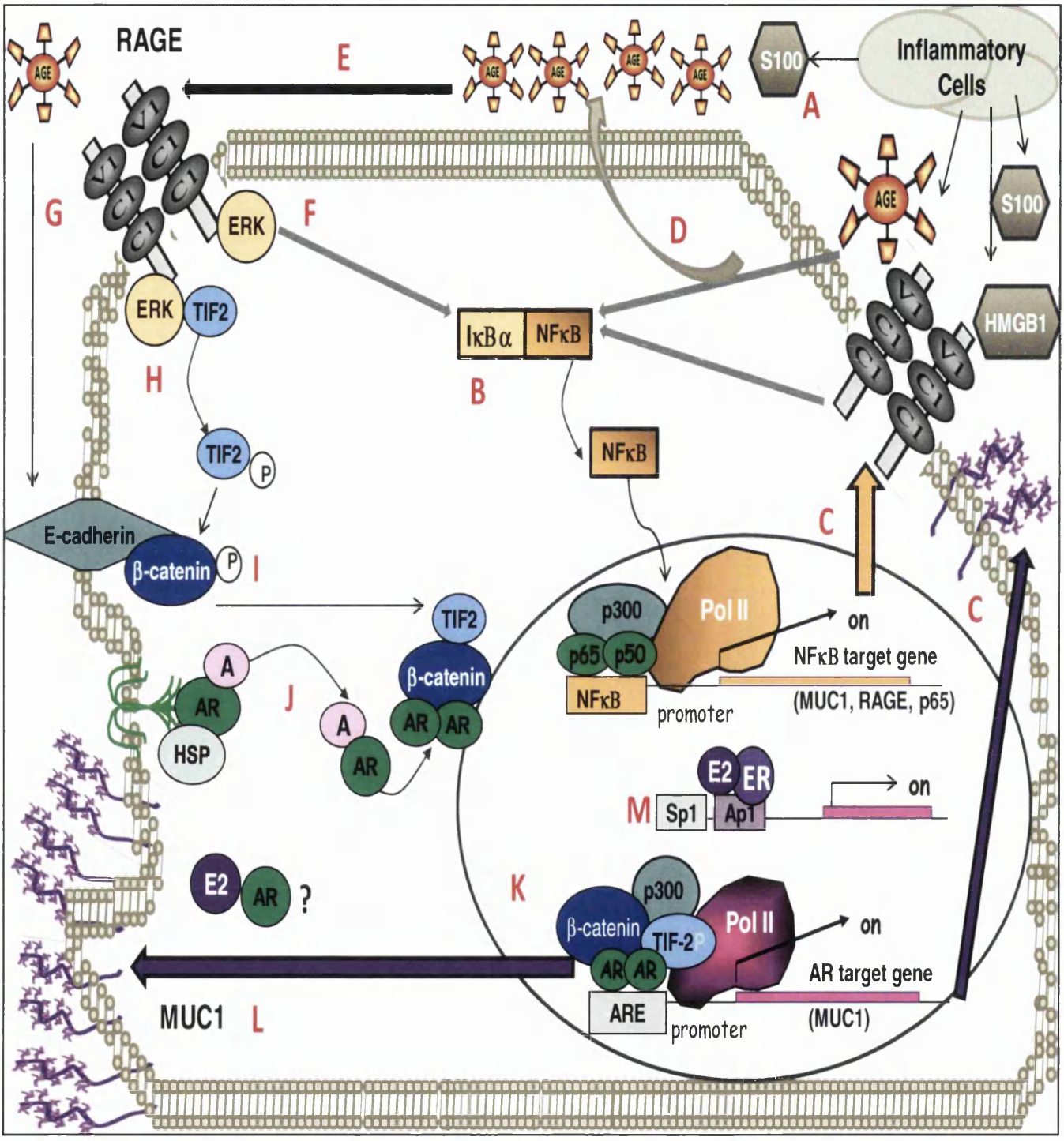

Figure 6-1 Putative positive feedback loop for RAGE regulation and its potential downstream targets

6.5 RAGE as a therapeutic target

This identification of RAGE expression in the endometrium may be significant for women with PCOS, endometriosis and endometrial cancer. Inflammatory processes involving RAGE could play an important role in these gynaecological diseases. The initial findings reported here on the regulatory pathways underlying RAGE modulation in the endometrium may present an avenue for exploitation towards the development of potential RAGE targeted therapeutics, or management of current treatment regimes through the use of RAGE as a clinical biomarker cf. Breast cancer and Tamoxifen. Expansion of the current study to a larger scale cohort of patients will confirm the importance of RAGE in these diseases. Furthermore, investigation into existing chemical entities such as RAGE, NFκB and ER modulators in our endometrial model will further elucidate the contribution and cross-talk of these pathways.

6.6 Study Limitations and Future Work

This study primarily focuses on the use of chromatin immunoprecipitation to show direct ER and NFκB protein-RAGE promoter interaction. While the ChIP experiments demonstrate that these proteins bind directly or indirectly via recruitment of other transcription factors to RAGE itself, this technique does not show the effect of these associations on transcriptional outcome. Neither does ChIP provide direct evidence of these proteins being up-stream of RAGE despite mRNA analysis suggesting that the NFκB and ER pathways are involved in its modulation in the endometrium. In order to strengthen these findings, future work would aim to combine these ChIP experiments with RAGE-luciferase reporter gene construct assays to measure promoter activity and expression in response to 17β estradiol, 4-hydroxytamoxifen and

AGE stimulation. In order to better characterise the candidate molecules of the NFκB and ER pathways that mediate the cellular response to AGEs and estrogen respectively, specific siRNA inhibitor/gene knock-down experiments could also be carried out. Moreover, future work could utilise confocal microscopy to assess RAGE expression prior to and post challenge with AGE in fertile and infertile PCO endometrium. Confocal studies in endometrial cells would also have the potential to show reputed AGE-induced NFκB nuclear translocation in line with previous work undertaken in PCO granulosa cells (Diamanti-Kandarakis, E. et al. 2007). Further limitations to this study are the known apoptotic effects of AGEs and more recently, the discovery that selective estrogen receptor modulator tamoxifen can induce apoptosis through an ER independent mechanism. In glioma cells not expressing ER, tamoxifen-induced cytotoxicity strongly correlated with a 4 fold increase in NFκB activity, cytosolic calcium influx and up-regulation of antiapoptotic genes. Conversely, inhibition of the NFκB pathway sensitized the cells to tamoxifen insult and lead to apoptosis (Hui, A-M et al. 2004). It is therefore important to recognise that the AGE- and tamoxifen-induced up-regulation of RAGE in the endometrium may not be solely due to ligand-receptor engagement or ER signalling but could also involve other factors arising from increased cellular toxicity and oxidative stress. In the future, AGE and TX dose experiments could perhaps be perfomed alongside caspase/cell death ELISA or MTT assays to ensure observed changes in RAGE expression are unrelated to reduced cell integrity, stress signals or cell death.

Bibliography

BIBLIOGRAPHY

Abe, M. and D. Kufe (1993). Characterization of cis-acting elements regulating transcription of the human DF3 breast carcinoma-associated antigen (MUC1) gene. *Proc Natl Acad Sci USA* **90** (1): 282-6.

Abe, R. and S. Yamagishi (2008). AGE-RAGE system and carcinogenesis. *Curr Pharm Des* **14** (10): 940-5.

Acconcia, F. et al. (2006). Estrogen and tamoxifen induce cytoskeletal remodeling and migration in endometrial cancer cells. *Endocrinology* **147** (3): 1203-12.

Adhikary, L. et al. (2004). Abnormal p38 mitogen-activated protein kinase signalling in human and experimental diabetic nephropathy. *Diabetologia* **47**: 1210-1222.

Agalou, S. et al. (2005). Advanced glycation end product free adducts are cleared by dialysis. *Ann N Y Acad Sci* **1043**: 734-9.

Ahmad, R. et al. (2009). MUC1-C oncoprotein functions as a direct activator of the nuclear factor-kappaB p65 transcription factor. *Cancer Res* **69** (17): 7013-21.

Ahmad, W. et al. (2008). Identification of AGE-precursors and AGE formation in glycation-induced BSA peptides. *BMB Reports* **41** (7): 516-522.

Ahmed, N. et al. (2005). Peptide mapping identifies hotspot site of modification in human serum albumin by methylglyoxal involved in ligand binding and esterase activity. **280**: 5724-5732.

Alkushi, A. et al. (2010). High-grade endometrial carcinoma: serous and grade 3 endometrioid carcinomas have different immunophenotypes and outcomes. *Int J Gynecol Pathol* **29** (4): 343-50.

Amini, M. et al. (2008). Prevalence of polycystic ovary syndrome in reproductive-aged women with type 2 diabetes. *Gynecol Endocrinol* **24** (8): 423-7.

Anderson, E. (2002). The role of oestrogen and progesterone receptors in human mammary development and tumorigenesis. *Breast Cancer Res* **4** (5): 197-201.

Aplin, J. D. et al. (2001). MUC1, glycans and the cell-surface barrier to embryo implantation. *Biochem Soc Trans* **29** (Pt 2): 153-6.

Arnold, J. T. et al. (2001). Endometrial stromal cells regulate epithelial cell growth in vitro: a new co-culture model. *Hum Reprod* **16** (5): 836-45.

Ashoor, S. H. a. Z., J.B. (1984). Malliard Browning of Common Amino Acids and Sugars. *Journal of Food Science* **49** (4): 1206-7.

Balen, A. (2001). Polycystic ovary syndrome and cancer. *Hum Reprod Update* **7** (6): 522-5.

Balen, A. (2004). The pathophysiology of polycystic ovary syndrome: trying to understand PCOS and its endocrinology. *Best Pract Res Clin Obstet Gynaecol* **18** (5): 685-706.

Ball, L. J. et al. (2009). Cell type- and estrogen receptor-subtype specific regulation of selective estrogen receptor modulator regulatory elements. *Mol Cell Endocrinol* **299**: 204-211.

Balmer, N. N. et al. (2006). Steroid receptor coactivator AIB1 in endometrial carcinoma, hyperplasia and normal endometrium: Correlation with clinicopathologic parameters and biomarkers. *Mod Pathol* **19** (12): 1593-605.

Bals-Pratsch, M. et al. (2011). Early Onset and High Prevalence of Gestational Diabetes in PCOS and Insulin Resistant Women Before and After Assisted Reproduction. *Exp Clin Endocrinol Diabetes* **119** (6): 338-42

Banu, S. K. et al. (2009). Selective inhibition of prostaglandin E2 receptors EP2 and EP4 induces apoptosis of human endometriotic cells through suppression of ERK1/2, AKT, NFkappaB, and beta-catenin pathways and activation of intrinsic apoptotic mechanisms. *Mol Endocrinol* **23** (8): 1291-305.

Barile, G. R. and A. M. Schmidt (2007). RAGE and its ligands in retinal disease. *Curr Mol Med* **7** (8): 758-65.

Barkhem, T., Carlsson, B., Nilsson, Y., Enmark, E., Gustafsson, J., Nilsson, S. (1998). Differential response of estrogen receptor alpha and estrogen receptor beta to partial agonists/antagonists. *Mol Pharmacol* **54**: 102-112.

Barnaby, O. S. et al. (2010). Quantitative analysis of glycation sites on human serum albumin using (16)O/(18)O-labeling and matrix-assisted laser desorption/ionization time-of-flight mass spectrometry. *Clin Chim Acta* **411** (15-16): 1102-10.

Barsalou, A. et al. (1998). Estrogen response elements can mediate agonist activity of anti-estrogens in human endometrial Ishikawa cells. *J Biol Chem* **273** (27): 17138-46.

Basta, G. et al. (2006). Circulating soluble receptor for advanced glycation end products is inversely associated with glycemic control and S100A12 protein. *J Clin Endocrinol Metab* **91** (11): 4628-34.

Basta, G. et al. (2002). Advanced glycation end products activate endothelium through signal-transduction receptor RAGE: a mechanism for amplification of inflammatory responses. *Circulation* **105** (7): 816-22.

Beckman, J. A. et al. (2007). Endothelial function varies according to insulin resistance disease type. *Diabetes Care* **30** (5): 1226-32.

Begum, M. R. et al. (2009). Prevention of gestational diabetes mellitus by continuing metformin therapy throughout pregnancy in women with polycystic ovary syndrome. *J Obstet Gynaecol Res* **35** (2): 282-6.

Bentrem, D. J. et al. (2001). Molecular Mechanism of Action at Estrogen Receptor α of a New Clinically Relevant Antiestrogen (GW7604) Related to Tamoxifen. *Endocrinology* **142** (2): 838-846.

Bergman, C. A. et al. (1997). Transforming growth factor-beta negatively modulates proliferation and c-fos expression of the human endometrial adenocarcinoma cell line HEC-1-A. *Gynecol Oncol* **65** (1): 63-8.

Bergqvist, A., C. et al. (2001). Interleukin 1beta, interleukin-6, and tumor necrosis factor-alpha in endometriotic tissue and in endometrium. Fertil Steril **75** (3): 489-95.

Bierhaus, A. et al. (2001). Diabetes-associated sustained activation of the transcription factor nuclear factor-kB. *Diabetes* **50**: 2792-2808.

Bierhaus, A. et al. (2005). Understanding RAGE, the receptor for advanced glycation end products. *J Mol Med* **83**: 876-886.

Bierhaus, A. et al. (1997). Advanced glycation end product (AGE)-mediated induction of tissue factor in cultured endothelial cells is dependent on RAGE. *Circulation* **96** (7): 2262-71.

Bitler, B. G. et al. (2010). MUC1 regulates nuclear localization and function of the epidermal growth factor receptor. *J Cell Sci* **123** (Pt 10): 1716-23.

Blauer, M., P. K. Heinonen, et al. (2008). Effects of tamoxifen and raloxifene on normal human endometrial cells in an organotypic in vitro model. *Eur J Pharmacol* **592** (1-3): 13-8.

Bohlender, J. M., Franke, S., Stein, G and Wolf, G. (2005). Advanced glycation end products and the kidney. *Am J Physiol Renal Physiol* **289**: F645-F659.

Bokhman, J. V. (1983). Two pathogenetic types of endometrial carcinoma. *Gynecol Oncol* **15** (1): 10-7.

Bombail, V. et al. (2008). Estrogen receptor related beta is expressed in human endometrium throughout the normal menstrual cycle. *Hum Reprod* **23** (12): 2782-90.

Boomsma, C. M. et al. (2008). Pregnancy complications in women with polycystic ovary syndrome. *Semin Reprod Med* **26** (1): 72-84.

Borjigin, J. and J. Nathans (1993). Bovine pancreatic trypsin inhibitor-trypsin complex as a detection system for recombinant proteins. *Proc Natl Acad Sci USA* **90** (1): 337-41.

Boulanger, E. et al. (2007). Mesothelial RAGE activation by AGEs enhances VEGF release and potentiates capillary tube formation. *Kidney Int* **71** (2): 126-33.

Bouma, B. et al. (2003). Glycation induces formation of amyloid cross-beta structure in albumin. *J Biol Chem* **278** (43): 41810-9.

Brasier, A. R. (2006). The NF-kappaB regulatory network. *Cardiovasc Toxicol* **6** (2): 111-30.

Brayman, M. J. et al. (2006). Progesterone receptor isoforms A and B differentially regulate MUC1 expression in uterine epithelial cells. *Mol Endocrinol* **20** (10): 2278-91.

Brayman, M. et al. (2004). MUC1: a multifunctional cell surface component of reproductive tissue epithelia. *Reprod Biol Endocrinol* **2**: 4.

Breitkopf, L. D. et al. (1993). Endometriosis: A guide to one of the most common causes of period pain and infertility. Hammersmith, London, Thorsons HarperCollins Publishers.

Brosens, J. et al. (1999). Progesterone receptor regulates decidual prolactin expression in differentiating human endometrial stromal cells. *Endocrinology* **140** (10): 4809-20.

Bucciarelli, L. G. et al. (2002). RAGE is a multi-ligand receptor of the immunoglobulin superfamily: implications for homeostasis and chronic disease. *Cell Mol Life Sci* **59**: 1117-1128.

Caglar, G. S. et al. (2011). The association of urinary albumin excretion and metabolic complications in polycystic ovary syndrome. *Eur J Obstet Gynecol Reprod Biol* **154** (1): 57-61.

Cai, W. et al. (2008). AGE-receptor-1 counteracts cellular oxidant stress induced by AGEs via negative regulation of p66shc-dependent FKHRL1 phosphorylation. *Am J Physiol Cell Physiol* **294** (1): C145-52.

Carroll, L. et al. (2007). Receptor for advanced glycation end products Glycine 82 Serine polymorphism and risk of cardiovascular events in rheumatoid arthritis. *Arthritis Res Ther* **9** (2): R39.

Carson, D. D. et al. (2006). MUC1 is a scaffold for selectin ligands in the human uterus. *Front Biosci* **11**: 2903-8.

Cassese, A. et al. (2008). In skeletal muscle advanced glycation end products (AGEs) inhibit insulin action and induce the formation of multimolecular complexes including the receptor for AGEs. *J Biol Chem* **283** (52): 36088-99.

Casslen, B. et al. (1998). Transforming growth factor beta1 in the human endometrium. Cyclic variation, increased expression by estradiol and progesterone, and regulation of plasminogen activators and plasminogen activator inhibitor-1. *Biol Reprod* **58** (6): 1343-50.

Castano, E. et al. (1997). Phosphorylation of serine-167 on the human oestrogen receptor is important for oestrogen response element binding and transcriptional activation. *Biochem J* **326**
(Pt 1): 149-57.

Castro-Rivera, E. and S. Safe (1998). Estrogen- and antiestrogen-responsiveness of HEC1A endometrial adenocarcinoma cells in culture. *J Steroid Biochem Mol Biol* **64** (5-6): 287-95.

Castro-Rivera, E. et al. (2001). Estrogen regulation of cyclin D1 gene expression in ZR-75 breast cancer cells involves multiple enhancer elements. *J Biol Chem* **276** (33): 30853-61.

Chadwick, C. C. et al. (2005). Identification of pathway-selective estrogen receptor ligands that inhibit NF-kappaB transcriptional activity. *Proc Natl Acad Sci USA* **102** (7): 2543-8.

Chan, E. L. and J. T. Murphy (2003). Reactive oxygen species mediate endotoxin-induced human dermal endothelial NF-kappaB activation. *J Surg Res* **111** (1): 120-6.

Chan, R. W. S. et al. (2004). Clonogenicity of Human Endometrial Epithelial and Stromal Cells. *Biol Reprod* **70**: 1738-1750.

Chavakis, T. et al. (2003). The pattern recognition receptor (RAGE) is a counterreceptor for leukocyte integrins: a novel pathway for inflammatory cell recruitment. *J Exp Med* **198** (10): 1507-15.

Chekir, C. et al. (2006). Accumulation of advanced glycation end products in women with preeclampsia: possible involvement of placental oxidative and nitrative stress. *Placenta* **27** (2-3): 225-33.

Chen, J. et al. (2010). Advanced glycation endproducts alter functions and promote apoptosis in endothelial progenitor cells through receptor for advanced glycation endproducts mediate overpression of cell oxidant stress. *Mol Cell Biochem* **335** (1-2): 137-46.

Chen, X., D. G. Walker, et al. (2007). RAGE: a potential target for Abeta-mediated cellular perturbation in Alzheimer's disease. *Curr Mol Med* **7** (8): 735-42.

Chinenov, Y. et al. (2001). Close encounters of many kinds: Fos-Jun interactions that mediate transcription regulatory specificity. *Oncogene* **20**: 2438-2452.

Chiu, W. C. et al. (2010). Oxidative stress enhances AP-1 and NF-kappaB-mediated regulation of beta(2)-glycoprotein I gene expression in hepatoma cells. *J Cell Biochem* **111** (4): 988-98.

Clancy, K. B. (2009). Reproductive ecology and the endometrium: physiology, variation, and new directions. *Am J Phys Anthropol* **140** Suppl 49: 137-54.

Cong, L. et al. (2007). Human adiponectin inhibits cell growth and induces apoptosis in human endometrial carcinoma cells, HEC-1-A and RL95 2. *Endocr Relat Cancer* **14** (3): 713-20.

Connor, P. et al. (1997). Epidermal growth factor activates protein kinase C in the human endometrial cancer cell line HEC-1-A. *Gynecol Oncol* **67** (1): 46-50.

Conway, G. S. et al. (1990). Effects of luteinizing hormone, insulin, insulin-like growth factor-I and insulin-like growth factor small binding protein 1 in the polycystic ovary syndrome. *Clin Endocrinol (Oxf)* **33** (5): 593-603.

Cooke, I. D., Salaiman, R.A., Lenton, E.A. and Parsons, R.J. (1981). Fertility and Infertility statistics: Their importance and application. *Clinical Obstetrics and Gynaecology* **8**: 3.

Cork, B. A. et al. (2002). Expression of interleukin (IL)-11 receptor by the human endometrium in vivo and effects of IL-11, IL-6 and LIF on the production of MMP and cytokines by human endometrial cells in vitro. *Mol Hum Reprod* **8** (9): 841-8.

Cortizo, A. M. et al. (2003). Advanced Glycation end-products (AGEs) induce concerted changes in the osteoblastic expression of their receptor RAGE and in the activation of extracellular signal-regulated kinases (ERK). *Mol Cell Biochem* **250**, 1-10.

Craggs-Hinton, C and Balen, A. Dr. (2008). Coping with Polycystic Ovary Syndrome. London, UK, Sheldon Press.

Critchley, H. O. and P. T. Saunders (2009). Hormone receptor dynamics in a receptive human endometrium. *Reprod Sci* **16** (2): 191-9.

Criteria (2004). Revised 2003 consensus on diagnostic criteria and long-term health risks related to polycystic ovary syndrome (PCOS). *Hum Reprod* **19** (1): 41-7.

Croce, M. V. et al. (2003). Tissue and serum MUC1 mucin detection in breast cancer patients. *Breast Cancer Res Treat* **81** (3): 195-207.

Csiszar, A. and Z. Ungvari (2008). Endothelial dysfunction and vascular inflammation in type 2 diabetes: interaction of AGE/RAGE and TNF-alpha signaling. *Am J Physiol Heart Circ Physiol* **295** (2): H475-6.

Daoud, S. et. al. (2001). Advanced glycation end products: activators of cardiac remodelling in primary fibroblasts from adult rat hearts. *Mol Med* **7**: 543-551.

Dardes, R. C. et al. (2002). Regulation of estrogen target genes and growth by selective estrogen-receptor modulators in endometrial cancer cells. *Gynecol Oncol* **85** (3): 498-506.

Dardes, R. C. et al. (2002). Effects of a new clinically relevant antiestrogen (GW5638) related to tamoxifen on breast and endometrial cancer growth in vivo. *Clin Cancer Res* **8** (6): 1995-2001.

Daverey, A. et al. (2009). Expression of estrogen receptor co-regulators SRC-1, RIP140 and NCoR and their interaction with estrogen receptor in rat uterus, under the influence of ormeloxifene. *J Steroid Biochem Mol Biol* **116**: 93-101.

DeLoia, J. A. et al. (1998). Regional specialization of the cell membrane-associated, polymorphic mucin (MUC1) in human uterine epithelia. *Hum Reprod* **13** (10): 2902-9.

Diamanti-Kandarakis, E. and A. Bergiele (2001). The influence of obesity on hyperandrogenism and infertility in the female. *Obes Rev* **2** (4): 231-8.

Diamanti-Kandarakis, E. et al (2009). Antimullerian hormone is associated with Advanced Glycosylated End products in women with Polycystic Ovary Syndrome. *Eur J Endocrinol* **160** (5): 847-53

Diamanti-Kandarakis, E. et al. (2005). Increased levels of serum advanced glycation end-products in women with polycystic ovary syndrome. *Clin Endocrinol (Oxf)* **62** (1): 37-43.

Diamanti-Kandarakis, E. et al. (2007). Immunohistochemical localization of advanced glycation end-products (AGEs) and their receptor (RAGE) in polycystic and normal ovaries. *Histochem Cell Biol* **127** (6): 581-9.

Diamanti-Kandarakis, E. et al. (2009). Hyperreninemia Characterizing Women with Polycystic Ovary Syndrome Improves after Metformin Therapy. *Kidney Blood Press Res* **32** (1): 24-31.

Diamanti-Kandarakis, E. et al. (2010). Metformin in polycystic ovary syndrome. *Ann N Y Acad Sci* **1205**: 192-8.

Diamanti-Kandarakis, E. et al. (2006). The role of genes and environment in the etiology of PCOS. *Endocrine* **30** (1): 19-26.

Diamanti-Kandarakis, E. et al. (2008). Increased serum advanced glycation end-products is a distinct finding in lean women with polycystic ovary syndrome (PCOS). *Clin Endocrinol (Oxf)* **69** (4): 634-41.

Diamanti-Kandarakis, E. et al. (2010). Androgens associated with advanced glycation end-products in postmenopausal women. *Menopause* **17** (6): 1182-7.

Diamanti-Kandarakis, E. et al. (2006). Indices of Low-Grade Inflammation in Polycystic Ovary Syndrome. *Ann N Y Acad Sci* **1092**: 175-186.

Dickerson, E. H. et al. (2010) Insulin resistance and free androgen index correlate with the outcome of controlled ovarian hyperstimulation in non-PCOS women undergoing IVF. *Hum Reprod* **25** (2): 504-9.

Dimitriadis, E. et al. (2005). Cytokines, chemokines and growth factors in endometrium related to implantation. *Hum Reprod Update* **11** (6): 613-30.

Dimitriadis, E. et al. (2006). Interleukin-11, IL-11 receptor alpha and leukemia inhibitory factor are dysregulated in endometrium of infertile women with endometriosis during the implantation window. *J Reprod Immunol* **69** (1): 53-64.

Ding, Q. and J. N. Keller (2005). Splice variants of the receptor for advanced glycosylation end products (RAGE) in human brain. *Neurosci Lett* **373** (1): 67-72.

Dobrzycka, B. and S. J. Terlikowski (2010). Biomarkers as prognostic factors in endometrial cancer. *Folia Histochem Cytobiol* **48** (3): 319-22.

Dougan, M. and G. Dranoff (2008). Inciting inflammation: the RAGE about tumor promotion. *J Exp Med* **205** (2): 267-70.

Drake, R. et al. (2010). Grey's Anatomy for Students. 2nd Ed. London, Churchill Livingstone.

Dunaif, A. et al. (1989). Profound peripheral insulin resistance, independent of obesity, in polycystic ovary syndrome. *Diabetes* **38** (9): 1165-74.

Dunaif, A. et al. (2001). Defects in insulin receptor signaling in vivo in the polycystic ovary syndrome (PCOS). *Am J Physiol Endocrinol Metab* **281** (2): E392-9.

Dyer, D. G. et. al. (1993). Accumulation of Malliard reaction products in skin collagen in diabetes and aging. *J Clin Invest* **91**: 2463-2469.

Ebert, M. P. et al. (2003). Loss of beta-catenin expression in metastatic gastric cancer. *J Clin Oncol* **21** (9): 1708-14.

Edelmann, R. J. et al. (1998). Psychological state and psychological strain in relation to infertility. *Journal of Community and Applied Social Psychology* **1** (4): 303-311.

Ellerman, J. E. et al. (2007). Masquerader: high mobility group box-1 and cancer. *Clin Cancer Res* **13** (10): 2836-48.

El-Osta, A. et al. (2008). Transient high glucose causes persistent epigenetic changes and altered gene expression during subsequent normoglycemia. *Journal of Experimental Medicine* **205** (10): 2409-2417.

Emanuele, E. et al. (2005). Circulating levels of soluble receptor for advanced glycation end products in Alzheimer disease and vascular dementia. *Arch Neurol* **62** (11): 1734-6.

Evans, J. L. et al. (2002). Oxidative stress and stress-activated signaling pathways: a unifying hypothesis of type 2 diabetes. *Endocr Rev* **23** (5): 599-622.

Evans, M. J. et al. (2001). Reciprocal antagonism between estrogen receptor and NF-kappaB activity in vivo. *Circ Res* **89** (9): 823-30.

Farnell, Y. Z. et al. (2003). Endometrial effects of selective estrogen receptor modulators (SERMs) on estradiol-responsive gene expression are gene and cell-specific. *J Steroid Biochem Mol Biol* **84**: 513-526.

Fasco, M. J. et al. (2000). Expression of an estrogen receptor alpha variant protein in cell lines and tumors. *Mol Cell Endocrinol* **162** (1-2): 167-80.

Feldman, I. et al. (2007). Identification of proteins within the nuclear factor-kappa B transcriptional complex including estrogen receptor-alpha. *Am J Obstet Gynecol* **196** (4): 394 e1-11; discussion 394 e11-3.

Fica, S. et al. (2008). Insulin resistance and fertility in polycystic ovary syndrome. *J Med Life* **1** (4): 415-22.

Figarola, J. et al. (2007). Anti-inflammatory effects of the advanced glycation end product inhibitor LR-90 in human monocytes. *Diabetes* **56** (3): 647-55.

Fitzgerald, D. C. et al. (2007). Tumour necrosis factor-alpha (TNF-alpha) increases nuclear factor kappaB (NFkappaB) activity in and interleukin-8 (IL-8) release from bovine mammary epithelial cells. *Vet Immunol Immunopathol* **116** (1-2): 59-68.

Fornes, R. et al. (2010). Changes in the expression of insulin signaling pathway molecules in endometria from polycystic ovary syndrome women with or without hyperinsulinaemia. *Mol Med* **16** (3-4): 129-36.

Fox, E. M. et al. (2008). ERβ in breast cancer- Onlooker, passive player, or active protector? *Steroids* **73**: 1039-1051.

Francis, L. W. et al. (2009). Progesterone induces nano-scale molecular modifications on endometrial epithelial cell surfaces. *Biol Cell* **101** (8): 481-93

Frasor, J. et al. (2008). Synergistic up-regulation of prostaglandin E synthase expression in breast cancer cells by 17beta-estradiol and proinflammatory cytokines. *Endocrinology* **149**(12): 6272-9.

Frolov, A. and R. Hoffmann (2010). Identification and relative quantification of specific glycation sites in human serum albumin. *Anal Bioanal Chem* **397** (6): 2349-56.

Fujii, E. Y. and M. Nakayama (2010). The measurements of RAGE, VEGF, and AGEs in the plasma and follicular fluid of reproductive women: the influence of aging. *Fertil Steril* **94** (2): 694-700.

Fujii, E. Y. et al. (2008). Concentrations of receptor for advanced glycation end products, VEGF and CML in plasma, follicular fluid, and peritoneal fluid in women with and without endometriosis. *Reprod Sci* **15** (10): 1066-74.

Fujita, T. (2010) AGE/RAGE axis in the development of abdominal aortic aneurysm. *Ann Surg* **252** (1): 203-5; author reply 205.

Furusawa, J. et al. (2009). Licochalcone A significantly suppresses LPS signaling pathway through the inhibition of NF-kappaB p65 phosphorylation at serine 276. *Cell Signal* **21**, 778-85.

Futterweit, W. D., Ryan, G. (2006). A Patient's Guide to PCOS: Understanding and Reversing Polycystic Ovary Syndrome. New York City, Henry Holt and Company LLC.

Galichet, A. et al. (2008). Calcium-regulated intramembrane proteolysis of the RAGE receptor. *Biochem Biophys Res Commun* **370** (1): 1-5.

Gao, J. X. et al. (2007). Association of Gly82Ser polymorphism of receptor for advanced glycation end products gene in a type 2 diabetic Chinese population. *Nan Fang Yi Ke Da Xue Xue Bao* **27** (2): 219-22.

Gao, X., et al. (2007). Tumor necrosis factor-alpha induces endothelial dysfunction in Lepr(db) mice. *Circulation* **115** (2): 245-54.

Gao, X., et al. (2008). AGE/RAGE produces endothelial dysfunction in coronary arterioles in type 2 diabetic mice. *Am J Physiol Heart Circ Physiol* **295** (2): H491-8.

Garg, K. et al. (2010). p53 overexpression in morphologically ambiguous endometrial carcinomas correlates with adverse clinical outcomes. *Mod Pathol* **23** (1): 80-92.

Gargett, C. E. and P. A. Rogers (2001). Human endometrial angiogenesis. *Reproduction* **121** (2): 181-6.

Garry, R. (2004). The endometriosis syndromes: a clinical classification in the presence of aetiological confusion and therapeutic anarchy. *Hum Reprod* **19** (4): 760-8.

Ge, J. et al. (2005). Advanced glycosylation end products might promote atherosclerosis through inducing the immune maturation of dendritic cells. *Arterioscler Thromb Vasc Biol* **25** (10): 2157-63.

Gebhardt, C. et al. (2006). S100A8 and S100A9 in inflammation and cancer. *Biochem Pharmacol* **72** (11): 1622-31.

Gendler, S. J. and A. P. Spicer (1995). Epithelial mucin genes. *Annu Rev Physiol* **57**: 607-34.

Gendler, S. J. et al. (1991). Structure and biology of a carcinoma-associated mucin, MUC1. *Am Rev Respir Dis* **144** (3 Pt 2): S42-7.

Germanova, A. et al. (2009). Soluble receptor for advanced glycation end products in physiological and pathological pregnancy. *Clin Biochem.* **43** (4-5): 442-6

Gielen, S. C. et al. (2008). Signaling by estrogens and tamoxifen in the human endometrium. *J Steroid Biochem Mol Biol* **109** (3-5): 219-23.

Gielen, S. C. et al. (2005). Tamoxifen treatment for breast cancer enforces a distinct gene-expression profile on the human endometrium: an exploratory study. *Endocr Relat Cancer* **12** (4): 1037-49.

Gilmore, T. D. (2006). Introduction to NF-κB: players, pathways, perspectives. *Oncogene* **25** (51): 6680-6684.

Giudice, L. C. (2006). Endometrium in PCOS: Implantation and predisposition to endocrine CA. *Best Pract Res Clin Endocrinol Metab* **20** (2): 235-44.

Glaros, S. et al. (2006). Activation function-1 domain of estrogen receptor regulates the agonistic and antagonistic actions of tamoxifen. *Mol Endocrinol* **20** (5): 996-1008.

Glenn, J. V. and A. W. Stitt (2009). The role of advanced glycation end products in retinal ageing and disease. *Biochim Biophys Acta* **1790** (10): 1109-16.

Glover, J. N. and S. C. Harrison (1995). Crystal structure of the heterodimeric bZIP transcription factor c-Fos-c-Jun bound to DNA. *Nature* **373** (6511): 257-61.

Glueck, C. J. et al. (2008). An observational study of reduction of insulin resistance and prevention of development of type 2 diabetes mellitus in women with polycystic ovary syndrome treated with metformin and diet. *Metabolism* **57** (7): 954-60.

Glueck, C. J. et al. (2001). Metformin to restore normal menses in oligo-amenorrheic teenage girls with polycystic ovary syndrome (PCOS). *J Adolesc Health* **29** (3): 160-9.

Goldin, A. et al. (2006). Advanced glycation end products: sparking the development of diabetic vascular injury. *Circulation* **114** (6): 597-605.

Gonzalez, F.et al. (2006). In vitro evidence that hyperglycaemia stimulates tumor necrosis factor-alpha release in obese women with polycystic ovary syndrome. *J Endocrinol* **188** (3): 521-9.

Greene, G. L. et al. (1986). Sequence and expression of human estrogen receptor complementary DNA. *Science* **231** (4742): 1150-4.

Grossin, N. et al. (2008). Severity of diabetic microvascular complications is associated with a low soluble RAGE level. *Diabetes & Metabolism* **34**: 392-395.

Gu, H. et al. (2008). Gly82Ser polymorphism of the receptor for advanced glycation end products is associated with an increased risk of gastric cancer in a Chinese population. *Clin Cancer Res* **14** (11): 3627-32.

Gugliucci, A (1996). Renal fate of circulating advanced glycated end products (AGE): Evidence for reabsorption and catabolism of AGE-peptides by renal proximal tubular cells. *Diabetologia* **39**: 149-160.

Guo, R. X. et al. (2004). Activation of phosphatidylinositol 3-kinase-protein kinase B (PI3K-PKB) induced by 17beta-estradiol in endometrial carcinoma cell (Ishikawa). *Zhonghua Fu Chan Ke Za Zhi* **39** (7): 469-73.

Guo, R. X. et al. (2006). Blockage of PI3K/PKB/P27kip1 signaling pathway can antagonize 17 beta-estradiol-induced Ishikawa proliferation and cell cycle progression. *Chin Med J (Engl)* **119** (3):242-5.

Guseva, N. V. et al. (2005). Characterization of estrogen-responsive epithelial cell lines and their infectivity by genital Chlamydia trachomatis. *Microbes Infect* **7** (15): 1469-81.

Guzeloglu-Kayisli, O. et al. (2008). DNA-binding ability of NF-kappaB is affected differently by ERalpha and ERbeta and its activation results in inhibition of estrogen responsiveness. *Reprod Sci* **15** (5): 493-505.

Hajek, Z. et al. (2008). Detection of feto-maternal infection/inflammation by the soluble receptor for advanced glycation end products (sRAGE): results of a pilot study. *J Perinat Med* **36** (5):399-404.

Hall, J. M. et al (1999). The estrogen receptor beta-isoform of the human estrogen receptor modulates ER alpha transcriptional activity and is a key regulator of the cellular response to estrogens and antiestrogens. *Endocrinology* **140** (12): 5566-5578.

Hall, J. M. et al (2002). Analysis of the molecular mechanisms of human estrogen receptors alpha and beta reveals differential specificity in target promoter regulation by xenoestrogens. *J Biol Chem* **277** (46): 44455-61.

Hall, J. M. et al. (2001). The multifaceted mechanisms of estradiol and estrogen receptor signaling. *J Biol Chem* **276** (40): 36869-72.

Hansen, B. et al. (2002). The physiological scavenger receptor function of hepatic sinusoidal endothelial and Kupffer cells is independent of scavenger receptor class A type I and II. Mol *Cell Biochem* **240** (1-2): 1-8.

Hanson, J. M. et al. (2001). MUC1 expression in primary breast cancer: the effect of tamoxifen treatment. *Breast Cancer Res Treat* **67** (3): 215-22.

Harashima, A. et al. (2006). Identification of mouse orthologue of endogenous secretory receptor for advanced glycation end-products: structure, function and expression. *Biochem J* **396** (1): 109-15.

Harnish, D. C. et al. (2000). The role of CBP in estrogen receptor cross-talk with nuclear factor-kappaB in HepG2 cells. *Endocrinology* **141** (9): 3403-11.

Harris, C., Carey, A. Dr. (2000). PCOS: A woman's guide to dealing with polycystic ovary syndrome. Hammersmith, London, UK, Thorsons of HarperCollins Publishers Ltd.

Harsem, N. et al. (2008). Advanced glycation end products in pregnancies complicated with diabetes mellitus or preeclampsia. *Hypertens Pregnancy* **27** (4): 374-86.

Hart, R. (2008). PCOS and infertility. *Panminerva Med* **50** (4): 305-14.

Hata, H. and H. Kuramoto (1992). Immunocytochemical determination of estrogen and progesterone receptors in human endometrial adenocarcinoma cells (Ishikawa cells). *J Steroid Biochem Mol Biol* **42** (2): 201-10.

Herynk, M. H. and S. A. Fuqua (2004). Estrogen receptor mutations in human disease. *Endocr Rev* **25** (6): 869-98.

Hess, J. et al. (2004). AP-1 subunits: quarrel and harmony among siblings. *J Cell Sci* **117** (Pt 25): 5965-73.

Hey, N. et al. (2003). Transmembrane and truncated (SEC) isoforms of MUC1 in the human endometrium and Fallopian tube. *Reprod Biol Endocrinol* 1: 2.

Hey, N. et al. (1994). The polymorphic epithelial mucin MUC1 in human endometrium is regulated with maximal expression in the implantation phase. *J Clin Endocrinol Metab* **78** (2): 337-42.

Hiwatashi, K. et al. (2008). A novel function of the receptor for advanced glycation end-products (RAGE) in association with tumorigenesis and tumor differentiation of HCC. *Ann Surg Oncol* **15** (3): 923-33.

Hjollund, N. H. et al. (1999). Is glycosylated haemoglobin a marker of fertility? A follow-up study of first-pregnancy planners. *Hum Reprod* **14** (6): 1478-82.

Hodge, J. E. (1953). Chemistry of browning reaction in model systems. *J Agric Food Chem* **1**: 928-943.

Hodge, J. E. (1967). Origin of Flavours in Food: Non-enzymatic Browning Reactions. Symposium on Food: The Chemistry and Physiology of Flavours. Westport, CT., AVI Publishing Co.

Hodgkinson, C. P. et al. (2008). Advanced glycation end-product of low density lipoprotein activates the toll-like 4 receptor pathway implications for diabetic atherosclerosis. *Arterioscler Thromb Vasc Biol* **28** (12): 2275-81.

Hofmann, M. A. et al. (1999). RAGE mediates a novel proinflammatory axis: a central cell surface receptor for S100/calgranulin polypeptides. *Cell* **97** (7): 889-901.

Homburg, R. (2009). Androgen circle of polycystic ovary syndrome. *Hum Reprod* **24** (7): 1548-55

Honda, H. et al. (2008). Serial analysis of gene expression reveals differential expression between endometriosis and normal endometrium. Possible roles for AXL and SHC1 in the pathogenesis of endometriosis. *Reprod Biol Endocrinol* **6**: 59.

Hori, O. et al. (1995). The receptor for advanced glycation end products (RAGE) is a cellular binding site for amphoterin. Mediation of neurite outgrowth and co-expression of rage and amphoterin in the developing nervous system. *J Biol Chem* **270** (43): 25752-61.

Horie, K., et al. (1997). Immunohistochemical colocalization of glycoxidation products and lipid peroxidation products in diabetic renal glomerular lesions: Implication for glycoxidative stress in the pathogenesis of diabetic nephropathy. *J Clin Invest* **100**: 2995-3004.

Horne, A. W. et al. (2005). The expression pattern of MUC1 glycoforms and other biomarkers of endometrial receptivity in fertile and infertile women. *Mol Reprod Dev* **72** (2): 216-29.

Horne, A. W. et al. (2006). The effects of sex steroid hormones and interleukin-1-beta on MUC1 expression in endometrial epithelial cell lines. *Reproduction* **131** (4): 733-42.

Hsu, H. Y. et al. (2001). Ligands of macrophage scavenger receptor induce cytokine expression via differential modulation of protein kinase signalling pathways. *J Bio Chem* **276**: 28719-28730.

Hudson, B. I. et al. (2008). Identification, classification, and expression of RAGE gene splice variants. *FASEB J* **22** (5): 1572-80.

Hudson, B. I. et al. (2008). Interaction of the RAGE cytoplasmic domain with diaphanous-1 is required for ligand-stimulated cellular migration through activation of Rac1 and Cdc42. *J Biol Chem* **283** (49): 34457-68.

Hui, A-M et al. (2004). Agents with Selective Estrogen Receptor (ER) Modulator Activity Induce Apoptosis *In vitro* and *In vivo* in ER-Negative Glioma Cells. *Cancer Research* **64** 9115-9123.

Huttunen, H. J. et al (1999). Receptor for Advanced Glycation End Products (RAGE) - mediated Neurite Outgrowth and Activation of NF-kB Require the Cytoplasmic Domain of the Receptor but Different Downstream Signalling Pathways. *J Biol Chem* **274** (28): 19919-19924.

Iacobini, C. et al. (2003). Role of galectin-3 in diabetic nephropathy. *J Am Soc Nephrol* **14** (8 Suppl 3): S264-70.

Ilchmann, A. et al. (2010). Glycation of a food allergen by the Maillard reaction enhances its T-cell immunogenicity: role of macrophage scavenger receptor class A type I and II. *J Allergy Clin Immunol* **125** (1): 175-83 e1-11.

Isdale, A. H. (1993). The ABC of the Diabetic Hand - Advanced Glycosylation End products, Browning and Collagen. *British Journal of Rheumatology* **32** (10): 859-861.

Ishibashi, T et al. (1998). Advanced Glycation End Products in Age-related Macular Degeneration. *Arch Ophthalmol* **116** (12): 1629-1632.

Ishihara, K. et al. (2003). The receptor for advanced glycation end-products (RAGE) directly binds to ERK by a D-domain-like docking site. *FEBS Lett* **550** (1-3): 107-13.

Jakus, V. et al. (1998). Importance of advanced glycation end products--AGE products. *Bratisl Lek Listy* **99** (7): 368-75.

Jang, Y. et al. (2007). Association of the Gly82Ser polymorphism in the receptor for advanced glycation end products (RAGE) gene with circulating levels of soluble RAGE and inflammatory markers in nondiabetic and nonobese Koreans. *Metabolism* **56** (2): 199-205.

Jayaraman, M. et al. (2009). Type 1 diabetes mellitus and polycystic ovary syndrome. *Endocr Pract* **15** (1): 80-1.

Jazaeri, O. et al. (1999). Expression of estrogen receptor alpha mRNA and protein variants in human endometrial carcinoma. *Gynecol Oncol* **74** (1): 38-47.

Johansson, J. et al. (2010). Intense electroacupuncture normalizes insulin sensitivity, increases muscle GLUT4 content, and improves lipid profile in a rat model of polycystic ovary syndrome. *Am J Physiol Endocrinol Metab* **299** (4): E551-9.

Johnson, S. M. et al. (2007). Ishikawa cells exhibit differential gene expression profiles in response to oestradiol or 4-hydroxytamoxifen. *Endocr Relat Cancer* **14** (2): 337-50.

Jones, R. L. et al. (2006). TGF-beta superfamily expression and actions in the endometrium and placenta. *Reproduction* **132** (2): 217-32.

Juhasz, M. et al. (2003). Dual role of serum soluble E-cadherin as a biological marker of metastatic development in gastric cancer. *Scand J Gastroenterol* **38** (8): 850-5.

Kaaks, R. et al. (2002). Obesity, endogenous hormones, and endometrial cancer risk: a synthetic review. *Cancer Epidemiol Biomarkers Prev* **11** (12): 1531-43.

Kalaitzidis, D. and T. D. Gilmore (2005). Transcription factor cross-talk: the estrogen receptor and NF-kappaB. *Trends Endocrinol Metab* **16** (2): 46-52.

Kang, R. et al. (2009). The receptor for advanced glycation end products (RAGE) sustains autophagy and limits apoptosis, promoting pancreatic tumor cell survival. *Cell Death Differ* **17** (4): 666-76

Katakami, N. et al. (2005) Decreased Endogenous Secretory Advanced Glycation End Product Receptor in Type 1 Diabetic Patients. *Diabetes Care* **28**: 2716-2721.

Kato, S. et al. (1995). Activation of the estrogen receptor through phosphorylation by mitogen-activated protein kinase. *Science* **270** (5241): 1491-4.

Kato, Y. et al (1981). Effect of some metals on the malliard reaction of ovalbumin. *J Agric Food Chem* **29** (3): 540-543.

Kelestimur, F. et al (2006). Prevalence of polycystic ovarian changes and polycystic ovary syndrome in premenopausal women with treated type 2 diabetes mellitus. *Fertil Steril* **86** (2): 405-10.

Kershah, S. M. et al (2004). Expression of estrogen receptor coregulators in normal and malignant human endometrium. *Gynecol Oncol* **92** (1): 304-13.

Kilhovd, B. K. et al (2005). High serum levels of advanced glycation end products predict increased coronary heart disease mortality in nondiabetic women but not in nondiabetic men: a population-based 18-year follow-up study. *Arterioscler Thromb Vasc Biol* **25** (4): 815-20.

King, A. E. et al (2010). An additive interaction between the NFkappaB and estrogen receptor signalling pathways in human endometrial epithelial cells. *Hum Reprod* **25** (2): 510-8.

King, A. E. et al (2001). The NF-kappaB pathway in human endometrium and first trimester decidua. *Mol Hum Reprod* **7** (2): 175-83.

Kislinger, T. et al (1999). N(epsilon)-(carboxymethyl)lysine adducts of proteins are ligands for receptor for advanced glycation end products that activate cell signalling pathways and modulate gene expression. *J Biol Chem* **274** (44): 31740-9.

Klinge, C. M. (2001). Estrogen receptor interaction with estrogen response elements. *Nucleic Acids Res* **29** (14): 2905-19.

Koga, T. et al (2007). TNF-alpha induces MUC1 gene transcription in lung epithelial cells: its signaling pathway and biological implication. *Am J Physiol Lung Cell Mol Physiol* **293** (3): L693-701.

Konishi, H. et al. (2004). Advanced glycation end products induce secretion of chemokines and apoptosis in human first trimester trophoblasts. *Hum Reprod* **19** (9): 2156-62.

Koos, R. D. et al. (2005). New insight into the transcriptional regulation of vascular endothelial growth factor expression in the endometrium by estrogen and relaxin. *Ann N Y Acad Sci* **1041**: 233-47.

Koschinsky, T. et al. (1997). Orally absorbed reactive glycation products (glycotoxins): an environmental risk factor in diabetic nephropathy. *Proc Natl Acad Sci USA* **94** (12): 6474-9.

Kovarik, A. et al. (1993). Analysis of the tissue-specific promoter of the MUC1 gene. *J Biol Chem* **268** (13): 9917-26.

Koyama, H. and Y. Nishizawa (2010). AGEs/RAGE in CKD: irreversible metabolic memory road toward CVD? *Eur J Clin Invest* **40** (7): 623-35.

Krajcovicova-Kudlackova, M. et al. (2002). Advanced glycation end products and nutrition. *Physiol Res* **51** (3): 313-6.

Kreiger, M. and Stern, D.M. (2001). Multiligand receptors and human disease. *J Clin Invest* **108** (5): 645-647.

Kuiper, G. G. et al. (1996). Cloning of a novel receptor expressed in rat prostate and ovary. *Proc Natl Acad Sci USA* **93** (12): 5925-30.

Kumar, A. et al. (2001). Activation of PKC-beta (1) in glomerular mesangial cells is associated with specific NF-kB subunit translocation. *Am J Physiol Renal Physiol* **281**: F613-F619.

Kuramoto, H. (1972). Studies of the growth and cytogenetic properties of human endometrial adenocarcinoma in culture and its development into an established line. *Acta Obstet Gynaecol Jpn* **19** (1): 47-58.

Kuramoto, H. et al. (1972). Establishment of a cell line of human endometrial adenocarcinoma in vitro. *Am J Obstet Gynecol* **114** (8): 1012-9.

Kurarmoto, H. et al. (2002). HEC-1 cells. *Hum Cell* **15** (2), 81-95.

Kurman, R. J. et al. (1985). The behavior of endometrial hyperplasia. A long-term study of untreated hyperplasia in 170 patients. *Cancer* **56** (2): 403-12.

Lagow, E. L. and D. D. Carson (2002). Synergistic stimulation of MUC1 expression in normal breast epithelia and breast cancer cells by interferon-gamma and tumor necrosis factor-alpha. *J Cell Biochem* **86** (4): 759-72.

Lai, T. H. et al. (2005). Differential expression of L-selectin ligand in the endometrium during the menstrual cycle. *Fertil Steril* **83** Suppl 1: 1297-302.

Lander, H. M. et al. (1997). Activation of the Receptor for Advanced Glycation End Products Triggers a p21ras-dependent Mitogen-activated Protein Kinase Pathway Regulated by Oxidant Stress. *J Biol Chem* **272** (28): 17810-17814.

Lapolla, A. et al. (2005). Advanced glycation end products/peptides: An *in vivo* investigation. *Ann NY Acad Sci* **1043**, 267-275.

Larsen, L. et al. (2005). Extracellular signal-regulated kinase is essential for interleukin-1-induced and nuclear factor kappaB-mediated gene expression in insulin-producing INS-1E cells. *Diabetologia* **48** (12): 2582-90.

Ledl, F. et al. (1999). The Malliard reaction in food and in the human body: new results in chemistry, biochemistry and medicine. *Angew Chem Int Ed Engl* **29**: 565-706.

Leon, L. et al. (2008). Activities of steroid metabolic enzymes in secretory endometria from untreated women with Polycystic Ovary Syndrome. *Steroids* **73** (1): 88-95.

Leslie, R. D. G. et al. (2003). Level of an Advanced Glycation End Product is Genetically Determined. *Diabetes* **52**: 2441-2444.

Lessey, B. A (2002). Implantation defects in infertile women with endometriosis. *Ann NY Acad Sci* **955**: 265-80.

Lessey, B. A. et al. (2006). Estrogen receptor-alpha (ER-alpha) and defects in uterine receptivity in women. *Reprod Biol Endocrinol* **4** Suppl 1, S9.

Li, J. H. et al. (2004). Advanced Glycation End Products Induce Tubular Epithelial-Myofibroblast Transition through the RAGE-ERK 1/2 MAP Kinase Signalling Pathway. *Am J Pathol* **164** (4): 1389-1397.

Li, J., and Schmidt, A.M. (1997). Characterization and Functional Analysis of the Promoter of RAGE, the receptor for Advanced Glycation End Products. *Journal of Biological Chemistry* **272** (26): 16498-16506.

Li, J. et al. (1998). Sp1-binding Elements in the Promoter of RAGE Are Essential for Amphoterin-mediated Gene Expression in Cultured Neuroblastoma Cells. *J Biol Chem* **273** (47): 30870-30878.

Li, Q. and I. M. Verma (2002). NF-kappaB regulation in the immune system. *Nat Rev Immunol* **2** (10): 725-34.

Li, X. et al. (2004). Single-chain estrogen receptors (ERs) reveal that the ERalpha/beta heterodimer emulates functions of the ERalpha dimer in genomic estrogen signalling pathways. *Mol Cell Biol* **24** (17): 7681-94.

Li, Y. et al. (2005). Free cholesterol-loaded macrophages are an abundant source of tumour necrosis factor-alpha and interleukin-6: model of NF-kappaB- and map kinase-dependent inflammation in advanced atherosclerosis. *J Biol Chem* **280** (23): 21763-72.

Ligtenberg, M. J. et al. (1992). Cell-associated episialin is a complex containing two proteins derived from a common precursor. *J Biol Chem* **267** (9): 6171-7.

Lim, M. et al. (2008). Induction of apoptosis of Beta cells of the pancreas by advanced glycation end-products, important mediators of chronic complications of diabetes mellitus. *Ann N Y Acad Sci* **1150**: 311-5.

Lin, F. L. et al. (2010). Advanced glycation end products down-regulate gap junctions in human hepatoma SKHep 1 cells via the activation of Src-dependent ERK1/2 and JNK/SAPK/AP1 signalling pathways. *J Agric Food Chem* **58** (15): 8636-42.

Lindsey, K. Q. et al. (2000). Neural regulation of endothelial cell-mediated inflammation. *J Investig Dermatol Symp Proc* **5** (1): 74-8.

Liu, J. et al. (2009). Advanced glycation end products and lipopolysaccharide synergistically stimulate proinflammatory cytokine/chemokine production in endothelial cells via activation of both mitogen-activated protein kinases and nuclear factor-kappaB. *Febs J* **276** (16): 4598-606.

Liu, Y. et al. (2010). AGEs increased migration and inflammatory responses of adventitial fibroblasts via RAGE, MAPK and NF-kappaB pathways. *Atherosclerosis* **208** (1): 34-42.

Livak, K. J. and T. D. Schmittgen (2001). Analysis of relative gene expression data using real-time quantitative PCR and the 2(-Delta Delta C(T)) Method. *Methods* **25** (4): 402-8.

Lloyd, K. O. et al. (1996). Comparison of O-linked carbohydrate chains in MUC-1 mucin from normal breast epithelial cell lines and breast carcinoma cell lines. Demonstration of simpler and fewer glycan chains in tumor cells. *J Biol Chem* **271** (52): 33325-34.

Lobo, R. A. and F. Z. Stanczyk (1994). New knowledge in the physiology of hormonal contraceptives. *Am J Obstet Gynecol* **170** (5 Pt 2): 1499-507.

Logsdon, C. D. et al. (2007). RAGE and RAGE ligands in cancer. *Curr Mol Med* **7** (8): 777-89.

Lovely, L. P. et al. (2000). Characterization of androgen receptors in a well-differentiated endometrial adenocarcinoma cell line (Ishikawa). *J Steroid Biochem Mol Biol* **74** (4): 235-41.

Lue, L. F. et al. (2009). Receptor for advanced glycation end products: its role in Alzheimer's disease and other neurological diseases. *Future Neurol* **4** (2): 167-177.

Luque-Ramirez, M. et al. (2010). Treatment of polycystic ovary syndrome (PCOS) with metformin ameliorates insulin resistance in parallel with the decrease of serum interleukin-6 concentrations. *Horm Metab Res* **42** (11): 815-20.

MacLaughlan, S. D. et al. (2007). Endometrial expression of Cyr61: a marker of estrogenic activity in normal and abnormal endometrium. *Obstet Gynecol* **110** (1): 146-54.

Makita, Z. (1992). Hemoglobin-AGE: a circulating marker of advanced glycosylation. *Science* **258**: 651-653.

Malliard, L.-C. (1912). Action des acides amines sur les sucres: formation des melanoides par voie methodique. *Cr Acad Sci* **154**: 66-68.

Margarit, L. et al. (2010). MUC1 as a discriminator between endometrium from fertile and infertile patients with PCOS and endometriosis. *J Clin Endocrinol Metab* **95** (12): 5320-9.

Margarit, L. et al. (2009). L-selectin ligands in human endometrium: comparison of fertile and infertile subjects. *Hum Reprod* **24** (11): 2767-77.

Masuda, H. et al. (2010). Stem cell-like properties of the endometrial side population: implication in endometrial regeneration. *PLoS One* **5** (4): e10387.

Matsumoto, K. et al. (2000). Endocytic uptake of advanced glycation end products by mouse liver sinusoidal endothelial cells is mediated by a scavenger receptor distinct from the macrophage scavenger receptor class A. *Biochem J* **352** Pt 1: 233-40.

Matthews, J. et al. (2006). Estrogen receptor (ER) beta modulates ER alpha-mediated transcriptional activation by altering the recruitment of c-Fos and c-Jun to estrogen responsive promoters. *Mol Endocrinol* **20** (3): 534-543.

Meduri, G. et al. (2000). Expression of vascular endothelial growth factor receptors in the human endometrium: modulation during the menstrual cycle. *Biol Reprod* **62** (2): 439-47.

Meseguer, M. et al. (2001). Human endometrial mucin MUC1 is up-regulated by progesterone and down-regulated in vitro by the human blastocyst. *Biol Reprod* **64** (2): 590-601.

Miki, Y. et al. (2009). Comparative effects of raloxifene, tamoxifen and estradiol on human osteoblasts in vitro: estrogen receptor dependent or independent pathways of raloxifene. *J Steroid Biochem Mol Biol* **113** (3-5): 281-9.

Miyata, T. et al. (1999). Alterations in non-enzymatic biochemistry in uremia: origin and significance of carbonyl stress in long-term uremic complications. *Kidney Int* **55**: 389-399.

Miyata, T. et al. (2000). Advanced glycation and lipoxidation end products: role of reactive carbonyl compounds generated during carbohydrate and lipid metabolism. *J Am Soc Nephrol* **11**: 1744-1752.

Moore, J. T. et al. (1998). Cloning and characterization of human estrogen receptor beta isoforms. *Biochem Biophys Res Commun* **247** (1): 75-8.

Mosselman, S. et al. (1996). ER beta: identification and characterization of a novel human estrogen receptor. *FEBS Lett* **392** (1): 49-53.

Mueller, M. D. et al. (2000). Regulation of vascular endothelial growth factor (VEGF) gene transcription by estrogen receptors alpha and beta. *Proc Natl Acad Sci USA* **97** (20): 10972-7.

Mukherjee, T. K. et al. (2005). Differential effect of estrogen receptor alpha and beta agonists on the receptor for advanced glycation end product expression in human microvascular endothelial cells. *Biochim Biophys Acta* **1745** (3): 300-9.

Mukherjee, T. K. et al. (2005). The role of reactive oxygen species in TNFalpha-dependent expression of the receptor for advanced glycation end products in human umbilical vein endothelial cells. *Biochim Biophys Acta* **1744** (2): 213-23.

Nabel, G. J. and Verma, I.M. (1993). Proposed NF-kB/IkB family nomenclature. *Genes Dev* **7** (11): 2063.

Nagai, R. et al. (1998). Conversion of Amadori product of Maillard reaction to Nepsilon-(carboxymethyl)lysine in alkaline condition. *FEBS Lett* **425** (2): 355-60.

Nagaoka, M. et al. (2002). Influence of amino acid numbers between two ligand cysteines of zinc finger proteins on affinity and specificity of DNA binding. *Biochem Biophys Res Commun* **296** (3): 553-9.

Nakajou, K. et al. (2005). CD36 is not involved in scavenger receptor-mediated endocytic uptake of glycolaldehyde- and methylglyoxal-modified proteins by liver endothelial cells. *J Biochem* **137** (5): 607-16.

Namiki, M (1988). Chemistry of Malliard reactions: recent studies on the browning reaction mechanism and the development of antioxidants and mutagens. *Advances in Food Research* London, Academic Press Inc. **32** 115-84.

Navo, M. A. et al. (2008). In vitro evaluation of the growth inhibition and apoptosis effect of mifepristone (RU486) in human Ishikawa and HEC1A endometrial cancer cell lines. *Cancer Chemother Pharmacol* **62** (3): 483-9.

Neeper, M. et al. (1992). Cloning and expression of a cell surface receptor for advanced glycosylation end products of proteins. *J Biol Chem* **267** (21): 14998-5004.

Nilsson, S. et al. (2001). Mechanisms of estrogen action. *Physiol Rev* **81** (4): 1535-65.

Nin, J. W. et al. (2011). Higher plasma levels of advanced glycation end products are associated with incident cardiovascular disease and all-cause mortality in type 1 diabetes: a 12-year follow-up study. *Diabetes Care* **34** (2): 442-7.

Nishida, M. (2002). The Ishikawa cells from birth to the present. *Hum Cell* **15** (3): 104-17.

Nishida, M. et al. (1985). Establishment of a new human endometrial adenocarcinoma cell line, Ishikawa cells, containing estrogen and progesterone receptors. *Nihon Sanka Fujinka Gakkai Zasshi* **37** (7): 1103-11.

Noguchi, T. et al. (2010). Evidence for activation of Toll-like receptor and receptor for advanced glycation end products in preterm birth. *Mediators Inflamm* **2010**: 490406.

Nutis, M. et al. (2008). Use of ultrasonographic cut point for diagnosing endometrial pathology in postmenopausal women with multiple risk factors for endometrial cancer. *J Reprod Med* **53** (10): 755-9.

O'Brien, J. E. et al. (2006). Estrogen-induced Proliferation of Uterine Epithelial Cells is Independent of Estrogen Receptor α Binding to Classical Estrogen response elements. *J Biol Chem* **281** (36): 26683-26692.

Oehler, M. K. and M. C. Rees (2003). Menorrhagia: an update. *Acta Obstet Gynecol Scand* **82** (5): 405-22.

Ohgami, N. et al. (2002). CD36 serves as a receptor for advanced glycation end-products (AGE). *J Diabetes Complications* **16**: 56-59.

Ohgami, N. et al. (2001). AGE and AGE-receptors. *Seikagaku* **73** (3): 200-4.

Ohgami, N. et al. (2001). Scavenger receptor class B type I-mediated reverse cholesterol transport is inhibited by advanced glycation end products. *J Biol Chem* **276** (16): 13348-55.

Okazaki, T. et al. (2003). Phosphorylation of serine 276 is essential for p65 NF-kappaB subunit-dependent cellular responses. *Biochem Biophys Res Commun* **300** (4): 807-12.

O'Regan, R. M. et al. (2002). Effects of raloxifene after tamoxifen on breast and endometrial tumor growth in athymic mice. *J Natl Cancer Inst* **94** (4): 274-83.

Origlia, N. et al. (2008). Receptor for advanced glycation end product-dependent activation of p38 mitogen-activated protein kinase contributes to amyloid-beta-mediated cortical synaptic dysfunction. *J Neurosci* **28** (13): 3521-30.

Otero, K. et al. (2001). Albumin-derived advanced glycation end-products trigger the disruption of the vascular endothelial cadherin complex in cultured human and murine endothelial cells. *Biochem. J* **359**: 567-574.

Ouslimani, N. et al. (2007). Metformin reduces endothelial cell expression of both the receptor for advanced glycation end products and lectin-like oxidized receptor 1. *Metabolism* **56** (3): 308-13.

Paech, K. et al. (1997). Differential ligand activation of estrogen receptors ERalpha and ERbeta at AP1 sites. *Science* **277** (5331): 1508-10.

Palomba, S., R. Pasquali, et al. (2009). Clomiphene citrate, metformin or both as first-step approach in treating anovulatory infertility in patients with polycystic ovary syndrome (PCOS): a systematic review of head-to-head randomized controlled studies and meta-analysis. *Clin Endocrinol (Oxf)* **70** (2): 311-21.

Panzer, U. et al. (2009). Resolution of renal inflammation: a new role for NF-kappaB1 (p50) in inflammatory kidney diseases. *Am J Physiol Renal Physiol* **297** (2): F429-39.

Pasquali, R. et al. (2006). The impact of obesity on reproduction in women with polycystic ovary syndrome. *Bjog* **113** (10): 1148-59.

Paszkiewicz-Gadek, A. et al. (2005). Effect of estradiol and raloxifene on MUC1 expression and adhesive properties of Ishikawa cells. *Oncol Rep* **14** (2): 583-9.

Pendaries, C. et al. (2002). The AF-1 activation-function of ERalpha may be dispensable to mediate the effect of estradiol on endothelial NO production in mice. *Proc Natl Acad Sci USA* **99** (4): 2205-10.

Peppa, M. and S. A. Raptis (2008). Advanced glycation end products and cardiovascular disease. *Curr Diabetes Rev* **4** (2): 92-100.

Peppa, M. et al. (2003). Glucose, Advanced Glycation End Products, and Diabetes Complications: What Is New and What Works. *Clin Diabetes* **21** (4): 186-187.

Perkins, N. D. (2007). Integrating cell-signalling pathways with NF-kB and IKK function. *Nat. Rev. Mol. Cell Biol* **8** (1): 49-62.

Pertynska-Marczewska, M. et al. (2009). Glycation endproducts, soluble receptor for advanced glycation endproducts and cytokines in diabetic and non-diabetic pregnancies. *Am J Reprod Immunol* **61** (2): 175-82.

Peters, T. J. (1996). All about albumin: biochemistry, genetics, and medical applications. Academic Press Limited, **2nd Ed**, San Diego, C.A.

Pillay, O. C. et al. (2006). The association between polycystic ovaries and endometrial cancer. *Hum Reprod* **21** (4): 924-9.

Pochampalli, M. R. et al. (2007). Transforming growth factor alpha dependent cancer progression is modulated by Muc1. *Cancer Res* **67** (14): 6591-8.

Ponce, C. et al. (2009). Nuclear factor kappaB pathway and interleukin-6 are affected in eutopic endometrium of women with endometriosis. *Reproduction* **137** (4): 727-37.
Popovici, R. M. et al. (2000). Discovery of new inducible genes in in vitro decidualized human endometrial stromal cells using microarray technology. *Endocrinology* **141** (9): 3510-3.

Prat, J. (2010). Classification and staging of endometrial sarcomas: one disease or two different tumor types? *Gynecol Oncol* **118** (1): 1-2.

Pricci, F. et al. (2000). Role of galectin-3 as a receptor for advanced glycosylation end products. *Kidney Int Suppl* **77**: S31-9.

Pugliese, G. et al. (2001). Accelerated diabetic glomerulopathy in galectin-3/AGE receptor 3 knockout mice. *Faseb J* **15** (13): 2471-9.

Pullerits, R. et al. (2006). Soluble receptor for advanced glycation end products triggers a proinflammatory cytokine cascade via beta2 integrin Mac-1. *Arthritis Rheum* **54**, 3898-907.

Punyadeera, C. et al. (2008). Effects of selective oestrogen receptor modulators on proliferation in tissue cultures of pre-and postmenopausal human endometrium. *J Steroid Biochem Mol Biol* **112**: 102-109.

Qiagen (2010). Critical Factors for Successful Real Time PCR. Real Time PCR Brochure.

Qin, Y. H. et al. (2009). HMGB1 enhances the proinflammatory activity of lipopolysaccharide by promoting the phosphorylation of MAPK p38 through receptor for advanced glycation end products. *J Immunol* **183** (10): 6244-50.

Quaedackers, M. E. et al (2007). Direct interaction between estrogen receptor alpha and NF-kappaB in the nucleus of living cells. *Molecular and Cellular Endocrinology* **273**, 42-50.

Quenby, S. et al. (2007). Different types of recurrent miscarriage are associated with varying patterns of adhesion molecule expression in endometrium. *Reprod Biomed Online* **14** (2): 224-34.

Ramasamy, R. et al. (2005). The RAGE axis and endothelial dysfunction: maladaptive roles in the diabetic vasculature and beyond. Trends *Cardiovasc Med* **15** (7): 237-43.

Ramasamy, R. et al. (2007). Arguing for the motion: yes, RAGE is a receptor for advanced glycation endproducts. *Mol Nutr Food Res* **51** (9): 1111-5.

Rasheed, Z. et al. (2011). Advanced glycation end products induce the expression of interleukin-6 and interleukin-8 by receptor for advanced glycation end product-mediated activation of mitogen-activated protein kinases and nuclear factor-{kappa}B in human osteoarthritis chondrocytes. *Rheumatology (Oxford)* **50** (5): 838-51.

Raucci, A. et al. (2008). A soluble form of the receptor for advanced glycation end-products (RAGE) is produced by proteolytic cleavage of the membrane-bound form by the sheddase a disintegrin and metalloprotease 10 (ADAM 10). *Faseb J* **22**: 3716-3727.

Riehl, A. et al. (2009). The receptor RAGE: Bridging inflammation and cancer. *Cell Commun Signal* **7**: 12.

Ritz, E. et al. (1999). End-stage renal failure in type 2 diabetes: A medical catastrophe of worldwide dimension. *Am J Kidney Dis* **34**: 795-808.

Roberts, M. et al. (2005). Differential regulation of interleukins IL-13 and IL-15 by ovarian steroids, TNF-alpha and TGF-beta in human endometrial epithelial and stromal cells. *Mol Hum Reprod* **11** (10): 751-60.

Rocken, C. et al. (2003). Advanced glycation end products and receptor for advanced glycation end products in AA amyloidosis. *Am J Pathol* **162** (4): 1213-20.

Rojas, A. et al. (2011) Fueling inflammation at tumor microenvironment: the role of multiligand/RAGE axis. *Carcinogenesis* **31**, 334-41.

Romano, A. et al. (2010). Identification of novel ER-alpha target genes in breast cancer cells: gene- and cell-selective co-regulator recruitment at target promoters determines the response to 17beta-estradiol and tamoxifen. *Mol Cell Endocrinol* **314** (1): 90-100.

Rosenbaum, D. et al. (1993). Insulin resistance in polycystic ovary syndrome: decreased expression of GLUT-4 glucose transporters in adipocytes. *Am J Physiol* **264**, E197-202.

Ryseck, R. P. and Bravo, R. (1991). c-JUN, JUN B, and JUN D differ in their binding affinities to AP-1 and CRE consensus sequences: effect of FOS proteins. *Oncogene* **6**: 533-542.

Saegusa, M et al. (2007). Crosstalk between NF-kappaB/p65 and beta-catenin/TCF4/p300 signalling pathways through alterations in GSK-3beta expression during trans-differentiation of endometrial carcinoma cells. *J Pathol* **213** (1): 35-45.

Sakamoto, T. et al. (2002). Estrogen receptor-mediated effects of tamoxifen on human endometrial cancer cells. *Mol Cell Endocrinol* **192** (1-2): 93-104.

Sano, H. et al. (1998). Insulin Enhances Macrophage Scavenger Receptor-mediated Endocytic Uptake of Advanced Glycation End Products. *J Biol Chem* **273** (15): 8630-8637.

Sasaki, C. Y. et al. (2005). Phosphorylation of RelA/p65 on serine 536 defines an I{kappa}B{alpha}-independent NF-{kappa}B pathway. *J Biol Chem* **280**, 34538-47.

Sato, T. et al. (2009). Effects of high-AGE beverage on RAGE and VEGF expressions in the liver and kidneys. *Eur J Nutr* **48** (1): 6-11.

Satyaswaroop, P. G. et al. (1978). Human endometrial cancer cell cultures for hormonal studies. *Cancer Res* **38** (11 Pt 2): 4367-75.

Saville, B. et al. (2000). Ligand-, cell-, and estrogen receptor subtype (alpha/beta)-dependent activation at GC-rich (Sp1) promoter elements. *J Biol Chem* **275** (8): 5379-87.

Sayin, N. C. et al. (2003). Elevated serum TNF-alpha levels in normal-weight women with polycystic ovaries or the polycystic ovary syndrome. *J Reprod Med* **48** (3): 165-70.

Scafonas, A. et al. (2008). Agonist-like SERM effects on ERalpha-mediated repression of MMP1 promoter activity predict in vivo effects on bone and uterus. *J Steroid Biochem Mol Biol* **110** (3-5): 197-206.

Schaefer, W. R. et al. (2010). In vitro-Ishikawa cell test for assessing tissue-specific chemical effects on human endometrium. *Reprod Toxicol* **30** (1): 89-93.

Schleicher, E. D. et al. (1997). Increased accumulation of the glycoxidation product N(epsilon)-(carboxymethyl)lysine in human tissues in diabetes and aging. *J Clin Invest* **99**: 457-468.

Schlueter, C. et al. (2003). Tissue-specific expression patterns of the RAGE receptor and its soluble forms--a result of regulated alternative splicing? *Biochim Biophys Acta* **1630** (1): 1-6.

Schmidt, A. M. et al. (1992). Isolation and characterization of two binding proteins for advanced glycosylation end products from bovine lung which are present on the endothelial cell surface. *J Biol Chem* **267** (21): 14987-97.

Schmidt, A. M. et al. (1999). Activation of receptor for advanced glycation end products: a mechanism for chronic vascular dysfunction in diabetic vasculopathy and atherosclerosis. *Circ Res* **84** (5): 489-97.

Scobie, G. A. et al. (2002). Human oestrogen receptors: differential expression of ER alpha and beta and the identification of ER beta variants. *Steroids* **67** (12): 985-92.

Shah, Y. M. and B. G. Rowan (2005). The Src kinase pathway promotes tamoxifen agonist action in Ishikawa endometrial cells through phosphorylation-dependent stabilization of estrogen receptor (alpha) promoter interaction and elevated steroid receptor coactivator 1 activity. *Mol Endocrinol* **19** (3): 732-48.

Shang, Y. and M. Brown (2002). Molecular determinants for the tissue specificity of SERMs. *Science* **295** (5564): 2465-8.

Shang, Y. et al. (2000). Cofactor dynamics and sufficiency in estrogen receptor-regulated transcription. *Cell* **103** (6): 843-52.

Sharma, I. et al. (2010). Implication of the RAGE-EN-RAGE axis in endometriosis. *Int J Gynaecol Obstet* **110** (3): 199-202.

Sheetz, M. J and King, G.L. (2002). Molecular understanding of hyperglycaemia 's adverse effects for diabetic complications. *JAMA* **288**: 2579-2588.

Sheikpranbabu, S. et al. (2009). The inhibition of advanced glycation end-products-induced retinal vascular permeability by silver nanoparticles. *Biomaterials* **31** (8): 2260-71

Sherman, M. E. (2000). Theories of endometrial carcinogenesis: a multidisciplinary approach. *Mod Pathol* **13** (3): 295-308.

Sherwin, J. R. et al. (2002). Soluble gp130 is up-regulated in the implantation window and shows altered secretion in patients with primary unexplained infertility. *J Clin Endocrinol Metab* **87** (8): 3953-60.

Shi, L. et al. (2009). Expression of ER-{alpha}36, a novel variant of estrogen receptor {alpha}, and resistance to tamoxifen treatment in breast cancer. *J Clin Oncol* **27** (21): 3423-9.

Shyu, M. K. et al. (2008). MUC1 expression is increased during human placental development and suppresses trophoblast-like cell invasion in vitro. *Biol Reprod* **79** (2): 233-9.

Singh, R. et al. (2001). Advanced glycation end-products: a review. *Diabetologia* **44**, 129-146.

Smedsrod, B. et al. (1997). Advanced glycation end products are eliminated by scavenger-receptor-mediated endocytosis in hepatic sinusoidal Kupffer and endothelial cells. *Biochem J* **322** (Pt 2): 567-73.

Soares, G. M. et al. (2009). Increased arterial stiffness in nonobese women with polycystic ovary syndrome (PCOS) without comorbidities: one more characteristic inherent to the syndrome? *Clin Endocrinol (Oxf)* **71** (3): 406-11.

Song, L. N. et al. (2003). Beta-catenin binds to the activation function 2 region of the androgen receptor and modulates the effects of the N-terminal domain and TIF2 on ligand-dependent transcription. *Mol Cell Biol* **23** (5): 1674-87.

Song, X. R. et al. (2010). Extracellular signal-regulated protein kinase activation in endometrium with polycystic ovary syndrome and its significance. *Zhonghua Fu Chan Ke Za Zhi* **45** (10): 767-71.

Sourris, K. C. and J. M. Forbes (2009). Interactions between advanced glycation end-products (AGE) and their receptors in the development and progression of diabetic nephropathy - are these receptors valid therapeutic targets. *Curr Drug Targets* **10** (1): 42-50.

Southern, L. et al. (2007). Immunohistochemical study of N-epsilon-carboxymethyl lysine (CML) in human brain: relation to vascular dementia. *BMC Neurol* **7**: 35.

Sparvero, L. J. et al. (2009). RAGE (Receptor for Advanced Glycation Endproducts), RAGE ligands, and their role in cancer and inflammation. *J Transl Med* **7**: 17.

Speir, E. et al. (2000). Competition for p300 regulates transcription by estrogen receptors and nuclear factor-kappaB in human coronary smooth muscle cells. *Circ Res* **87** (11): 1006-11.

Srikrishna, G. and H. H. Freeze (2009). Endogenous damage-associated molecular pattern molecules at the crossroads of inflammation and cancer. *Neoplasia* **11** (7): 615-28.

Srikrishna, G. (2002). N-glycans on the receptor for advanced glycation end products influence amphoterin binding and neurite outgrowth. *J Neurochemistry* **80**: 998-1008.

Stavreus-Evers, A. et al. (2001). Formation of pinopodes in human endometrium is associated with the concentrations of progesterone and progesterone receptors. *Fertil Steril* **76** (4): 782-91.

Stein, I. F. and Leventhal, M.L. (1935). Amenorrhea associated with bilateral polycystic ovaries. *Am J Obstet Gyneacol* **29**: 181-191.

Sternberg, D. I. et al. (2008). Blockade of receptor for advanced glycation end product attenuates pulmonary reperfusion injury in mice. *J Thorac Cardiovasc Surg* **136** (6): 1576-85.

Stoikos, C. J. et al. (2008). A distinct cohort of the TGFbeta superfamily members expressed in human endometrium regulate decidualization. *Hum Reprod* **23** (6): 1447-56.

Strowitzki, T. et al. (2006). The human endometrium as a fertility-determining factor. *Hum Reprod Update* **12** (5): 617-30.

Sturchler, E. et al. (2008). Site-specific blockade of RAGE-Vd prevents amyloid-beta oligomer neurotoxicity. *J Neurosci* **28** (20): 5149-58.

Stygar, D. et al. (2003). Effects of SERM (selective estrogen receptor modulator) treatment on growth and proliferation in the rat uterus. *Reprod Biol Endocrinol* **1**: 40.

Sugaya, K. et al. (1994). Three genes in the human MHC class III region near the junction with the class II: gene for receptor of advanced glycosylation end products, PBX2 homeobox gene and a notch homolog, human counterpart of mouse mammary tumor gene int-3. *Genomics* **23** (2): 408-19.

Sugino, N. et al. (2002). Expression of vascular endothelial growth factor (VEGF) and its receptors in human endometrium throughout the menstrual cycle and in early pregnancy. *Reproduction* **123** (3): 379-87.

Sugiyama, T. et al. (2007). Angiotensin II receptor blocker inhibits abnormal accumulation of advanced glycation end products and retinal damage in a rat model of type 2 diabetes. *Exp Eye Res* **85** (3): 406-12.

Sun, C. et al. (2009). Advanced glycation end products depress function of endothelial progenitor cells via p38 and ERK 1/2 mitogen-activated protein kinase pathways. *Basic Res Cardiol* **104** (1): 42-9.

Suzuki, D. et al. (2006). Relationship between the expression of advanced glycation end-products (AGE) and the receptor for AGE (RAGE) mRNA in diabetic nephropathy. *Intern Med* **45** (7): 435-41.

Tabibzadeh, S. et al. (1999). Regulation of TNF-alpha mRNA expression in endometrial cells by TNF-alpha and by oestrogen withdrawal. *Mol Hum Reprod* **5** (12): 1141-9.

Takeuchi, M. and S. Yamagishi (2008). Possible involvement of advanced glycation end-products (AGEs) in the pathogenesis of Alzheimer's disease. *Curr Pharm Des* **14** (10): 973-8.

Takeuchi, M. et al. (2000). Immunological evidence that non-carboxymethyllysine advanced glycation end-products are produced from short chain sugars and dicarbonyl compounds in vivo. *Mol Med* **6** (2): 114-25.

Talbott, E. O. et al. (2001). Cardiovascular risk in women with polycystic ovary syndrome. *Obstet Gynecol Clin North Am* **28** (1): 111-33, vii.

Tan, S. et al. (2005). Insulin resistance syndrome and polycystic ovary syndrome: implications for diagnosis and treatment. *Panminerva Med* **47** (4): 211-7.

Tanaka, N. et al. (2000). The receptor for advanced glycation end products is induced by the glycation products themselves and tumor necrosis factor-alpha through nuclear

factor-kappa B, and by 17beta-estradiol through Sp-1 in human vascular endothelial cells. *J Biol Chem* **275** (33): 25781-90.

Tang, T. et al. (2010). Insulin-sensitising drugs (metformin, rosiglitazone, pioglitazone, D-chiro-inositol) for women with polycystic ovary syndrome, oligo amenorrhoea and subfertility. *Cochrane Database Syst Rev* **1**: CD003053.

Tanikawa, T. et al. (2009). Advanced Glycation End Products Induce Calcification of Vascular Smooth Muscle Cells through RAGE/p38 MAPK. *J Vasc Res* **46**: 572-580.

Tesarova, P. et al. (2007). Receptor for advanced glycation end products (RAGE)--soluble form (sRAGE) and gene polymorphisms in patients with breast cancer. *Cancer Invest* **25** (8): 720-5.

Thathiah, A. et al. (2004). Tumor necrosis factor alpha stimulates MUC1 synthesis and ectodomain release in a human uterine epithelial cell line. *Endocrinology* **145**: 4192-203.

Thornalley, P. J. (1990). The glycoxylase system, new developments towards functional characterization of a metabolic pathway fundamental to biological life. *Journal of Biochemistry* **269**: 1-11.

Thornalley, P. J. (1998). Cell activation by glycated proteins. AGE receptors, receptor recognition factors and functional classification of AGEs. *Cell Mol Biol* **44**: 1013-1033.

Thornalley, P. J. et al. (2000). Mass spectrometric monitoring of albumin in uremia. *Kidney Intl* **58**, 2228-2234.

Tian, B. and Brasier, A.R. (2003). Identification of a nuclear factor kB-dependent gene network. *Recent Prog Horm Res* **58**: 95-130.

Tian, B. et al. (2005). A TNF-induced gene expression program under oscillatory NF-kappaB control. *BMC Genomics* **6**: 137.

Tian, J. et al. (2007). Toll-like receptor 9-dependent activation by DNA-containing immune complexes is mediated by HMGB1 and RAGE. *Nat Immunol* **8** (5): 487-96.

Toprak, S. et al. (2001). Insulin resistance in nonobese patients with polycystic ovary syndrome. *Horm Res* **55**, 65-70.

Tremblay, G. B. et al. (1999). Dominant activity of activation function 1 (AF-1) and differential stoichiometric requirements for AF-1 and -2 in the estrogen receptor alpha-beta heterodimeric complex. *Mol Cell Biol* **19** (3): 1919-27.

Truica, C. et al. (2003). beta-Catenin Affects Androgen Receptor Transcriptional Activity and Ligand Specificity. *Cancer Res* (Advances in Brief) **60**: 4709-4713.

Trukhacheva, E. et al. (2009). Estrogen receptor (ER) beta regulates ERalpha expression in stromal cells derived from ovarian endometriosis. *J Clin Endocrinol Metab* **94** (2): 615-22.

Tse, A. K. et al. (2010). 1alpha,25-Dihydroxyvitamin D3 inhibits transcriptional potential of nuclear factor kappa B in breast cancer cells. *Mol Immunol* **47** (9): 1728-38.

Tsuji, A. et al. (2008). Induction of Receptor for Advanced Glycation End Products by EBV Latent Membrane Protein 1 and Its Correlation with Angiogenesis and Cervical Lymph Node Metastasis in Nasopharyngeal Carcinoma. *Clin Cancer Res* **14** (17): 5368 - 5375.

Tuttle, K. R. et al. (2005). Amino acids injure mesangial cells by advanced glycation end products, oxidative stress, and protein kinase C. *Kidney Int* **67** (3): 953-68.

Ulrich, P. and Cerami, A. (2001). Protein glycation, diabetes, and aging. *Recent Prog Horm Res* **56**: 1-21.

Uribarri, J. et al. (2010). Advanced glycation end products in foods and a practical guide to their reduction in the diet. *J Am Diet Assoc* **110** (6): 911-16 e12.

Van Beijnum, J. et al. (2008). Convergence and amplification of toll-like receptor (TLR) and receptor for advanced glycation end products (RAGE) signaling pathways via high mobility group B1 (HMGB1). *Angiogenesis* **11** (1): 91-9.

Van den Akker, O. (2002). The Complete Guide to Infertility: Diagnosis, treatment, options. London, Free Association Books.

Van Zoelen, M. et al. (2009). Role of toll-like receptors 2 and 4, and the receptor for advanced glycation end products in high-mobility group box 1-induced inflammation in vivo. *Shock* **31** (3): 280-4.

Villablanca, A. C. et al. (2009). 17-β Estradiol Prevents Early-Stage Atherosclerosis in Estrogen Receptor-Alpha Deficient Female Mice. *J Cardiovasc Trans Res* **2**: 289-299.

Villavicencio, A.K. et al. (2006). Androgen and estrogen receptors and co-regulators levels in endometria from patients with polycystic ovarian syndrome with and without endometrial hyperplasia. *Gynecol Oncol* **103** (1): 307-14.

Vlassara, H. et al. (1995). Identification of galectin-3 as a high-affinity binding protein for advanced glycation end products (AGE): a new member of the AGE-receptor complex. *Mol Med* **1** (6): 634-46.

Von Wolff, M. et al. (1999). Tumour necrosis factor-alpha (TNF-alpha) in human endometrium and uterine secretion: an evaluation by immunohistochemistry, ELISA and semiquantitative RT-PCR. *Mol Hum Reprod* **5** (2): 146-52.

Wa, C. et. al. (2007). Characterization of glycation adducts on human serum albumin by matrix-assisted laser desorption/ionization time-of-flight mass spectrometry. *Clin Chim Acta* **385** (1-2): 48-60.

Walter, P. et al. (1985). Cloning of the human estrogen receptor cDNA. *Proc Natl Acad Sci USA* **82** (23): 7889-93.

Wang, A. et al. (1998). The effects of FSH,LH and insulin on steroids production by granulosa cells from polycystic ovaries syndrome. *Zhonghua Yi Xue Za Zhi* **78** (11): 830-2.

Wang, L. et al. (2008). Receptor for advanced glycation end products (RAGE) mediates neuronal differentiation and neurite outgrowth. *J Neurosci Res* **86** (6): 1254-66.

Wei, X. et al. (2005). Human MUC1 oncoprotein regulates p53-responsive gene transcription in the genotoxic stress response. *Cancer Cell* **7** (2): 167-78.

Wei, X. et al. (2006). MUC1 oncoprotein stabilizes and activates estrogen receptor alpha. *Mol Cell* **21** (2): 295-305.

Weihua, Z. et al. (2000). Estrogen receptor (ER) beta, a modulator of ERalpha in the uterus. *Proc Natl Acad Sci USA* **97** (11): 5936-41.

Wendt, T. M. et al. (2003). RAGE Drives the Development of Glomerulosclerosis and Implicates Podocyte Activation in the Pathogenesis of Diabetic Neuropathy. *Am J Pathol* **162** (4): 1123-1137.

Wendt, T. M. et al. (2003). Glucose, Glycation, and RAGE: Implications for Amplification of Cellular Dysfunction in Diabetic Nephropathy. *J Am Soc Nephrol* (Frontiers in Nephrology) **14**: 1383-1395.

Weyant, M. J. et al. (2001). Reciprocal expression of ERalpha and ERbeta is associated with estrogen-mediated modulation of intestinal tumorigenesis. *Cancer Res* **61** (6): 2547-51.

WHO, W. H. O. (1992). Scientific Group on recent advances in medically assisted conception. Geneva. WHO monograph Technical Series 820.

Wieslander, A. et al. (2001). Exogenous uptake of carbonyl stress compounds promoting AGE formation from peritoneal dialysis. *Contrib Nephrol* **131**: 82-89.

Wijayanti, N. et al. (2008). Inhibition of phorbol ester-dependent peroxiredoxin I gene activation by lipopolysaccharide via phosphorylation of RelA/p65 at serine 276 in monocytes. *Free Radic Biol Med* **44** (4): 699-710.

Wilder, J. et al. (2004). Tamoxifen-associated malignant endometrial tumors: pathologic features and expression of hormone receptors estrogen-alpha, estrogen-beta and progesterone; a case controlled study. *Gynecol Oncol* **92** (2): 553-8.

Witek, A. et al. (2007). Coexpression index of estrogen receptor alpha mRNA isoforms in simple, complex hyperplasia without atypia, complex atypical hyperplasia and adenocarcinoma. *Gynecol Oncol* **106** (2): 407-12.

Wu, X. et al. (2000). Expression of insulin-receptor substrate-1 and -2 in ovaries from women with insulin resistance and from controls. *Fertil Steril* **74** (3): 564-72.

Xanthis, A. et al. (2009). Receptor of Advanced Glycation End Products (RAGE) Positively Regulates CD36 Expression and Reactive Oxygen Species Production in Human Monocytes in Diabetes. *Angiology* **60** (6): 772-9

Xie, J. et al. (2008). Structural basis for pattern recognition by the receptor for advanced glycation end products (RAGE). *J Biol Chem* **283** (40): 27255-69.

Yamagishi, S. et al. (2008). Olmesartan blocks advanced glycation end products (AGEs)-induced angiogenesis in vitro by suppressing receptor for AGEs (RAGE) expression. *Microvasc Res* **75**, 130-4.

Yan, S. D. et al. (1996). RAGE and amyloid-beta peptide neurotoxicity in Alzheimer's disease. *Nature* **382** (6593): 685-91.

Yan, S. F. et al. (2009). Receptor for AGE (RAGE) and its ligands-cast into leading roles in diabetes and the inflammatory response. *J Mol Med* **87** (3): 235-47.

Yan, S. F. et al. (2009). The receptor for advanced glycation endproducts (RAGE) and cardiovascular disease. *Expert Rev Mol Med* **11**: e9.

Yang, F. et al. (2002). Linking beta-catenin to androgen-signaling pathway. *J Biol Chem* **277** (13): 11336-44.

Yang, J. et al. (2009). Reciprocal regulation of 17beta-estradiol, interleukin-6 and interleukin-8 during growth and progression of epithelial ovarian cancer. *Cytokine* **46** (3): 382-91.

Yao, D. and M. Brownlee (2010). Hyperglycaemia -induced reactive oxygen species increase expression of the receptor for advanced glycation end products (RAGE) and RAGE ligands. *Diabetes* **59** (1): 249-55.

Yeh, C.-H. et al. (2001). Requirement for p38 and p44/p42 Mitogen-Activated Protein Kinases in RAGE-Mediated Nuclear Factor-kappa B Transcriptional Activation and Cytokine Secretion. *Diabetes.* **50**: 1495-1504.

Yim, M. B. et al. (2001). Protein glycation: creation of catalytic sites for free radical generation. *Ann. N.Y. Acad. Sci* **928**: 48-53.

Yonekura, H. et al. (2003). Novel splice variants of the receptor for advanced glycation end-products expressed in human vascular endothelial cells and pericytes, and their putative roles in diabetes-induced vascular injury. *Biochem J* **370** (Pt 3): 1097-109.

Yoon, Y. W. (2008). Pathobiological role of advanced glycation endproducts via mitogen-activated protein kinase dependent pathway in the diabetic vasculopathy. *Exp Mol Med* **40**, 398-406.

Zaretsky, J. et al. (2006). MUC1 gene overexpressed in breast cancer: structure and transcriptional activity of the MUC1 promoter and role of estrogen receptor alpha (ERalpha) in regulation of the MUC1 gene expression. *Mol Cancer* **5**: 57.

Zargar, A. H. et al. (2005). Prevalence of ultrasonography proved polycystic ovaries in North Indian women with type 2 diabetes mellitus. *Reprod Biol Endocrinol* **3**: 35.

Zhang, H. M. et al. (2009). Association of 1704G/T and G82S polymorphisms in the receptor for advanced glycation end products gene with diabetic retinopathy in Chinese population. *J Endocrinol Invest* **32** (3): 258-62.

Zhang, H., Park, Y., Wu, J., Chen, X., Lee, S., Yang, J., Dellsperger, K. C., and Zhang, C. (2009). Role of TNF-alpha in vascular dysfunction. *Clin Sci (Lond)* **116**, 219-30.

Zhang, H. et al. (2008). Role of soluble receptor for advanced glycation end products on endotoxin-induced lung injury. *Am J Respir Crit Care Med* **178** (4): 356-62.

Zhang, L. and Q. Liao (2010). Effects of testosterone and metformin on glucose metabolism in endometrium. *Fertil Steril* **93** (7): 2295-8.

Zhang, L. et al. (2008). Receptor for advanced glycation end products is subjected to protein ectodomain shedding by metalloproteinases. *J Biol Chem* **283** (51): 35507-16.

Zhong, H. et al. (1998). Phosphorylation of NF-kappa B p65 by PKA stimulates transcriptional activity by promoting a novel bivalent interaction with the coactivator CBP/p300. *Mol Cell* **1** (5): 661-71.

Zhou, G. et al. (2001). Role of AMP-activated protein kinase in mechanism of metformin action. *J Clin Invest* **108** (8): 1167-74.

Zhu, L. and J. W. Pollard (2007). Estradiol-17beta regulates mouse uterine epithelial cell proliferation through insulin-like growth factor 1 signaling. *Proc Natl Acad Sci USA* **104** (40):15847-51.

Appendix

APPENDIX

A: RNA Protocol for RNeasy Kit Qiagen

Procedure:

1. Cells grown in a monolayer (do not use more than 1 x 107 cells): Cells can be either lysed directly in the cell-culture vessel (up to 10 cm diameter) or trypsinized and collected as a cell pellet prior to lysis.

2. Disrupt the cells by adding Buffer RLT. For pelleted cells, loosen the cell pellet thoroughly by flicking the tube. Add the appropriate volume of Buffer RLT (see Table 5). Vortex or pipet to mix, and proceedto step 3.

3. Pipet the lysate directly into a QIAshredder spin column placed in a 2 ml collection tube, and centrifuge for 2 min at full speed. Proceed to step 4.

4. Add 1 volume of 70% ethanol to the homogenized lysate, and mix well by pipetting. Do not centrifuge.

5. Transfer up to 700 µl of the sample, including any precipitate that may have formed, to an RNeasy spin column placed in a 2 ml collection tube (supplied). Close the lid gently, and centrifuge for 15 s at _8000 x g (_10,000 rpm). Discard the flow-through.

6. Add 700 µl Buffer RW1 to the RNeasy spin column. Close the lid gently, and centrifuge for 15 s at _8000 x g (_10,000 rpm) to wash the spin column membrane. Discard the flow-through.

7. Add 500 µl Buffer RPE to the RNeasy spin column. Close the lid gently, and centrifuge for 15 s at _8000 x g (_10,000 rpm) to wash the spin column membrane. Discard the flow-through.

8. Add 500 µl Buffer RPE to the RNeasy spin column. Close the lid gently, and centrifuge for 2 min at _8000 x g (_10,000 rpm) to wash the spin column membrane.

9. Optional: Place the RNeasy spin column in a new 2 ml collection tube (supplied), and discard the old collection tube with the flow-through. Close the lid gently, andcentrifuge at full speed for 1 min.

10. Place the RNeasy spin column in a new 1.5 ml collection tube (supplied). Add 30–50 µl RNase-free water directly to the spin column membrane. Close the lid gently, and centrifuge for 1 min at _8000 x g (_10,000 rpm) to elute the RNA.

11. If the expected RNA yield is >30 µg, repeat step 10 using another 30–50 µl RNasefree water, or using the eluate from step 10 (if high RNA concentration is required). Reuse the collection tube from step 10.

If using the eluate from step 10, the RNA yield will be 15–30% less than that obtained using a second volume of RNase-free water, but the final RNA concentration will be higher.

B: Chromatin Immunoprecipitation (ChIP)

B1: Optimization of Chromatin Shearing by Sonication

Prior to immunoprecipitation, shearing conditions to yield chromatin suitable for use in ChIP were optimised during a six month secondment at Active Motif Europe, Rixensart, Belgium. Five aliquots of fixed chromatin in 350µL Shearing Buffer were subject to sonication of different pulse number (5 or 10 times), pulse length (30 sec, 1 min 40 sec, 2 min 30 and 3 min 20) and power (30% or 40% amplitude), using a hand-held probe sonicator with a 3mm stepped micro-tip (Vibracell VC 130, Sonics). Chromatin was efficiently sheared on ice to 200-300bp using 5 intermittent pulses of 40% amplitude lasting 1 min 40 sec. Shearing conditions for the use of the Bioruptor sonicator (Diagenode) maintained at a constant water temperature of 4°C were previously optimised at Swansea University to be 30 sec pulses (on) with 30 sec rest (off) between each pulse for a total period of 30 min. All reagents were supplied in the ChIP-IT Express kit (Active Motif) unless stated otherwise.

B2: DNA Clean up and Quantification

50µL aliquots of sheared chromatin reserved from each sample were thawed (if necessary). 150µL of distilled MilliQ water (Millipore) and 10µL of 5M NaCl (SIGMA) were added to all samples and heated overnight at 65°C in a water bath or thermocycler to reverse cross-links. Samples were re-incubated at 37°C for 15 min with 2µL RNase A, and 42°C for 1.5 h with 10µL Proteinase K to remove RNA and protein respectively that may be bound to the chromatin. To determine DNA concentration by spectrophotometer, samples were precipitated in 200µL phenol/chloroform 1:1 (pH8) or with isoamyl alcohol in a ratio of 25:24:1(SIGMA), briefly vortexed and centrifuged at maximum rpm for 5 min. Supernatant was transferred to 1.7mL tube and supplemented with 20µL 3M Sodium Acetate pH 5.2 (SIGMA) and 500µL of 100% Ethanol (Fisher Scientific), vortexed thoroughly and placed at -80°C for 1 h. Samples were centrifuged maximum speed at 4°C for 10 min, supernatant discarded and pellet left undisturbed. 500mL 70% Ethanol was added to the pellet and centrifuged at 4°C for 5 min. Supernatant was removed and pellet allowed to air dry. The chromatin was then resuspended in 30mL distilled MilliQ water and quantified by OD at λ260nm on the

Nanodrop Spectrophotometer (Thermo). The amount of chromatin to be used in ChIP was adjusted per sample to 5µg. All reagents used for DNA clean up procedure were supplied in ChIP-IT Express Kit (Active Motif) unless stated otherwise.

B3: Optimisation of ChIP Primers

	Promoter	Primer Set	Optimal Dilution	[Primer] (µM)	Efficiency (%)	Slope	Y Intercept	R^2
A	RAGE	p65 Site 1 ER Ap1 Site	1:20	5.0	96.971	-3.397	14.735	0.999
B	RAGE	p65 Site 2	1:100	0.2	101.02	-.3.298	16.88	0.999
C	RAGE	p65 Site 3	1:100	0.2	100.76	-3.304	17.146	0.999
D	RAGE	ER Sp1 Site 1 ER Sp1 Site 2	1:20	5.0	94.071	-3.473	15.931	0.996
E	RAGE	ER Sp1 Site 3	1:100	0.2	92.99	-3.505	17.561	0.999
F	MUC1	p65 Site 1	1:100	0.2	95.62	-3.641	19.672	0.991
G	MUC1	p65 Site 2	1:100	0.2	97.35	-3.598	18.447	0.990

Figure 7-1 Table to show the primer efficiencies and working concentrations of the genomic primers designed for ChIP on the RAGE and MUC1 promoters.

C: Melt Curves for genomic RT-PCR primers

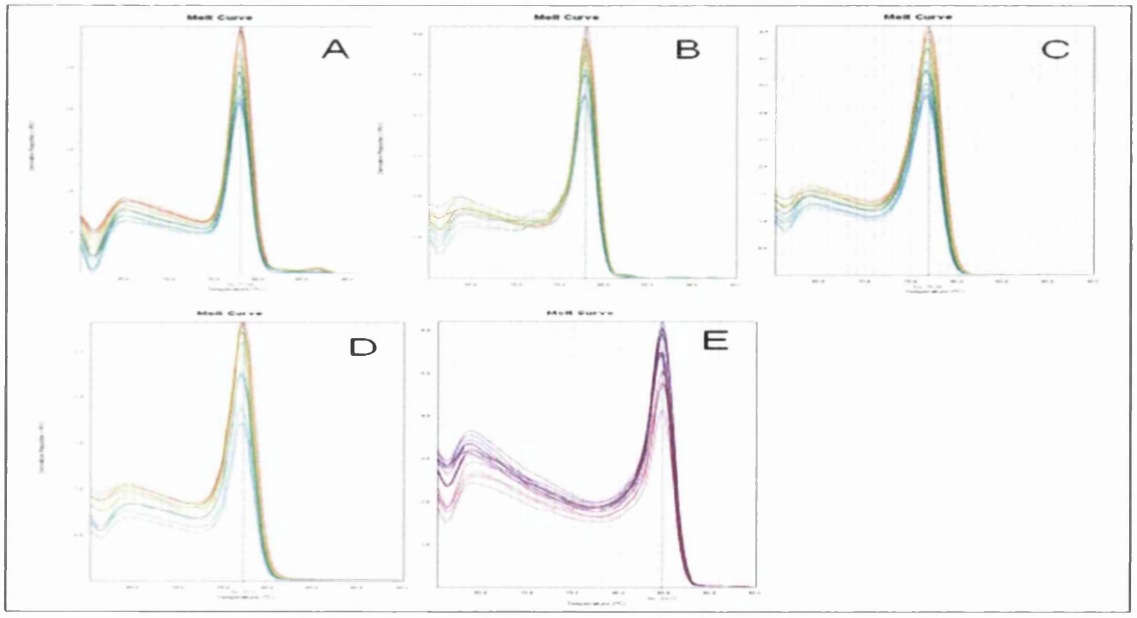

Figure 7-2 Melt curves of the genomic primers for the NFκB, Ap1 and Sp1 sites on the RAGE promoter used in ChIP.

The melt curves A-E above correspond to the primer information shown in Figure 7-1 in section B3 of the Appendix. These melt curves show no indication of primer dimer formation and amplify a specific singular product at the required PCR temperature (60°C).